DESIGN METHODS FOR MICROWAVE FILTERS AND MULTIPLEXERS

by

SAOD ABDUL AZIZ ALSEYAB
B.Sc., M.Sc.

Submitted in fulfilment of the requirements
for the degree of
Doctor of Philosophy

The University of Leeds
Department of Electrical and Electronic Engineering

October 1979

Research carried out between June 1976 and June 1979,
under the Supervision of Professor J.D. Rhodes.

PAGE NUMBERS ARE CUT OFF IN THE ORIGINAL

ABSTRACT

This thesis is concerned with developing synthesis and design procedures for microwave filters and multiplexers. The core of this thesis presents the following topics.

1) New classes of lumped lowpass prototype filters satisfying generalized Chebyshev characteristics have been investigated. Exact synthesis procedures are given using a relatively new technique termed the alternating pole synthesis technique to solve the accuracy problem. The properties of these filters and their pract.cal advantages have been discussed. Tables of element values for commonly used specifications are included.

2) A new design procedure has been developed for bandpass channel multiplexers connected at a common junction. This procedure is for multiplexers having any number of Chebyshev channel filters, with arbitrary degrees, bandwidths and inter-channel spacings. The procedure has been modified to allow the design of multi-octave bandwidth combline channel filter multiplexers. It is shown that this procedure gives very good results for a wide variety of specifications, as demonstrated by the computer analysis of several multiplexers examples and by the experimental results.

3) A compact exact synthesis method is presented for a lumped bandpass prototype filter up to degree 30 and satisfies a generalized Chebyshev response. This prototype has been particularly utilized in designing microwave broadband combline filters.

4) Different forms of realization have been discussed and used in design and construction of different devices. This includes a new technique to realize TEM networks in coaxial structure form having equal diameter coupled circular cylindrical rods between parallel ground planes. Other

forms of realization have been discussed ranging from equal diameter posts, direct coupled cavity waveguide filters to microwave integrated circuits using suspended substrate stripline structure. The experimental results are also given.

In addition, the fundamentals of lumped circuits and distributed circuits have been briefly reviewed. The approximation problem was also discussed.

ACKNOWLEDGEMENTS

I wish to express my sincere gratitude to the people of Yorkshire whose hospitality and friendly nature will stay alive in my memory for long years to come. I would like especially to thank the many members of the Department of Electrical and Electronic Engineering at Leeds University. First of all, I am in debt to Professor J.D. Rhodes who supervised the research which led to this thesis in his unique and distinguished way, for all the help and encouragement during the work. It is a privilege indeed working with him.

My thanks should go to:

Mr. P. Clark

Mr. J.L. Gibbs and his staff of the Workshop. Messrs. R.C. Hawkes, J.L. Clarke and N. Banting for their efforts in building the devices.

The technical staff of Dec-10 system of the Department of Computer Studies at Leeds University for use of the facilities and their ready help whenever needed.

Miss S.D. Salman for preparing neat drawings of all the illustrations and graphs in this thesis.

Mr. S.J. Aljadir who devoted a lot of his time for going through the final manuscript and correcting many spelling and grammatical mistakes.

Mrs. S. Moore and Mrs. J. Lowe for their expert typing.

Mr. A. Payne for his help in photocopying this thesis.

Finally, The Ministry of Higher Education and Scientific Research of the Government of Iraq for the financial support without which I would not be here in the first place.

CONTENTS

CHAPTER 1

FUNDAMENTALS OF LUMPED CIRCUITS THEORY

1.1 INTRODUCTION.

Filtering is a fundamental signal process in electronics, it includes such diverse operations as channeling, demodulating, equalizing, detecting, decoding, phase slitting, integrating and differentiating. Nowadays, any two-port network that is designed to process signals is loosely called a filter, whether it is linear or non linear, time invariant or time-varying, and whether the signal is continuous or digital.

The word "filter" is used in this thesis to designate a linear, time invariant passive lossless two-port network terminated by a resistive load that allows analogue signals in certain frequency band(s) which are called passband(s) and suppresses all others which are called stopband(s). In general, filters may contain purely passive elements (inductors L's, capacitors C's, resistors R's), they may be of an active RC type, they may contain mechanical resonators (quartz crystals and other piezoelectric resonators), or they may be built of distributed parameter components (microwave or active distributed RC filters). For all or most of these different types of ralizations, the synthesis and design theory is common and became a highly specialized field within electronic engineering.

The filter designer has several design methods to choose, the simplest and oldest being the image parameter method. This method is useful for the design of LC, piezoelectric crystal, and mechanical filter and, in fact, is still being used extensively for the latter types. The network theory (insertion-loss) design technique is an exact method for LC filters operating between resistive terminations. Under

normal conditions, it provides the simplest and hence the least expensive design. In the past the price one pays for this is a vastly increased complexity in computations. But today sets of explicit design formulas and algorithms are available for numerous types of filters, which enable even the non-specialist to design filters using no more than a pocket calculator or a microcomputer.

Filters are present in any communication system and for a certain extent in many systems and equipments that depend on selective network. However, their major application is in frequency division multiplex systems and this is the main concern of this work.

1.2 BASIC CONCEPTS.

A filter is assumed here to be a passive network with single-input, single-output as shown symbolically in Fig. 1. and is composed of only linear, time invariant elements. A network of this type generally satisfies the following constraints on its input variable (the excitation) X(t) and its output variables (the response) Y(t) [1]:

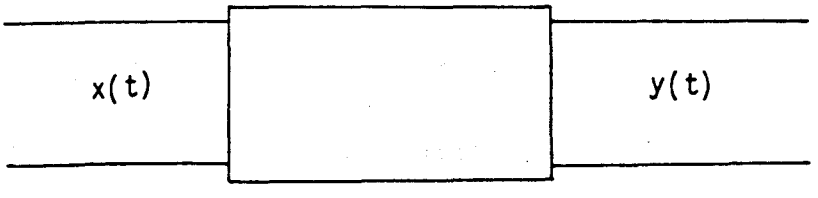

Fig. 1.1. Single-Input, Single Out-put Filter.

a) Linearity: If $X_1(t) \rightarrow$ (implies) $Y_1(t)$

and $X_2(t) \rightarrow Y_2(t)$

Then, linearity means

$$a\,X_1(t) + b\,X_2(t) \rightarrow a\,Y_1(t) + b\,Y_2(t)$$

where, a and b are arbitrary constants.

t represents time variable.

b) Time-invariance: It means that the network parameters do not change as functions of time. Thus

$$X(t) \rightarrow y(t)$$

then

$$X(t+t_0) \rightarrow y(t+t_0)$$

where to is an arbitrary time interval.

c) Passivity: A network is said to be passive, if it may only absorb or store energy. That is, it does not provide amplification nor returns more energy to the source than is supplied. If v(t) and i(t) are the input voltage and current respectively, then, the passivity restriction requires:

$$\text{total delivered energy} = \int_{-\infty}^{t} v(\tau)\, i(\tau)\, d\tau \geq 0 \quad t > -\infty$$

d) Causality: A network is causal if it yields no response until after an excitation is applied.

If $x(t) \rightarrow y(t)$

then $x(t) = 0, \quad t \leq t_0 \quad , \quad X(t) = X_1(t), \quad t > t_0$

implies $Y(t) = 0, \; t \leq t_0 \quad , \quad Y(t) = Y_1(t), \; t > t_0$

e) Real time function: when a signal X(t), which is a real function of real time, is imposed upon the network, it must give rise to a response Y(t), which is also a real function of real time.

If $X_0(t) = X_r(t) + j\, X_i(t)$

$Y_0(t) = Y_r(t) + j\, Y_i(t)$

then, the real time function restriction requires:

$$X_i(t) = 0 \rightarrow Y_i(t) = 0$$

$$X(t) = X_r(t) \rightarrow Y(t) = Y_r(t)$$

The linear relationship between the response and the excitation which characterizes the network can be expressed either in the time domain or in the frequency domain.

Consider X(t) and Y(t) to be continuous functions of time, so they can be related through a convolution integral [2] as follows:

$$Y(t) = \int^{\infty} h(t-\tau)\, X(\tau)\, d\tau \qquad (1.1)$$

where h(t) is the response of the network to a unit impulse applied at t = o.

This time domain relationship can be converted to the frequency domain by taking the Laplace transform of (1.1), yielding

$$Y_o(p) = H(p)\, X_1(p)$$

or $$H(p) = Y_o(p)/X_1(p) \qquad (1.2)$$

where $Y_o(p)$, $X_1(p)$, H(p) are the Laplace transforms of Y(t), X(t) and h(t) respectively.

H(p) is referred to as the "transfer function" of the network. $P = \sigma + j\omega$ is the lumped complex frequency variable.

The Laplace transformation F(p) for a function f(t) is defined as:

$$F(p) = \mathcal{L}\, f(t) = \int_0^{\infty} f(t)\, e^{-pt}\, dt. \qquad (1.3)$$

1.2.1. Lumped Element Networks.

A lumped element network is a combination of resistors, capacitors, inductors and coupled elements (i.e. coupled coils including transformers and coupled capacitors). In this type of networks, the electrical and magnetic fields and electric energy dissipation in the form of heat may be considered as concentrated in separate elements of the network. Changes in voltages and currents in these networks are expressed only as time functions independently, of the spatial coordinates [3]. If $v(t)$ and $i(t)$ are the time dependent voltage and current associated with a particular element, then, the elements are defined by the following relationships:

a) A resistor (R) ohms $\quad v(t) = R\, i(t)$

b) An inductor (L) Henries $\quad v(t) = -L \dfrac{di(t)}{dt}$ or $i(t) = \displaystyle\int_0^t v(\tau)\, d\tau$

c) A capacitor (c) Farads $\quad i(t) = C \dfrac{dv(t)}{dt}$ or $v(t) = \dfrac{1}{C} \displaystyle\int_0^t i(\tau)\, d\tau$

d) An ideal transformer (n) turn ratio $\quad v_1(t) = n\, v_2(t)$ or $i_1(t) = \dfrac{1}{n}\, i_2(t)$

where 1 and 2 indicate the primary and secondary coils respectively. The relationships defining the coupled elements are excluded because the networks to be considered are free of them.

Applying the Laplace transformation to $f(t) = v(t)/i(t)$ and assuming zero initial conditions, results in the concept of "impedance". Hence the impedance of a resistor R, inductor L and a capacitor C are R, LP and $1/CP$ respectively.

1.2.2. Driving Point Functions and Transfer Functions.

For a general network consisting of any arbitrary connections of a finite number of RLC elements the impedance function

$$Z(p) = F(p) = V(p)/I(p) \tag{1.4}$$

is known as the "driving-point impedance" if V(p) and I(p) belong to the same terminal pair (port). If each belongs to a different port, then z(p) is known as the "transfer impedance". Furthermore the reciprocal of the driving point impedance is the "driving point admittance".

$$Y(p) = I(p)/V(p) \tag{1.5}$$

The word "immittance" is sometimes used to mean either Z(p) or Y(p). The transfer admittance function may be defined by equation (1.5) if the variables of the right hand side are taken at differnt ports. However, no physical significance can be attached to the definition of a transfer admittance function as a reciprocal of transfer impedance function.

Driving point and transfer functions are important quantities in circuit theory and in practical network applications. These functions usually appear in the form of rational functions (ratios of two finite polynomials) in terms of the variable P. The coefficients of the numerator and denominator polynomials are real and positive. The zeros of the numerator polynomial are called "Zeros" of the function while the zeros of the denominator are called the "poles" of the function.

A driving-point function may have zeros and poles in the left half p-plane and on the imaginary axis. Taking z(p) as a typical case, it is generally constructed in the form

$$z(p) = \frac{N(p)}{D(p)}$$

or

$$z(p) = \frac{m_1(p) + n_1(p)}{m_2(p) + n_2(p)} \tag{1.6}$$

where $m_1(p)$, $m_2(p)$ and $n_1(p)$, $n_2(p)$ are the even and odd parts of the numerator and denominator polynomials respectively.

In general any driving-point function z(p) is positive real (p.r.) [4].

i.e. z(p) is real for p real

Re $z(p) \geq 0$ for Re $p \geq 0$

Where "Re" stands for real part of a complex quantity. However, some driving point functions are of the LC form and thus have all their poles and zeros on the imaginary axis. An impednace of this form is called a "reactance function", and an admittance, a "susceptance function". If z(p) is a reactance function, then it is an odd function i.e. a ratio of even and odd polynomials or a ratio of odd and even polynomials.

$$Z_{LC}(p) = \frac{m(p)}{n(p)} \text{ or } \frac{n(p)}{m(p)} \tag{1.7}$$

where m(p) and n(p) are even and odd polynomials respectively.

On the other hand, a driving point impedance may have none of its poles on the imaginary axis, such a function is called "minimum reactive" impedance. Similarly, a driving-point admittance without poles on the imaginary axis is called "minimum susceptive". A corresponding set of definitions is applied to transfer functions. A transfer function of a stable network must have no poles ir the right half p-plane; however, its zeros are in general not restricted in this way. A transfer function that does have none of its zeros in the right half is called a "minimum phase" function, otherwise it is "non-minimum phase".

Minimum phase transfer functions normally describe linear stable physical systems where electromagnetic energy may only travel from the input to the output port along a single path and the "Ladder" structure type of networks shown in Fig. 1.2 is an example of them.

Ladder networks and their minimum phase transfer functions will be discussed extensively in this thesis, while the nonmimum phase transfer functions which describe multipath structures and realized by a rather special type of networks (e.g. linear phase filters) are considered beyond the scope of this thesis.

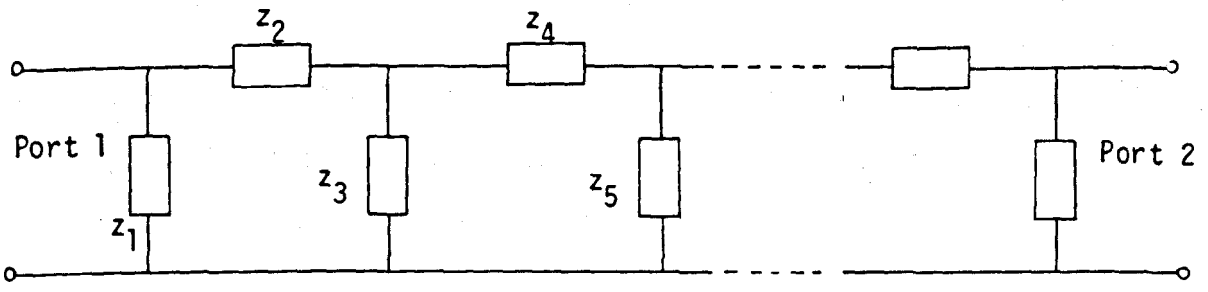

Fig. 1.2. Ladder Structure.

1.2.3. Properties of Driving-Point Immittance Functions [5].

The properties of the driving point immittance function F(p) may be summarized in:

a) F(p) is positive real function i.e.

Re F(p) $\geq$ 0 for Re P $\geq$ 0

F(p) is real for P real

This is the necessary and sufficient conditior for F(p) to be realizable as an input immittance of a physical network.

Furthermore, if F(p) is positive real, then one can define a function

$$\rho(p) = \pm \frac{F(p)-1}{F(p)+1} \qquad (1.8)$$

where $\rho(p)$ is a bounded real function i.e.

$\rho(p)$ is real for p real

$0 \leq |\rho(p)| < 1$ for Re $P > 0$

b) The poles and zeros of the driving-point function are either real, or occur in complex conjugate pairs.

c) The poles and zeros occur in the left half p-plane or on the $j\omega$-axis (numerator and denominator are both Hurwitz polynomials).

d) Poles and zeros on the $j\omega$ axis are simple, i.e. can never have multiplicity (or degree) greater than unity.

e) As a corollary of (d) above: The degree of the numerator and denominator polynomials of the driving point functions cannot differ by more than one.

1.2.4. Properties of Transfer Functions [5]

The properties of transfer functions may be summarized in:

a) The poles and zeros of a transfer function are either real, or occur in complex conjugate pairs.

b) The poles of transfer functions all occur in the left hand p-plane or on the $j\omega$-axis. No restriction on the occurrence of the zeros.

c) Poles on the $j\omega$-axis are simple (of multiplicity of 1).

The properties of driving-point functions and transfer functions are given briefly in section 1.2.3. and 1.2.4, the proofs and detailed

discussions are omitted here because they are not needed and they can be found in any standard text on networkssynthesis (e.g. 4,5).

1.3 TWO-PORT NETWORK PARAMETERS.

Two-port network are of general importance in filter theory. Consider the general two port network N, shown diagrammatically in Fig. 1.3.

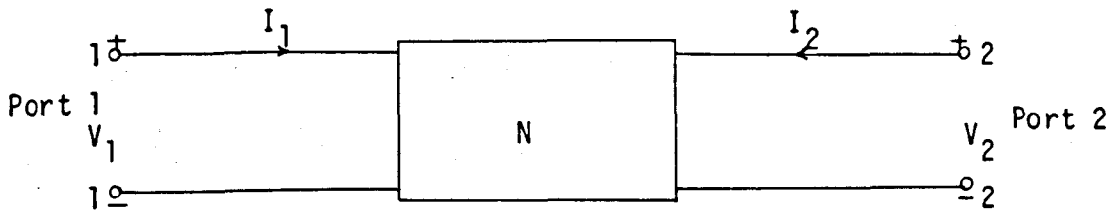

Fig. 1.3. Two-Port Network.

The behaviour of the network at its accessible ports can be described by relating the voltage V_1 and current I_1 at port 1 to the corresponding quantities at port 2. The relationships between V_1, V_2, I_1 and I_2 can be expressed by means of linear equations. Hence choosing any two of the four variables and the remaining two variables can be expressed in terms of them as linear relationships. The linearity due to the linear properties of the network. In this sense there are six sets of two-port parameters. They are called "z-parameters","y-parameters", "ABCD and reverse ABCD parameters", and "h- and g- parameters".

The four parameters of each set are related to the parameters of other sets by simple formulas deduced by applying basic circuit laws and algebric manipulations.

The h-and g- parameters are not commonly used in passive networks, their main application being in circuits having transistors or mixed current-voltage sources and they are not needed as far as this thesis is

concerned, therefore they will not be discussed here.

1.3.1. The z-Parameters.

The z-parameters are z_{11}, z_{12}, z_{21} and z_{22} which are functions of the frequency variable p and each having the dimension of impedance they are also referred to as "the open circuit impedance parameters" and being defined by the equations:

$$V_1 = z_{11} I_1 + z_{12} I_2 \qquad \text{(a)}$$
$$V_2 = z_{21} I_1 + z_{22} I_2 \qquad \text{(b)} \qquad (1.9)$$

or in matrix form

$$\begin{bmatrix} V_1 \\ V_2 \end{bmatrix} = \begin{bmatrix} z_{11} & z_{12} \\ z_{21} & z_{22} \end{bmatrix} \begin{bmatrix} I_1 \\ I_2 \end{bmatrix} \qquad (1.10)$$

Define

$$[z] = \begin{bmatrix} z_{11} & z_{12} \\ z_{21} & z_{22} \end{bmatrix} \qquad (1.11)$$

and

$$\Delta z = z_{11} z_{22} - z_{12} z_{21} \qquad (1.12)$$

The extension to n-port network is straightforward, Instead of two impedance equations, there are n equations which can be expressed in matrix form by

$$[V] = [z]_{nxn} \; [I] \qquad (1.13)$$

where

$$[z]_{nxn} = \begin{bmatrix} z_{11} & z_{12} & \cdots & z_{1n} \\ z_{21} & z_{22} & \cdots & z_{2n} \\ - & - & - & - \\ z_{n1} & z_{2n} & \cdots & z_{nn} \end{bmatrix} \qquad (1.14)$$

The elements of the matrix are defined by

$$z_{rk} = \left.\frac{Vr}{I_k}\right|_{I_1 = I_2 = \ldots = I_{k-1} = I_{k+1} \ldots = I_n = o} \tag{1.15}$$

1.3.2. The y-parameters.

These four parameters y_{11}, y_{12}, y_{21} and y_{22} are the dual of the z-parameters. Each of them is a function of P and having the dimensions of admittance. They are also called the short-circuit admittance parameters and defined by the following two equations:

$$\left.\begin{aligned} I_1 &= y_{11} V_1 + y_{12} V_2 \qquad (a) \\ I_2 &= y_{21} V_1 + y_{22} V_2 \qquad (b) \end{aligned}\right\} \tag{1.16}$$

or in matric form:

$$\begin{bmatrix} I_1 \\ I_2 \end{bmatrix} = \begin{bmatrix} y_{11} & y_{12} \\ y_{21} & y_{22} \end{bmatrix} \begin{bmatrix} V_1 \\ V_2 \end{bmatrix} \tag{1.17}$$

Define

$$[y] = \begin{bmatrix} y_{11} & y_{12} \\ y_{21} & y_{22} \end{bmatrix} \tag{1.18}$$

and

$$\Delta y = y_{11} y_{22} - y_{12} y_{21} \tag{1.19}$$

The y-parameters for n-port network can be described by an nxn matrix as:

$$[y]_{nxn} = \begin{bmatrix} y_{11} & y_{12} & \cdots & y_{1n} \\ y_{21} & y_{22} & \cdots & y_{2n} \\ - & - & - & - \\ y_{n1} & y_{n2} & \cdots & y_{nn} \end{bmatrix} \tag{1.20}$$

The elements of the matrix are defined by

$$y_{rk} = \frac{I_r}{V_k}\Bigg|_{V_1=V_2 \ldots V_{k-1} = V_{k+1} \ldots = V_n = 0} \qquad (1.21)$$

1.3.3. The Forward And Reverse Transfer Matrix Parameters:

The four parameters are well known as A, B, C. and D and often designated as transmission parameters, chain parameters, general circuit parameters, or simply as the ABCD parameters. They relate the input quantities to the output quantities by means of the follow two equations:

$$\left.\begin{aligned} V_1 &= AV_2 - BI_2 \qquad \ldots.(a) \\ I_1 &= CV_2 - DI_2 \qquad \ldots.(b) \end{aligned}\right\} \qquad (1.22)$$

or simply in matrix form as:

$$\begin{bmatrix} V_1 \\ I_1 \end{bmatrix} = \begin{bmatrix} A & B \\ C & D \end{bmatrix} \begin{bmatrix} V_2 \\ -I_2 \end{bmatrix} \qquad (1.23)$$

and the transfer matrix is referred to as:

$$[T] = \begin{bmatrix} A & B \\ C & D \end{bmatrix} \qquad (1.24)$$

Define

$$\Delta T = AD - BC \qquad (1.25)$$

The dimensions of these four parameters are different. The parameters A and D are dimensionless, while B and C have the dimensions of impedance and admittance respectively.

The reverse transfer matrix parameters can be obtained from the forward ones, because they are simply relating the output variables V_2 and I_2 to their input counterparts. Thus the reverse matrix $[T_r]$ is given by:

$$[T_r] = \begin{bmatrix} A_r & B_r \\ C_r & D_r \end{bmatrix} = \frac{1}{\Delta T} \begin{bmatrix} D & B \\ C & A \end{bmatrix} \tag{1.26}$$

The forward and reverse transfer parameter are widely used in analysis of networks connected in cascade as shown in Fig. 1.4.

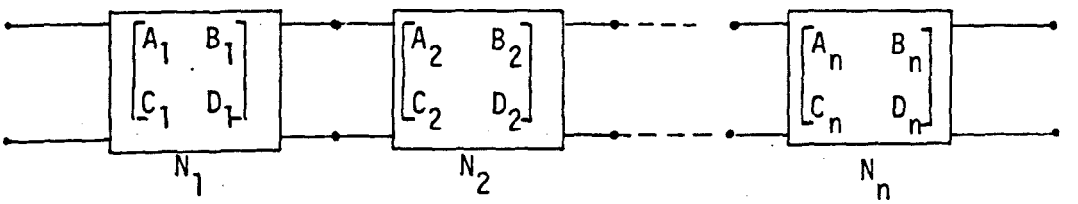

Fig. 1.4. Cascade-Connected Networks N_i

They simplify the calculation and reduce it only to a matrix multiplication which is in turn the most appropriate case for computer handling of the problem.

The overall transfer matrix $\begin{bmatrix} A & B \\ C & D \end{bmatrix} = \begin{bmatrix} A_1 & B_1 \\ C_1 & D_1 \end{bmatrix} \begin{bmatrix} A_2 & B_2 \\ C_2 & D_2 \end{bmatrix} \cdots \begin{bmatrix} A_n & B_n \\ C_n & D_n \end{bmatrix}$

(1.27)

1.3.4. Relationships Between z, y and ABCD Parameters.

Although the 'y' and 'z' parameters are duals the individual y-parameters is not the reciprocal of the corresponding z-parameter for the same network. The relationship between each z and y parameters can be obtained by arranging the relations (1.10) and (1.17) into the dual form, which gives:

$$\begin{bmatrix} z_{11} & z_{12} \\ z_{21} & z_{22} \end{bmatrix} = \begin{bmatrix} y_{11} & y_{12} \\ y_{21} & y_{22} \end{bmatrix}^{-1} = \frac{1}{\Delta y} \begin{bmatrix} y_{22} & -y_{12} \\ -y_{21} & y_{11} \end{bmatrix} \tag{1.28}$$

or

$$\begin{bmatrix} y_{11} & y_{12} \\ y_{21} & y_{22} \end{bmatrix} = \begin{bmatrix} z_{11} & z_{12} \\ z_{21} & z_{22} \end{bmatrix}^{-1} = \frac{1}{\Delta z} \begin{bmatrix} z_{22} & -z_{12} \\ -z_{21} & z_{11} \end{bmatrix} \tag{1.29}$$

The relationship between z-parameters and the ABCD-parameters can be obtained by the same argument of re-arranging and comparing the defining equations.

Re-write equation (1.9b) as

$$I_1 = \frac{1}{z_{21}} V_2 - \frac{z_{22}}{z_{21}} I_2 \tag{1.30}$$

Substitute for I_1 in equation (1.9a) to give

$$V_1 = \frac{z_{11}}{z_{21}} V_2 - \frac{\Delta z}{z_{21}} I_2 \tag{1.31}$$

comparing equations (1.30) and (1.31) with (1.22a and b) leads to the following relationship between the z and ABCD parameters

$$\begin{bmatrix} A & B \\ C & D \end{bmatrix} = \begin{bmatrix} \frac{z_{11}}{z_{21}} & \frac{\Delta z}{z_{21}} \\ \frac{1}{z_{21}} & \frac{z_{22}}{z_{21}} \end{bmatrix} \tag{1.32}$$

Alternatively

$$\begin{bmatrix} z_{11} & z_{12} \\ z_{21} & z_{22} \end{bmatrix} = \begin{bmatrix} \frac{A}{C} & \frac{\Delta T}{C} \\ \frac{1}{C} & \frac{C}{D} \end{bmatrix} \tag{1.33}$$

The relationship between y and ABCD parameters can be derived by rearringing equations (1.16.a and b) and comparing the resulting equations with (1.22.a and b) in the similar way in which the relationship between z and ABCD parameters have been obtained.

1.4 SYMMETRICAL AND RECIPROCAL TWO-PORT NETWORKS.

Symmetrical networks are defined as, the networks whose ports cannot be distinguished or whose external characteristics are unchanged when the network is reversed. Hence, in terms of the network parameters, the symmetry conditions are:

$$\left.\begin{aligned} z_{11} &= z_{22} \\ y_{11} &= y_{22} \\ \text{and} \quad A &= D \end{aligned}\right\} \tag{1.34}$$

On the other hand, reciprocal networks are networks which satisfy the reciprocity principle. In general any network consisting of linear, finite, time invariant and bilateral resistors, inductors, capacitors and ideal transformers is reciprocal.

The reciprocity conditions can be expressed in terms of the two-port parameters as:

$$\left.\begin{aligned} z_{12} &= z_{21} \\ y_{12} &= y_{21} \\ \text{and} \quad \Delta T &= AD - BC = 1 \end{aligned}\right\} \tag{1.35}$$

1.5 LOSSLESS NETWORKS.

Lossless networks are particularly important because most filter circuits dealt with later in this thesis are lossless. The lossless networks mainly consist of LC elements. Their driving point immittance functions are of the form defined in equation (1·7).

1.5.1. One Port lossless Network:

For one port the driving point function is usually written as (Taking a driving point impedance as a typical case).

$$Z_{LC}(p) = K \frac{(P^2+S_1^2)\ (P^2+S_3^2)}{P(P^2+P_2^2)(P^2+P_4^2)} \tag{1.36}$$

or

$$Z_{LC}(p) = K \frac{P(P^2+S_1^2)(P^2+S_3^2)}{(P^2+P_2^2)(P^2+P_4^2)} \tag{1.37}$$

where K is a scaling factor. The zeros occur at $P = \pm S_r$ and the poles at $P = \pm P_r$.

At the origin there is either a pole or a zero and there is either a pole or a zero at infinity depending on whether the numerator or the denominator polynomial has the highest degree.

$Z_{LC}(P)$ has the following properties.

a) Its poles and zeros are simple and occur only on the imaginary axis in an alternating manner.

b) The constant multiplier K is positive. Since $Z_{LC}(P)$ must be positive real, and since its poles are on the imaginary axis they must be simple with real positive residues. Therefore $Z_{LC}(P)$ can be expanded in a partial fraction general form as

$$Z_{LC}(P) = k_\infty p + \frac{K_o}{p} + \sum_{r=2,4,6}^{n} \frac{2\,K_r\,P}{p^2 + P_r^2} \tag{1.38}$$

where all the "k's" are real positive residues. If there is no pole at infinity $k_\infty = 0$ and if there is no pole at the origin $k_o = 0$. Similarly, the driving-point admittance function may be written as

$$Y_{LC}(P) = a_\infty P + \frac{a_o}{P} + \sum_{r=1,3,5}^{n} \frac{2\,a_r\,P}{P^2 + P_r^2} \tag{1.39}$$

where all the "a's" are positive real residues.

1.5.2. Two-Port Lossless Network.

Consider a reciprocal two-port network defined by its [z] matrix. And z_{11}, z_{12} and z_{22} are reactance functions. Hence, they may be expanded in partial fraction form similar to (1.38)

$$\left.\begin{aligned} z_{11} &= k_{11}^{(\infty)} P + \frac{k_{11}^{(0)}}{P} + \sum_{r=1}^{n} \frac{2 k_{11}^{(r)} P}{P^2 + P_r^2} \\ z_{22} &= k_{22}^{(\infty)} P + \frac{k_{22}^{(0)}}{P} + \sum_{r=1}^{n} \frac{2 k_{22}^{(r)} P}{P^2 + P_r^2} \\ z_{12} &= k_{12}^{(\infty)} P + \frac{k_{12}^{(0)}}{P} + \sum_{r=1} \frac{2 k_{12}^{(r)} P}{P^2 + P_r} \end{aligned}\right\} \qquad (1.40)$$

z_{12} cannot have a pole which is not a pole of z_{11} and z_{22}, but it is possible for z_{11} or z_{22} to possess poles not common with the other two impedances. These non-common poles are called "private poles", and can be removed as series elements consisting of parallel LC circuit. A network whose z_{11}, z_{22} and z_{12} have the same poles is called "compact". The necessary and sufficient condition for a given [z] matrix with z_{11}, z_{22} and z_{12} being reactance functions, to be realized as two-port LC (lossless) networks is:

$$k_{11}^{(i)} \; k_{22}^{(i)} - k_{12}^{2(i)} \geq 0, \quad k_{11}^{(i)} > 0, \quad k_{22}^{(i)} > 0$$

at every pole on the imaginary axis.

The transfer matrix of two port lossless network generally has the following properties.

a) A and D are even rational functions in P with no zero at the origin.

b) B and C are odd rational function in P.

1.6 TWO-PORT NETWORK TERMINATED BY AN ARBITRARY LOAD.

Consider the passive two-port network N defined by either set of its parameters and terminated by an arbitrary load of impedance $Z_\ell = \frac{1}{Y_\ell}$ at port 2 as shown in Fig. 1.5.

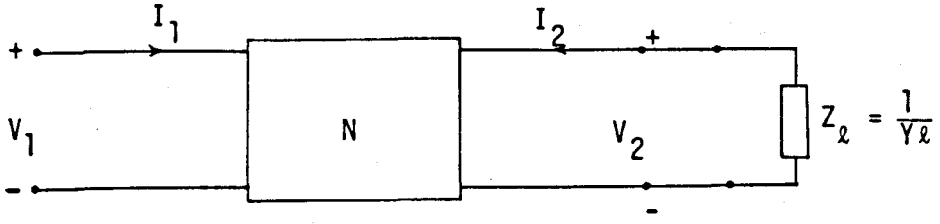

Fig. 1.5. Two-port network terminated by load.

The input impedance (driving point impedance) at port 1 is defined as

$$Z_{in}(p) = \frac{V_1}{I_1} \tag{1.41}$$

and the transfer impedance

$$Z_t(p) = \frac{V_2}{I_1} \tag{1.42}$$

To find $Z_{in}(p)$ and $Z_t(p)$ in terms of the z-parameters let

$$I_2 = -\frac{V_2}{Z_\ell} \tag{1.43}$$

Substitute for I_2 in equations (1.9a and b) giving

$$V_1 = z_{11} I_1 - \frac{z_{12}}{Z_\ell} V_2 \tag{1.44}$$

$$V_2 = z_{21} I_1 - \frac{z_{22}}{Z_\ell} V_2 \tag{1.45}$$

Hence

$$V_2 = \frac{z_{21} I_1}{1 + (z_{22}/Z_\ell)} \tag{1.46}$$

Substitute for V_2 in (1.32) gives

$$Z_{in}(p) = \frac{V_1}{I_1} = \frac{\Delta z + z_{11} Z_\ell}{Z_\ell + z_{22}} \tag{1.47}$$

$Z_t(p)$ can be obtained from (1.46) as

$$Z_t(p) = \frac{V_2}{I_1} = \frac{z_{21} Z_\ell}{Z_\ell + z_{22}} \tag{1.48}$$

Similarly, the driving point admittance at port 1 defined by

$$Y_{in}(p) = \frac{I_1}{V_1} \tag{1.49}$$

and the transfer admittance

$$Y_t(p) = \frac{I_2}{V_1} \tag{1.50}$$

can be expressed in terms of the y-parameters as:

$$Y_{in}(p) = \frac{\Delta y + y_{11} Y_\ell}{Y_\ell + Y_{22}} \tag{1.51}$$

$$Y_t(p) = \frac{y_{21} Y_\ell}{Y_\ell + y_{22}} \tag{1.52}$$

Expressions can be developed also for $Z_{in}(p)$ and $Z_t(p)$ or $Y_{in}(p)$ and $Y_t(p)$ in terms of the ABCD-Parameters. Substitute for I_2 as given by equation (1.43) in equations (1.22 a and b), results in:

$$V_1 = (A + B/Z_\ell)\, V_2 \tag{1.53}$$

$$I_1 = (C + D/Z_\ell)\, V_2 \tag{1.54}$$

so that, the driving point impedance at port 1 is given by:

$$Z_{in}(p) = \frac{V_1}{I_1} = \frac{AZ_\ell + B}{CZ_\ell + D} \tag{1.55}$$

and

$$Z_t(p) = \frac{V_2}{I_1} = \frac{Z_\ell}{CZ_\ell + D} \tag{1.56}$$

or

$$Y_t(p) = \frac{-I_2}{V_1} = \frac{1}{AZ_\ell + B} \tag{1.57}$$

1.7 INSERTION LOSS OF DOUBLY TERMINATED NETWORK [5]

In equation (1.2), a general definition was given to the transfer function H(p) of a two port network as the ratio of the transformed output variable to the transformed input variable, and it has been shown in the previous sections that there exist at least two variable (voltage and current) at each port of the considered two port network. Furthermore, the transfer function was considered as transfer impedance and admittance in equations (1.42) and (1.50) respectively. In this section the transfer function will be considered as the ratio of the output to the input voltage, and this definition is used in deriving a formula for the insertion loss which may be defined as "the ratio of the available power from the generator P_o to the power delivered to the load P_ℓ .

Consider the connection shown in Fig. 1.6 when a voltage generator V_g with a series connected resistance Rg is connected to a resistive load R_ℓ by an ideal transformer of turn ratio 1:n.

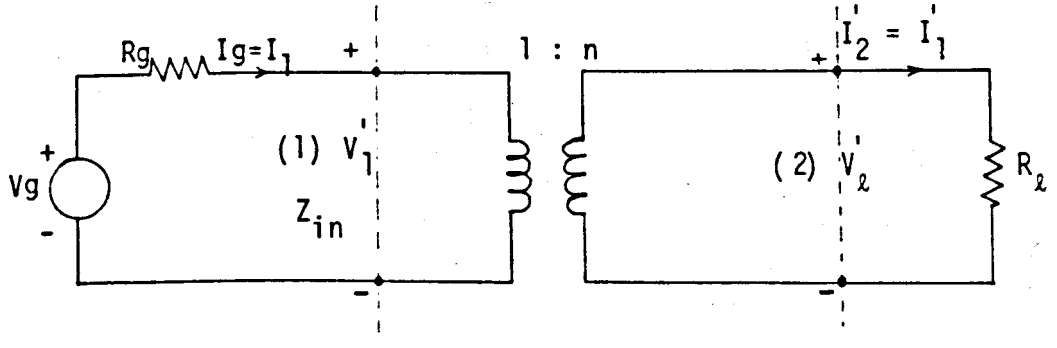

Fig. 1.6. Transformer-connected generator and load.

It is well known from the basic principles of circuit analysis that the maximum available power for delivery to the load is equal to half the power delivered by the generator and the other half is dissipated in its own series resistance and this can only happen when the load and generator resistances are equal.

From Fig. 1.6 the input impedance at port 1 is given by

$$Z_{in} = \frac{R_\ell}{n^2} \tag{1.58}$$

and can be made equal to Rg by choosing n to be

$$n = \left(\frac{R_\ell}{Rg}\right)^{\frac{1}{2}} \tag{1.59}$$

$$V_1' = \frac{1}{n} V_\ell' = \left(\frac{Rg}{R_\ell}\right)^{\frac{1}{2}} V_\ell \tag{1.60}$$

Since the same current I'_1 is flowing through Rg and Z_{in}, across which is the voltage V_1', also equal powers are developed in both of them. This means that the voltage across Rg and Z_{in} are each equal to V_1'. The generator voltage Vg is developed across these two resistances, this leads to the relation

$$Vg = 2 V_1' = 2\left(\frac{Rg}{R_\ell}\right)^{\frac{1}{2}} V_\ell'$$

or

$$\frac{V_\ell'}{Vg} = \frac{1}{2}\left(\frac{R_\ell}{Rg}\right)^{\frac{1}{2}} \tag{1.61}$$

Now the ideal transformer can be removed and a two-port network N defined by its ABCD parameters is inserted between Rg and R_ℓ as shown in Fig. 1.7.

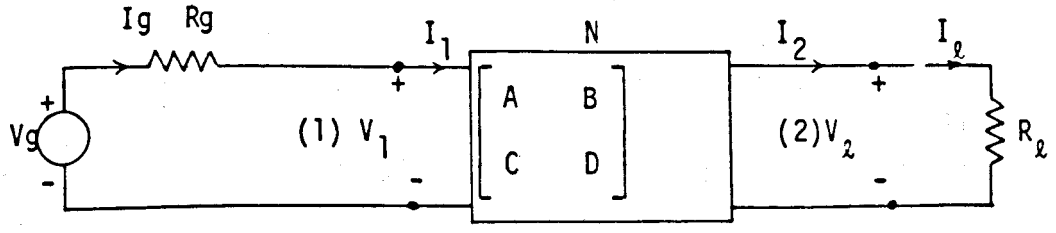

Fig. 1.7. Doubly terminated two-port network.

The voltage Vg and current Ig delivered from the generator may be related to the voltage V_ℓ and current I_ℓ across the load by using the overall transfer matrix of the series resistance Rg and the network N as

$$\begin{bmatrix} Vg \\ Ig \end{bmatrix} = \begin{bmatrix} A+CRg & B+DRg \\ C & D \end{bmatrix} \begin{bmatrix} V_\ell \\ I_\ell \end{bmatrix} \tag{1.62}$$

and from it, deduce

$$Vg = (A + CRg)\, V_\ell + (B + DRg)\, I_\ell \tag{1.63}$$

But I_ℓ can be related to V by

$$I_\ell = \frac{V_\ell}{R_\ell} \tag{1.64}$$

Thus

$$V_g = (A+C\,Rg + \frac{B}{R_\ell} + D\,\frac{Rg}{R_\ell})\, V_\ell$$

or

$$\frac{V_g}{V_\ell} = (A+\frac{B}{R_\ell} + C\,Rg + D\,\frac{Rg}{R_\ell}) \tag{1.65}$$

Now, the ratio of the voltage across the load resistor when there is a maximum power transfer to the actual voltage across it, i.e. V'_ℓ/V_ℓ can be obtained from equations (1.61) and (1.65) as

$$\frac{V'_\ell}{V_\ell} = \frac{1}{2}\left\{ A\left(\frac{R}{Rg}\right)^{\frac{1}{2}} + \frac{B}{(R_\ell Rg)^{\frac{1}{2}}} + C\,(R_\ell R_g)^{\frac{1}{2}} + D\left(\frac{R_g}{R_\ell}\right)^{\frac{1}{2}} \right\} \tag{1.66}$$

Since the insertion loss power ratio = $\frac{P_o}{P_\ell}$ (1.67)

and the voltage V'_ℓ and V_ℓ are delivered across the same R_ℓ

$$\therefore \quad \frac{P_o}{P} = \left| \frac{V'_\ell}{V} \right|^2 = \frac{1}{4} \left| A\left(\frac{R_\ell}{R_g}\right)^{\frac{1}{2}} + \frac{B}{(R_\ell R_g)^{\frac{1}{2}}} + C\,(R_\ell R_g)^{\frac{1}{2}} + D\left(\frac{R_g}{R_\ell}\right)^{\frac{1}{2}} \right|^2 \tag{1.68}$$

Equation (1.68) is a general expression for any passive linear time invariant two port network terminated at port 1 and 2 by R_g and R_ℓ respectively. It can be simplified for a special but very important case when $R_g = R_\ell = 1$ ohm to give

$$\frac{P_o}{P_\ell} = \frac{1}{4} \left| A + B + C + D \right|^2 \tag{1.69}$$

And for a lossless network at real frequencies when A and D are real and B and C are imaginary it becomes

$$\frac{P_o}{P_\ell}\,(\text{lossless}) = 1 + \frac{1}{4}(A-D)^2 + \frac{1}{4}(B-C)^2 \tag{1.70}$$

1.8 THE IMAGE PARAMETERS AND IMAGE-MATCHED NETWORKS.

1.8.1. The Image Parameters.

The image parameters for a reciprocal two port network are a set of three parameters, two image impedances z_{I_1} and z_{I_2} and an image propagation function ν.

Image impedances z_{I_1} and z_{I_2} may be connected respectively to port 1 and 2, and each of them is defined as the driving point impedance at its port if the second port is terminated in the other image impedance. The image parameters may be expressed in terms of other sets of parameters, the most convenient of which are the transfer matrix parameters.

Consider a network terminated at port 2 in the impedance z_{I_2}, thus, its driving point impednace at port 1 is given by

$$z_{1\,in} = \frac{A\,z_{I_2}+B}{C\,z_{I_2}+D} = z_{I_1} \tag{1.71}$$

and the driving impedance at port 2, z_{I_2} when port 1 is terminated in z_{I_1} is given by

$$z_{2\,in} = \frac{D\,z_{I_1}+B}{C\,z_{I_1}+A} = z_{I_2} \tag{1.72}$$

Solving (1.71) and (1.72) for Z_{I_1} and Z_{I_2}, results in

$$z_{I_1} = \left(\frac{AB}{CD}\right)^{\frac{1}{2}} \quad ; \quad z_{I_2} = \left(\frac{DB}{CA}\right)^{\frac{1}{2}} \tag{1.73}$$

and the image propagation function γ may be defined by

$$\frac{V_1}{V_2} = \frac{z_{I_1}}{z_{I_2}}\,e^{\nu} \tag{1.74}$$

where $\nu = \alpha + j\beta$

α is the attentuation function

β is the phase function

If $z_\ell = z_{I_2}$ is used in equation (1.53) it gives

$$\frac{V_1}{V_2} = A + B/z_{I_2} \tag{1.75}$$

Thus

$$\left(\frac{z_{I_1}}{z_{I_2}}\right)^{\frac{1}{2}} e^{\nu} = A + B/z_{I_2} \tag{1.76}$$

Substituting for z_{I_1} and z_{I_2} by their values given in (1.73) results in:

$$e^{\nu} = (AD)^{\frac{1}{2}} + (BC)^{\frac{1}{2}} \tag{1.77}$$

Now, it can be shown that

$$\cosh = \frac{e^{\nu} + e^{-\nu}}{2} = (AD)^{\frac{1}{2}} \tag{1.78}$$

$$\sinh = \frac{e^{\nu} - e^{-\nu}}{2} = (BC)^{\frac{1}{2}} \tag{1.79}$$

$$\frac{z_{I_1}}{z_{I_2}} = \frac{A}{D} \quad , \quad z_{I_1}\, z_{I_2} = \frac{B}{C} \tag{1.80}$$

The relationship between the transfer matrix parameters and the image parameters can be established as:

$$A = \left(\frac{A}{D}\right)^{\frac{1}{2}} \cdot (AD)^{\frac{1}{2}} = \left(\frac{z_{I_1}}{z_{I_2}}\right)^{\frac{1}{2}} \cosh \nu$$

$$B = \left(\frac{B}{C}\right)^{\frac{1}{2}} \cdot (BC)^{\frac{1}{2}} = (z_{I_1}\, z_{I_2})^{\frac{1}{2}} \sinh \nu$$

$$C = \left(\frac{C}{D}\right)^{\frac{1}{2}} (BC)^{\frac{1}{2}} = \frac{\sin h\, \nu}{(z_{I_1}\, z_{I_2})^{\frac{1}{2}}}$$

and

$$D = \left(\frac{D}{A}\right)^{\frac{1}{2}} (AD)^{\frac{1}{2}} = \left(\frac{z_{I_2}}{z_{I_1}}\right)^{\frac{1}{2}} \cosh \nu$$

i.e. in matrix notation:

$$\begin{bmatrix} A & B \\ C & D \end{bmatrix} = \begin{bmatrix} \left(\frac{z_{I_1}}{z_{I_2}}\right)^{\frac{1}{2}} \cosh & (z_{I_1} z_{I_2})^{\frac{1}{2}} \sin h\nu \\ \frac{\sin h\nu}{(z_{I_1} z_{I_2})^{\frac{1}{2}}} & \left(\frac{z_{I_2}}{z_{I_1}}\right)^{\frac{1}{2}} \cos h\, \nu \end{bmatrix} \qquad (1.81)$$

1.8.2. Image-matched Lossless Networks.

The concept of image-matching means that a network is matched if it is terminated in its image impedances. It can be easily proved by substituting for the transfer parameters (given by their image-parameter equivalent form of (1.81)) in the insertion loss expression (1.68) and let

$$R_g = z_{I_1} \quad ; \quad R_\ell = Z_{i_2} \qquad (1.82)$$

this results in

$$\frac{P_o}{P_\ell} = \frac{1}{4} \left|2 \cosh\nu + 2\sinh\nu\right|^2 = |e^{\nu}|^2 \qquad (1.83)$$

$$= |\, e^{\alpha+j\beta} \,|^2$$

Hence $\frac{P_o}{P_\ell} = e^{2\alpha}$

α is either positive or zero, since the insertion loss must be greater or equal to unity by definition. For a lossless network α equal zero and $\frac{P_o}{P_\ell} = 1$ always holds under the assumption of (1.82), i.e. the network is perfectly matched.

1.9 SCATTERING PARAMETERS (MATRIX) [1] .

The scattering parameters originated in the theory of transmission lines. They are defined in such a way that the various quantities of interest in power transmission have very simple expressions in terms of them. Thus, they are indispensable in the design of microwave networks and in any other situation when the concept of power is much more important than the concepts of voltage and current. One other important property of the scattering parameters is that every linear, passive, time invariant network has a scattering matrix, comparing with other parameters, for example, a two port consisting of a series of impedance and a ground wire has no impednace matrix, or a shunt two port branch has no admittance matrix.

1.9.1. Definition of Scattering Variables:

The scattering variables are termed as incident and reflected voltages or incident and reflected currents. The linear relations between such variables and the well known voltage and current at the input of one port network shown in Fig. 1.8 are defined in terms of the general equations:

$$a = \alpha_{11} \dot{V}' + \alpha_{12} I' \tag{1.84}$$

$$b = \alpha_{21} \dot{V}' + \alpha_{22} I' \tag{1.85}$$

where a is the incident voltage or current

b is the reflected voltage or current

α_{ij} are arbitrary constants which define the transformation. They can be chosen to make a and b particularly convenient to use in physical problems when a power transfer is under consideration.

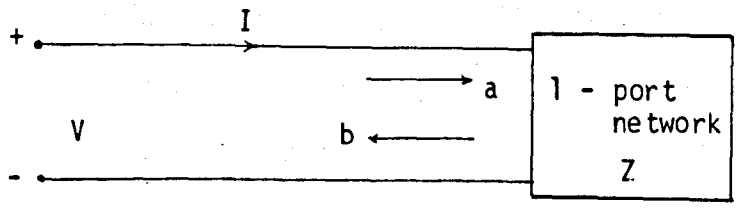

Fig. 1.8. Definition of scattering variables.

A simple choice of α_{ij} that yields this results for network design problems is

$$\alpha_{11} = \alpha_{12} = \frac{1}{2(R_1)^{\frac{1}{2}}} \quad , \quad \alpha_{21} = -\alpha_{22} = \frac{1}{2}(R_1)^{\frac{1}{2}} \tag{1.86}$$

where R_1 is real positive constant termedthe port normalizing number and has the dimensions of resistance. It is usually chosen equal to the source resistance.

Equations (1.84)and(1.85) can be rewritten as:

$$a = \frac{1}{2}\left\{\left[\frac{V'}{(R_1)^{\frac{1}{2}}} + I'(R_1)^{\frac{1}{2}}\right]\right. \tag{1.87}$$

$$b = \frac{1}{2}\left\{\left[\frac{V'}{(R_1)^{\frac{1}{2}}} - I'(R_1)^{\frac{1}{2}}\right]\right. \tag{1.88}$$

defining the normalized voltage and current as

$$V = \frac{V'}{(R_1)^{\frac{1}{2}}} \quad , \quad I = I'(R_1)^{\frac{1}{2}} \tag{1.89}$$

Thus

$$a = \frac{1}{2}[V + I] \tag{1.90}$$

$$b = \frac{1}{2}[V - I] \tag{1.91}$$

The ratio of the reflected quantity b to the incident quantity a is defined as the "reflection coefficient" at port 1 given by:

$$S_{11} = b/a = \frac{V-I}{V+I} = \frac{Z-1}{Z+1} \tag{1.92}$$

where Z is the normalized driving point impedance of the network.

1.9.2. Scattering parameters of two-port network:

Consider a two port network N shown in Fig. 1.9 and defined by its impedance matrix as:

$$\begin{bmatrix} V_1 \\ \\ V_2 \end{bmatrix} = [z] \begin{bmatrix} I_1 \\ \\ I_2 \end{bmatrix}$$

$$[V] = [z]\,[I] \tag{1.93}$$

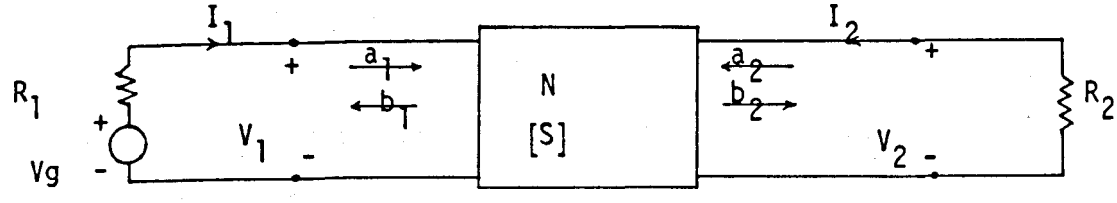

Fig. 1.9 Scattering parameter representation for two-port network.

For such a network, two new matrices can be constructed as follows,

$$[a] = \begin{bmatrix} a_1 \\ a_2 \end{bmatrix} = \frac{1}{2} \begin{bmatrix} R_1^{-\frac{1}{2}} & 0 \\ 0 & R_2^{-\frac{1}{2}} \end{bmatrix} [V] + \frac{1}{2} \begin{bmatrix} R_1^{\frac{1}{2}} & 0 \\ 0 & R_2^{\frac{1}{2}} \end{bmatrix} [I] \tag{1.94}$$

$$[b] = \begin{bmatrix} b_1 \\ b_2 \end{bmatrix} = \frac{1}{2} \begin{bmatrix} R_1^{-\frac{1}{2}} & 0 \\ 0 & R_2^{-\frac{1}{2}} \end{bmatrix} [V] - \frac{1}{2} \begin{bmatrix} R_1^{\frac{1}{2}} & 0 \\ 0 & R_2^{\frac{1}{2}} \end{bmatrix} [I] \tag{1.95}$$

where $[a]$ and $[b]$ are linear combinations of $[V]$ and $[I]$, R_1 and R_2 are port 1 and port 2 normalizing numbers. R_1 and R_2 are not necessarily taken equal to the individual port termination, but their values are usually chosen so as to simplify the form of the power transfer equations. The linear relationships between a and b can be written as:

$$b_1 = S_{11}\, a_1 + S_{12}\, a_2 \tag{1.96}$$

$$b_2 = S_{21}\, a_1 + S_{22}\, a_2 \tag{1.97}$$

or in matrix form

$$[b] = [S]\,[a] \tag{1.98}$$

[S] is called the "scattering matrix" of the two port and defined by

$$[S] = \begin{bmatrix} S_{11}(p) & S_{12}(p) \\ S_{21(p)} & S_{22}(p) \end{bmatrix} \tag{1.99}$$

where

S_{11} is "the reflection coefficient of port 1" obtained by terminating port 2 with its matching load i.e. $a_2 = o$.

$$S_{11} = \left.\frac{b_1}{a_1}\right|_{a_2=0} \tag{1.100}$$

S_{22} is "port 2 reflection coefficient" obtained by terminating port 1 with its matching load i.e. $a_1 = o$

$$S_{22} = \left.\frac{b_2}{a_2}\right|_{a_1=o} \tag{1.101}$$

S_{21} is the "forward transmission coefficient" with port 2 terminated in its matching load i.e. $a_2=o$.

$$S_{21} = \left.\frac{b_2}{a_1}\right|_{a_2=o} \tag{1.102}$$

and S_{12} is the "reverse transmission coefficient" with port 1 terminated in its matching load i.e. $a_1 = o$.

$$S_{12} = \left.\frac{b_1}{a_2}\right|_{a_1=o} \tag{1.103}$$

Each of the four scattering parameters is a function of the frequency variable p.

However, scattering matrix is not only a two-port property but it may be applied to networks with an arbitrary number "n" of ports,

in this case it takes the form of (nxn) matrix as

$$[S]_{nxn} = \begin{bmatrix} S_{11} & S_{12} \cdots S_{1n} \\ S_{21} & S_{22} \cdots S_{2n} \\ \text{- - - - -} \\ \text{- - - - -} \\ S_{n1} & S_{n2} \quad S_{nn} \end{bmatrix} \tag{1.104}$$

and the elements of the matrix are defined by

$$S_{rk} = \frac{b_r}{a_k} \Bigg|_{a_1=a_2 \text{ ---- } = a_{k-1} = a_{k+1} = \text{ ---- } a_n=0} \tag{1.105}$$

1.9.3. Relationship Between The Scattering Parameters and Other Parameters.

Relationships can be obtained between the scattering parameters and other sets of two-port parameters such as z, y, ABCD etc. As an example, the relationship between z and the scattering parameters is given here. Starting from equations (1.94) and (1.95). [V] and [I] may be expressed in terms of [a] and [b] as

$$[V] = \begin{bmatrix} R_1^{\frac{1}{2}} & 0 \\ 0 & R_2^{\frac{1}{2}} \end{bmatrix} \quad ([a] + [b]) = \begin{bmatrix} R_1^{\frac{1}{2}} & 0 \\ 0 & R_2^{\frac{1}{2}} \end{bmatrix} ([1] + [S])\,[a] \tag{1.106}$$

$$[I] = \begin{bmatrix} R_1^{-\frac{1}{2}} & 0 \\ 0 & R_2^{-\frac{1}{2}} \end{bmatrix} \quad ([a] - [b]) = \begin{bmatrix} R_1^{-\frac{1}{2}} & 0 \\ 0 & R_2^{-\frac{1}{2}} \end{bmatrix} ([1] - [S])\,[b] \tag{1.107}$$

Substitute for [V] and [I] in (1.93) will result in

$$\begin{bmatrix} R_1^{-\frac{1}{2}} & 0 \\ 0 & R_2^{-\frac{1}{2}} \end{bmatrix} [z] \begin{bmatrix} R_1^{-\frac{1}{2}} & 0 \\ 0 & R_2^{-\frac{1}{2}} \end{bmatrix} = ([1] + [S])\,([1] - [S])^{-1} \tag{1.108}$$

where the left hand side of equation (1.108) is the normalized impedance matrix[z']

$$\therefore [z'] = ([1] + [S])\,([1] - [S])^{-1} \tag{1.109}$$

1.9.4. Properties of The Scattering Matrix.

The 2 x 2 scattering matrix [S] of a two-port network normalised to R_1 at port 1 and R_2 at port 2 which is given in (1.99) has the following properties.

(a) The four entries in [S] are rational functions and real for real P.

(b) [S] is analytic in $Re \geq P$ 0.

(c) The 2 x 2 hermetian matrix [1] - $[S^+(j\omega)]$ $[S(j\omega)]$ is non-negative definite for all ω, where [1] is a unitary matrix and + denotes the adjoint matrix (complex conjugate of the transpose matrix).

(d) The network is reciprocal if and only if $S_{12}(p) = S_{21}(p)$. That is if and only if $[S] = [S]_t$ where t means transpose.

(e) The network is lossless if and only if [S] possesses the attributes (a), (b) and meets the unitary constraint

$$[S^+(j\omega)][S(j\omega)] = [1] \qquad (1.110)$$

for all ω

(f) Any 2 x 2 matrix [S] satisfies (a), (b) and (c) is a scattering matrix of lumped, passive two port. Moreover, if $S_{12}(p) = S_{21}(p)$ the network is reciprocal and if $[S(j\omega)]$ is unitary, the network is lossless.

1.10. DOUBLY TERMINATED LOSSLESS NETWORK.

The problem of transferring energy from a generator with a resistive series impedance to a resistive load is one of the commonest problems in network theory. A coupling lossless two port network inserted between the resistive generator and the load operates as a filter. The problem of designing such a reciprocal lossless two port network to achieve a prescribed transfer function is one of synthesis and the necessary equations for the synthesis of the lossless network can be found from the fact that all the power leaving the generator must be

consumed in the resistive load. Consider the network N shown in Fig. 1.9 is a lossless one. From equations (1.94) and (1.95), the following relationships can be written

$$\left.\begin{aligned} V_1 &= (a_1+b_1)\, R_1^{\frac{1}{2}} && \text{(a)} \\ V_2 &= (a_2+b_2)\, R_1^{\frac{1}{2}} && \text{(b)} \\ I_1 &= (a_1-b_1)\, R_1^{-\frac{1}{2}} && \text{(c)} \end{aligned}\right\} \qquad (1.111)$$

and

$$I_2 = (a_2-b_2)\, R_2^{-\frac{1}{2}} \qquad \text{(d)}$$

From Fig. 1.9 it appears

$$\left.\begin{aligned} a_2 &= 0 \quad \text{(no incident wave from Port 2)} \\ V_2 &= -R_2 I_1 \\ \text{and} \qquad V_g &= R_1 I_1 + V_1 = 2\, R_1^{\frac{1}{2}}\, a_1 \end{aligned}\right\} \qquad (1.112)$$

Now, the ratio of $P_\ell(\omega^2)$, the average ac power delivered to the load R_2, to $P_g(\omega^2)$, the available ac generator power is defined as "the transducer power gain" $G(\omega^2)$. Hence

$$G(\omega^2) = \frac{P_\ell(\omega^2)}{P_g(\omega^2)} \qquad (1.113)$$

But

$$P_g(\omega^2) = \frac{|V_g|^2}{4R_1} \qquad (1.114)$$

$$\therefore \quad G(\omega^2) = \frac{4|I_2|^2 R_1 R_2}{|V_g|^2} = \frac{|b_2|^2}{|a_1|^2} \qquad (1.115)$$

Since

$$S_{21} = \frac{b_2}{a_1}\Big|_{a_2=0}$$

$$\therefore\ G(j\omega) = |S_{21}(j\omega)|^2 \tag{1.116}$$

and so

$$0 \leq |S_{21}(j\omega)|^2 \leq 1 \tag{1.117}$$

Since the power delivered to the load cannot exceed the available power from the generator when the coupling network is passive.

Another important function for the synthesis is the driving point function at port 1 which can be expressed as the input impedance by

$$Z_{in}(p) = \frac{V_1}{I_1} = R_1 \frac{(a_1+b_1)}{a_1-b_1} \tag{1.118}$$

But

$$b_1 = S_{11}(p)a_1$$

Since $a_2 = o$

Hence

$$\frac{Z_{in}(p)}{R_1} = \frac{1+ S_{11}(p)}{1- S_{11}(p)} \tag{1.119}$$

$Z_{in}(p)$ must be a positive real function since it is the input impedance of a passive RLC network, consequently $S_{11}(p)$ is bounded real i.e. it satisfies the two conditions

$$\begin{aligned} &1)\ S_{11}(p) \text{ is real for P real} \\ &2)\ |S_{11}(p)| < 1 \quad \text{for } R_e\, P > 0 \end{aligned} \tag{1.120}$$

or $S_{11}(p)$ analytic in $R_e p > 0$ and

$|S_{11}(j\omega)| \leq 1$

From the unitary constraint given in equation (1.110), the relationship between the reflection coefficient and the transmission coefficient of a reciprocal lossless network can be constructed as:

$$|S_{11}(j\omega)|^2 + |S_{12}(j\omega)|^2 = 1 \qquad (1.121)$$

or in more general form as:

$$S_{11}(p)\, S_{11}(-p) + S_{12}(p)\, S_{12}(-p) = 1 \qquad (1.122)$$

Thus, if $S_{12}(p)$ is given as a bounded real function, then on $S_{11}(p)$ satisfying the condition (1.121) may be constructed as a bounded real, and from which $Z_{in}(p)$ may be determined according to equation (1.119) and consequently the element values can be obtained and the whole procedure is termed as the "synthesis problem". Usually $S_{12}(p)$ is not given, but must be selected, the problem of selecting a suitable $S_{12}(p)$ is an "approximation problem" and it will be discussed in Chapter 2.

1.10.1. Darlington's theorem: [6]

This theorem states that: "Any positive real driving point impedance function can be realized by a lossless network terminated in one ohm resistor" and quoted here as a generalization to the argument given in the last section. The proof of this theorem is a standard part of most network synthesis text e.g.[4] or of course in the original paper by Darlington [6] so, there is no need to be repeated here.

1.11 Zeros of Transmission.

The zeros of transmission are the values of the complex frequency p for which no power appears in the load.

Consider the lossless two port network N shown in Figure 1.10.

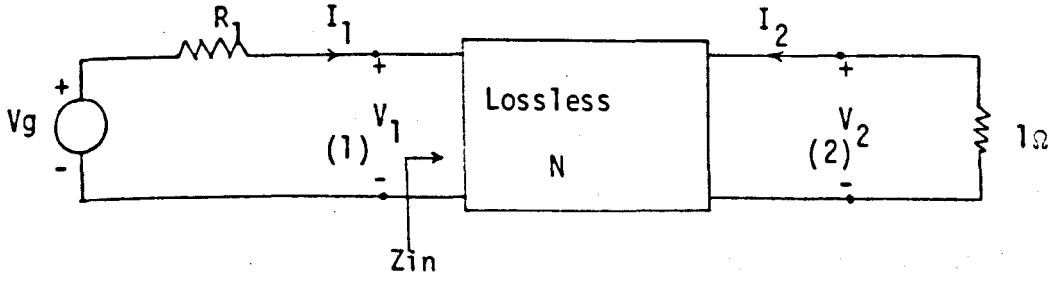

Fig. 1.10. Two- port lossless network.

driven at port 1 by a voltage generator V_g of a resistive internal impedance R_1 and terminated by 1 ohm resistance at Port 2. If z is the impedance matrix of the lossless network then from equation (1.47) the input impedance at port 1 is

$$Z_{in}(p) = z_{11} - \frac{z_{12}^2}{1+z_{22}} \tag{1.123}$$

and from (1.46) the transfer impedance is given by

$$Z_{21}(p) = Z_t(p) = \frac{V_2}{I_1} = \frac{z_{12}}{1+z_{22}} \tag{1.124}$$

Now, form the following:

$$Z_{in}(p) + Z_{in}(-p) = z_{11}(p) - \frac{z_{12}^2(p)}{1+z_{22}(p)} + z_{11}(-p) - \frac{z_{12}^2(-p)}{1+z_{22}(-p)}$$

Since N is lossless, hence $z_{11}(p)$, $z_{12}(p)$ and $z_{22}(p)$ are odd functions i.e.

$$z_{11}(-p) = -z_{11}(p)$$

$$z_{22}(-p) = -z_{22}(p)$$

$$z_{12}(-p) = -z_{12}(p)$$

Therefore

$$Z_{in}(p) + Z_{in}(-p) = \frac{-2\, z_{12}^2\,(p)}{1-z_{22}^2(p)} \tag{1.125}$$

But

$$Z_{21}(p)\; Z_{21}(-p) = \frac{-\, z_{12}^2\,(p)}{1-z_{22}^2(p)} \tag{1.126}$$

so, from (1.125) and (1.126)

$$Z_{21}(p)\; Z_{21}(-p) = \frac{1}{2}\,(Z_{in}(p) + Z_{in}(-p)) \tag{1.127}$$

This relationship is closely related to the power entering at port 1 of the lossless network and the power dissipated in the 1 ohm load and it can be shown as follows

The power dissipated in the load $P = V_2(j\omega)\, V_2(-j\omega)/1$ (1.128)

while the power entering at port 1

$$P_{in} = I_1(j\omega)\, I_1(-j\omega)\, R_e\, Z_{in}(j\omega) \tag{1.129}$$

and $P = P_{in}$ (for lossless networks)

Hence $$Z_{21}(j\omega)\, Z_{21}(-j\omega) = R_e\, Z_{in}(j\omega) \tag{1.130}$$

But the $R_e\, Z_{in}(j\omega) = \frac{1}{2}\left(Z_{in}(j\omega) + Z_{in}(-j\omega)\right)$

Then, by replacing $j\omega$ by p leads to the relationship given in (1.127). However, for a lossless network the zeros of transmission are the zeros of $Z_{21}(p)\, Z_{21}(-p)$ or the zeros of the even part of $Z_{in}(p)$. It can also be shown by using the duality that the transmission zeros are the zeros of $Y_{21}(p).\, Y_{21}(-p)$ or the zeros of the even part of $Y_{in}(p)$.

On the other hand, it can be generally considered that the zeros of transmission are the zero of $|S_{12}(j\omega)|^2$ and this definition will be adopted through this thesis for the doubly terminated networks.

$$P_\ell = \frac{1}{2} I_1(j\omega)\, I_1(-j\omega)\left(Z_{in}(j\omega) + Z_{in}(-j\omega)\right)$$

$$= \frac{1}{2}\, \frac{V_g}{R_1+Z_{in}(j\omega)}\, \frac{V_g^*}{R_1+Z_{in}(-j\omega)}\left(Z_{in}(j\omega) + Z_{in}(-j\omega)\right)$$

and

$$P_g = \frac{V_g\, V_g^*}{4\, R_1}$$

Hence

$$|S_{12}(j\omega)|^2 = \frac{P_\ell}{P_g} = \frac{2\left(Z_{in}(j\omega) + Z_{in}(-j\omega)\right)R_1}{\left(R_1+Z_{in}(j\omega)\right)\left(R_1+Z_{in}(-j\omega)\right)} \tag{1.131}$$

or after replacing $j\omega$ by p

$$S_{12}(p).S_{12}(-p) = \frac{2\left(Z_{in}(p)+Z_{in}(-p)\right)R_1}{\left(R_1+Z_{in}(p)\right)\left(R_1+Z_{in}(-p)\right)} \tag{1.132}$$

From (1.132) the transmission zeros are the zeros of the even part of $Z_{in}(p)$ and additional ones which are poles of $Z_{in}(p)$, since $Z_{in}(p)$ has all of its poles on the imaginary axis.

1.12 CONCLUDING REMARKS.

This chapter has presented a brief summary of the fundamentals of passive linear circuit theory. It has reviewed the basic definitions and relations of two port networks with special attention to lossless networks. The main reason to introduce this chapter is to serve as a background material particularly for the next chapter which deals mainly with lumped lossless prototype filters and their synthesis procedures. Little attention has been given to the proofs and the derivation details since they can be found in the standard texts on circuit theory and the appropriate references are given instead.

CHAPTER 2

APPROXIMATION AND SYNTHESIS OF PROTOTYPE FILTERS

2.1 INTRODUCTION.

It has been mentioned in chapter 1 that any lossless coupling network matching a given resistive load to a resistive generator can be synthesized to achieve a preassigned transducer power gain characteristic $|S_{12}(j\omega)|^2$ over a frequency band of interest. Such coupling network acts as a filter. The response of this filter in its simplest case "the low pass case" is necessarily an approximation to the response of a fictitious device called the "Ideal Low Pass Filter" (ILPF) shown in Fig. 2.1. However, this infinitely selective ideal response cannot be achieved with a finite number of network elements and furthermore the network is physically unrealizable because it is non-causal.

The problem of seeking a mathematical function which approximates the ideal response is called "the approximation problem". The resulting function must on one hand meet the specification of the filter and on the other hand be realizable by a practical network. The realizability requirement restricts the mathematical functions to be rational function of the variable (P) for passive lumped networks.

There are three popular rational function approximation schemes: the maximally flat (Butterworth) response, the equiripple passband (Chebyshev) response, and the elliptic (Cauer-parameter) response. The latter is equiripple in both the pass band and the stopband. Special attention will be given to the equiripple passband (Chebyshev) response, since the other two have not been used in this thesis. The corresponding network realizations are of the ladder types. These are attractive from the engineering view point in that they are unbalanced and contain no coupling coils.

In this chapter the three popular rational function approximation schemes are reviewed. At first the lowpass prototype filters are considered and the available explicit formulas for the element values of some well known ladder networks are given; This is because some of them will be used later on in this thesis in designing the individual channel filters of a multiplexer. A part of this chapter is devoted for a new class of filters satisfying a generalized Chebyshev function response and for the computerized synthesis methods. New tables of the element values are provided. Finally, the method of achieving other types of filter amplitude responses and their corresponding networks, such as, high-pass, band-pass and band-stop from the given low-pass prototype by applying the appropriate frequency transformation is given.

2.2. THE IDEAL LOW-PASS FILTER (ILPF).

The ILPF response is shown in Fig. 2.1 and if a steady state behaviour is assumed, then it can be described by

$$\left.\begin{aligned} S_{12}(j\omega) &= K(\omega)\, e^{-j\psi(\omega)} \\ \text{From which the amplitude is given by:} \\ |S_{12}(j\omega)|^2 &= |K(\omega)|^2 = A(\omega) \qquad |\omega| < \omega_c \\ &= 0 \qquad\qquad\quad |\omega| > \omega_c \\ \text{and the phase is given by:} \\ -\text{Arg}|S_{12}(j\omega)| &= -\psi(\omega) = -T_g\,\omega \end{aligned}\right\} \qquad (2.1)$$

The ILPF has the property that if a signal in time domain with a band-limited spectrum is applied at its input, it will appear at the output with no amplitude or phase distortion i.e. it is an exact replica on the input signal. The only change is a delay by a constant time displacement T_g. It is more convenient sometimes to use the normalized ILPF i.e.

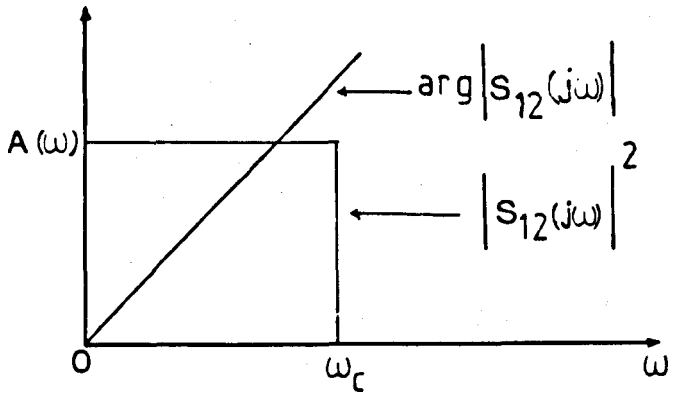

Fig. 2.1 The ideal low pass filter response

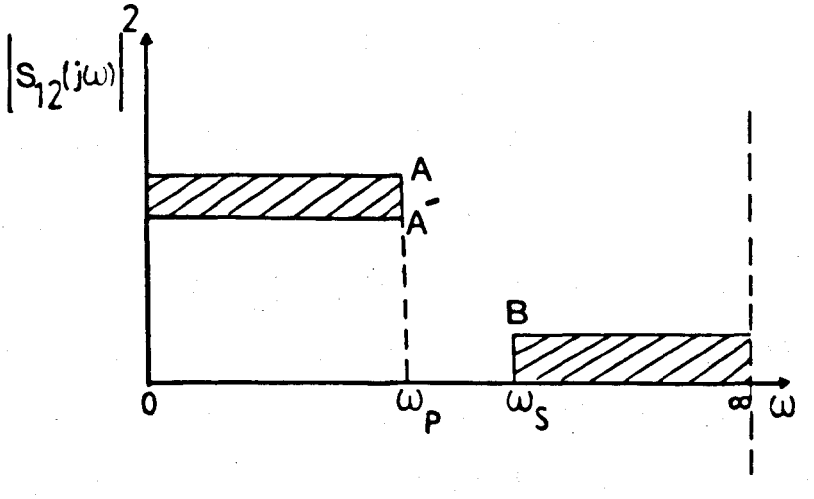

Fig. 2.2 Low pass prototype specification

$$A(\omega) = 1 \quad \text{and} \quad \omega_c = 1$$

The physically realizable filter has a response which may approximate the ILPF response either in the amplitude or phase and sometimes in both.

Filters discussed in this thesis are approximated only in the amplitude response in an optimum manner defined by one way or another as shown in the following sections.

2.3 MINIMUM PHASE TRANSFER FUNCTIONS.

As it has been defined in Chapter 1; the transfer function of a stable network is a minimum phase one if it is devoid of poles and zeros in the right half plane.

If

$$S_{12}(p) = \frac{N(p)}{D(p)} \tag{2.2}$$

is a minimum phase transfer function then:

N(p) and D(p) are Hurwitz polynomials i.e.

$$N(p) \neq 0, \quad D(p) \neq 0 \qquad \text{for Re } p > 0$$

The name "minimum phase" arises from the fact that for a given $|S_{12}(j\omega)|^2$ the phase shift of Arg $S_{12}(j\,\omega)$ is minimum over the frequency range $-\infty \leq \omega \leq \infty$. The ladder structure is an example of minimum phase networks. However, with minimum phase network there is a unique relationship between the amplitude and phase response at real frequencies which appears as a Hilbert transform pair [2].

From equation (2.2), the steady-state behaviour is given by:

$$S_{12}(j\omega) = \frac{N(j\omega)}{D(j\omega)} = e^{-\alpha(\omega)+j\psi(\omega)} \tag{2.3}$$

The amplitude response is defined by

$$A(\omega) = \left|\frac{N(j\omega)}{D(j\omega)}\right| = e^{-\alpha(\omega)} \tag{2.4}$$

which is normally bounded

So

$$\alpha(\omega) = - \ln A(\omega) \tag{2.5}$$

and the phase reponse is given by:

$$\psi(\omega) = \tan^{-1}\left\{\frac{N(j\omega) - N(-j\omega)}{j(N(j\omega)+N(-j\omega))}\right\} - \tan^{-1}\left\{\frac{D(j\omega) - D(-j\omega)}{j(D(j\omega)+D(-j\omega))}\right\} \tag{2.6}$$

The relationships between $\alpha(\omega)$ and $\psi(\omega)$ are:

$$-\psi(\omega) = \frac{\omega}{\pi}\int_{-\infty}^{\infty} \frac{\alpha(X)}{X^2-\omega^2}\, dX \tag{2.7}$$

$$\alpha(\omega) = \alpha(0) + \frac{\omega^2}{\pi}\int_{-\infty}^{\infty} \frac{\psi(X)}{X(X^2-\omega^2)}\, dX \tag{2.8}$$

where X is just a dummy variable.

2.4 THE APPROXIMATION PROBLEM (AMPLITUDE CONSTRAINTS ONLY)

A real finite lumped network is characterized by its amplitude characteristics and may be described by

$$|S_{12}(j\omega)|^2 = \frac{\sum_{i=0}^{m} a_i \omega^{2i}}{\sum_{i=0}^{n} b_i \omega^{2i}} \tag{2.9}$$

where $|S_{12}(j\omega)|^2$ is a finite continuous rational function of degree n in ω^2. This function may approximate the ILPF characteristics within a certain prescribed error to give a physically realiable low-pass response specification constrained as shown in Fig. 2.2 and given by:

$$\left.\begin{aligned} A \geq |S_{12}(j\omega)|^2 \geq A' \qquad & |\omega| < \omega_p \\ |S_{12}(j\omega)|^2 \leq B \qquad & |\omega| > \omega_s \end{aligned}\right\} \tag{2.10}$$

Now the three most popular types of response will be reviewed following closely the approach used in [7]. It is believed that the Chebyshev response is essential in this thesis while the other two (maximally flat and elliptic function) are briefly reviewed for the sake of comparison.

2.4.1. The Maximally Flat Response.

Butterworth polynomials can be used to approximate the function in Fig. 2.2. If $\omega_p \to 0$ and $A' \to A$, then a maximally flat solution about the origin is approached. This zero bandwidth approximation is termed "maximally flat" response in the passband because it results in the maximum number of derivatives of $|S_{12}(j\omega)|^2$ being made equal to zero at $\omega = 0$. Similarly if $\omega_s \to \infty$ and $B \to 0$, then the response can be made maximally flat by equating the maximum number of derivative of $|S_{12}(j\omega)|^2$ at $\omega = \infty$ to zero. The maximally flat amplitude response of $S_{12}(p)$ of degree n is sketched in Fig. 2.3 with the bandedge frequency ω_p being normalized to unity Let

$$|S_{12}(j\omega)|^2 = A\left(\frac{1+a_1\omega^2+a_2\omega^4+ \ldots + a_{n-1}\omega^{2n-2}}{1+b_1\omega^2+b_2\omega^4+ \ldots + b_{n-1}\omega^{2n-2}+b_n\omega^{2n}}\right) \tag{2.11}$$

where $b_n > 0$

This satisfies the conditions

$$|S_{12}(0)|^2 = A \tag{2.12}$$

and

$$|S_{12}(\infty)|^2 = 0 \tag{2.13}$$

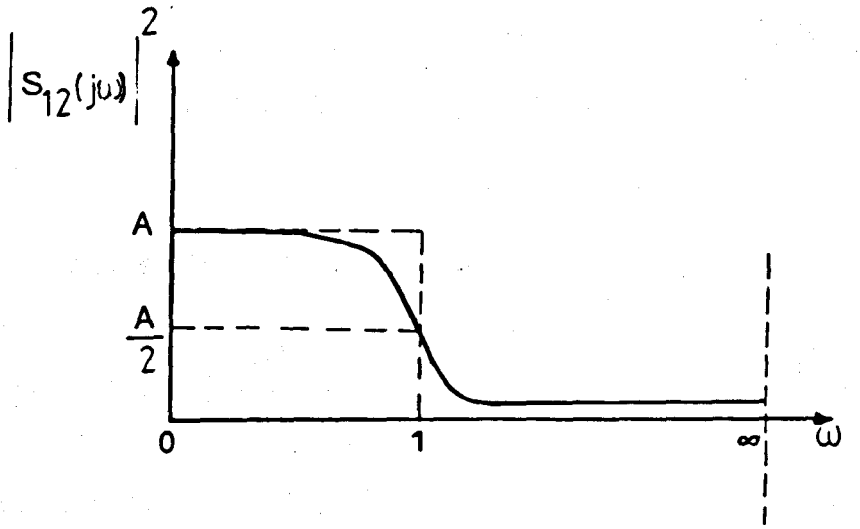

Fig. 2.3 The normalized maximally flat response

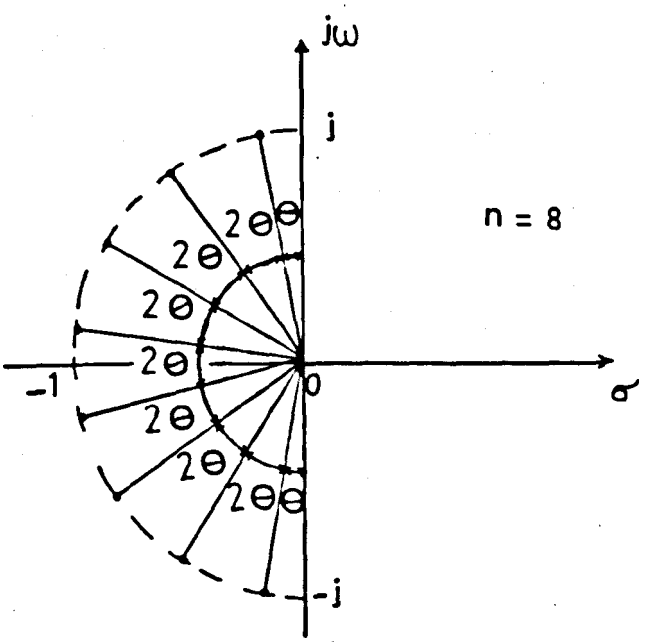

Fig. 2.4 Pole distribution for the maximally flat response

Since equation (2.11) is of degree 2n in ω, hence the maximum number of derivatives, with respect to ω that may be equated to zero is (2n-1) at both $\omega = 0$ and $\omega = \infty$

a) The maximally flat condition at $\omega = 0$:

From equation (2.11)

$$|S_{12}(j\omega)|^2 - A = A \left\{ \frac{(a_1-b_1)\omega^2+(a_2-b_2)\omega^4+ \ldots. +(a_{n-1}-b_{n-1})\omega^{2n-2}-b_n\omega^{2n}}{1+b_1\omega^2+b_2\omega^4+ \ldots. + b_{n-1}\omega^{2n-2} + b_n\omega^{2n}} \right\} \quad (2.14)$$

Since it is required that (2.14) and its first (2n-1) derivatives be zero at $\omega=0$, then the power series expansion about $\omega=0$ must be of the form

$$|S_{12}(j\omega)|^2 - A = C_n\omega^{2n} + C_{n+1}\omega^{2n+2} + \ldots. \quad (2.15)$$

which implies

$$a_i = b_i \quad \text{for } i = 1,2, \ldots (n-1) \quad (2.16)$$

b) The maximally flat condition at $\omega = \infty$:

The maximally flat condition at $\omega=\infty$ can be applied if the numerator and the denominator of (2.11) are divided by ω^{2n} to give

$$|S_{12}(j\omega)|^2 = A \left(\frac{a_{n-1}\omega^{-2}+ a_{n-2}\omega^{-4} + \ldots. a_1\omega^{-2n+2}+\omega^{-2n}}{b_n+b_{n-1}\omega^{-2}+ \ldots. + b_1\omega^{-2n+2}+\omega^{-2n}} \right) \quad (2.17)$$

The power series expansion of (2.17) about $\omega=\infty$ takes the form

$$|S_{12}(j\omega)|^2 = d_n\omega^{-2n} + d_{n+1}\omega^{-2n-2} + \ldots. \quad (2.18)$$

which gives

$$a_i = 0 \quad \text{for} \quad i = 1, 2, \ldots. n-1 \quad (2.19)$$

Hence, from (2.16)

$$b_i = 0 \quad \text{for} \quad i = 1, 2, \ldots. n-1 \quad (2.20)$$

consequently (2.11) becomes

$$|S_{12}(j\omega)|^2 = \frac{A}{1 + b_n\omega^{2n}}$$

b_n is usually set equal to unity without changing the prescribed maximally flat behaviour, so that

$$|S_{12}(j\omega)|^2 = \frac{A}{1+\omega^{2n}} \tag{2.21}$$

Then the half power or 3dB point is always at $\omega = 1$ regardless of the degree of the transfer function. $S_{12}(p)$ can be constructed from (2.21) by replacing ω^2 by $(-p^2)$, hence

$$S_{12}(p)\, S_{12}(-p) = \frac{A}{1+(-p^2)^n} \tag{2.22}$$

The poles of $S_{12}(p)$, $S_{12}(-p)$ occur when

$$(-p^2)^n = -1$$

$$= e^{j(2r-1)\pi} \qquad r = 1 \to 2n$$

or
$$p_r = j\, e^{j\,\theta_r}$$
$$= -\sin\theta_r + j\cos\theta_r \tag{2.23}$$

where $\theta_r = \frac{(2r-1)\pi}{2n}$

and

p_r is a typical pole

To construct $S_{12}(p)$ as a bounded real function, the left half plane poles must be chosen, i.e. for $r = 1 \to n$

$$S_{12}(p) = \frac{A^{\frac{1}{2}}}{\prod_{r=1}^{n} \pi\,(p - jp^{j\,\theta_r})} \tag{2.24}$$

All the zeros of $S_{12}(p)$ are at infinity, while the poles are distributed on a unit-semicircle in the left half plane at equal angular spacing as shown in Fig. 2.4.

It is usually convenient to set $A = 1$, then equation (2.21) becomes

$$|S_{12}(j\omega)|^2 = \frac{1}{1+\omega^{2n}} \tag{2.25}$$

Thus

$$|S_{11}(j\omega)|^2 = 1 - |S_{12}(j\omega)|^2 = \frac{\omega^{2n}}{1+\omega^{2n}}$$

and

$$S_{11}(p)\, S_{11}(-p) = \frac{(-p^2)^n}{1+(-p^2)^n} \tag{2.26}$$

Hence, $S_{11}(p)$ can be constructed as a bounded real function with all its zeros at the origin and its poles lie in the left half plane as given by (2.24). Therefore

$$S_{11}(p) = \frac{\pm\, p^n}{\prod_{r=1}^{n} (p - j\, e^{j\theta_r})} \tag{2.27}$$

Then, $Z_{in}(p)$ can be formed and synthesized to yield the low-pass prototype element values.

2.4.2. The Equiripple Response.

It has been pointed out in the last sub-section that the maximally flat approximation is a zero bandwidth approximation. This is because it is of the Maclaurian's expansion type which gives an accurate solution at a single point, and in the low-pass filter case that point is the origin ($\omega=0$). However, if an approximation is required to be accurate over a certain frequency range, then the equiripple solution is the most appropriate.

Consider the amplitude response of a finite lumped network of degree n and

$$F_n^2(\omega^2) = |S_{12}(j\omega)|^2 \tag{2.28}$$

as a rational function of degree n in ω^2 required to be within the shaded area of Fig. 2.2 for $0 \leq \omega \leq \omega_p$ and $\omega \geq \omega_s$. For simplicity ω_p is normalized

to unity. Since $F_n(\omega^2)$ must be a rational function, then the derivative $d\,F_n(\omega^2)/d\omega$ is zero at the origin and infinity and may be zero up to $2(n-1)$ times in the interval $0 < \omega < \infty$. If these zeros occur only when $F_n(\omega^2)$ attains the limits of the specification, i.e. A, A', B and zero, then it is an equiripple solution as sketched in Fig. 2.5 for $n = 5$. The number of ripples in each band is the same since $F_n(\omega^2)$ and its derivative cannot simultaneously be zero more that n/2, for n even, or (n-1)/2, for n odd, times in the interval $o < \omega < \infty$.

The equipripple solution has another important property away from being a finite bandwidth approximation, that it is the minimum degree solution to the problem of minimizing the maximum deviation of a rational function in each band of the two band specifications described in Fig. 2.2, so it is often called a "mini-max" approximation. This can be shown fairly easily by considering another function $F_m'(\omega^2)$ of degree m in ω^2 as a solution to the approximation problem to meet the specification given in Fig. 2.2. A typical $F_m'(\omega^2)$ is represented by the dashed line in Fig. 2.5. Thus the error function

$$e(\omega^2) = F_n(\omega^2) - F_m'(\omega^2) \qquad (2.29)$$

must be zero at least n times in the interval $o \leq \omega \leq 1$, n times in the interval $\omega_s \geq \omega \geq \infty$ and once in the interval $1 \geq \omega \geq \omega_s$. Thus the total number of times with $e(\omega^2)$ being zero is at least $(2n+1)$. Hence from (2.29) either $m > n$ or $e(\omega^2)$ is equal to zero. Therefore the equiripple solution is a minimum degree (optimum) solution with irriduceable error (mini-max).

The response which is equiripple in both the pass band and the stopband is called "the elliptic function response" and the response which has an equiripple passband and maximally flat stopband is called

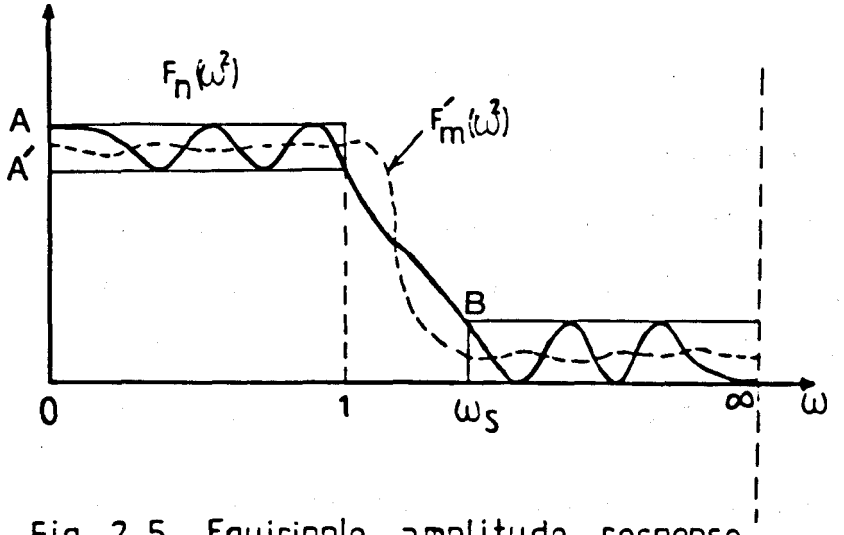

Fig. 2.5 Equiripple amplitude response (n = 5)

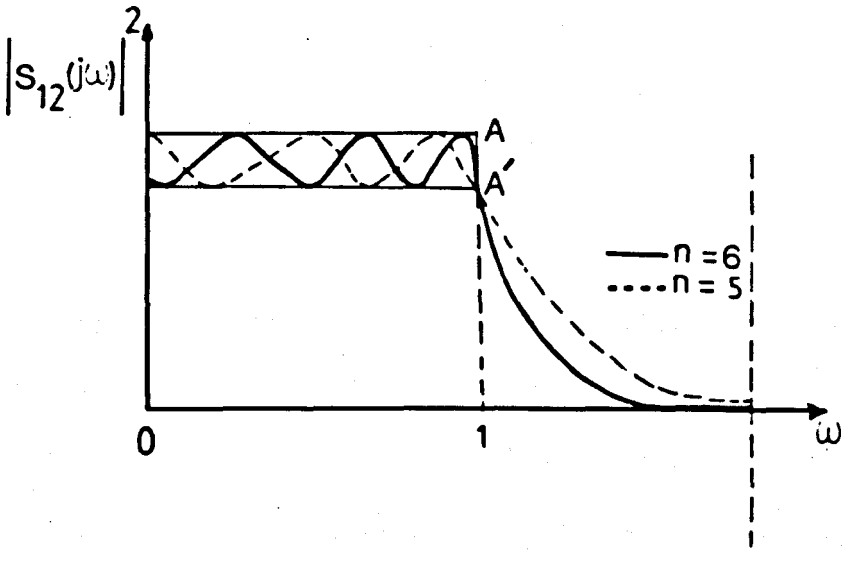

Fig. 2.6 Conventionl Chebyshev response

"the Chebyshev response" and this response will be discussed first.

2.4.3. The Chebyshev Response.

This case may be obtained as $\omega_s \to \infty$, B = o and the first (2n-1) derivatives must be set to zero at ∞ to give a maximally flat stopband while the equiripple solution in the interval $o \leq \omega \leq 1$ i.e. the passband, is still the optimum solution to the problem of a polynomial in ω^2, constrained to lie in the rectangular area between A and A'.

The terminology "conventional Chebyshev response" will be used here to differentiate this response from other equiripple passband and maximally flat stopband response which satisfies a generalized Chebyshev rational function and will be discussed later in this chapter. The conventional Chebyshev response is sketched in Fig. 2.6 and may be expressed as

$$|S_{12}(j\omega)|^2 = \frac{A}{1+\varepsilon^2 T_n^2(\omega)} \qquad (2.30)$$

where

$$A' = \frac{A}{(1+\varepsilon^2)} \qquad (2.31)$$

and $T_n^2(\omega)$ is an even polynomial in ω which attains the maximum value of unity at the maximum number of points in the interval $|\omega| \leq 1$.
$T_n(\omega)$ is a Chebyshev polynomial which has the following properties:

(a) $T_n(\omega)$ is either an even or an odd polynomial depending upon whether n is even or odd. More specifically one can write

$$T_n(-\omega) = T_n(\omega) \qquad \text{for n even}$$

$$T_n(-\omega) = -T_n(\omega) \qquad \text{for n odd}$$

(b) Every coefficient of $T_n(\omega)$ is an integer, the one associated with ω^n being 2^{n-1}. Thus, in the limit as ω approaches to infinity,

$$T_n(\omega) \to 2^{n-1}\,\omega^n \tag{2.32}$$

(c) In the interval $-1 \leq \omega \leq 1$, all the Chebyshev polynomials have the equiripple property. Varying between a maximum of 1 and a minimum of -1. Outside this interval their magnitude increases monotonically as ω increases, and approaches to infinity in accordance with (2.32). Sketches of the polynomials for n=5 and n=6 are shown in Fig. 2.7 .

(d) As indicated in Fig. 2.7 the polynomials possess special values at $\omega = 0, 1$ or -1:

$$\begin{aligned} T_n(0) &= (-1)^{n/2} && n \text{ even} \\ &= 0 && n \text{ odd} \end{aligned} \tag{2.33}$$

$$\begin{aligned} T_n(\pm 1) &= 1 && n \text{ even} \\ &= \pm 1 && n \text{ odd} \end{aligned} \tag{2.34}$$

However, $T_n(\omega)$ is uniquely defined by its required behaviour. Properties (c) amd (d) give

$$\left.\frac{d\,T_n(\omega)}{d\,\omega}\right|_{|T_n(\omega)| \equiv 1} = 0 \qquad \text{except for } |\omega| = 1 \tag{2.35}$$

Hence a differential equation can be constructed as follows:

$$\frac{d\,T_n(\omega)}{d\omega} = C\,\frac{\sqrt{1-T_n^2(\omega)}}{\sqrt{1-\omega^2}} \tag{2.36}$$

where C is a constant and the right hand side must be of degree (n-1), since $1-T_n^2(\omega)$ contains zeros of multiplicity 2 in the interval $|\omega|<1$ and simple zeros at $\omega = \pm 1$, then the factor $\sqrt{1-\omega^2}$ is cancelled.

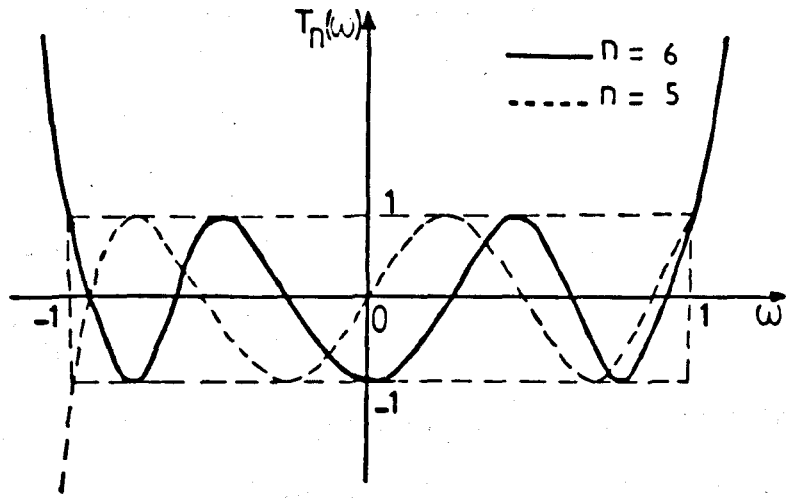

Fig. 2.7 $T_n(\omega)$ plotted as a function of ω

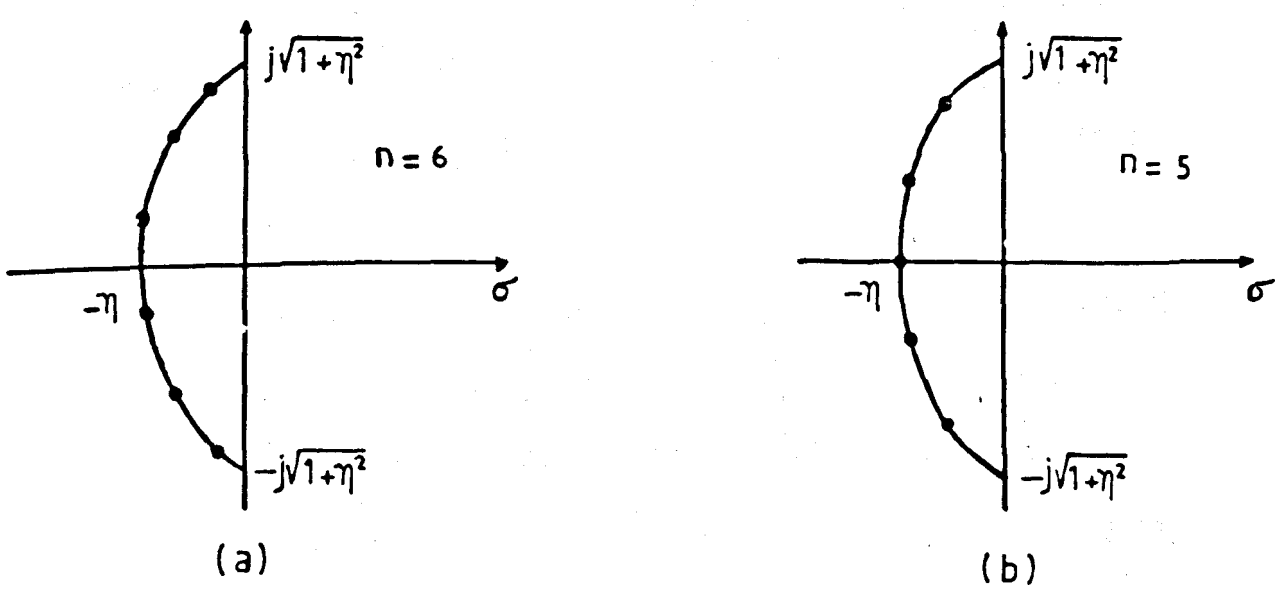

Fig. 2.8 Pole distribution for Chebyshev response

(a) n = 6

(b) n = 5

Separating the variables of equation (2.36) gives

$$\frac{d\,T_n(\omega)}{\sqrt{1-T_n^2(\omega)}} = C\,\frac{d\omega}{\sqrt{1-\omega^2}} \tag{2.37}$$

and the integration results in

$$\cos^{-1} T_n(\omega) = C\cos^{-1}\omega + K \tag{2.38}$$

where K is the constant of integration. This must be zero from property (a). Furthermore, for $T_n(\omega)$ to be an nth-degree polynomial, it must have zeros at n distinct values of ω, this condition leads to the conclusion that C = n and (2.38) may be written as

$$\begin{aligned} T_n(\omega) &= \cos(n\cos^{-1}\omega) \\ &= \cosh(n\cosh^{-1}\omega) \end{aligned} \tag{2.39}$$

and the zeros of the polynomial are given by

$$\omega_r = \cos[(2r-1)\pi/2n] \qquad r=1\rightarrow n \tag{2.40}$$

However, the Chebyshev polynomial $T_n(\omega)$ can be constructed for any degree n from the following recurrence formula

$$T_{n+1}(\omega) = 2\omega T_n(\omega) - T_{n-1}(\omega) \tag{2.41}$$

with the initial conditions

$$T_0(\omega) = 1, \qquad T_1(\omega) = \omega \tag{2.42}$$

Now, it is required to construct $S_{12}(p)$ from (2.30) for the low-pass case where all the zeros are at $\omega=\infty$ and the poles occur when

$$\varepsilon^2 T_n^2(\omega) = -1 \tag{2.43}$$

To simplify the calculations define a positive auxiliary parameter η as

$$\eta = \sinh\left(\frac{1}{n}\sinh^{-1}\frac{1}{\varepsilon}\right) \tag{2.44}$$

Then

$$T_n^2(\omega) = -1/\varepsilon^2 = -\sinh^2(n \sinh^{-1} \eta)$$

$$= \sin^2(n \sin^{-1} j\eta) \qquad (2.45)$$

Hence

$$n\cos^{-1}\omega = n \sin^{-1} j\eta + \frac{(2r-1)\pi}{2} \qquad (2.46)$$

replacing ω by P/j and rearranging gives

$$P = -j \cos\{\sin^{-1} j\eta + \frac{(2r-1)\pi}{2n}\} \qquad \text{for } r = 1 \to 2n \qquad (2.47)$$

A typical pole P_r is given by

$$P_r = \sigma_r + j\omega_r = j \cos\{\sin^{-1} j\eta + \frac{(2r-1)\pi}{2n}\}$$

$$= \eta \sin\theta_r + j\sqrt{1+\eta^2}\cos\theta_r \qquad (2.48)$$

where

$$\theta_r = \frac{(2r-1)\pi}{2n}$$

Hence

$$\frac{\sigma_r^2}{\eta^2} + \frac{\omega_r^2}{1+\eta^2} = 1 \qquad (2.49)$$

This is the equation of an ellipse whose major semi-axis is $\sqrt{1+\eta^2}$ and whose minor semi-axis is η. This ellipse is the locus of the pole distribution in the complex plane as shown in Fig. 2.8 for degree 5 and 6.

To construct $S_{12}(p)$ as a bounded real function the left half plane poles must be chosen i.e. $r = 1 \to n$ and all the zeros are at $P = \infty$. Furthermore from equation (2.30) and from property (d) of the Chebyshev polynomials. The following equations can be written;

$$S_{12}(0) = A^{\frac{1}{2}} \quad \text{for n odd} \qquad (2.50)$$

and:

$$S_{1=}(0) = \frac{A^{\frac{1}{2}}}{\sqrt{1+\varepsilon^2}} \text{ for n even} \qquad (2.51)$$

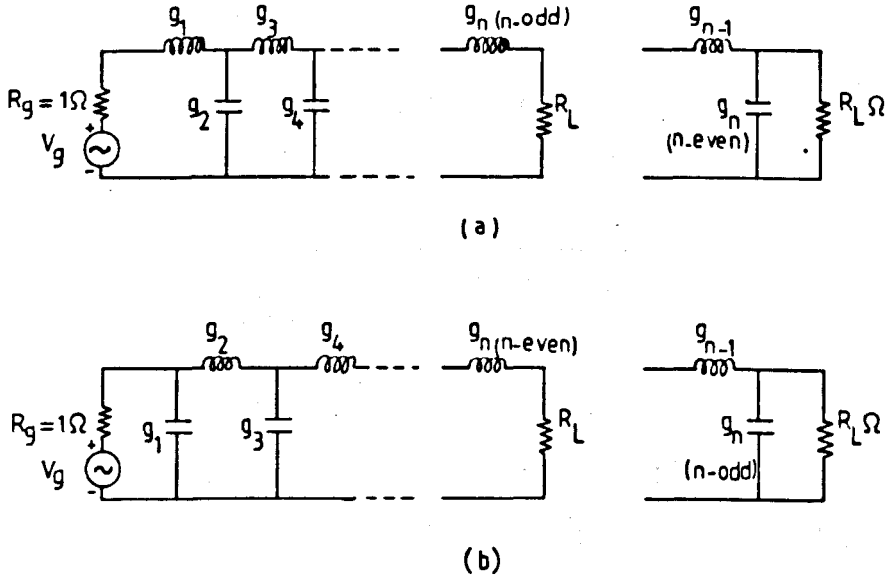

Fig. 2.9 Prototype ladder networks satisfying either a maximally flat or conventional Chebyshev response

Using these conditions a general formula for $S_{12}(p)$ of degree n even or odd has been derived in |7| and given as

$$S_{12}(p) = \frac{A^{\frac{1}{2}} \prod_{r=1}^{n} \{\eta^2 + \sin^2(r\pi/n)\}^{\frac{1}{2}}}{\prod_{r=1}^{n} \{p + j\cos(\sin^{-1} j + (2r-1)\pi/2n)\}} \qquad (2.52)$$

If this equation is rewritten as

$$S_{12}(p) = \frac{A^{\frac{1}{2}} \prod_{r=1}^{n} \{\eta^2 + \sin^2(r\pi/n)\}^{\frac{1}{2}}}{\prod_{r=1}^{n} \{p + j\sqrt{1+\eta^2}\cos((2r-1)\pi/2n) + \eta\sin((2r-1)\pi/2n)\}} \qquad (2.53)$$

and if P is replaced by ηp and letting $\eta \to \infty$ (2.54)

Then equation (2.53) becomes

$$S_{12}(p) = \frac{A^{\frac{1}{2}}}{\prod_{r=1}^{n} \{P - j\, e^{j(2r-1)\pi/2n}\}} \qquad (2.55)$$

which is the maximally flat transfer function. Therefore it can be stated that the maximally flat is the limiting case of the Chebyshev case and can be always recovered by using the conditions in (2.54).

Since all the transmission zeros of the maximally flat and the conventional Chebyshev low pass response lie at infinity, therefore the filters can be realized as ladder networks of the general forms shown in Fig. 2.9. Such networks, which can form the bases for many types of filters are known as "low-pass prototype networks". Extensive tables for their element values can be found in many hand books on filter design e.g. [8], [9], also explicit formulas for the element values are available for these filters and will be discussed later in this chapter.

2.4.4. The Elliptic Function Response [7].

The elliptic function response is an equiripple response in both the passband and the stopband and may be expressed for a low-pass case as

$$|S_{12}(j\omega)|^2 = \frac{A}{1 + \varepsilon^2 F_n^2(\omega)} \qquad (2.56)$$

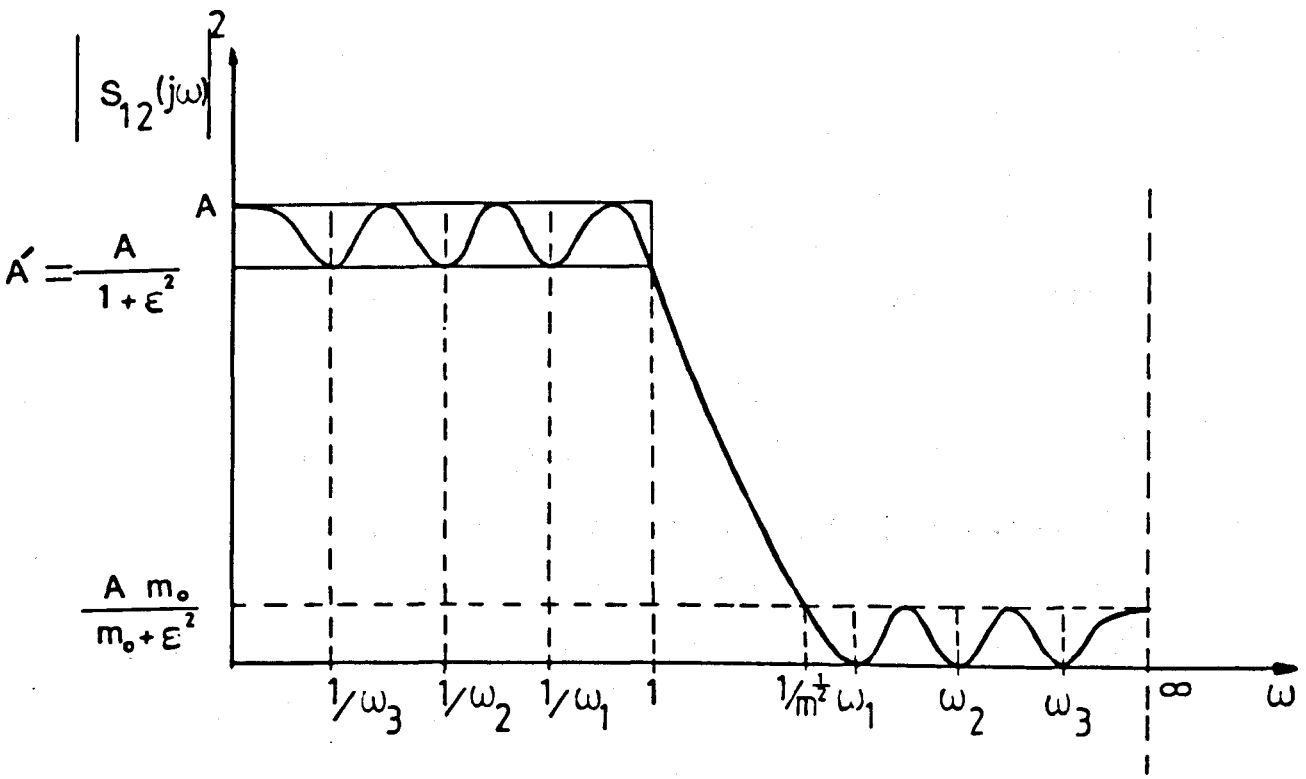

Fig. 2.10 Elliptic function response

and sketched for n=6 in Fig. 2.10 where $F_n(\omega)$ is a Jacobian elliptic rational function of degree n in ω, which oscillate the maximum number of times between ± 1 for $|\omega| \leq 1$ and $|F_n(\omega)| \geq 1/m_o^{\frac{1}{2}}$ for $|\omega| \geq 1/m^{\frac{1}{2}}$ and the turning points are the maximum or the minimum points of $F_n(\omega)$ i.e.

$$\left.\begin{aligned} &\frac{dF_n(\omega)}{d\omega}\Big|_{|F_n(\omega)|=1} = 0 \qquad \text{except when } |\omega|=1 \\ &\text{and} \\ &\frac{d\,F_n(\omega)}{d\,\omega}\Big|_{|F_n(\omega)|=1/m_o^{\frac{1}{2}}} = 0 \quad \text{except when } |\omega| = \frac{1}{m^{\frac{1}{2}}} \end{aligned}\right\} \tag{2.57}$$

Hence, $F_n(\omega)$ can be defined by the following differential equation

$$\frac{d\,F_n(\omega)}{d\,\omega} = \frac{C_n\sqrt{(1-F_n^{\,2}(\omega)(1-m_oF_n^{\,2}(\omega))}}{\sqrt{(1-\omega^2)(1-m\omega^2)}} \tag{2.58}$$

whose right hand side being of the correct degree (n-1), since $(1-F_n^{\,2}\omega\,))$ and $(1-m_oF_n^{\,2}(\omega))$ contain zeros of multiplicity 2 except at $|\omega| = 1$ and $1/m^{\frac{1}{2}}$ and this leads to the cancellation of the factors $\sqrt{1-\omega^2}$ and $\sqrt{1-m\omega^2}$.

Separating the variables of (2.58) results in:

$$\frac{d\,F_n(\omega)}{\sqrt{(1-F_n^{\,2}(\omega))(1-m_oF_n^{\,2}(\omega))}} = \frac{C_n\,d\omega}{\sqrt{(1-\omega^2)(1-m\omega^2)}} \tag{2.59}$$

and integrating gives

$$c\,d_o^{-1}\,F_n(\omega) = C_n\,Cd^{-1}\,\omega = u \tag{2.60}$$

with the constant integration being zero since $F_n(\omega)$ is an even or odd function and the mathematical symbols are the same as in reference [7] which also gives the details of the derivations yielding

$$F_n(\omega) = \frac{B\prod_{r=1}^{n}\{\omega-cd[(2r-1)K/n]\}}{\prod_{r=1}^{n}\{1-\omega m\,cd[(2r-1)K/2]\}} \tag{2.61}$$

where $C_n = \frac{nK_o}{K}$ and the conditional requirement:

$\frac{K_o}{K_o'} = \frac{K}{nK'}$ which relates the elliptic parameters m_o and m

B is a constant whose value is obtained from the fact $F_n(1) = 1$, hence

$$B = \prod_{r=1}^{n} \left\{ \frac{1-m\ cd[(2r-1)\ K/n]}{1-cd[(2r-1)\ K/n]} \right\} \qquad (2.62)$$

Inspection of $F_n(\omega)$ in equation (2.61) shows that its poles are the reciprocals of its zeros. Because of this reciprocal relationship between the zeros and poles, it can be concluded that

$$F_n\left(\frac{1}{\omega}\right) = \frac{1}{F_n(\omega)} \qquad (2.63)$$

Hence, the function $F_n(\omega)$ has the important property that its value at any frequency ω_o in the interval $0 \leq \omega < 1$ is the reciprocal of its value at the reciprocal frequency $1/\omega_o$ in the interval $1 < \omega \leq \infty$. Furthermore, the zeros of $F_n(\omega)$ lie within the passband while all the poles of $F_n(\omega)$ lie in the stopband.

Now, with $F_n(\omega)$ having these properties, equation (2.56) gives $|S_{12}(j\omega)|^2$ as a bounded function satisfying an elliptic function response with transmission zeros at finite points on the $j\omega$-axis and at infinity. Because $S_{12}(p)$ possesses zeros on finite real frequency axis, a ladder network realization as shown in Fig. 2.9 is not possible. However, a partial pole extracting technique can be used in the computation of the element values resulting in a network realization shown in Fig. 2.11. This realization has been used by Saal [10] and the realizability conditions given in [11] and [12] must be observed in order to avoid the appearance of negative element values whenever possible. Tables for the element values of these prototype networks can be found in e.g. [9] and [10]. On the other hand Rhodes [7] used the property of $F_n(\omega)$ given in equation (2.63) to derive the transfer function of a high-pass prototype described by:

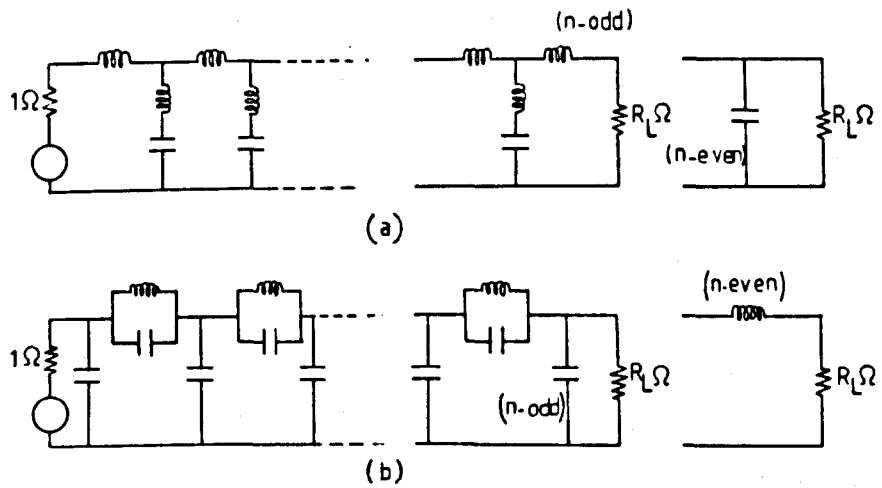

Fig. 2.11 Low-pass prototypes satisfying an elliptic function response

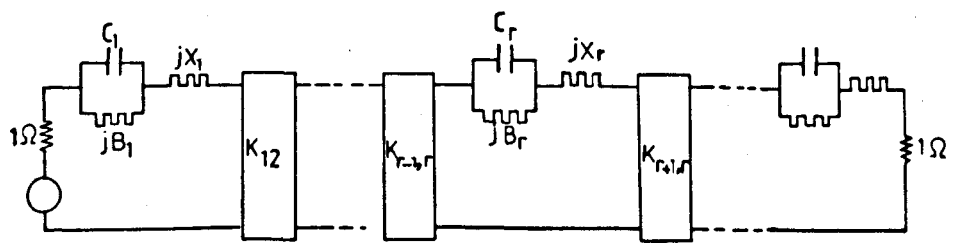

Fig. 2.12 The natural prototype network satisfying a high pass elliptic function response

$$S_{12}(p) = A^{\frac{1}{2}} \prod_{r=1}^{n} \left\{ \frac{[1+m\,\eta^2 Sn^2(2rK/n)]^{\frac{1}{2}}[P+jcd((2r-1)K/n)]}{[1+m\,\eta^2 cd^2((2r-1)K/n)]^{\frac{1}{2}}[P+jcd(Sn^{-1}j\eta+(2r-1)K/n)]} \right\} \quad (2.64)$$

where η is an auxiliary parameter defined by

$$j\eta = Sn\left(\frac{K}{nK_o}\, Sn_o^{-1}\, \frac{j}{\varepsilon}\right) \quad (2.65)$$

Then he derived the explicit formulas for the element values of a ladder type network shown in Fig. 2.12 satisfying a high-pass elliptic function response and called it the "natural prototype" [13]. This prototype incorporates the concept of impedance inverter and frequency invariant reactance. The latter is an imaginary element originally introduced by Baum [14] and widely used afterwards. Both the inverter and the frequency invariant reactance will be discussed further later on in this thesis. However, the main application of the natural prototype is in the design of narrow bandwidth band-pass or band-stop filters.

2.5 THE EXPLICIT DESIGN FORMULAS.

The lumped element low-pass prototype filters are important types of networks, since they are used in designing many other classes of filters such as low-pass, high-pass, band-pass and band-stop microwave filters. Element values of the low-pass prototypes can be generally obtained by network synthesis methods, for example, Darlington's method [6]. However, there exist concise equations known as "the explicit formulas" which enable the designer to calculate the element values directly without the need to go through any synthesis procedure.

In this section a review is given for the explicit design formulas of the prototype which will be used or referred to in the following chapters of this thesis. The development of explicit design formulas started with Norton's discovery [15] of formulas for Ladder networks, then Bennett [16] extended Norton's work by giving the explicit formulas for

the element values of Ladder networks exhibiting a maximally flat response and terminated in equal resistances at both ends similar to those shown in Fig. (2.9). These formulas are given in [16] and stated as:

$$\left.\begin{aligned} R_g &= 1 \ \Omega \\ g_r &= 2 \sin\left[\frac{(2r-1)\pi}{2n}\right] \qquad r = 1 \rightarrow n \\ R_L &= 1 \ \Omega \end{aligned}\right\} \tag{2.66}$$

After that, there were several contributions among them was that by Belevitch [17] who derived the formulas for matched ladder networks satisfying a conventional Chebyshev passband response. If the prototypes shown in Fig. 2.9 satisfy a conventional Chebyshev response then the elements values are calculated using the following formulas [17].

$$\begin{aligned} R_g &= 1 \ \Omega \\ g_1 &= \frac{2\sin(\pi/2n)}{\sinh\left[(1/n)\sinh^{-1}(1/\epsilon)\right]} \\ g_r g_{r+1} &= \frac{4\sin\{(2r-1)\pi/2n\}\sin\{(2r+1)\pi/2n\}}{\sinh^2\left[(1/n)\sinh^{-1}(1/\epsilon)\right]+\sin^2(r\pi/n)} \\ & \qquad\qquad r = 1 \rightarrow (n-1) \end{aligned} \tag{2.67}$$

The value of the load resistance R_L depends on the value of n. In equation (2.50), assuming the normalized gain case, i.e. A = 1, results in:

$S_{12}(0) = 1$, therefore $R_L = 1\Omega$ for n is odd. For n is even, using equation (2.51) and assuming A = 1 gives:

$$S_{12}(0) = \frac{1}{\sqrt{1+\epsilon^2}}$$

i.e.

$$|S_{12}(0)|^2 = \frac{1}{1+\epsilon^2} = \frac{4\,R_L}{(R_L+1)^2}$$

Hence

$$R_L = \left[\varepsilon + \sqrt{1+\varepsilon^2}\right]^2 \qquad (2.68)$$

Most of the attempts to find the explicit formulas did not give proofs and no proof was known for the general case of arbitrary resistive termination before Takahasi's work [18], [19] became known. Takahasi gave a proof that yields the formulas as a final result. His approach depends on a number of properties of the Chebyshev and related polynomials in two or three variables. Rhodes [7] followed a different approach to derive the explicit formulas for the element values of the "modified low pass prototypes" with arbitrary gain A i.e. For any ratio of resistance terminations and exhibiting either a maximally flat or conventional Chebyshev response. His formulas for the matched case (A=1, R_g = 1 and R_L = 1) of the modified low pass prototypes shown in Fig. 2.12 and satisfy a conventional Chebyshev response are used in this thesis whenever required.

2.5.1. The Modified Low-Pass Prototype Ladder Network.

The modified low-pass prototype ladder network is shown in Fig. 2.13. It consists of either series inductors separated by ideal impedance inverters or shunt capacitors separated by ideal admittance inverters. It has the property of being always terminated by 1Ω load resistance for A=1, regardless of even or odd values of n. This is because of the impedance (admittance) scaling due to the presence of the inverters which makes the network symmetrical. The original low pass prototype shown in Fig. 2.9 in case of conventional Chebyshev response is symmetrical and terminated by 1Ω load resistance only when n is odd. On the other hand, it is antimetric when n is even and the load resistance has the value given by (2.68).

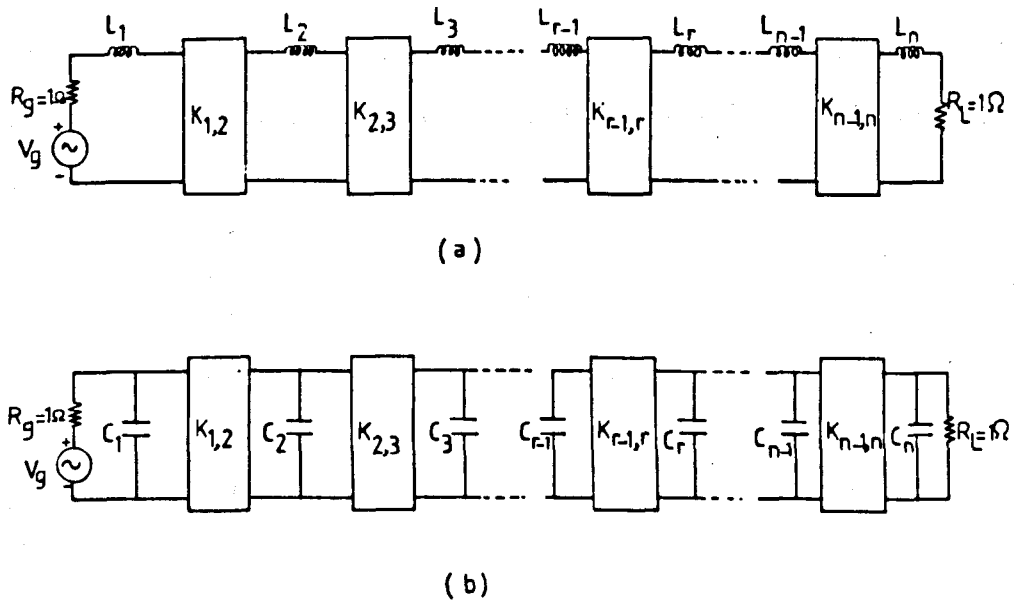

Fig. 2.13 The modified doubly terminated low-pass prototype ladder networks.
(a) and (b) are duals

The ideal impedance inverter is a two port network operates like a quarter wavelength line of characteristic impedance K at all frequencies. It is defined by the following transfer matrix.

$$\begin{bmatrix} 0 & jK \\ j/K & 0 \end{bmatrix} \tag{2.69}$$

However, if an impednace inverter is terminated in an impedance Z_2 at one end as shown in Fig. 2.14.a, the impedance Z_1 seen looking in at the other end is

$$Z_1 = \frac{K^2}{Z_2} \tag{2.70}$$

The ideal admittance inverter of characteristic admittance J is shown in Fig. 2.14b. It is considered to be the dual of the ideal impedance inverter if J = 1/K and

$$Y_1 = \frac{J^2}{Y_2} \tag{2.71}$$

Because of the inverting action indicated by (2.70) and (2.71), a series inductor between two impedance inverters looks like a shunt capacitor from its exterior terminals. Likewise, a shunt capacitor between two admittance inverters looks like a series inductor from its exterior terminals. Making use of this property, the prototype networks shown in Fig. 2.9 can be converted to either of the equivalent forms in Fig. 2.13 preserving the same transmission response and allowing internal impedance (admittance) scaling within the networks. Thus, the modified low pass prototype is obtained.

2.5.2. Explicit Formulas For Element Values in Conventional Chebyshev Filters [7]

The explicit design formulas for element values of the modified

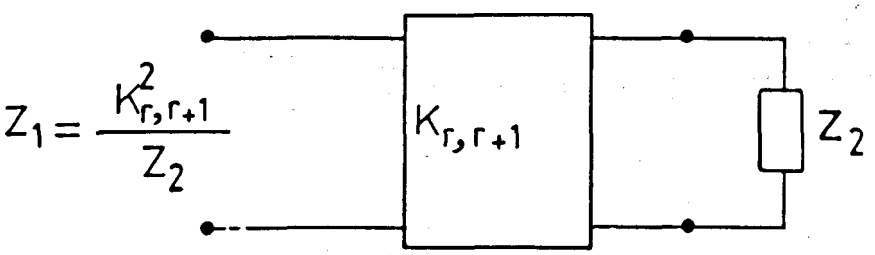

(a)

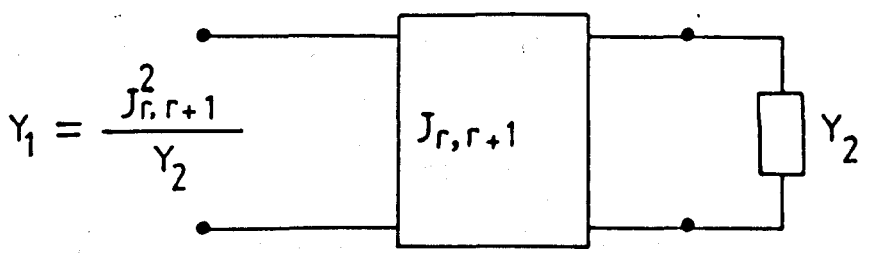

(b)

Fig. 2.14 (a) Definition of an ideal impedance inverter

(b) Definition of an ideal admittance inverter

low-pass prototypes shown in Fig. 2.13, satisfying a conventional Chebyshev response and terminated at both ends in 1 ohm resistance i.e. the matched case of A equal to unity, may be derived as follows:

Rewriting equation (2.52) with A=1 as

$$S_{12}(p) = \frac{\prod_{r=1}^{n} [n^2+\sin^2(r\pi/n)]^{\frac{1}{2}}}{\prod_{r=1}^{n} \{P+ j \cos[\sin^{-1}(jn)+(2r-1)\pi/2n]\}} \tag{2.72}$$

and since

$$S_{11}(p)\, S_{11}(-p) = 1 - S_{12}(p)S_{12}(-p) \tag{2.73}$$

Then

$$S_{11}(p) = \frac{\prod_{r=1}^{n} [p+j\cos((2r-1)\pi/2n)]}{\prod_{r=1}^{n} \{p+j\cos[\sin^{-1}jn+(2r-1)\pi/2n]\}} \tag{2.74}$$

To obtain the network in Fig. 2.13a, the positive sign of $S_{11}(p)$ must be chosen to form the input impedance as

$$Z_n(p) = \frac{1 + S_{11}(p)}{1 - S_{11}(p)} \tag{2.75}$$

which can be described by a continued fraction expansion;

$$Z_n(p) = L_1p + \cfrac{K_{1,2}^2}{L_2P + \cfrac{K_{2,3}^2}{L_3P+ \cfrac{K^2_{3,4}}{\ddots \cfrac{}{L_rp+ \cfrac{K^2_{r,r+1}}{L_{r+1}P+ \ddots \cfrac{K^2_{n-1,n}}{L_np+1}}}}}} \tag{2.76}$$

For the dual network of Fig. 2.13b, the negative sign of $S_{11}(p)$ must be chosen to form the input admittance as

$$Y_n(p) = \frac{1 - S_{11}(p)}{1 + S_{11}(p)} \tag{2.77}$$

Similarly, the continued fraction expansion may be written as:

$$Y_{in}(p) = c_1 p + \cfrac{J_{1,2}^2}{c_2 p + \cfrac{J_{2,3}^2}{c_3 p + \cfrac{J_{3,4}^2}{\ddots + \cfrac{\ddots}{c_r p + \cfrac{J_{r,r+1}^2}{c_{r+1} p + \ddots + \cfrac{J_{n-1,n}^2}{c_n p + 1}}}}}} \tag{2.78}$$

Taking equation (2.76) as a typical case, the synthesis cycle commences by extracting the series inductor L_1

as

$$L_1 = \left.\frac{Z_n(p)}{p}\right|_{p=\infty} > 0 \tag{2.79}$$

leaving

$$Z'_{n-1}(p) = Z_n(p) - L_1 p \tag{2.80}$$

Then the impedance inverter $K_{1,2}$ is extracted to give

$$Z_{n-1}(p) = \frac{K_{1,2}^2}{Z'_{n-1}(p)} \tag{2.81}$$

where $K_{1,2}$ may be chosen as any arbitrary scaling factor and $Z_{n-1}(p)$ is positive real function. The typical rth cycle may be written as

$$Z'_{n-r} = Z_{n-(r-1)} - L_r P \qquad (2.82a)$$

and

$$Z_{n-r} = \frac{K^2_{r,r+1}}{Z'_{n-r}} \qquad (r=1\rightarrow n) \qquad (2.82b)$$

Then

$$Z_{n-(r-1)}(p) = L_r P + \frac{K^2_{r,r+1}}{Z_{n-r}(p)} \qquad (2.82c)$$

The cycle may be repeated until the Ladder structure is expressed as a cascade of series inductors $L_r(r=1\rightarrow n)$ separated by ideal impedance inverters $K_{r,r+1}$ $(r=1\rightarrow n-1)$, allowing the terminating resistors to be 1 ohm. However, if explicit formulas for the element values are available then there is no need to follow this lengthy synthesis procedure.

It has been shown in [7] that the two important properties required to derive the explicit design formulas are:

(a) The reflection coefficient $S_{11}(p)$ of degree n in p given in (2.74) degenerates into a function of degree u in the same variable if $\eta = \pm j\sin(\frac{u\pi}{n})$

(b) The transfer function $S_{12}(p)$ given in (2.72), if evaluated at the first point of perfect transmission i.e. $|S_{12}(j\omega)|^2=1$ at $\omega = -\cos(\pi/2n)$, it will give

$$S_{12}(-j\cos(\pi/2n)) = \prod_{r=1}^{n}\left[\frac{\sin(r\pi/n) - j\eta}{\sin(r\pi/n) + j\eta}\right]^{\frac{1}{2}} \qquad (2.83)$$

which is a bounded real all-pass function in the auxiliary variable η.

Now, inspecting equation (2.81), at the zeros of $K_{1,2,}$ the impedance $Z_{n-1}(p)$ vanishes leaving $Z_n(p)$ of degree one in p (single series inductor). Using the same argument for equation (2.82b) which indicates that $Z_{n-r}(p)$ will vanish at the zeros of $K_{r,r+1}$, leaving $Z_n(p)$ of degree u in p at these points, where u = r. Furthermore, it has been

shown in [7] that the zeros of $K_{r,r+1}$ are chosen to occur when $\eta = \pm j\sin\frac{r\pi}{n}$ i.e. the zeros of $K^2_{r,r+1}$ are the zeros of $(\eta^2+\sin^2(r\pi/n))$. But these zeros are the zero of the transfer function given in (2.83). Thus, the only realization of a function with such characteristic is a cascade form of passive and all-pass sections forming a two port network with an overall transfer matrix of the form

$$\prod_{r=1}^{n-1} \frac{1}{\sqrt{\eta^2+\sin^2\left(\frac{r\pi}{n}\right)}} \begin{bmatrix} \sin\left(\frac{r\pi}{n}\right) & j\eta \\ j\eta & \sin\left(\frac{r\pi}{n}\right) \end{bmatrix} \qquad (2.84)$$

Each of whose basic sections may be decomposed into

$$\begin{bmatrix} 1 & -j\frac{\sin(r\pi/n)}{\eta} \\ 0 & 1 \end{bmatrix} \begin{bmatrix} 0 & j\frac{\sqrt{\eta^2+\sin^2\left(\frac{r\pi}{n}\right)}}{\eta} \\ j\frac{\eta}{\sqrt{\eta^2+\sin^2\left(\frac{r\pi}{n}\right)}} & 0 \end{bmatrix} \begin{bmatrix} 1 & -j\frac{\sin(r\pi/n)}{\eta} \\ 0 & 1 \end{bmatrix} \qquad (2.85)$$

Comparison between the centre matrix of (2.85) and (2.69) shows that it is a transfer matrix of an impedance inverter of characteristic impedance

$$K_{r,r+1} = \frac{\sqrt{\eta^2+\sin^2(r_\pi/n)}}{\eta} \qquad (r = 1 \to n-1) \qquad (2.86)$$

Also from (2.85) it can be concluded that between the impedance inverters of characteristic impedances $K_{r-1,r}$ and $K_{r,r+1}$ there is a series element of impedance

$$\frac{-j}{\eta}\left[\sin\left(\left(\frac{r-1}{n}\right)\pi\right)+\sin\left(\frac{r\pi}{n}\right)\right] \qquad (2.87)$$

Since this impedance is evaluated at $p = -j\cos(\pi/2n)$ therefore, the series inductor of inductance L_r can be obtained as:

$$L_r = \frac{-j[\sin((r-1)\pi/n)+\sin(r\pi/n)]}{-j\eta\cos(\pi/2n)}$$

Hence,

$$L_r = \frac{2}{\eta} \sin\,[(2r-1)\pi/2n] \qquad (r=1\rightarrow n) \tag{2.88}$$

Equations (2.86) and (2.88) are the explicit formulas for the element values of the low pass prototype shown in Fig. 2.13a satisfying a conventional Chebyshev response. For the dual network shown in Fig. 2.13b the same formulas can be used where $K_{r,r+1}$ in this case is the characteristic admittance of the admittance inverter and $C_r = L_r$. In both cases the auxiliary parameter η is defined as in equation (2.44).

For the maximally flat response case, the explicit design formulas [7] are

$$\left.\begin{aligned} L_r \text{ or } C_r &= 2 \sin\,[(2r-1)\pi/2n] \quad r = 1 \rightarrow n \\ K_{r,r+1} &= 1 \qquad\qquad\qquad\qquad\quad r = 1 \rightarrow n-1 \end{aligned}\right\} \tag{2.89}$$

2.5.3. The Singly Terminated Low-Pass Prototype.

A filter is called "doubly terminated" if it has resistive loading at both the generator and the load ends. On the other hand a filter is called "singly terminated" if it has a resistive termination at the load end only. The singly terminated low pass prototype is designed to be driven by an ideal source. In Fig. 2.15a the first element of the singly terminated prototype filter is a series connected one and the source is a zero-internal impedance, voltage generator of voltage Vg. Fig. 2.15 b shows a singly terminated low pass prototype whose first element is shunt connected and the source is a zero-internal admittance, current generator of current Ig. For a singly terminated filter the definition of a transducer power gain given in equation (1.116) does not apply since a zero internal impedance (admittance), voltage (current)

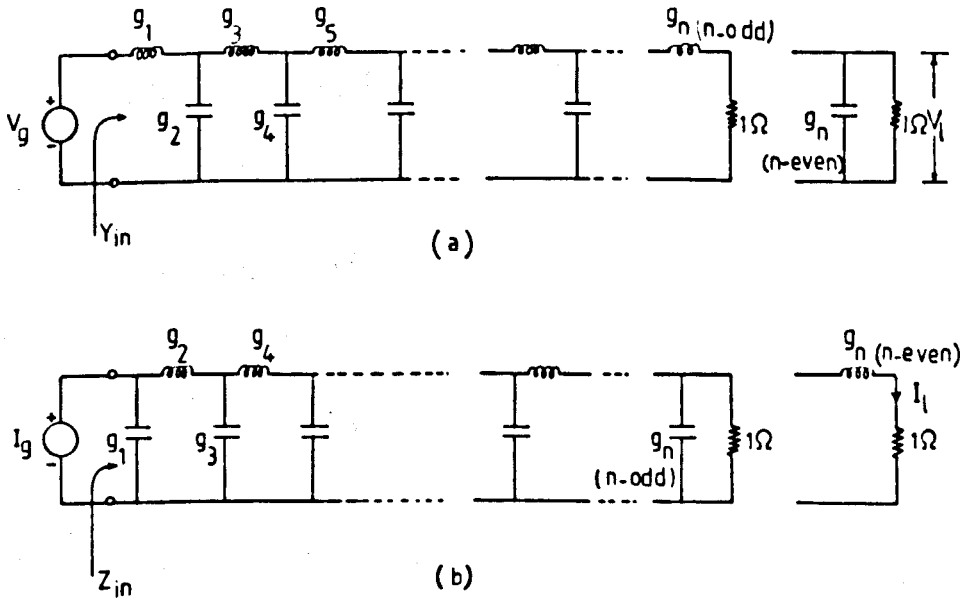

Fig. 2.15 The singly terminated, low-pass prototype filter

(a) Driven by a zero impedance voltage generator

(b) Driven by a zero admittance current generator

generator has infinite available power. However, the power absorbed by the network in Fig. 2.15a is given by

$$P = |V_g|^2 R_e Y_{in}(j\omega) \tag{2.90}$$

where $R_e Y_{in}(j\omega)$ is the real part of the input admittance. Since all the power must be absorbed in the 1 ohm resistive load, Therefore.

$$|V_g|^2 R_e Y_{in}(j\omega) = |V_\ell|^2 \times 1$$

or

$$\left|\frac{V_\ell}{V_g}\right|^2 = R_e Y_{in}(j\omega) \tag{2.91}$$

But from equation (1.130) and by using the dual quantities

$$R_e Y_{in}(j\omega) = Y_{21}^2(j\omega) \tag{2.92}$$

Thus

$$\left|\frac{V_\ell}{V_g}\right|^2 = Y_{21}^2(j\omega) \tag{2.93}$$

Similarly, for the dual network shown in Fig. (2.15b)

$$\left|\frac{I_\ell}{I_g}\right|^2 = Z_{21}^2(j\omega) \tag{2.94}$$

Hence, it can be concluded from equations (2.93) and (2.94) that the most appropriate manner to describe the transfer function of a singly terminated prototype is in terms of the transfer admittance $Y_{21}(p)$ or the transfer impedance $Z_{21}(p)$.

The singly terminated prototype has limited applications in its own as a filter. However, its main application is in the design of diplexers and multiplexers.

Orchard [20]gives explicit formulas for the element values of the singly terminated low-pass prototype satisfying either a

maximally flat or a conventional Chebyshev response. The element values of the networks shown in Fig. 2.15 and exhibiting a maximally flat behaviour may be obtained by using the following relationships:

$$\left.\begin{aligned} g_1 &= \sin(\pi/2n) \\ g_r g_{r+1} &= \frac{\sin[(2r-1)\pi/2n]\sin[(2r+1)\pi/2n]}{\cos^2(r\pi/n)} \qquad (r=1\rightarrow n) \\ R_L &= 1\ \Omega \end{aligned}\right\} \qquad (2.95)$$

and for the conventional Chebyshev response the explicit formulas are

$$\left.\begin{aligned} g_1 &= \frac{\sin(\pi/2n)}{\eta} \\ g_r g_{r+1} &= \frac{\sin[(2r-1)\pi/2n]\sin[(2r+1)\pi/2n]}{\{\eta^2+\sin^2(r\pi/2n)\}\cos^2(r\pi/2n)} \qquad (r=1\rightarrow n) \\ R_L &= 1\ \Omega \end{aligned}\right\} \qquad (2.96)$$

where

$$\eta = \sinh\left[\frac{1}{n}\sinh^{-1} 1/\varepsilon\right]$$

If it is required to use the modified singly terminated low pass prototype shown in Fig. 2.16 , then the explicit formulas given by Rhodes [7] may be used to obtain the element values in the Chebyshev case as:

$$\left.\begin{aligned} L_r \text{ or } C_r &= \frac{\sin[(2r-1)\pi/2n]}{\eta} \qquad r=1\rightarrow n \\ K_{r,r+1} &= \frac{\sin(r\pi/2n)\sqrt{\eta^2+\cos^2(r\pi/2n)}}{\eta} \qquad r=1\rightarrow n-1 \end{aligned}\right\} \qquad (2.97)$$

and in the maximally flat case as:

$$\left.\begin{aligned} L_r \text{ or } C_r &= \sin[(2r-1)\pi/2n] \qquad r=1\rightarrow n \\ K_{r,r+1} &= \sin(r\pi/2n) \qquad r=1\rightarrow n-1 \end{aligned}\right\} \qquad (2.98)$$

where $K_{r,r+1}$ is either a characteristic impedance of an impedance inverter in Fig. 2.16a or a characteristic admittance of an admittance inverter

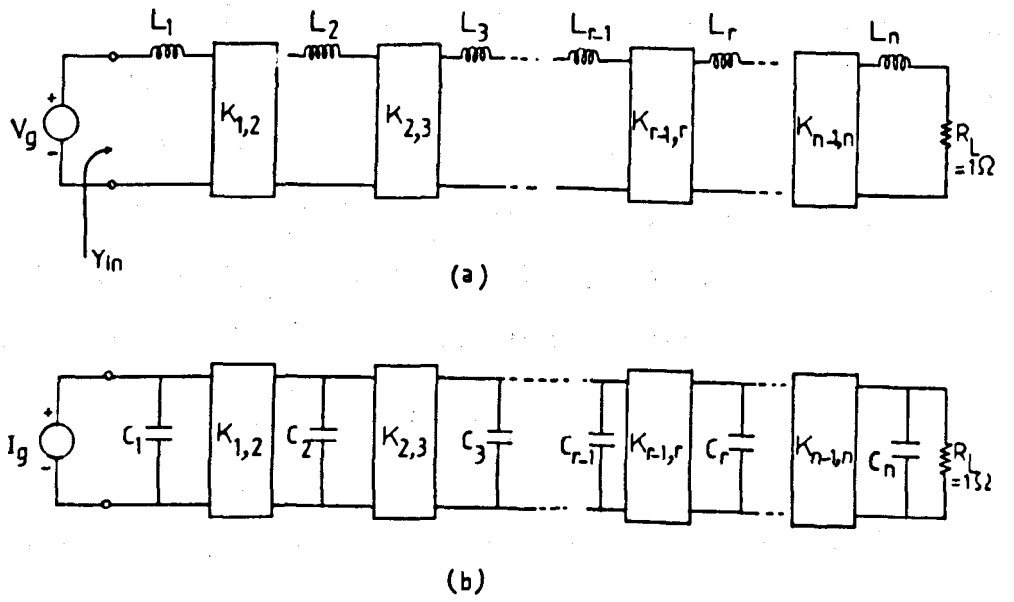

Fig. 2.16 The modified singly terminated low-pass prototype filter

(a) and (b) are duals

in Fig. 2.16b.

2.6 THE GENERALIZED CHEBYSHEV RESPONSE

For LC ladder low-padd prototypes shown in Fig. 2.9, when all the transmission zeros of the transfer function are at infinity and the network is required to satisfy an equiripple passband behaviour, the solution to the approximation problem requires use of Chebyshev polynomials. In some classes of networks, where the class is defined by the location of the transmission zeros, and if an equiripple passband amplitude response is required, then rational Chebyshev function must be used. The term "generalized Chebyshev function" is used in order to distinguish it from the Chebyshev polynomials. Hence, the generalized Chebyshev response may be described by

$$|S_{12}(j\omega)|^2 = \frac{A}{1 + \varepsilon^2 F_n^2(\omega)} \tag{2.99}$$

where $F_n(\omega)$ is the generalized Chebyshev rational function of degree n in ω with prescribed poles shown schematically in Fig. 2.17. This function has been used in different forms for different applications e.g. [21], [22], and one compact form is given in [7]. However, to obtain $F_n(\omega)$ which is optimally equipripple between ± 1 in the interval $|\omega| \leq 1$, let

$$F_n(\omega) = \frac{P_n(\omega)}{E(\omega)} \tag{2.100}$$

where $P_n(\omega)$ is an nth degree polynomial

$E(\omega)$ is an even polynomial of degree $2m \leq n$ in ω and defined by the location of the transmission zeros as

$$E(\omega) = \prod_{i=1}^{m} (1 - \omega^2/\omega_i^2) \tag{2.101}$$

where ω_i are the location of the transmission zeros which are given independently of $P_n(\omega)$.

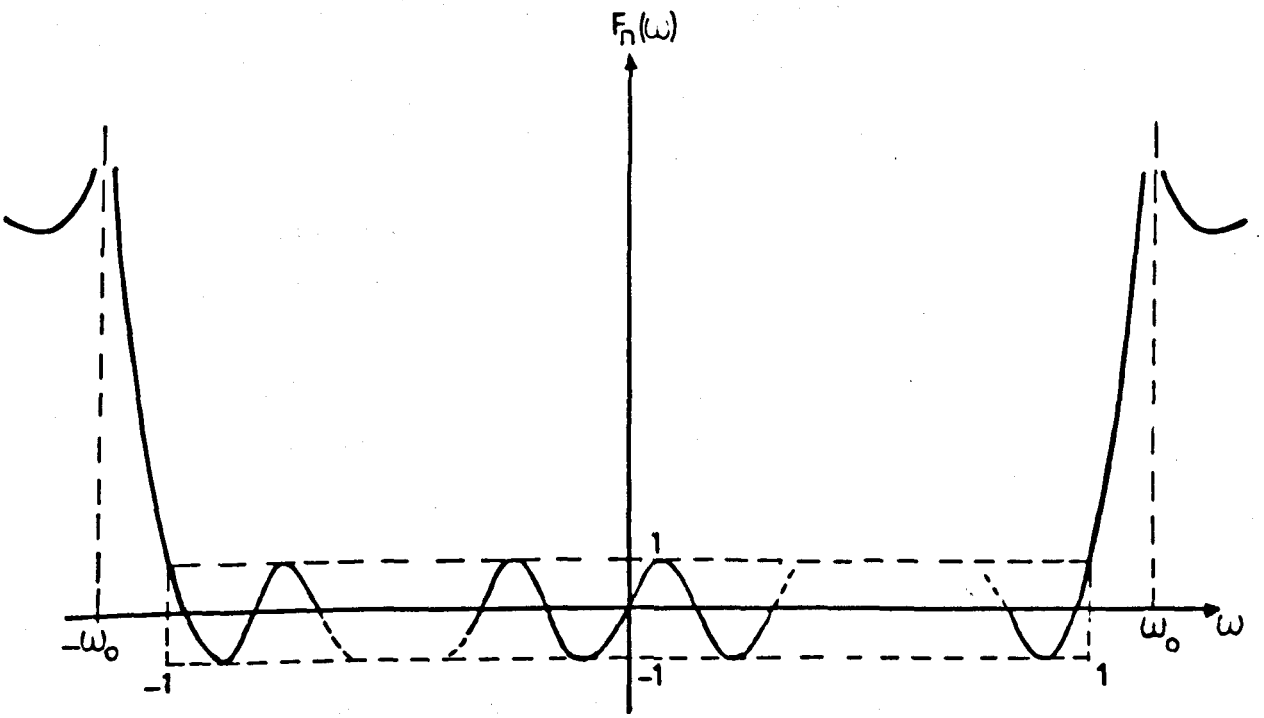

Fig. 2.17 The generalized Chebyshev rational function

For $F_n(\omega)$ to be an equiripple between $\pm$ 1 with the maximum number of turning points in the interval $-1<\omega<1$ as required, it must satisfy a differential equation of the form

$$\frac{d\,F_n(\omega)}{d\,\omega} = \frac{\sqrt{F_n^2(\omega)-1}}{\sqrt{\omega^2-1}} \quad \frac{Q(\omega^2)}{E(\omega)} \tag{2.102}$$

where $Q(\omega^2)$ is a polynomial introduced to correct the degree of the numerator. It can be determined from the condition that $F_n(\omega)$ is a rational function of degree n. Here, for simplicity, let

$$F_n(\omega) = \cosh U \tag{2.103}$$

and use the transformation

$$\omega = \frac{1}{\sqrt{1-Z^2}} \quad \text{or} \quad Z = \sqrt{1 - \frac{1}{\omega^2}} \tag{2.104}$$

This transformation stretches the interval $-1\leq\omega\leq1$ over the whole imaginary axis of Z

Thus,

$$\frac{d\,F_n(\omega)}{du} = \sinh U \tag{2.105}$$

and

$$\frac{dZ}{d\omega} = \frac{1}{\omega^2\sqrt{\omega^2-1}} \tag{2.106}$$

substituting in (2.102) gives

$$\frac{d\,F_n(\omega)}{d\,\omega} = \sinh U \frac{dU}{d\omega} = \frac{\sinh U}{\sqrt{\omega^2-1}} \quad \frac{Q(\omega^2)}{\prod_{i=1}^{m}(1-\frac{\omega^2}{\omega_i^2})} \tag{2.107}$$

Hence

$$\frac{dU}{d\omega} = \frac{Q(\omega^2)}{\sqrt{\omega^2-1}\prod_{i=1}^{m}(1-\omega^2/\omega_i^2)} \tag{2.108}$$

$$\frac{dU}{dZ} = \frac{\omega^2 Q(\omega^2)}{\prod_{i=1}^{m}(1-\omega^2/\omega_i{}^2)} = \frac{R(Z)}{\prod_{i=1}^{m}(Z^2{}_i - Z^2)} \tag{2.109}$$

where

$$R(Z) = K\,\omega^2\,Q(\omega^2)\Big|_{\omega = \frac{1}{\sqrt{1-Z^2}}}$$

K is a constant

and

$$Z_i = \sqrt{1 - 1/\omega^2{}_i} \tag{2.110}$$

Then, equation (2.109) may be written as

$$\frac{dU}{dZ} = \sum_{i=1}^{m}\left\{\frac{k_i}{Z_i - Z} + \frac{k'_i}{Z_i + Z}\right\} + B(Z) \tag{2.111}$$

where

B(Z) is a polynomial in Z with the assumption that the transmission zeros Z_i or ω_i are distinct.

Integrating (2.111) results in

$$U = \sum_{i=1}^{m}\{k'_i\,\ell n(Z+Z_i) - k_i\,\ell_n(Z_i - Z)\} + \int B(Z)\,dZ \tag{2.112}$$

Hence,

$$F_n(\omega) = \cosh\left[\sum_{i=1}^{m}\{k'_i\,\ell_n(Z+Z_i) - k_i\ell_n(Z_i - Z)\} + \int B(z)\,dz\right]$$

For $F_n(\omega)$ to be a rational function in ω, then

$$k_i = k'_i \quad \text{and} \quad B(Z) = 0$$

Thus,

$$F_n(\omega) = \left[\cosh\ \ell n\ \sum_{i=1}^{m}\left(\frac{Z+Z_i}{Z_i - Z}\right)^{k_i}\right]$$

$$= \frac{1}{2}\left[\prod_{i=1}^{m}\left(\frac{Z+Z_i}{Z_i - Z}\right)^{k_i} + \prod_{i=1}^{m}\left(\frac{Z_i - Z}{Z_i + Z}\right)^{k_i}\right] \tag{2.113}$$

which may be written as

$$F_n(\omega) = \frac{1}{2}\left\{\left(\frac{1+Z}{1-Z}\right)^{q_1/2\ q_2/2} \prod_{i=1} \left(\frac{Z-Z_i}{-Z-Z_i}\right) + \left(\frac{1-Z}{1+Z}\right)^{q_1/2\ q_2/2} \prod_{i=1} \left(\frac{-Z-Z_i}{Z-Z_i}\right)\right\} \qquad (2.114)$$

where the factor (1+Z) represents the transmission zeros at infinity.

$F_n(\omega)$ is even for q_1+q_2 even and odd for q_1+q_2 odd, for $q_2=0$ this function degenerates to the case of the Chebyshev polynomial.

To simplify the expression of $F_n(\omega)$ even further,

Define

$$H(Z) = \prod_{i=1}^{\eta_2} (Z-Z_i) \qquad (2.115)$$

$$Z = U + jV \qquad (2.116)$$

$$P = \sigma + j\omega \qquad (2.117)$$

and

$$P = \frac{1}{\sqrt{Z^2-1}} \text{ or } Z = \sqrt{1 + 1/p^2} \qquad (2.118)$$

However, $F_n(\omega)$ is required to have the maximum number of turning points in the interval $-1 \leq \omega \leq 1$, i.e. along the entire imaginary axis of Z=jv

Let

$$F_n(\omega) = \cos\theta \qquad (2.119)$$

Hence

$$\theta = 2\text{Arg}\left|H(jv)\ (1+jv)^{q_1/2}\right| \qquad (2.120)$$

The maximum variation in θ in the interval $-\infty < V < \infty$ requires H(Z) to be a strict Hurwitz polynomial in Z. Additionally, $|F_n(\omega)| = 1$ along the entire imaginary axis. For the purposes of the network realization, all Z_i must be either real or occur in complex-conjugate pairs. Furthermore, if

$$\left.\begin{aligned} \phi_i &= \text{Arg}(Z-Z_i)\Big|_{Z=jv} = \tan^{-1}\frac{V}{-Z_i} = \cos^{-1}\left(\frac{1}{\sqrt{1+V^2/Z_1^2}}\right) \\ \phi &= \text{Arg}\,(1+Z)\Big|_{Z=jv} = \tan^{-1} V = \cos^{-1}\left(\frac{1}{\sqrt{1+V^2}}\right) \end{aligned}\right\} \qquad (2.21)$$

Then $F_n(\omega)$ may be written in the trigonometric form:

$$F_n(\omega) = \frac{1}{2}\left[e^{j(q_1\phi+\sum_{i=1}^{q_2}\phi_i)} + e^{-j(q_1\phi+\sum_{i=1}^{q_2}\phi_i)}\right] \qquad (2.122)$$

Thus

$$F_n(\omega) = \cos\left[q_1\,\phi + \sum_{i=1}^{q_2}\phi_i\right] \qquad (2.123)$$

or in a hyperbolic form as:

$$F_n(\omega) = \cosh\left[q_1\,\phi + \sum_{i=1}^{q_2}\phi_i\right] \qquad (2.124)$$

where

$$\phi = \cosh^{-1}\left(\frac{1}{\sqrt{1-Z^2}}\right) \qquad (2.125a)$$

and

$$\phi_i = \cosh^{-1}\left(\frac{1}{\sqrt{1-Z^2/Z_1^2}}\right) \qquad (2.125b)$$

Substituting for Z by its value given in (2.118) results in

$$\left.\begin{aligned} \phi &= \cosh^{-1}\frac{P}{J} \\ \phi_i &= \cosh^{-1}\sqrt{\frac{P^2(1+P_i^2)}{P^2-P_i^2}} \end{aligned}\right\} \qquad (2.126)$$

Replacing p by $j\omega$ and P^2 by $(-\omega^2)$ results in

$$\left.\begin{aligned} \phi &= \cosh^{-1}\omega \\ \phi_i &= \cosh^{-1}\left[\frac{\omega^2(\omega_1^2-1)}{(1-\omega^2)}\right]^{\frac{1}{2}} \end{aligned}\right\} \qquad (2.127)$$

2.7 THE GENERALIZED CHEBYSHEV LOW-PASS PROTOTYPE FILTERS.

This section presents a synthesis procedure for very selective classes of low pass prototype networks which have important applications in the design of TEM mode microwave broadband filters, diplexers and multiplexers particularly for printed circuit forms of realization. These networks satisfy a generalized Chebyshev response with an equiripple passband, have an odd number of transmission zeros at infinity and an even multiple of transmission zeros at a finite point on the jω-axis. These prototypes are excellent alternatives to the elliptic function prototypes when a minimum impedance variation in the network is required.

2.7.1. Prototypes Having A Single Transmission Zero at Infinity [23].

The generalized Chebyshev insertion loss response L of the doubly terminated low-pass prototype network and its dual shown in Fig. (2.18a,b) is given by

$$L = 1 + \varepsilon^2 \cosh^2\{(N-1)\cosh^{-1}\left[\omega\left(\frac{\omega_0^2-1}{\omega_0^2-\omega^2}\right)^{\frac{1}{2}}\right] + \cosh^{-1}\omega\} \qquad (2.128)$$

where

$$L = \frac{1}{|S_{12}(j\omega)|^2} \qquad (2.129)$$

The transmission zeros are of order $(N-1)$ at $\omega = \pm\omega_0$ and one at infinity N is an odd number equal to the degree of the network

$$\varepsilon = [10^{(R.L./10)} - 1]^{-\frac{1}{2}} \qquad (2.130)$$

and

R.L. is the minimum passband return loss (dB). The return loss measured in deciBells is usually defined by:

$$\text{Return loss (dB)} = 10 \log \frac{1}{|S_{11}(j\omega)|^2} \qquad (2.131)$$

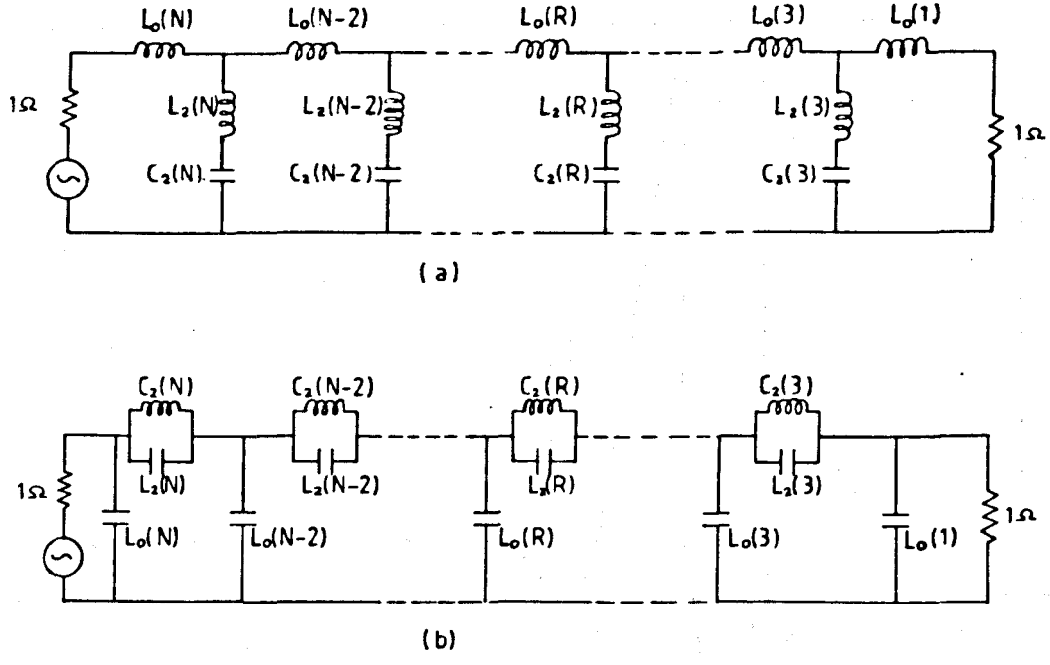

Fig. 2.18 The generalized Chebyshev low-pass prototype networks with single transmission zero at infinity and even multiple at finite real frequency

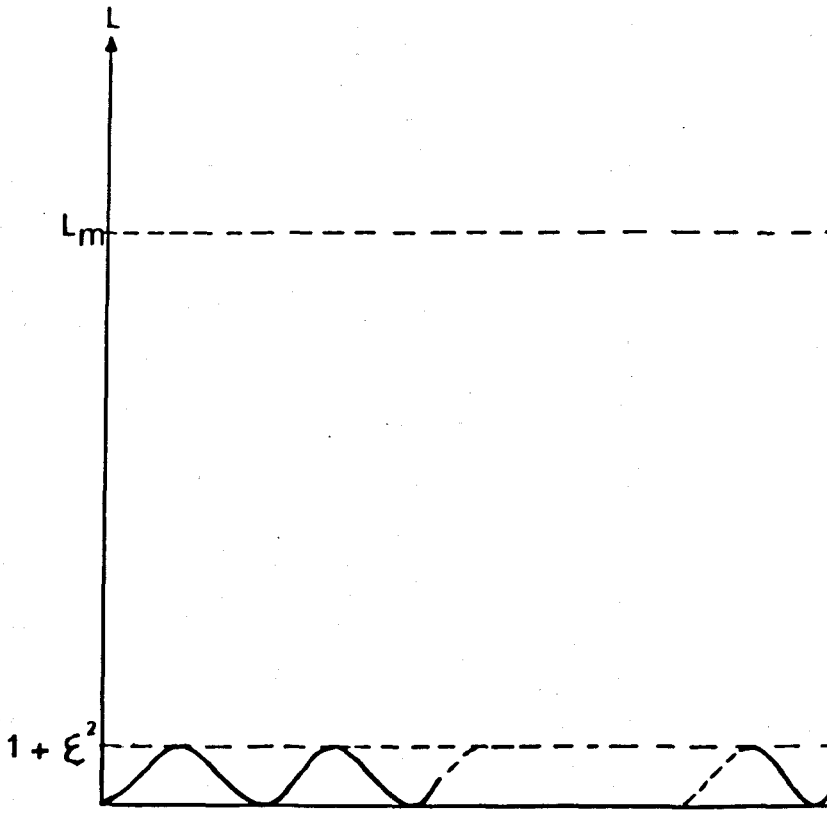

Fig. 2.19 The generalized Chebyshev

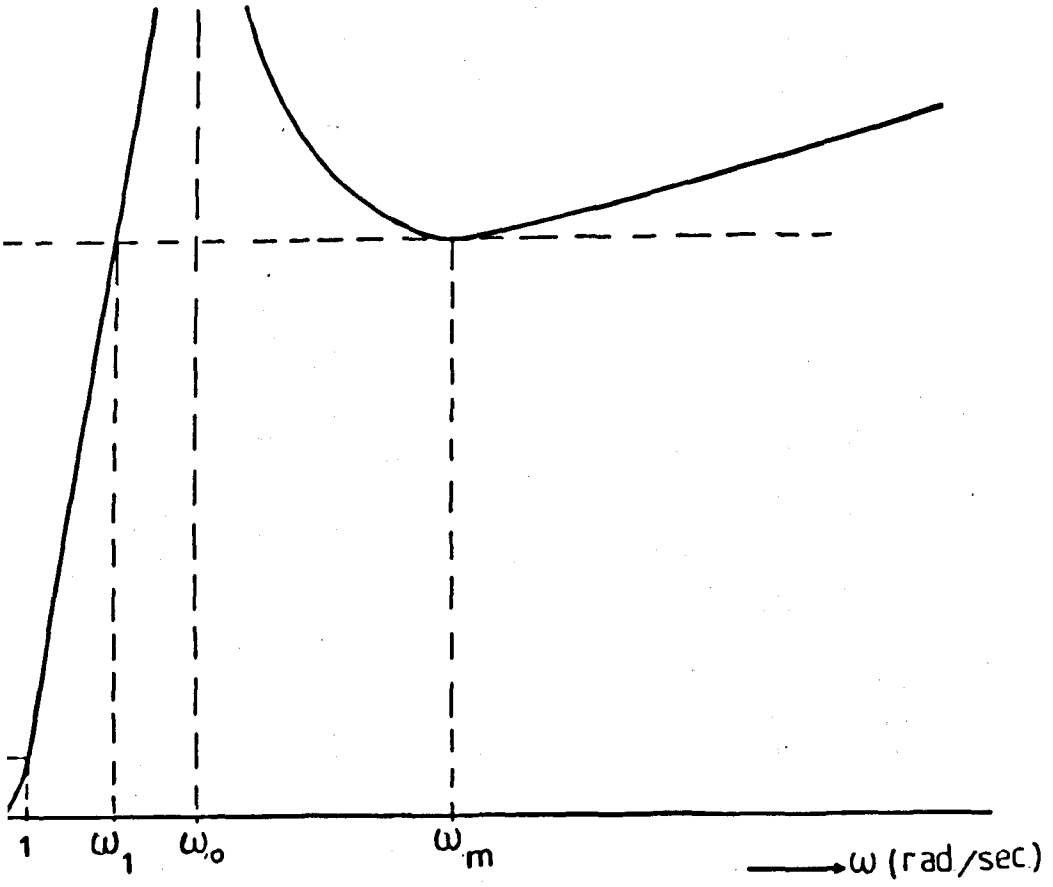

insertion loss response

Similarly, the insertion loss measured in (dB) is given by:

$$\text{Insertion loss (dB)} = 10 \log \frac{1}{|S_{12}(j\omega)|^2} \qquad (2.132)$$

The insertion loss response L is illustrated in Fig. 2.19, where ω_m is the frequency of the minimum insertion loss level L_m in the stopband and ω_1 is the stopband edge frequency. ω_m and ω_1 are derived numerically by iteration for the given values of N, R.L. and L_m measured in (dB). If equation (2.128) is written in a general form as

$$L = 1 + \varepsilon^2 F_N^2(\omega) \qquad (2.133)$$

where $F_n(\omega)$ is a general Chebyshev function then ω_m is defined as

$$\left.\frac{d F_N(\omega)}{d\omega}\right|_{\omega = \omega_o} = 0$$

Yielding

$$\omega_m^2 = \omega_o^2 + (N-1)\,\omega_o\,(\omega_o^2-1)^{\frac{1}{2}} \qquad (2.134)$$

After finding these important points, one can proceed to find the element values by using the standard Darlington Procedure i.e. by forming the reflection coefficient $S_{11}(p)$ from

$$S_{11}(p).\, S_{11}(-p) = \frac{\varepsilon^2 P_N(p)}{1-\varepsilon^2 P_N^2(p)} \qquad (2.135)$$

where

$$P = \sigma + j\omega \quad , \quad P_N(p) = j\, F_n(\omega)$$

By forming a Hurwitz factorization of the denominator and the numerator, the driving point impedance is given by:

$$Z(p) = \frac{1 + S_{11}(p)}{1 - S_{11}(p)} \qquad (2.136)$$

However, it is not possible to carry out the computerized synthesis of high degree network of this type by extracting elements in the p-plane in the conventional manner without losing a significant amount of accuracy. Therefore different techniques have been used.

The Z-Transformed Variable Technique.

The well known Z-transformed variable technique described in [24], [25] among others, is attempted here first as a solution to the synthesis accuracy problem. This technique is based upon replacing the variable p^2 by an expression in Z^2 as

$$Z^2 = 1 + 1/p^2 \quad \text{or} \quad p^2 = \frac{1}{Z^2-1} \tag{2.137}$$

where Z is the transformed complex frequency.

This transformation for the low pass case is used in preference to any other mathematical form because it is the only simple function that gives a one to one correspondence between the two variables in both directions of the transformation. Moreover, it preserves the degree of any rational function whose variable is so changed. Additionally it stretches the passband $|\omega| \leq 1$ over the entire imaginary axis; hence it separates the critical frequencies (Poles and Zeros) which are, in the p-plane, tightly clustered around the cutoff frequency and this last property is the main factor in improving the accuracy of the synthesis. This is because the loss of the accuracy in the filter design occurs when the information about the filter is stored in the coefficient of the polynomials forming numerators and denominators of $S_{11}(p)$ and $Z_{in}(p)$ or $Y_{in}(p)$. A very small change in these coefficients results in a large change in the element values of the ladder networks, in other words, the element values are extremely sensitive to error in the coefficients. If the critical frequencies are more widely separates as it is the case when the

Z-transformed variable is used, hence, all the polynomials concerned become very much better conditioned. The net result is that the sensitivity of the ladder elements to the coefficients of the polynomials in the variable Z is much less than their sensitivity to those of the P-variable case.

The synthesis of the network shown in Fig. 2.18 using the Z-transformed variable is illustrated by the following numerical example.

NUMERICAL EXAMPLE No. 1.

Given: the degree of the network N = 7

R.L. = The minimum return loss in the passband = 20 dB

L_m = The minimum insertion loss in the stopband = 40 dB

Required: to find the elements values of this network shown in Fig. 2.20.

Start by calculating the constant ε from equation (2.142)

$$\varepsilon = \left[10^{20/10} - 1\right]^{-\frac{1}{2}} = 0.1$$

and the location of the finite transmission zeros ω_o from

$$L_m = 10 \text{ Log } \{1 + \varepsilon^2 \cosh^2\{(N-1)\cosh^{-1}\left[\omega_m\left(\frac{\omega_o^2-1}{\omega_o^2-\omega_m^2}\right)^{1/2}\right] + \cosh^{-1}\omega_m\}\} \quad (2.138)$$

Substitute for ω_m by the value given in (2.134) and solve numerically for ω_o to obtain

$$\omega_o = 1.41544 \quad \text{rad/sec}$$

The numerical factorization of the denominator and the numerator of equation (2.135) is carried out and the left half plane (p-plane) poles are chosen to form the denominator of $S_{11}(p)$. These are

$$P_1 = -0.0485419 \pm j1.03771$$

$$P_2 = -.0.181441 \pm j0.947114$$

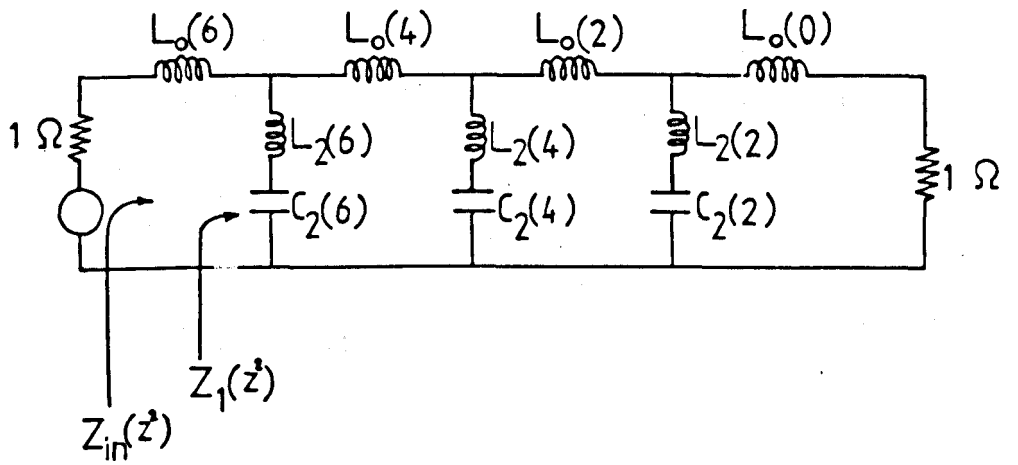

Fig. 2.20 Low-pass prototype of degree 7
"Numerical example No. 1"

$$P_3 = -0.425805 \pm j0.671126$$

$$P_4 = -0.635948$$

let the typical complex pole be $P_r = -X_r \pm jy_r \qquad r=1\rightarrow(N-1)/2$

and the real pole $P_m = -X_m$ where $m = (N+1)/2$

The zeros of $S_{11}(p)$ are on the imaginary axis. Their values are

$$P_1' = \pm j\ 0.986073$$

$$P_2' = \pm j\ 0.860628$$

$$P_3' = \pm j\ 0.541943$$

$$P_4' = 0$$

let the typical zero be $P_r' = \pm j\ K_r$ where $r = 1\rightarrow (N-1)/2$.

Thus,

$$S_{11}(p) = \frac{P[P^2 + K_1^2][P^2 + K_2^2]\ [P^2 + K_3^2]}{[P + X_m][P^2+2X_1+(X_1^2+Y_1^2)][P^2+2X_2+(X_2^2+Y_2^2)]\ [P^2+2x_3+(X_3^2+Y_3^2)]} \qquad (2.139)$$

replacing P by $\frac{1}{\sqrt{Z^2-1}}$ and P^2 by $\frac{1}{Z^2-1}$

gives

$$S_{11}(Z^2) = \frac{B_{(0)}+B_{(2)}Z^2+B_{(4)}Z^4+B_{(6)}Z^6}{A_1(0)+A_1(2)Z^2+A_1(4)Z^4+A_1(6)Z^6+\sqrt{Z^2-1}\{A_2(0)+A_2(2)Z^2+A_2(4)Z^4+A_2(6)Z^6\}} \qquad (2.140)$$

where the numerical values of the numerator coefficients are:

$$B_{(0)} = 0.005066, \quad B_{(2)} = 0.194667, \quad B_{(4)} = 0.588745,$$

$$B_{(6)} = 0.211522$$

and the numerical values of the denominator coefficients are:

$A_1(0) = 0.0308842$, $A_1(2) = -0.59255$, $A_1(4) = 0.190558$, $A_1(6) = 1.37111$.

and

$A_2(0) = -0.040755$, $A_2(2) = -0.08525$, $A_2(4) = 1.67007$, $A_2(6) = 0.403182$.

Now, $Z_{in}(Z^2)$ can be formed as

$$Z_{in}(Z^2) = \frac{1+S_{11}(Z^2)}{1-S_{11}(Z^2)}$$

$$= \frac{E(0)+E(2)Z^2+E(4)Z^4+E(6)Z^6+\sqrt{Z^2-1}\,\{A_2(0)+A_2(2)Z^2+A_2(4)Z^4+A_2(6)Z^6\}}{F(0)+F(2)Z^2+F(4)Z^4+F(6)Z^6+\sqrt{Z^2-1}\{A2(0)+A_2(2)Z^2+A_2(4)Z^4+A_2(6)Z^6\}} \quad (2.141)$$

where

$$E(i) = A_1(i) + B(i)$$

$$F(i) = A_1(i) - B(i)$$

and their numerical values are:

$E(0) = 0.0359502$ $E(2) = -0.397883$, $E(4) = 0.779303$,
$E(6) = 1.58264$

$F(0) = 0.058182$, $F(2) = -0.787217$, $F(4) = -0.398187$,
$F(6) = 1.15959$

The element values can be obtained by using the zero shifting technique in a similar manner to that used in P-plane synthesis [26]. The impedance of a series inductor $L_o(r)P$ in the P-plane becomes

$$\frac{L_o(r)}{\sqrt{Z^2-1}} \quad \text{in the z-plane}$$

All these series inductors are partially extracted except the last one which is completely extracted. The first series inductor is partially extracted such that

$$\frac{L_o(6)}{\sqrt{Z^2-1}} = Z_{in}(Z)^2 \Big|_{Z^2=Z_o^2} \quad (2.142)$$

where $Z_o^2 = 1/(1-1/\omega^2_o)$ (2.143)

and since $Z_{in}(Z^2)$ has a pole at $Z^2=1$

Therefore,

$$F(0) + F(2)Z^2+F(4)Z^4+F(6)Z^6=(Z^2-1)[F_1(0)+F_1(2)Z^2+F_1(4)Z^4]$$

Hence,

$$Z_{in}(Z^2) = \frac{E(0)+E(2)Z^2+E(4)Z^4+E(6)Z^6+\sqrt{Z^2-1}\{A_2(0)+A_2(2)Z^2+A_2(4)Z^4+A_2(6)Z^6\}}{(Z^2-1)[F_1(0)+F_1(2)Z^2+F_1(4)Z^4]+\sqrt{Z^2-1}\{A_2(0)+A_2(2)Z^2+A_2(4)Z^4+A_2(6)Z^6\}} \tag{2.144}$$

And

$$L_o(6) = \left.\frac{E(0)+E(2)Z^2+E(4)Z^4+E(6)Z^6+\sqrt{Z^2-1}\{A_2(0)+A_2(2)Z^2+A_2(4)Z^4+A_2(6)Z^6\}}{\sqrt{Z^2-1}\{F_1(0)+F_1(2)Z^2+F_1(4)Z^4\}+[A_2(0)+A_2(2)Z^2+A_2(4)Z^4+A_2(6)Z^6]}\right|_{Z^2=Z_o^2}$$

Or

$$L_o(6) = \left.\frac{\sum_{i=0}^{6} E(i)Z^i}{\sum_{i=0}^{6} A_2(i)Z^i}\right|_{Z^2=Z_o^2} = \left.\frac{\sum_{i=0}^{6} A_2(i)Z^i}{\sum_{i=0}^{4} F_1(i)Z^i}\right|_{Z^2=Z_o^2} \tag{2.145}$$

$$Z_1(Z^2) = Z_{in}(Z^2) - \frac{L_o(6)}{\sqrt{Z^2-1}} \tag{2.146}$$

$$Z_1(Z^2) = \frac{E_1(0)+E_1(2)Z^2+E_1(4)Z^4+E_1(6)Z^6+\sqrt{Z^2-1}\{E_2(0)+E_2(2)Z^2+E_2(4)Z^4+E_2(6)Z^6\}}{(Z^2-1)[F_1(0)+F_1(2)Z^2+F_1(4)Z^4]+\sqrt{Z^2-1}\{A_2(0)+A_2(2)Z^2+A_2(4)Z^4+A_2(6)Z^6\}} \tag{2.147}$$

where

$$E_1(i) = E(i) - L_o(6)\, A_2(i) \qquad i = 0,2,\text{--}6$$

$$E_2(i) = A_2(i) - L_o(6)\, F_1(i) \qquad i = 0,2,4$$

$$E_2(6) = A_2(6)$$

The shunt connected branch which is a series connection of an inductor $L_2(6)$ and a capacitor $C_2(6)$ must be completely extracted by removing a pole at $Z^2 = Z_o^2$. Such that

$$Y_2(Z^2) = Y_1(Z^2) - Y' \tag{2.148}$$

where

$$Y_1(Z^2) = \frac{1}{Z_1(Z^2)} \quad \text{and} \quad Y' = \frac{C_2(6)\sqrt{Z^2-1}}{Z^2-Z_o^2}$$

$$Y' = Y_1(Z^2)\Big|_{Z^2=Z_o^2} \tag{2.149}$$

But $Y_1(Z^2)$ can be written as

$$Y_1(Z^2) = \frac{(Z^2-1)\left[F_1(0)+F_1(2)Z^2+F_1(4)Z^4\right]+\sqrt{Z^2-1}\left[A_2(0)+A_2(2)Z^2+A_2(4)Z^4+A_2(6)Z^6\right]}{(Z^2-Z_o^2)\{\left[E_3(0)+E_3(2)Z^2+E_3(4)Z^4\right]+\sqrt{Z^2-1}\left[E_4(0)+E_4(2)Z^2+E_4(4)Z^4\right]\}}$$

where (2.150)

$$(Z^2-Z_o)\left[E_3(0)+E_3(2)Z^2+E_3(4)Z^4\right]=E_1(0)+E_1(2)Z^2+E_1(4)Z^4+E_1(6)Z^6$$

and

$$(Z^2-Z_o)\left[E_4(0)+E_4(2)Z^2+E_4(4)Z^4\right]= E_2(0)+E_2(2)Z^2+E_2(4)Z^4+E_2(6)Z^6$$

Thus, $C_2(6)$ may be calculated from

$$C_2(6) = \frac{F_1(0)+F_1(2)Z^2+F_1(4)Z^4}{E_4(0)+E_4(2)Z^2+E_4(4)Z^4}\Bigg|_{Z^2=Z_o^2} \tag{2.151}$$

and $L_2(6)$ from the relationship

$$L_2(6) = 1/(C_2(6)\ \omega_o^2) \tag{2.152}$$

From (2.148)

$$Y_2(Z^2) = \frac{\left[G(0)+G(2)Z^2+G(4)Z^4+G(6)Z^6\right]+\sqrt{Z^2-1}\left[H(0)+H(2)Z^2+H(4)Z^4+H(6)Z^6\right]}{(Z^2-Z_o)\{\left[E_3(0)+E_3(2)Z^2+E_3(4)Z^4\right]+\sqrt{Z^2-1}\left[E_4(0)+E_4(2)Z^2+E_4(4)Z^4\right]\}} \tag{2.153}$$

where

$$G(i) = F(i) - C_2(6)\ G_1(i) \quad i = 0,2,4,6$$

$$G_1(0) = -E_4(0)$$

$$G_1(i) = -\left[E_4(i) - E_4(i-2)\right] \quad i = 2,4,6$$

$$H(i) = A_2(i) - C_2(6)\ E_3(i) \quad i = 0,2,4,6$$

Since $Z^2-Z_o^2$ is a factor of the numerator of $Y_2(Z^2)$ Then

$$Y_2(Z^2) = \frac{G_2(0)+G_2(2)Z^2+G_2(4)Z^4+\sqrt{Z^2-1}\,[H_1(0)+H_1(2)Z^2+H_1(4)Z^4]}{E_3(0)+E_3(2)Z^2+E_3(4)Z^4+\sqrt{Z^2-1}\,[E_4(0)+E_4(2)Z^2+E_4(4)Z^4]} \qquad (2.154)$$

where

$$[G_2(0)+G_2(2)Z^2+G_2(4)Z^4]\,[Z^2-Z_o^2] = G(0)+G(2)Z^2+G(4)Z^4+G(4)Z^6$$

$$[H_1(0)+H_1(2)Z^2+H_1(4)Z^4]\,[Z^2-Z_o^2] = H(0)+H(2)Z^2+H(4)Z^4+H(6)Z^6$$

Then

$$Z_2(Z^2) = 1/Y_2(Z^2) \qquad (2.155)$$

and the synthesis cycle is repeated until all the elements of the network are obtained. The element values of this example are given in Table EX.1.

N=7, L_m = 40 dB R.L. = 20 dB	
$L_o(6)$	0.59781
$L_2(6)$	0.572575
$C_2(6)$	0.871735
$L_o(4)$	1.36485
$L_2(4)$	0.440682
$C_2(4)$	1.13264
$L_o(2)$	1.36485
$L_2(2)$	0.572575
$C_2(2)$	0.871735
$L_o(1)$	0.59781

Table EX.1.: Element Values of the Network Shown in Fig. 2.20.

However, a severe deterioration in the accuracy was noticed when similar networks of degree greater than 11 was attempted using the Z-transformed variable technique. Even for a degree 11 network which was synthesized using this technique to satisfy a minimum passband return loss of 20 dB and a minimum stopband insertion loss of 40 dB, a drop in the minimum return loss level in band to 19.49 dB and to 18.77 dB at the band edge was noticed. Hence a relatively new technique termed "the alternating pole synthesis technique" [23] is used. A little accuracy is lost for networks up to and including degree 19.

The Alternating Pole Synthesis Technique [23].

By using Bartlett's bisection theorem, the transmission coefficient $S_{12}(p)$ of the passive lossless linear network (N) shown in Fig. 2.21 may be written as, [7]

$$S_{12}(p) = \frac{Z_o - Z_e}{(1 + Z_e)(1 + Z_o)} \tag{2.156}$$

where Z_o and Z_e are the odd and even mode impedances of a symmetrical network respectively. $Z_o(Z_e)$ is the input impedance when a short circuiting (open circuiting) plane is inserted along the line of symmetry as shown in Fig. 2.21b and c respectively and they are reactance functions.

The reflection coefficient $S_{11}(p)$ may also be written as:

$$S_{11}(p) = \frac{1 - Z_e Z_o}{(1+Z_o)(1+Z_e)} \tag{2.157}$$

To find the element values of the network, it is necessary to construct either Z_o or Z_e uniquely from the poles of $S_{11}(p)$. This can be done as follows:-

Rewrite $S_{12}(j\omega)$as:

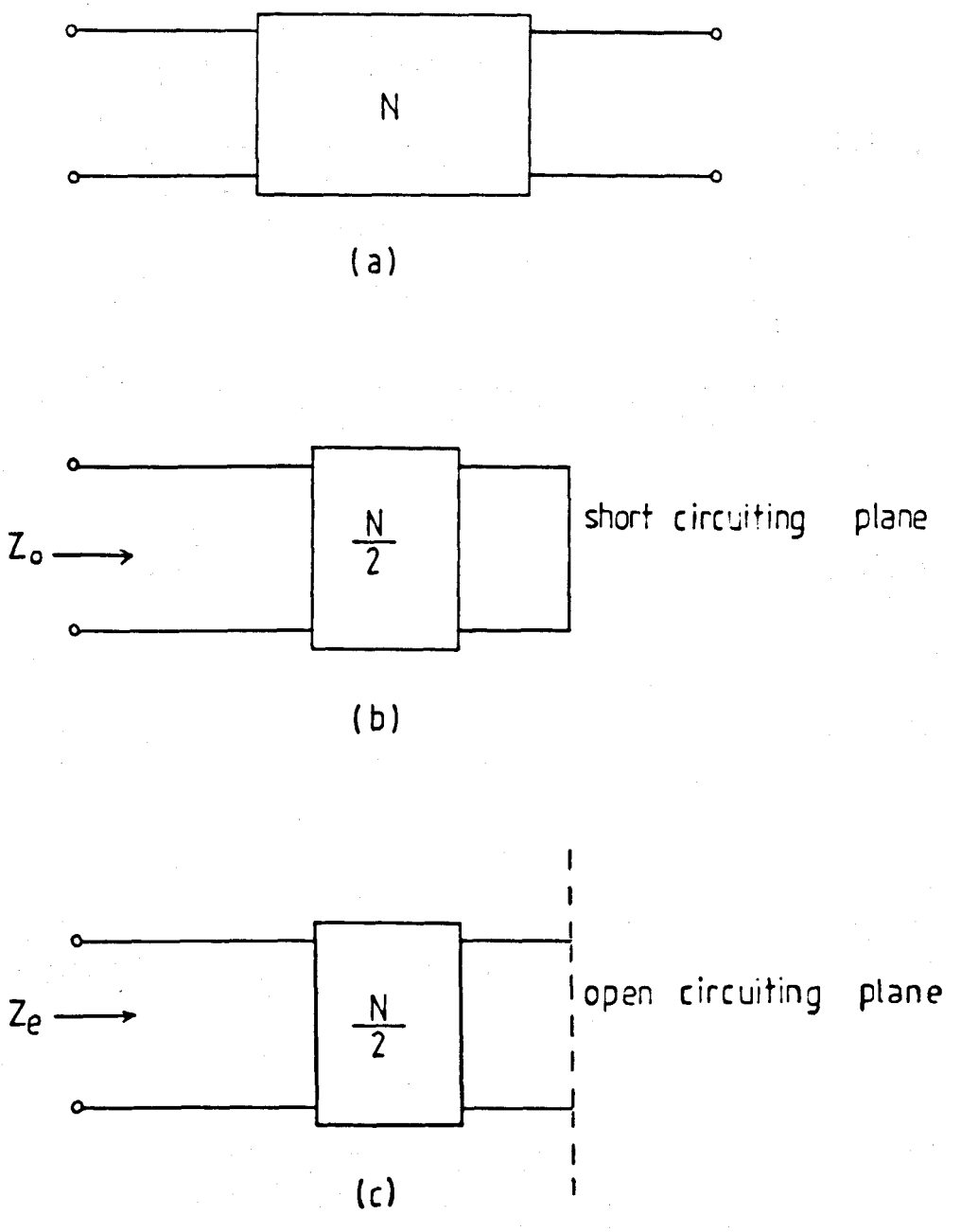

Fig. 2.21 (a) Symmetrical network N
(b) Odd mode impedance Z_o
(c) Even mode impedance Z_e

$$\left|S_{12}(j\omega)\right|^2 = \frac{1}{1 + \dfrac{\left|S_{11}(j\omega)\right|^2}{\left|S_{12}(j\omega)\right|^2}} \tag{2.158}$$

Hence, from equation (2.156) and (2.157) we have

$$\left|S_{12}(j\omega)\right|^2 = \frac{1}{1 - \left(\dfrac{1 - Z_e Z_o}{Z_o - Z_e}\right)^2} \tag{2.159}$$

But

$$\left|S_{12}(j\omega)\right|^2 = \frac{1}{1 + \varepsilon^2 F_N^{\,2}(\omega)} = \frac{1}{(1 + j\varepsilon F_N(\omega))(1 - j\varepsilon F_N(\omega))} \tag{2.160}$$

therefore

$$j\varepsilon F_N(\omega) = \pm \left(\frac{1 - Z_e Z_o}{Z_o - Z_e}\right) \tag{2.161}$$

Consequently,

$$\frac{1}{1 + j\varepsilon F_N(\omega)} = \frac{Z_o - Z_e}{(1 + Z_o)(1 - Z_e)} \tag{2.162}$$

and

$$\frac{1}{1 - j\varepsilon F_N(\omega)} = \frac{Z_e - Z_o}{(1 + Z_e)(1 - Z_o)} \tag{2.163}$$

replacing ω by (P/j) we have

$$\frac{1}{1 + j\varepsilon F_N(P/j)} = \frac{Z_o - Z_e}{(1 + Z_o)(1 - Z_e)} = \frac{1}{1 + \varepsilon P_N(p)} \tag{2.164}$$

and

$$\frac{1}{1 - j\varepsilon F_N(P/j)} = \frac{Z_e - Z_o}{(1 + Z_e)(1 - Z_o)} = \frac{1}{1 - \varepsilon P_N(p)} \tag{2.165}$$

From equation (2.164), we have

Numerator of $(1 + \varepsilon P_N(p))$ = Numerator of $\left[(1 + Z_o)(1 - Z_e)\right]$ (2.166)

Since Z_o and Z_e are reactance functions, then the left half zeros of $(1 + \varepsilon P_N(p))$ are zeros of $(1 + Z_o)$.

Similarly from equation (2.165)

$$\text{Numerator of } (1 - \varepsilon P_N(p)) = \text{Numerator of } \left[(1 + Z_e)(1 - Z_o)\right] \tag{2.167}$$

so, the left half zeros of $(1 - \varepsilon P_N(p))$ are the zeros of $(1 + Z_e)$. However, if a polynomial $D_1(p)$ is constructed from the left hand zeros of $(1 + \varepsilon P_N(p))$ it must be Hurwitz and may be written as

$$D_1(p) = E_1(p) + O_1(p) \tag{2.168}$$

where $E_1(p)$ and $O_1(p)$ are even and odd parts respectively and the reactance function Z_e may be constructed as,

$$\therefore \quad Z_e = \frac{E_1(p)}{O_1(p)} \text{ or } \frac{O_1(p)}{E_1(p)} \tag{2.169}$$

Meanwhile, following the same argument another Hurwitz polynomial $D_2(p)$ may be constructed from the left half zeros of $(1 - \varepsilon P_N(p))$ as

$$D_2(p) = E_2(p) + O_2(p) \tag{2.170}$$

resulting in

$$Z_o = \frac{E_2(p)}{O_2(p)} \text{ or } \frac{O_2(p)}{E_2(p)} \tag{2.171}$$

Thus, to synthesize the network one needs only to form the numerator of $(1 + \varepsilon P_N(p))$ and to solve for the roots numerically. The LHP roots are associated with the zeros of $(1 + Z_o)$ and the RHP roots with the zeros of $(1 - Z_e)$. For $(1 + \varepsilon P_N(p))$, it has been found that the roots of the numerator taken in order from the largest imaginary part, alternate between the LHP and the RHP. For N = 7 this is illustrated in Fig. 2.22.

This is the reason why the synthesis procedure may be described as the alternating pole technique and indicates why accuracy is retained in the p-plane due to the inherent maximum separation of pole locations.

Fig. 2.22 Typical

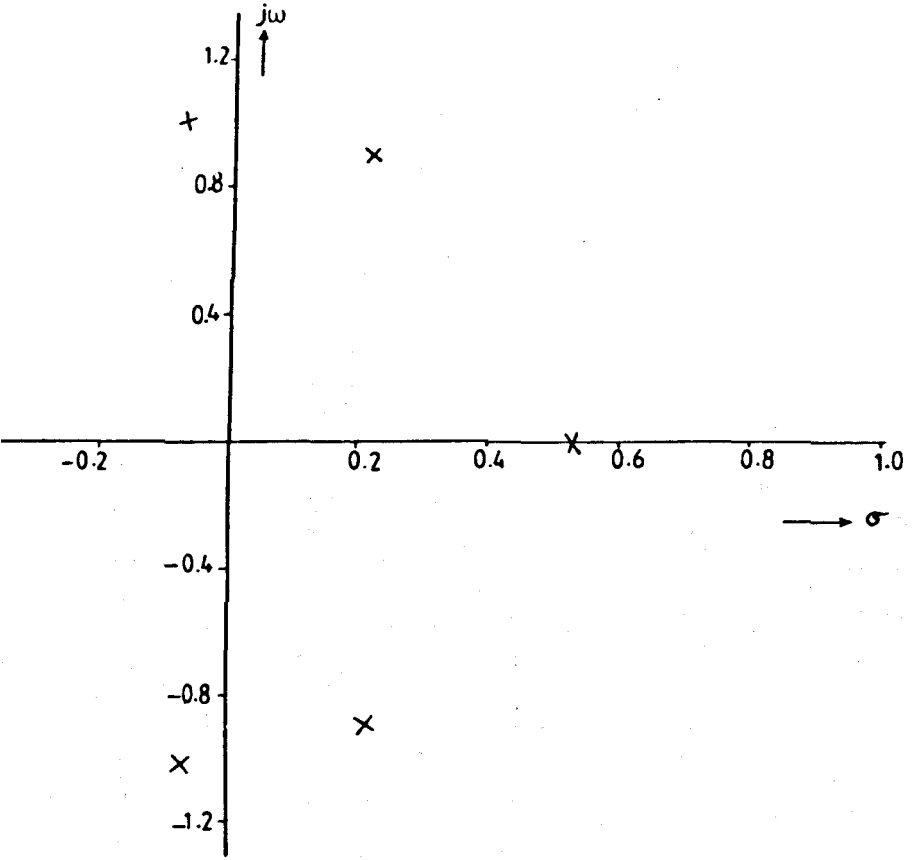

zero location for $(1 + \varepsilon P_N(p))$ for N = 7

Results

For the prototype network shown in Fig. 2.18, all the element values provided in tables (1→8) have been obtained by using the alternating pole technique to construct either Z_e or Z_o whichever has the highest degree. It has been found that networks of degree 7, 11, 15 and 19 can be synthesized by constructing Z_e, while networks of degree 5, 9, 13 and 17 can be synthesized by constructing Z_o. However in either case the element values may be extracted by using the zero shifting technique. (the synthesis cycle is shown in Fig. 2.23).

Let $Z(p) = Z_e$ or Z_o

and $Z(p) = E(p)/O(p)$

The series element $L_o(R)$ is obtained by:

$$L_o(R) = \frac{Z(j\omega_o)}{j\omega_o}$$

$$Z_1(p) = \frac{E^1(p)}{O(p)} \rightarrow Y_1(p) = \frac{1}{Z_1(p)} = \frac{O(p)}{E^1(p)}$$

The admittance of the shunt resonant section is:

$$Y^1(p) = \frac{P/L_2(R)}{p^2 + \omega_2{}^2}$$

where

$$\omega_o{}^2 = 1/(L_2(R).C_2(R))$$

and the residue K_2 of $Y_1(p)$ at $P = \pm j\omega_o$ is given by:

$$K_2 = \left.\frac{O(p)}{\frac{d}{dp}(E^1(p))}\right| \quad p = \pm j\omega_o$$

$$L_2(R) = 1/(2\,K_2)$$

Then, the cycle is repeated to extract the rest of the elements. The whole synthesis procedure has been programmed on a computer, and the element values

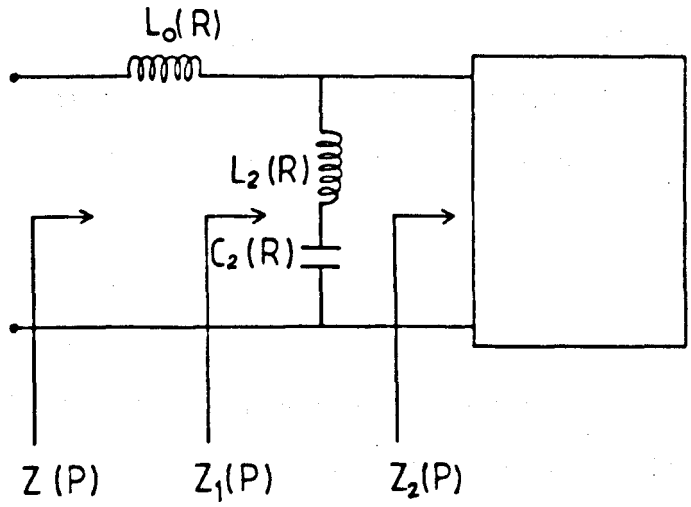

Fig. 2.23 The synthesis cycle of the prototype shown in Fig. 2.18

can be obtained easily for the given values of N, L_m and R.L. Besides better accuracy, other advantages of the relatively new technique of alternating pole over the Z-transformed variable are its simplicity and also its application to bandpass networks in a similar manner. The application of the Z-transformed variable technique to bandpass networks requires tedious and complicated algebraic operations especially at the element extraction stage. However, the alternating pole techniques can not be used in the synthesis of non-symmetrical networks, but this is not a very serious limitation since these networks are less common than the symmetrical ones.

Practical Advantages of this Prototype.

This prototype has a very important practical advantage, for some application in that it is possible for certain minimum stop band insertion loss levels and minimum passband return loss levels, to synthesis the network shown in Fig. 2.18 with the numerical values of $L_o(N)$ and $L_o(1)$ equal to zero. These prototypes with zero end-element values make the realization of many structures much easier. Hence, the classified tables provided in this section include element values of networks having end elements of zero value in addition to the standard set with minimum stopband insertion loss levels of 40, 50 and 60 dB.

This prototype has also the practical advtange of the selectivity and the stopband response can be further improved for the same return loss by simply adding more sections in the middle of the network. For example an increase of about 9 dB per section is obtained in the stopband insertion loss of a network of degree 17 designed to satisfy L_m = 60 dB and R.L. = 20 dB. The computer simulation of the network insertion loss and the return loss response before and after adding one more section at the middle are shown in Fig. 2.24 and Fig. 2.25 respectively.

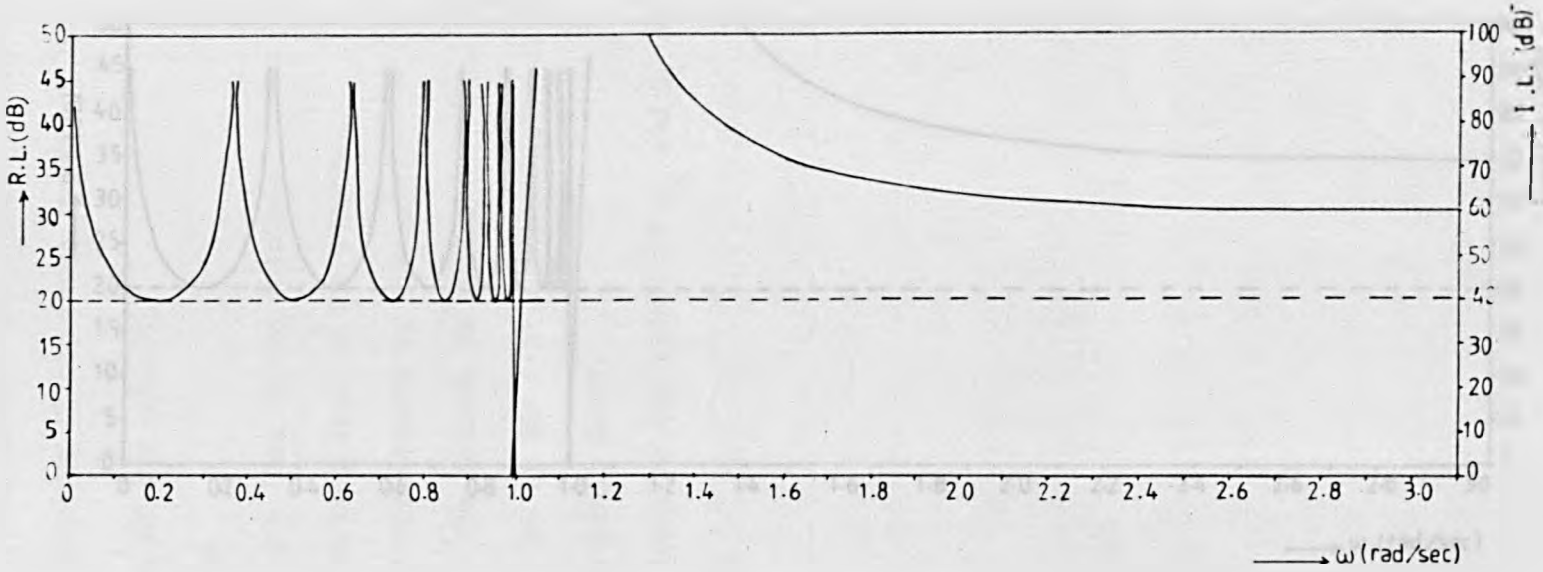

Fig.2.24 Insertion loss (I.L.) and return loss (R.L) response of degree 17 network satisfying a generalized Chebyshev response L_m= 60 dB, R.L.= 20 dB

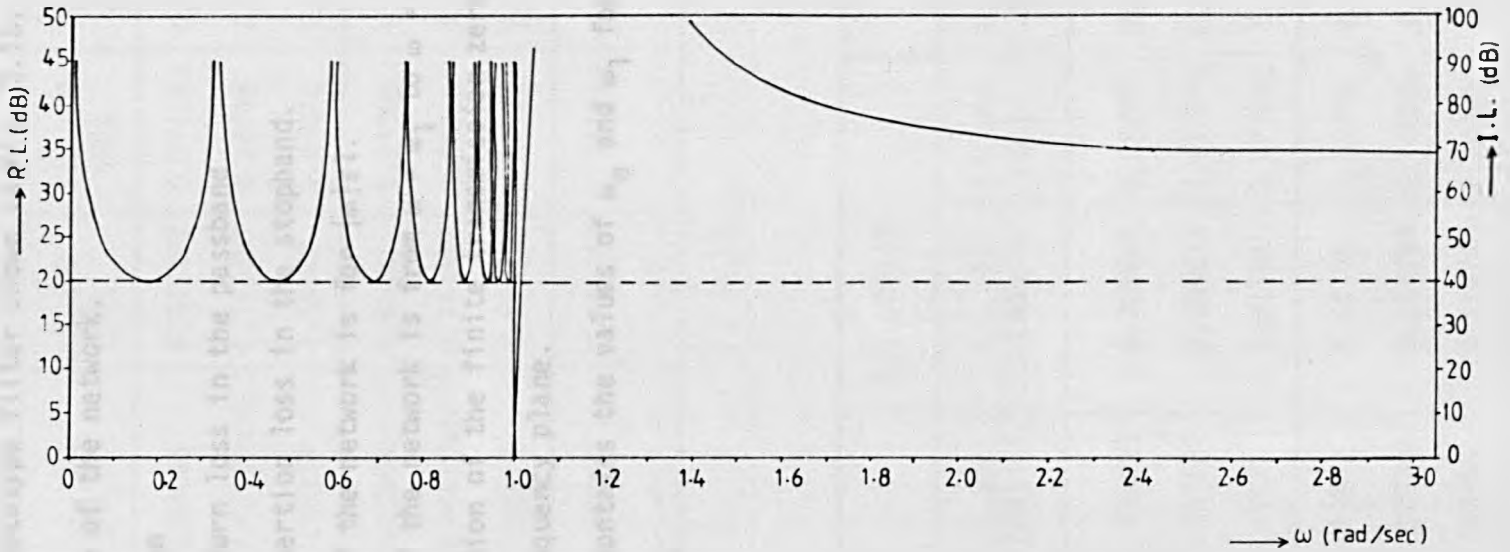

Fig. 2.25 Insertion loss and return loss response of a network originally designed to satisfy the specification given in Fig. 2.24, after adding one section at the middle

Key To The Tables

Table (1→8) contain the element values for different degrees of the low-pass prototype filter shown in Fig. 2.18.

N is the degree of the network.

R is the section

R.L. is the return loss in the passband

I.L. is the insertion loss in the stopband.

The passband of the network is for $|\omega| \leq 1$.

The stopband of the network is from $\omega = \omega_1$ to $\omega = \infty$.

ω_0 is the location of the finite transmission zero on the j -axis of the complex frequency plane.

Table No. (9) contains the values of ω_0 and ω_1 for the different specifications.

TABLE (1)

N = 5		R.L.≥20(dB)			R.L.≥26(dB)		
R	element	I.L.≥60 (dB)	I.L.≥50 (dB)	I.L.≥40 (dB)	I.L.≥60 (dB)	I.L.≥50 (dB)	I.L.≥40 (dB)
	$L_o(5)$	0.89085	0.845187	0.774793	0.702537	0.666004	0.608975
5	$L_2(5)$	9.40429×10^{-2}	0.151697	0.24796	7.48542×10^{-2}	0.120903	0.197917
	$C_2(5)$	1.25524	1.19029	1.09216	1.21304	1.15844	1.07507
	$L_o(3)$	1.68008	1.6144	1.51788	1.50242	1.45581	1.3871
3	$L_2(3)$	9.40429×10^{-2}	0.151697	0.24796	7.48542×10^{-2}	0.120903	0.197917
	$C_2(3)$	1.25524	1.19029	1.09216	1.21304	1.15844	1.07507
1	$L_o(1)$	0.89085	0.845187	0.774793	0.702537	0.666004	0.608975

TABLE (2)

N = 7		R.L.≥20(dB)			R.L.≥26(dB)		
R	element	I.L.≥60 (dB)	I.L.≥50 (dB)	I.L.≥40 (dB)	I.L.≥60 (dB)	I.L.≥50 (dB)	I.L.≥40 (dB)
7	$L_o(7)$	0.786251	0.705668	0.59781	0.616933	0.546048	0.449416
	$L_2(7)$	0.267567	0.386612	0.572575	0.228085	0.330539	0.491102
	$C_2(7)$	1.1207	1.01161	0.871735	1.11113	1.01061	0.880119
	$L_o(5)$	1.61077	1.50131	1.36486	1.50415	1.41923	1.31304
5	$L_2(5)$	0.222361	0.311793	0.440692	0.180832	0.253124	0.356454
	$C_2(5)$	1.34854	1.25436	1.13261	1.40148	1.31969	1.21258
	$L_o(3)$	1.61077	1.50131	1.36486	1.50415	1.41923	1.31304
3	$L_2(3)$	0.267567	0.386612	0.572575	0.228086	0.330539	0.491102
	$C_2(3)$	1.1207	1.01161	0.871735	1.11113	1.01061	0.880119
1	$L_o(1)$	0.786251	0.705668	0.59781	0.616933	0.546048	0.449416

TABLE (3)

N = 9		R.L≥20(dB)			R.L.≥26(dB)		
R	element	I.L.≥60 (dB)	I.L.≥50 (dB)	I.L.≥40 (dB)	I.L.≥60 (dB)	I.L.≥50 (dB)	I.L.≥40 (dB)
9	$L_o(9)$	0.644682	0.544275	0.418398	0.482705	0.388214	0.266948
	$L_2(9)$	0.500829	0.691391	0.990478	0.448353	0.622573	0.898558
	$C_2(9)$	0.934737	0.808492	0.661355	0.93117	0.80858	0.664228
7	$L_o(7)$	1.43923	1.31699	1.18012	1.3741	1.2757	1.16659
	$L_2(7)$	0.38518	0.506465	0.674728	0.322058	0.421909	0.558494
	$C_2(7)$	1.21539	1.1037	0.970846	1.29633	1.19315	1.06867
5	$L_o(5)$	1.49928	1.3644	1.20707	1.45196	1.33938	1.20668
	$L_2(5)$	0.38518	0.506465	0.674728	0.322058	0.421909	0.558494
	$C_2(5)$	1.21539	1.1037	0.970846	1.29633	1.19315	1.06867
3	$L_o(3)$	1.43923	1.31699	1.18012	1.3741	1.2757	1.16659
	$L_2(3)$	0.500829	0.691391	0.990478	0.448353	0.622573	0.898558
	$C_2(3)$	0.934737	0.808492	0.661355	0.93117	0.80858	0.664228
1	$L_o(1)$	0.644682	0.544275	0.418398	0.482705	0.388214	0.266948

TABLE (4)

N = 11		R.L.≥20(dB)			R.L.≥26(dB)		
R	element	I.L.≥60 (dB)	I.L.≥50 (dB)	I.L.≥40 (dB)	I.L.≥60 (dB)	I.L.≥50 (dB)	I.L.≥40 (dB)
11	$L_o(11)$	0.50507	0.394402	0.259439	0.340444	0.230296	9.19182×10^{-2}
	$L_2(11)$	0.782383	1.06259	1.51523	0.730409	1.00277	1.45156
	$C_2(11)$	0.762399	0.636015	0.497766	0.752568	0.626214	0.487296
9	$L_o(9)$	1.27764	1.16099	1.04028	1.23913	1.14543	1.05203
	$L_2(9)$	0.557858	0.708652	0.917621	0.475431	0.60097	0.772211
	$C_2(9)$	1.06925	0.953674	0.821938	1.15618	1.04489	0.915995
7	$L_o(7)$	1.33125	1.19351	1.04132	1.3107	1.19145	1.05863
	$L_2(7)$	0.545154	0.689826	0.886124	0.461143	0.580255	0.738673
	$C_2(7)$	1.09416	0.979701	0.851153	1.192	1.08219	0.957584
5	$L_o(5)$	1.33125	1.19351	1.04132	1.3107	1.19145	1.05863
	$L_2(5)$	0.557858	0.708652	0.917621	0.475431	0.60097	0.772211
	$C_2(5)$	1.06925	0.953674	0.821938	1.15618	1.04489	0.915995
3	$L_o(3)$	1.27764	1.16099	1.04028	1.23913	1.14543	1.05203
	$L_2(3)$	0.782383	1.06259	1.51523	0.730409	1.00277	1.45156
	$C_2(3)$	0.762399	0.636015	0.497766	0.752568	0.626214	0.487296
1	$L_o(1)$	0.50507	0.394402	0.259439	0.340444	0.230296	9.19182×10^{-2}

TABLE (5)

N = 13		R.L.≥20(dB)			R.L.≥26(dB)		
R	element	I.L.≥60 (dB)	I.L.≥50 (dB)	I.L.≥40 (dB)	I.L.≥60 (dB)	I.L.≥50 (dB)	I.L.≥44.4 (dB)
13	$L_0(13)$	0.377667	0.26111	0.119979	0.203178	8.09507×10^{-2}	0.000000
	$L_2(13)$	1.11432	1.51126	2.17528	1.08375	1.49632	1.840330
	$C_2(13)$	0.618399	0.499843	0.376128	0.598405	0.478328	0.408889
11	$L_0(11)$	1.14686	1.04349	0.943709	1.12863	1.04896	1.008050
	$L_2(11)$	0.733459	0.914577	1.16974	0.633633	0.786007	0.894539
	$C_2(11)$	0.939512	0.82595	0.699457	1.0235	0.910592	0.841206
9	$L_0(9)$	1.17922	1.04781	0.908234	1.17235	1.05629	0.988051
	$L_2(9)$	0.709398	0.877742	1.10576	0.60624	0.744918	0.840395
	$C_2(9)$	0.971378	0.860611	0.739932	1.06974	0.96082	0.895402
7	$L_0(7)$	1.1893	1.05497	0.910559	1.1864	1.06688	0.995779
	$L_2(7)$	0.709398	0.877742	1.10576	0.60624	0.744918	0.840395
	$C_2(7)$	0.971378	0.860611	0.739932	1.06974	0.96082	0.895402
5	$L_0(5)$	1.17922	1.04781	0.908234	1.17235	1.05629	0.988051
	$L_2(5)$	0.733459	0.914577	1.16974	0.633633	0.786007	0.894539
	$C_2(5)$	0.939512	0.82595	0.699457	1.0235	0.910592	0.841206
3	$L_0(3)$	1.14686	1.04349	0.943709	1.12863	1.04896	1.008050
	$L_2(3)$	1.11432	1.51126	2.17528	1.08375	1.49632	1.840330
	$C_2(3)$	0.618399	0.499843	0.376128	0.598405	0.478328	0.408889
1	$L_0(1)$	0.377667	0.26111	0.119979	0.203178	8.09507×10^{-2}	0.000000

TABLE (6)

N = 15		R.L.≥20 (dB)			R.L.≥26 (dB)	
R	element	I.L.≥60 (dB)	I.L.≥50 (dB)	I.L.≥40 (dB)	I.L.≥60 (dB)	I.L.≥54.28 (dB)
15	$L_o(15)$	0.263531	0.142742	4.34057×10^{-2}	7.37286×10^{-2}	0.000000
	$L_2(15)$	1.50353	2.05244	2.65354	1.52631	1.84187
	$C_2(15)$	0.502423	0.394767	0.318868	0.4724	0.409424
13	$L_o(13)$	1.04645	0.958726	0.902256	1.04665	1.00962
	$L_2(13)$	0.910809	1.1253	1.32799	0.795546	0.89438
	$C_2(13)$	0.829381	0.72002	0.63715	0.906332	0.84316
11	$L_o(11)$	1.05262	0.931096	0.843625	1.05339	0.991252
	$L_2(11)$	0.872537	1.06455	1.23813	0.751377	0.837903
	$C_2(11)$	0.86576	0.761107	0.683394	0.95961	0.899991
9	$L_o(9)$	1.06299	0.936686	0.844274	1.0682	1.00298
	$L_2(9)$	0.866998	1.05645	1.22631	0.745017	0.830259
	$C_2(9)$	0.871291	0.766941	0.68998	0.967803	0.908277
7	$L_o(7)$	1.06299	0.936686	0.844274	1.0682	1.00298
	$L_2(7)$	0.872537	1.06455	1.23813	0.751377	0.837903
	$C_2(7)$	0.86576	0.761107	0.683394	0.95961	0.899991
5	$L_o(5)$	1.05262	0.931096	0.843625	1.05339	0.991252
	$L_2(5)$	0.910809	1.1253	1.32799	0.795546	0.89438
	$C_2(5)$	0.829381	0.72002	0.63715	0.906332	0.84316
3	$L_o(3)$	1.04645	0.958726	0.902256	1.04665	1.00962
	$L_2(3)$	1.50353	2.05244	2.65354	1.52631	1.84187
	$C_2(3)$	0.502423	0.394767	0.318868	0.4724	0.409424
1	$L_o(1)$	0.263531	0.142742	4.34057×10^{-2}	7.37286×10^{-2}	0.000000

TABLE (7)

	N = 17	R.L.≥20 (dB)		R.L.≥26(dB)
R	Element	I.L.≥60 (dB)	I.L.≥50 (dB)	I.L.≥64 (dB)
17	$L_o(17)$	0.161439	3.69278×10^{-2}	0.00000
	$L_2(17)$	1.95691	2.69927	1.84298
	$C_2(17)$	0.410484	0.314437	0.409755
15	$L_o(15)$	0.971446	0.899493	1.01058
	$L_2(15)$	1.09013	1.34192	0.89449
	$C_2(15)$	0.736867	0.632489	0.844248
13	$L_o(13)$	0.949788	0.839276	0.992952
	$L_2(13)$	1.03277	1.24849	0.837039
	$C_2(13)$	0.77779	0.679824	0.902194
11	$L_o(11)$	0.957438	0.840482	1.00646
	$L_2(11)$	1.02282	1.23337	0.826949
	$C_2(11)$	0.785354	0.688154	0.913202
9	$L_o(9)$	0.960208	0.841718	1.01056
	$L_2(9)$	1.02282	1.23337	0.826949
	$C_2(9)$	0.785354	0.688154	0.913202
7	$L_o(7)$	0.957438	0.840482	1.00646
	$L_2(7)$	1.03277	1.24849	0.837039
	$C_2(7)$	0.77779	0.679824	0.902194
5	$L_o(5)$	0.949788	0.839276	0.992952
	$L_2(5)$	1.09013	1.34192	0.89449
	$C_2(5)$	0.736867	0.632489	0.844248
3	$L_o(3)$	0.971446	0.899493	1.01058
	$L_2(3)$	1.95691	2.69927	1.84298
	$C_2(3)$	0.410484	0.314437	0.409755
1	$L_o(1)$	0.161439	3.69278×10^{-2}	0.00000

TABLE (8).

N = 19		R.L.≥20 (dB)		R.L.≥26(dB)
R	Element	I.L.≥60 (dB)	I.L.≥5C (dB)	I.L.≥73.8 (dB)
19	$L_o(19)$	7.01418×10^{-2}	2.58668×10^{-2}	0.000000
	$L_2(19)$	2.47716	2.77852	1.843780
	$C_2(19)$	0.338366	0.306852	0.409976
17	$L_o(17)$	0.916813	0.894362	1.011150
	$L_2(17)$	1.27072	1.3668	0.894733
	$C_2(17)$	0.659616	0.623791	0.844838
15	$L_o(15)$	0.867497	0.830341	0.993900
	$L_2(15)$	1.18825	1.26911	0.836653
	$C_2(15)$	0.705396	0.671807	0.903486
13	$L_o(13)$	0.871112	0.831443	1.008500
	$L_2(13)$	1.1737	1.25149	0.825451
	$C_2(13)$	0.714142	0.681263	0.915747
11	$L_o(11)$	0.87399	0.834233	1.014340
	$L_2(11)$	1.17116	1.24544	0.823168
	$C_2(11)$	0.71569	0.684576	0.918287
9	$L_o(9)$	0.87399	0.834233	1.014340
	$L_2(9)$	1.1737	1.25149	0.825451
	$C_2(9)$	0.714142	0.681263	0.915747
7	$L_o(7)$	0.871112	0.831443	1.008500
	$L_2(7)$	1.18825	1.26911	0.836653
	$C_2(7)$	0.705396	0.671807	0.903486
5	$L_o(5)$	0.867497	0.830341	0.993900
	$L_2(5)$	1.27072	1.3668	0.894733
	$C_2(5)$	0.659616	0.623791	0.844838
3	$L_o(3)$	0.916813	0.894362	1.011150
	$L_2(3)$	2.47715	2.77852	1.843780
	$C_2(3)$	0.338366	0.306852	0.409976
1	$L_o(1)$	7.01418×10^{-2}	2.58668×10^{-2}	0.000000

TABLE (9)

Degree	RADIAN Frequency	R.L.≥ 20(dB)			R.L. ≥ 26(dB)		
		I.L.≥60 (dB)	I.L.≥50 (dB)	I.L.≥40 (dB)	I.L.≥60 (dB)	I.L.≥50 (dB)	I.L.≥40 (dB)
5	ω_0	2.91054	2.35334	1.92161	3.31859	2.67205	2.16790
	ω_1	2.42435	1.97656	1.63445	2.75453	2.23212	1.82887
7	ω_0	1.82616	1.59903	1.41544	1.98641	1.7302	1.52105
	ω_1	1.52581	1.35817	1.2278	1.64656	1.45437	1.30204
9	ω_0	1.46154	1.33752	1.23555	1.54766	1.40943	1.2944
	ω_1	1.24632	1.16429	1.10137	1.30556	1.21129	1.13705
11	ω_0	1.29479	1.21642	1.15146	1.34879	1.26194	1.18901
	ω_1	1.13086	1.08535	1.05122	1.16412	1.11133	1.07046
13							I.L.≥44.4 (dB)
	ω_0	1.20465	1.15057	1.10554	1.24176	1.18202	1.152787
	ω_1	1.07552	1.04829	1.02833	1.09571	1.06377	1.04939
15						I.L.≥54.28 (dB)	
	ω_0	1.15056	1.11095	1.08713	1.17767	1.151554	
	ω_1	1.04636	1.02917	1.02005	1.05929	1.0468	
17					I.L.≥64 (dB)		
	ω_0	1.11575	1.08545		1.15074		
	ω_1	1.02994	1.0186		1.04523		
19					I.L.≥73.8 (dB)		
	ω_0	1.09227	1.0822		1.150182		
	ω_1	1.0202	1.01679		1.04394		

2.7.2. Prototypes Having 3-Transmission Zeros at Infinity.

The doubly terminated low pass prototype network and its dual shown in Fig. 2.26a, b satisfy a generalized Chebyshev response described by:

$$L = 1 + \varepsilon^2 \cosh^2\{(N-3)\cosh^{-1}\left[\omega\left(\frac{\omega_o^2-1}{\omega_o^2-\omega^2}\right)^{\frac{1}{2}}\right] + 3\cosh^{-1}\omega\} \qquad (2.172)$$

where the transmission zeros are of order (N-3) at $\omega = \pm \omega_o$ and three at infinity. N is an odd number equal to the degree of the network. Other symbols have the same definition as in section 2.7.1.

The insertion loss response of this prototype looks similar to that shown in Fig. 2.19. However, ω_m and ω_1 are derived numerically by iteration for the given values of N, L_m and R.L.

If equation (2.172) is written in general from as:

$$L = 1 + \varepsilon^2 F_N^2(\omega) \qquad (2.173)$$

where $F_N(\omega)$ is a general Chebyshev rational function, then ω_m is defined as:

$$\left.\frac{dF_N(\omega)}{d\omega}\right|_{\omega=\omega_m} = 0 \qquad (2.174)$$

yielding,

$$\omega_m^2 = \omega_o^2 + \frac{(N-3)}{3}\omega_o(\omega_o^2-1)^{\frac{1}{2}} \qquad (2.175)$$

After finding these points, the element values can be obtained by using the alternating pole synthesis technique to form either Y_e or Y_o, where $Y_e(Y_o)$ are the duals of $Z_e(Z_o)$ respectively. The synthesis procedure is illustrated in the following example.

Numerical Example No. 2.

Given: The degree N=9, L_m = 60 dB, R.L. = 20 dB

Required to find the element value of the network shown in

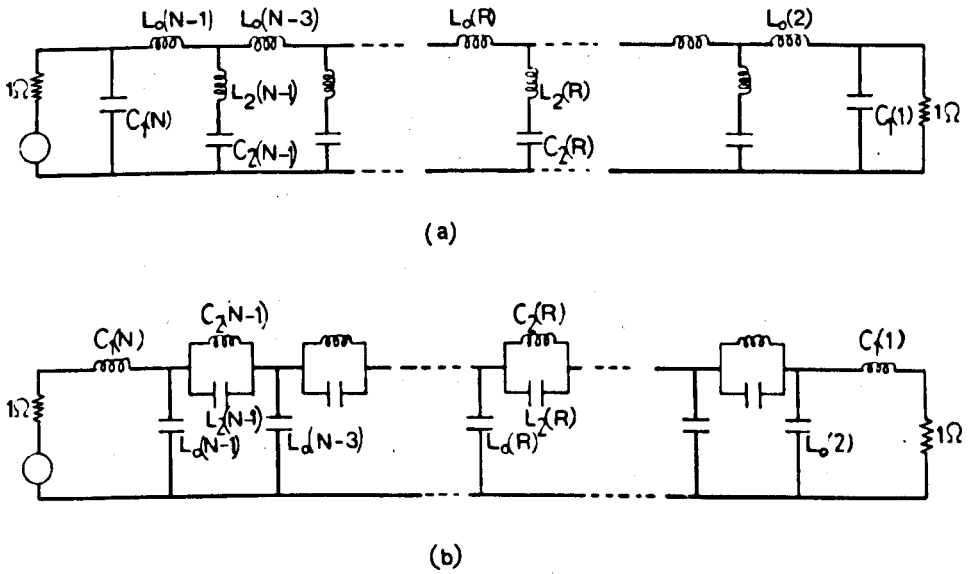

Fig. 2.26 A generalized Chebyshev low-pass prototype filter having 3-transmission zeros at infinity and (N-3) at a finite frequency.
(b) The dual circuit

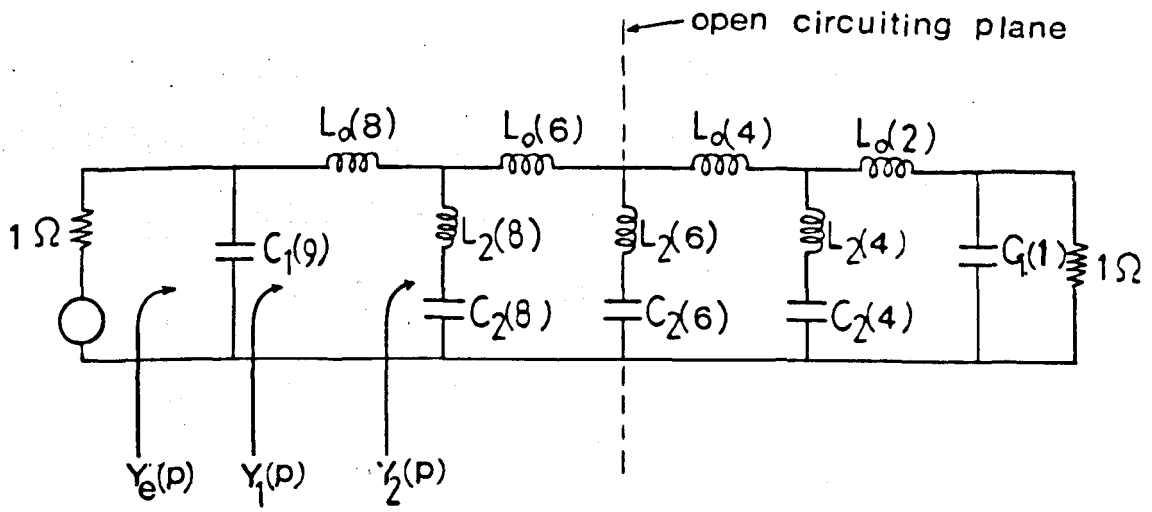

Fig. 2.27 A network of degree 9
"Example No. 2"

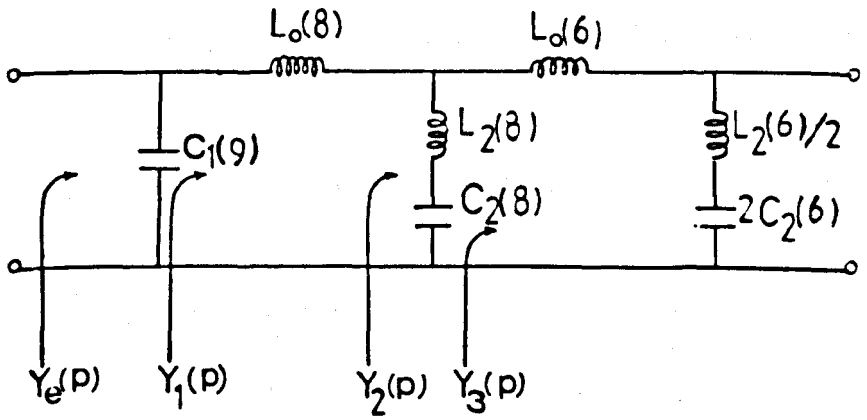

Fig. 2.28 The synthesis cycle of example No. 2

Fig. 2.27.

The constant $\epsilon = 0.1$

The numerical solution gives: $\omega_0 = 1.32599$ rad/sec and the poles of $S_{11}(p)$ as

$$P_{1,9} = -0.0303334 \pm j\ 1.02275$$

$$P_{2,8} = -0.10604 \pm j\ 0.96344$$

$$P_{3,7} = -0.225112 \pm j\ 0.80937$$

$$P_{4,6} = -0.377114 \pm j\ 0.490176$$

$$P_5 = -0.455417$$

The network can be synthesized by constructing Y_e which is obtained by forming a Hurwitz polynomial such as

$$D(p) = [P + 0.0303334 - j\ 1.02275][P + 0.0303334 + j\ 1.02275]$$
$$[P + 0.225112 - j\ 0.80937][P + 225112 + j\ 0.80937]$$
$$[P + 0.455417]$$
$$= 0.455417 + 1.31691P + 1.793\ P^2 + 2.72394\ P^3 + 1.30779\ P^4 + 1.35339\ P^5$$

Rearranging the odd and even terms in P results in $D(p) = O(p) + E(p)$ where

$$O(p) = 1.31691P + 2.72394\ P^3 + 1.35339\ P^5$$

and $$= A(1)\ P + A(3)\ P^3 + A\ (5)\ P^5$$

$$E(p) = 0.455417 + 1.793\ P^2 + 1.30779\ P^4$$

$$= B(0) + B(2)\ P^2 + B(4)\ P^4$$

Hence

$$Y_e(p) = \frac{O(p)}{E(p)}$$

The synthesis procedure commences with the extraction of the shunt capacitor $C_1(9)$ by completely removing a pole at infinity from $Y_e(p)$ to

leave:

$$Y_1(p) = Y_e(p) - C_1(9)\, P$$

where

$$C_1(9) = \left.\frac{Y_e(p)}{P}\right|_{P=\infty} = \frac{A(5)}{B(4)} = 1.03487$$

Hence

$$Y_1(p) = \frac{A_1(1)P + A_1(3)P^3}{B(0)+B(2)P^2+B(4)P^4}$$

$$A_1(1) = A(1) - C_1(9)\, B(0) = 0.845557$$

$$A_1(3) = A(3) - C_1(9)\, B(2) = 0.868418$$

$$Z_1(p) = \frac{1}{Y_1(p)}$$

The series inductance $L_0(8)$ is extracted by a zero shifting step such that

$$L_0(8) = \frac{Z_1(j\omega_0)}{j\omega_0} = \frac{1}{j\omega_0}\,\frac{B(0)-B(2)\omega_0{}^2+B(4)\omega_0{}^4}{jA_1(1)\omega_0-j\,A_1(3)\omega_0{}^3} = 1.12352$$

$$Z_2(p) = Z_1(p) - L_0(8)p$$

$$= \frac{B_1(0)+B_1(2)P^2+B_1(4)P^4}{A_1(1)P+A_1(3)P^3}$$

where

$$B_1(0) = B(0)$$

$$B_1(2) = B(2) - A_1(1)\, L_0(8) = 0.842999$$

$$B_1(4) = B(4) - A_1(3)\, L_0(8) = 0.332105$$

$$Y_2(p) = \frac{1}{Z_2(p)}$$

$$Y_3(p) = Y_2(p) - \frac{P/L_2(8)}{P^2+\omega_0{}^2}$$

$L_2(8)$ can be calculated by finding the residue K_8 at $\pm j\omega_0$ of $Y_2(p)$. Thus

$$K_8 = \left. \frac{A_1(p)\, P + A_1(3)\, P^3}{\frac{d}{dP}\{B_1(0)+B_1(2)P^2+B_1(4)P^4\}^2} \right|_{P = \pm j\omega_o}$$

$$=1.04847$$

$L_2(8) = 1/(2\ K8) = 0.476885$

$C_2(8) = 1/(L_2(8)\ \omega_o^2) = 1.19263$

and the cycle is repeated to obtain the remaining element values of half the network shown in Fig. 2.28. Hence, the element values of the other half are obtained since the network is symmetrical. The complete element values of this example are included in Table (12).

Results.

For the prototype network shown in Fig. 2.26 all the element values provided in Tables (10→15) in this section have been obtained by using the alternating pole technique to construct either Y_e or Y_o whichever has the highest degree. It has been found that networks of degree 5, 9 and 13 can by synthesized by constructing Y_e, while networks of degree 7, 11, and 15 can be synthesized by constructing Y_o. However, in either case the element values may be obtained by using a similar procedure to that used in example No. 2. Table No. (16) contains the values of ω_o and ω_1 for the different specifications and the corresponding element values are given in tables (10→15).

Comparing the values of ω_1 in table (16) with those in table (8) for the same specifications except for the degree 5 case indicates that the generalized Chebyshev low pass prototype with three transmission zeros at infinity is more selective than that having a single transmission zero at infinity.

Key to the Tables

Tables (10→15) contain the element values for different degrees of the low-pass prototype filter shown in Fig. (2.26).

N is the degree of the network.

R is the section.

R.L. is the return loss in the passband.

I.L. is the insertion loss in the stopband.

The passband of the network is for $|\omega| \leq 1$.

The stopband of the network is from $\omega = \omega_1$ to $\omega = \infty$.

ω_o is the location of the finite transmission zero on the j -axis of the complex frequency plane.

Table No. (16) contains the values of ω_o and ω_1 for the different specifications.

Table (10)

N=5		R.L. ≥ 20 dB			R.L. ≥ 26 dB		
R	Element	I.L.≥60 (dB)	I.L.≥50 (dB)	I.L.≥40 (dB)	I.L.≥60 (dB)	I.L.≥50 (dB)	I.L.≥40 (dB)
5	$C_1(5)$	0.97692	0.980116	0.985092	0.771053	0.773927	0.778435
4	$L_o(4)$	1.30282	1.26448	1.2068	1.25245	1.22001	1.17048
	$L_2(4)$	8.54378×10^{-2}	0.138258	0.227543	7.36741×10^{-2}	0.119383	0.196755
	$C_2(5)$	1.62304	1.5241	1.37499	1.4518	1.37501	1.25759
2	$L_o(2)$	1.30282	1.26448	1.2068	1.25245	1.22001	1.17048
1	$C_1(1)$	0.97692	0.980116	0.985022	0.771053	0.773927	0.778435

TABLE(11)

N=7		R.L.≥20(dB)			R.L. ≥26(dB)		
R	Element	I.L.≥60 (dB)	I.L.≥50 (dB)	I.L.≥40 (dB)	I.L.≥60 (dB)	I.L.≥50 (dB)	I.L.≥40 (dB)
7	$C_1(7)$	1.01858	1.02211	1.02647	0.816773	0.820282	0.824706
6	$L_o(6)$	1.2363	1.16791	1.08027	1.21518	1.15125	1.06753
	$L_2(6)$	0.256163	0.3682	0.541922	0.233173	0.335228	0.492702
	$C_2(6)$	1.45916	1.29965	1.10006	1.36698	1.23372	1.06387
4	$L_o(4)$	1.2498	1.1300	0.984147	1.30698	1.19918	1.06617
	$L_2(4)$	0.256163	0.3682	0.541922	0.233173	0.335228	0.492702
	$C_2(4)$	1.45916	1.29965	1.10006	1.36698	1.23372	1.06387
2	$L_o(2)$	1.2363	1.16791	1.08027	1.21518	1.15125	1.06753
1	$C_1(1)$	1.01858	1.02211	1.02647	0.816773	0.820282	0.824706

TABLE (12)

N = 9		R.L. ≥20 (dB)			R.L.≥ 26 (dB)		
R	Element	I.L.≥60	I.L.≥50	I.L.≥40	I.L.≥60	I.L.≥50	I.L.≥40
9	$C_1(9)$	1.03487	1.03721	1.03969	0.83549	0.837985	0.840714
	$L_o(8)$	1.12352	1.04292	0.947416	1.10722	1.0264	0.928279
8	$L_2(8)$	0.476885	0.654003	0.930679	0.450961	0.618263	0.877829
	$C_2(8)$	1.19263	1.01488	0.813568	1.13819	0.980696	0.799104
	$L_o(6)$	1.07413	0.944115	0.8009	1.15782	1.03493	0.898068
6	$L_2(6)$	0.428164	0.569346	0.771466	0.394432	0.521907	0.70086
	$C_2(6)$	1.32834	1.16578	0.98147	1.30131	1.16176	1.00088
	$L_o(4)$	1.07413	0.944115	0.8009	1.15782	1.03493	0.898068
4	$L_2(4)$	0.476885	0.654003	0.930679	0.450961	0.618263	0.877829
	$C_2(4)$	1.19263	1.01488	0.813568	1.13819	0.980696	0.799104
2	$L_o(2)$	1.12352	1.04292	0.947416	1.10722	1.0264	0.928279
1	$C_1(1)$	1.03487	1.03721	1.03969	0.83549	0.837985	0.840714

TABLE(13)

N = 11		R.L. ≥ 20 (dB)			R.L. ≥ 26 (dB)		
R	Element	I.L.≥60 (dB)	I.L.≥50 (dB)	I.L.≥40 (dB)	I.L.≥60 (dB)	I.L.≥50 (dB)	I.L.≥40 (dB)
11	$C_1(11)$	1.0416	1.04297	1.04428	0.843579	0.845115	0.846644
10	$L_o(10)$	1.01792	0.935065	0.840267	0.994819	0.907422	0.804735
	$L_2(10)$	0.729441	0.984313	1.39582	0.710293	0.959304	1.36035
	$C_2(10)$	0.958626	0.787121	0.60441	0.918352	0.760814	0.590439
8	$L_o(8)$	0.908631	0.786767	0.661279	0.995387	0.877259	0.755266
	$L_2(8)$	0.61751	0.794605	1.04755	0.576811	0.736593	0.959128
	$C_2(8)$	1.13239	0.975041	0.80535	1.13087	0.990848	0.837434
6	$L_o(6)$	0.93471	0.807267	0.672323	1.03347	0.908381	0.77411
	$L_2(6)$	0.61751	0.794605	1.04755	0.576811	0.736593	0.959128
	$C_2(6)$	1.13239	0.975041	0.80535	1.13087	0.990848	0.837434
4	$L_o(4)$	0.908631	0.786767	0.661279	0.995387	0.877259	0.755266
	$L_2(4)$	0.729441	0.984313	1.39582	0.710293	0.959304	1.36035
	$C_2(4)$	0.958626	0.787121	0.60441	0.918352	0.760814	0.590439
2	$L_o(2)$	1.01792	0.935065	0.840267	0.994819	0.907422	0.804735
1	$C_1(1)$	1.0416	1.04297	1.04428	0.843579	0.845115	0.846644

TABLE(14)

N = 13		R.L. ≥ 20(dB)		R.L.≥ 26 (dB)	
R	Element	I.L≥ 60 (dB)	I.L.≥50 (dB)	I.L.≥60 (dB)	I.L.≥50 (dB)
13	$C_1(13)$	1.04459	1.04538	0.84729	0.848212
12	$L_o(12)$	0.928797	0.847254	0.894132	0.804545
	$L_2(12)$	1.01275	1.36487	1.01212	1.36929
	$C_2(12)$	0.773517	0.616731	0.736698	0.589614
10	$L_o(10)$	0.778798	0.670841	0.862227	0.756986
	$L_2(10)$	0.810049	1.02504	0.764112	0.958028
	$C_2(10)$	0.96708	0.821198	0.975811	0.842726
8	$L_o(8)$	0.80446	0.687232	0.900696	0.783025
	$L_2(8)$	0.795651	1.00249	0.746468	0.931278
	$C_2(8)$	0.98458	0.839663	0.998876	0.866932
6	$L_o(6)$	0.804469	0.687232	0.900696	0.783025
	$L_2(6)$	0.810049	1.02504	0.764112	0.958028
	$C_2(6)$	0.96708	0.831198	0.975811	0.842726
4	$L_o(4)$	0.778798	0.670841	0.862227	0.756986
	$L_2(4)$	1.01275	1.36487	1.01212	1.36929
	$C_2(4)$	0.773517	0.616731	0.736698	0.589614
2	$L_o(2)$	0.928797	0.847254	0.894132	0.804545
1	$C_1(1)$	1.04459	1.04538	0.84729	0.848212

TABLE(15)

N = 15		R.L.≥20 (dB)	R.L.≥26 (dB)
R	Element	I.L.≥60 dB	I.L.≥60 dB
15	$C_1(15)$	1.04601	0.849109
14	$L_o(14)$	0.85466	0.806586
	$L_2(14)$	1.33100	1.36481
	$C_2(14)$	0.629993	0.59235
12	$L_o(12)$	0.680414	0.759946
	$L_2(12)$	1.00399	0.953938
	$C_2(12)$	0.835194	0.847481
10	$L_o(10)$	0.699487	0.788953
	$L_2(10)$	0.977594	0.921391
	$C_2(10)$	0.857741	0.877417
8	$L_o(8)$	0.704337	0.79654
	$L_2(8)$	0.977594	0.921391
	$C_2(8)$	0.857741	0.877417
6	$L_o(6)$	0.699487	0.788953
	$L_2(6)$	1.00399	0.953938
	$C_2(6)$	0.835194	0.847481
4	$L_o(4)$	0.680414	0.759946
	$L_2(4)$	1.331	1.36481
	$C_2(4)$	0.629993	0.59235
2	$L_o(2)$	0.85466	0.806586
1	$C_1(1)$	1.04601	0.849109

TABLE (16)

		R.L≥ 20(dB)			R.L.≥ 26(dB)		
Degree	Frequency	I.L.≥60 (dB)	I.L.≥50 (dB)	I.L.≥40 (dB)	I.L.≥60 (dB)	I.L.≥50 (dB)	I.L.≥40 (dB)
5	ω_0	2.68541	2.17845	1.7878	3.05766	2.46817	2.01033
	ω_1	2.52739	2.04812	1.69345	2.88554	2.3175	1.90012
7	ω_0	1.63565	1.44559	1.29516	1.77125	1.55497	1.38122
	ω_1	1.4999	1.33773	1.21229	1.61703	1.43071	1.28362
9	ω_0	1.32599	1.22745	1.14922	1.3958	1.28424	1.19397
	ω_1	1.21737	1.14178	1.0848	1.27249	1.18496	1.11696
11	ω_0	1.19586	1.13609	1.08873	1.23816	1.17053	1.1158
	ω_1	1.1087	1.06853	1.03927	1.13856	1.09134	1.05564
13	ω_0	1.12983	1.08995		1.15808	1.11293	
	ω_1	1.05953	1.03646		1.07704	1.04948	
15	ω_0	1.09205			1.11218		
	ω_1	1.03489			1.04574		

2.8 IMPEDANCE AND FREQUENCY SCALING.

In low-pass prototype networks which are the natural results of most synthesis techniques, the values of the terminating resistances are usually regarded to be 1 ohm and the cut off frequency is at ω equal 1 rad/sec. However, the values of the LC elements of such networks are impractical and are rarely, if ever, encountered in real life. However, their use simplifies the arithmetical calculations and make the tabulation of the element values more meaningful. If the prototype network designed to work at 1 ohm impedance level at one or more ports and then required to work at a practical level of R_o ohm, the conversion is called "impedance scaling". This simply means multiplying the terminating resistances by R_o and each inductor L becomes R_oL and each capacitor C becomes C/R_o.

On the other hand the "frequency scaling" is also a straightforward operation which transforms the cutoff frequency of the low-pass prototype from ω equal 1 rad/sec to the required value ω_o rad/sec. Since the resistances in the network, are frequency independent, they remain unchanged by the frequency scaling, but the reactive elements must be changed, hence an inductor of impedance ωL is transformed to $\frac{\omega}{\omega_o}L$, similarly a capacitor of impedance $1/\omega C$ is changed to $\frac{\omega_o}{\omega C}$, i.e.

$$L \rightarrow L/\omega_o \quad , \qquad C \rightarrow C/\omega_o$$

If the impedance and frequency scaling are required simultaneously, all the resistances in the network must be multiplied by R_o, all the inductors by R_o/ω_o and all capacitors by $1/\omega_o R_o$.

2.9 FREQUENCY TRANSFORMATION

Electric filters may be categorized according to the location of their passbands or stopbands on the $j\omega$-axis into four main types, the low-pass, the high-pass, the band-pass and band-stop filters. However, the

low-pass case can be easily adapted to other cases by means of different transformations of the lumped complex frequency variable. Let $p'=\sigma'+j\omega'$ be the complex frequency variable for the normalized (cut off at $\omega = 1$) low-pass function and $p = \sigma + j\omega$ be the new complex frequency variable. Hence the frequency transformation is a function of the form

$$p' = f(p) \tag{2.176}$$

which maps one or several frequency ranges of interest to the frequency range of the passband of the low-pass characteristics. Thus, in moving the passband, the different types of filter characteristics can be obtained and the desired network is obtained from the low-pass one by replacing each inductance L by a one-port whose impedance is $Lf(p)$, and each capacitance C by a one-port whose admittance is $Cf(p)$.

2.9.1. Low-Pass To High-Pass Transformation.

The transformation

$$p' = \frac{\omega_o}{p} \tag{2.177}$$

is used to transform the normalized low-pass to high-pass, which maps the interval from $j\omega_o$ to $+\infty$ in the p-plane into the interval $-j1$ to 0 in the p'-plane, and from $-j\omega_o$ to $-\infty$ in the p-plane into $j1$ to 0 in the p'-plane and vice versa as indicated in Fig. 2.29.

If L' and C' represent the inductance and capacitance in the normalized low-pass network, then the high pass element L_h and C_h can be obtained by

$$\left.\begin{aligned} L'p' \rightarrow L' \frac{\omega_o}{p} &= \frac{1}{C_h p} \\ \frac{1}{C'p'} \rightarrow \frac{1}{C'} \frac{\omega_o}{p} &= L_h p \end{aligned}\right\} \tag{2.178}$$

where

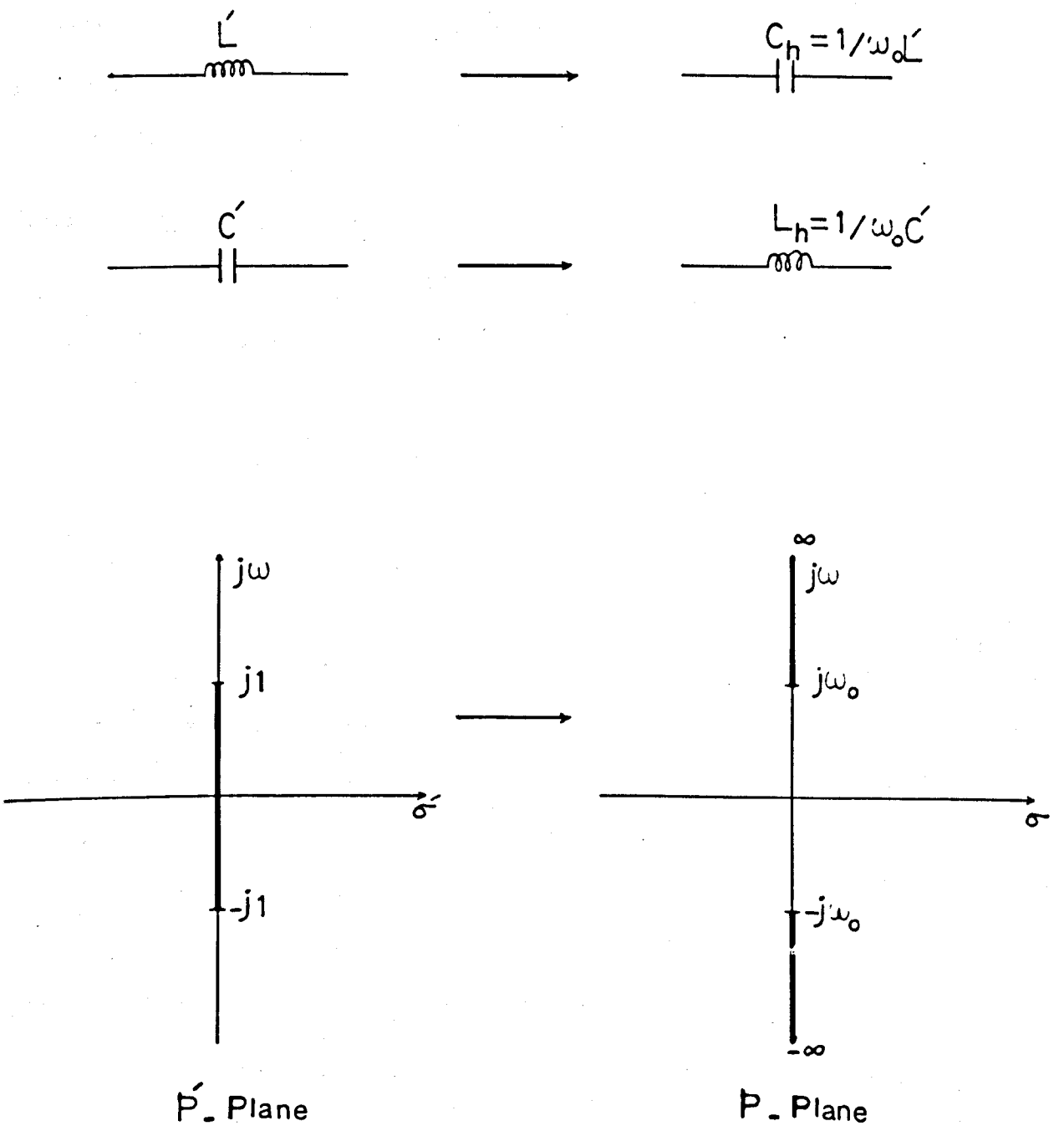

Fig. 2.29 Transformation from low-pass to high-pass

$$C_h = 1/\omega_o L' \quad \text{and} \quad L_h = 1/\omega_o C' \tag{2.179}$$

Thus, to obtain a high pass network from its corresponding normalized low-pass realization, each inductance L' is simply replaced by a capacitance C_h and each capacitance C' is replaced by an inductance L_h. If the high-pass network is also required to be normalized i.e. $\omega_o=1$, then the relationships given in (2.179) become simple inverse.

2.9.2. Low-Pass To Bandpass Transformation.

The transformation from the normalized low-pass to band-pass can be achieved by considering the transformation

$$p' = \frac{\omega_o}{B}\left[\frac{p}{\omega_o} + \frac{\omega_o}{p}\right] \tag{2.180}$$

where

$$\omega_o = \sqrt{\omega_1\omega_2} \tag{2.181}$$

$$B = \omega_2 - \omega_1 \tag{2.182}$$

ω_2 and ω_1 are the upper and lower passband edge frequencies, ω_o is the geometric midband frequency and B is the bandwidth. The quantity B/ω_o is an important bandpass filter design parameter and it is known as "the relative bandwidth". This transformation maps the interval $j\omega_1$ to $j\omega_2$ and $-j\omega_1$ to $-j\omega_2$ in the p-plane into the interval -jl to jl in the p'-plane as indicated in Fig. 2.30.

The required band-pass network is obtained by replacing each element in the normalized low-pass by a one-port whose impedance at any point in the band-pass interval is the same as the impedance of the replaced element at the corresponding point in the low-pass interval.

i.e.
$$\left.\begin{aligned} L'p' &= L'\frac{\omega_o}{B}\left[\frac{p}{\omega_o} + \frac{\omega_o}{p}\right] \\ &= \frac{L'}{B}p + \frac{L'}{B}\omega_o^2\frac{1}{p} \\ &= L_{b1}p + \frac{1}{C_{b1}p} \end{aligned}\right\} \tag{2.183}$$

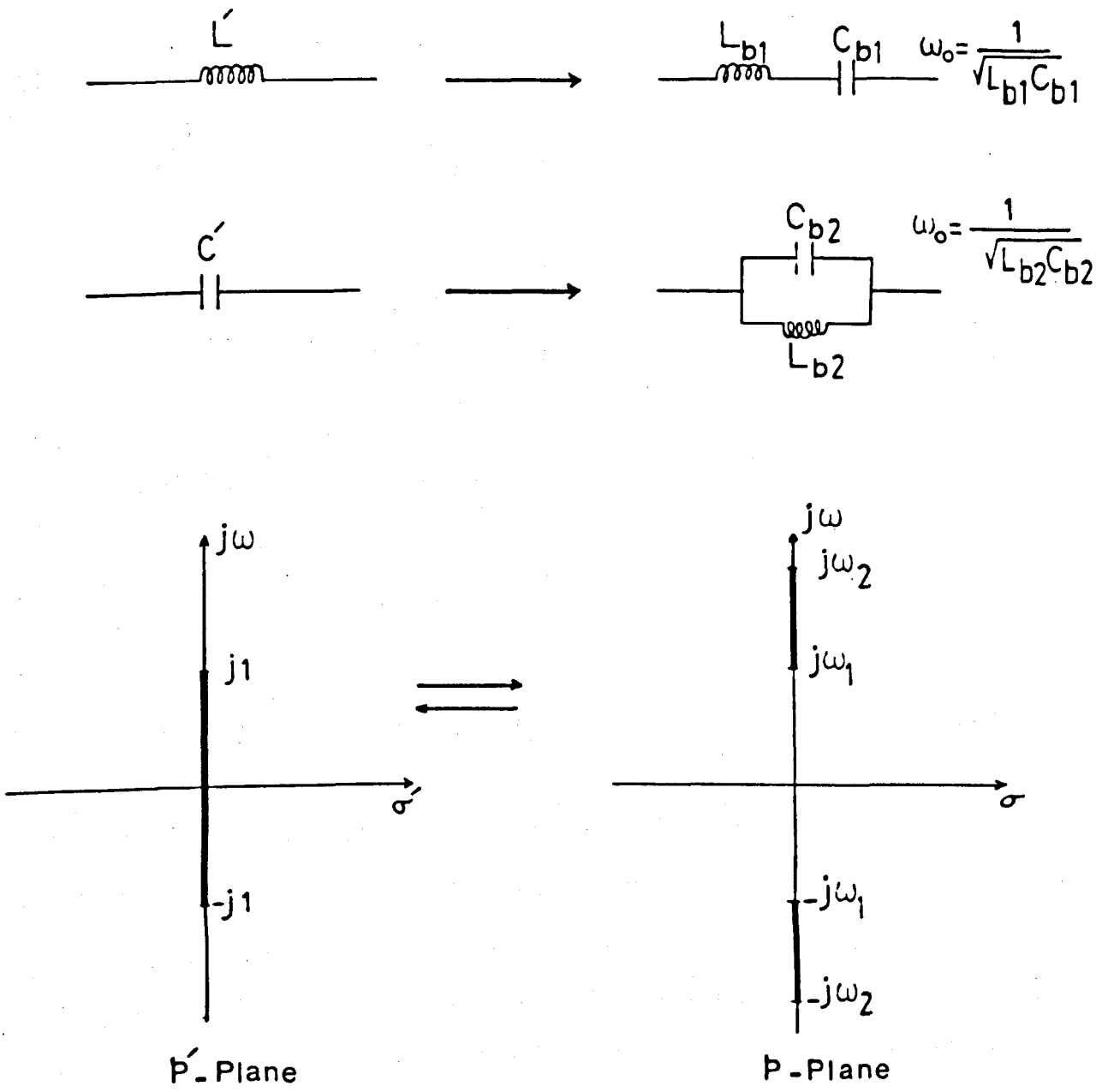

Fig. 2.30 Transformation from low-pass to band-pass

where

$$L_{b1} = \frac{L'}{B} \quad \text{and} \quad C_{b1} = \frac{B}{L'\omega_o^2} \tag{2.184}$$

Similarly,

$$\left.\begin{aligned} \frac{1}{C'p'} &= \frac{1}{C'\frac{\omega_o}{B}\left(\frac{p}{\omega_o} + \frac{\omega_o}{p}\right)} \\ &= \frac{1}{\frac{C'}{B}p + \frac{C'\omega_o^2}{B}\frac{1}{p}} \end{aligned}\right\} \tag{2.185}$$

Hence

$$\left.\begin{aligned} C'p' &= \frac{C'}{B}p + \frac{C'\omega_o^2}{B}\frac{1}{p} \\ &= C_{b2}p + \frac{1}{L_{b2}p} \end{aligned}\right\}$$

where

$$C_{b2} = \frac{C'}{B} \quad \text{and} \quad L_{b2} = \frac{B}{C'\omega_o^2} \tag{2.186}$$

Thus, it can be concluded from the above relationships that, to obtain a bandpass network from its corresponding normalized low-pass, each inductance L' in the low pass is replaced by a series combination of an inductor with inductance L_{b1} and a capacitor with a capacitance C_{b1} meanwhile each capacitance C' in the low-pass is replaced by a parallel combination of an inductor with inductance L_{b2} and a capacitor with a capacitance C_{b2} as shown in Fig. 2.30.

If it is required to transform the normalized low pass to a normalized bandpass (the most convenient normalization is $\omega_o = 1$) then the transformation given in (2.180) becomes

$$p' = a\,(p'' + 1/p'') \tag{2.187}$$

where $p'' = \sigma'' + j\omega''$

or

$$\omega' = a(\omega'' - 1/\omega'') \tag{2.188}$$

where

$$\omega'' = \frac{\omega}{\omega_0} \tag{2.189}$$

Thus,

$$\omega_1'' = 1/\omega_2'' \tag{2.190}$$

$$a = \frac{1}{\omega_2'' - \omega_1''} \tag{2.191}$$

ω_1'' and ω_2'' are the lower and upper normalized bandedge frequencies, and consequently the normalized bandpass network is obtained.

When the low-pass contains resonant branches as in the generalized Chebyshev cases, the direct transformation results in unappropriate combinations of elements for practical applications. Hence, it must be replaced by the equivalent preferred structure derived in [26], [9] and shown in Fig. 2.31 a,b , where a parallel resonant circuit forming a series branch in the lowpass is transformed into two parallel circuits connected in series in the bandpass structure and a series resonant circuit forming a shunt branch in the low-pass is transformed into two shunt connected, series resonant circuits in the band pass. The normalized element values of the preferred structure are given by [9].

$$\left.\begin{aligned} C^+ &= \frac{1}{L^-} = a\,C'\,(1+\ \omega_r^{2}-) \\ C^- &= \frac{1}{L^+} = a\,C'\,(1+\omega_r^{2}+) \\ L^+ &= \frac{1}{C^-} = a\,L'\,(1+\omega^2{}_r-) \\ L^- &= \frac{1}{C^+} = a\,L'\,(1+\omega^2{}_r+) \end{aligned}\right\} \tag{2.192}$$

where

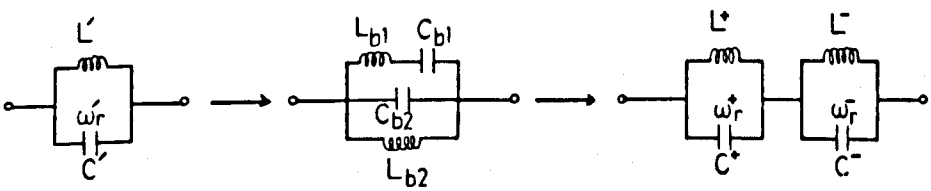

(a)

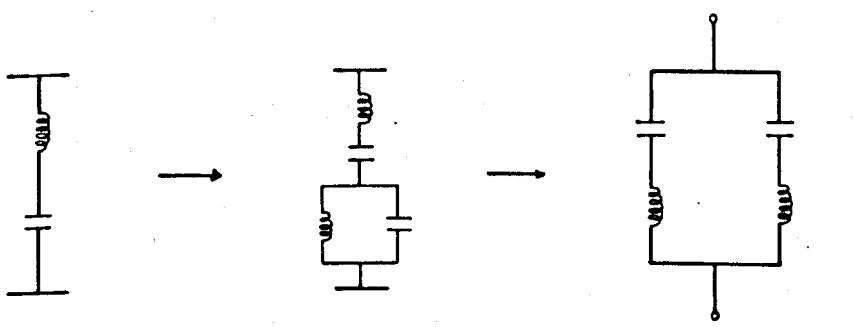

Low pass

Direct band pass structure

Preferred band pass structure

(b)

Fig. 2.31 Transformation of low pass resonant section to band pass equivalent circuit

(a) A typical section

(b) Dual section

$$\omega_r^{\pm} = \sqrt{1 + \left(\frac{\omega_r}{2a}\right)^2} \pm \frac{\omega_r}{2a} \tag{2.193}$$

$$\omega_r = \frac{1}{\sqrt{L'C'}} \tag{2.194}$$

and equation (2.193) is a special case of the general expression obtained by solving equation (2.186) for ω'' (the bandpass normalized real frequency) in terms of ω' (the low pass normalized real frequency) and is given by

$$\omega'' = \sqrt{1 + \left(\frac{\omega'}{2a}\right)^2} \pm \frac{\omega'}{2a} \qquad 0 < \omega' < \infty \tag{2.195}$$

Hence, equation (2.193) gives the two resonant frequencies $\omega_r^{\pm}$ of the preferred bandpass structure as a direct result of substituting the low-pass resonant frequency ω_r.

2.9.3. Low-Pass to Band-Stop Transformation

The frequency transformation required in this case is given by

$$p' = \frac{1}{\frac{\omega_0}{B}\left(\frac{p}{\omega_0} + \frac{\omega_0}{p}\right)} \tag{2.196}$$

which maps the desired intervals $-j\omega_1$ to $-j\omega_2$ and $j\omega_1$ to $+j\omega_2$ in the p-plane into the interval -jl to +jl in the p'-plane and vice versa, as shown in Fig. 2.32 and all the symbols have the same definitions as in the band pass case (section 2.9.2.). Here, $(\omega_2 - \omega_1)$ means the band width of the stopband. Using a similar argument to that in the previous section the bandstop network can be obtained from its corresponding normalized low-pass realization if each inductance L' in the low-pass is replaced by a parallel combination of an inductor with inductance L_{s1} *and a capacitor of* Capacitance C_{s1} *and in the same time each* capacitance C' in the low-pass realization is replaced by a series combination of an inductor with inductance L_{s2} and a capacitor of capacitance C_{s2}, whose

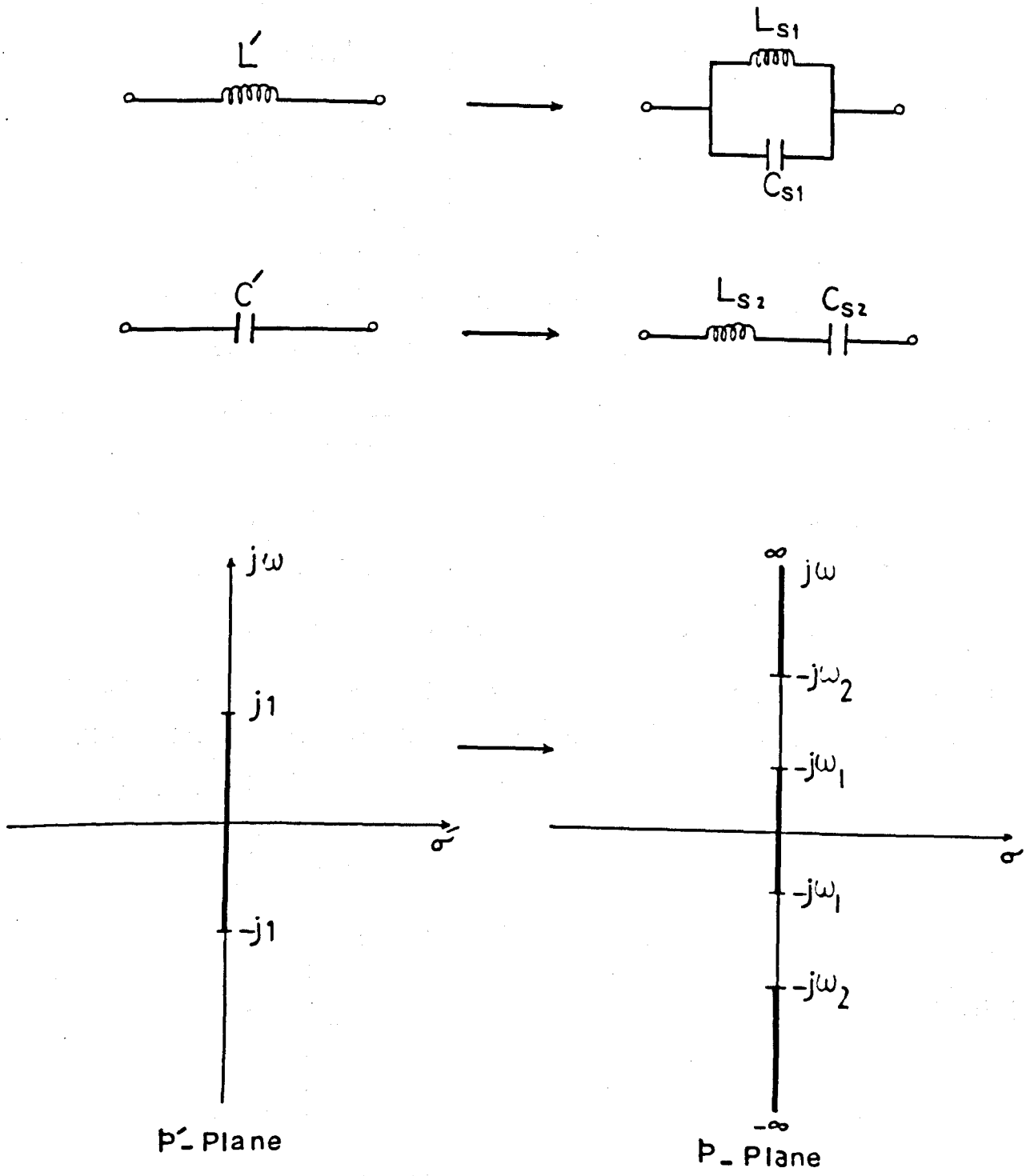

Fig. 2.32 Transformation from low-pass to band-stop

values are given by:

$$\left.\begin{aligned} L_{s1} &= L'B/\omega_o{}^2 \\ C_{s1} &= 1/L'B \\ L_{s2} &= 1/C'B \\ C_{s2} &= C'B/\omega_o{}^2 \end{aligned}\right\} \qquad (2.197)$$

However, if a normalized bandstop is required, then the most convenient normalization is to set ω_o equal 1. Hence the transformation given in (2.196) becomes

$$p' = \frac{1}{a(p''+1/p'')} \qquad (2.198)$$

and the normalized element values can be obtained by replacing B in equation (2.197) by 1/a with $\omega_o = 1$

When a low pass realization containing resonant branches is required to be transformed into the preferred bandstop structure shown in Fig. 2.33, the following formulas for the normalized element values maybe used [26], [9] .

$$\begin{aligned} C_s^- &= \frac{a}{L'}(1 + \omega_{rs}^{2+}) \\ C_s^+ &= \frac{a}{L'}(1 + \omega_{rs}^{2-}) \\ L_s^- &= \frac{1}{C_s^-} \\ L_s^+ &= \frac{1}{C_s^+} \end{aligned} \qquad (2.199)$$

where

$$\omega_{rs}^{\pm} = \sqrt{1 + \left(\frac{1}{2\omega_r a}\right)^2} \pm \left(\frac{1}{2\omega_r a}\right) \qquad (2.200)$$

which is the analogous form of that of the normalized bandpass filter given in (2.194).

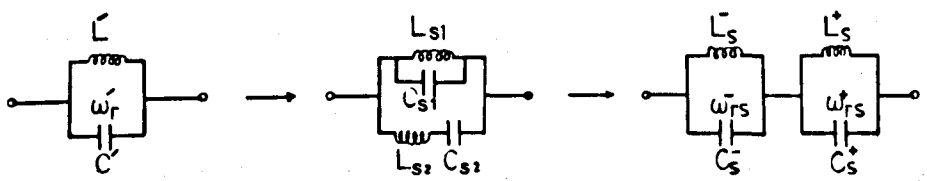

(a)

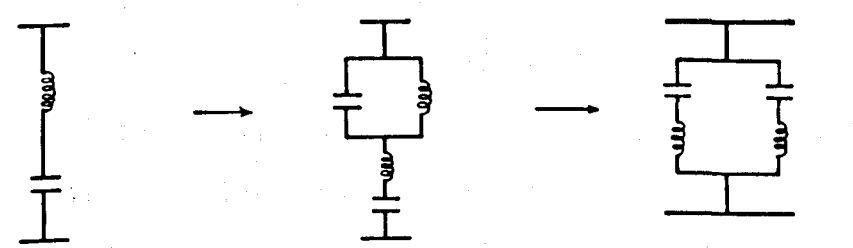

Low-pass

Direct band-stop structure

Preferred band-stop structure

(b)

Fig. 2.33 Transformation of low-pass resonant section to band-stop equivalent circuit

(a) A typical section

(b) Dual section

2.10 CONCLUDING REMARKS.

This chapter starts by reviewing what is considered to be the three most popular amplitude approximation methods. Special attention is given to the equiripple type. Several design methods for different prototype filters have been included ranging from the explicit formulas to the computerized synthesis methods. The synthesis accuracy problem is discussed and a relatively new solution has been adopted and terms the alternating pole technique. A comparison of this technique with the z-transformed variable technique is illustrated.

Each filter discussed in this chapter has been chosen for its merit to act as a prototype channel filter in an interacting channel filter multiplexer. For example, the modified low-pass prototype will be used later in designing a bandpass channel multiplexer which in turn may be realized in a waveguide structure for microwave applications. The generalized Chebyshev response is also discussed and new classes of very selective filters satisfying this response are introduced, their properties and applications are given and new tables of the element values for typical requirements are provided. Additionally, since this chapter concentrated on the low-pass prototype filters, it was logical to devote some space to the transformation of the low-pass into the other main types of filters such as the high-pass, band-pass and band-stop filters. The transformation of the modified low-pass prototype which contains inverters will be discussed later in this thesis.

CHAPTER 3

DESIGN PROCEDURE FOR BAND-PASS CHANNEL MULTIPLEXERS CONNECTED AT A COMMON JUNCTION.

3.1 BASIC CONCEPTS

Filters are at the heart of multichannel systems and a large percentage of the manufactured filters are used in these systems especially in the microwave region of the frequency spectrum. Nowadays the applications of the multichannel systems are numerous ranging from the frequency division multiplex (F.D.M.) system for microwave radio relay links, earth stations and satellite transponders to the military use in airborne, seaborne and ground equipments for electronic counter-measures (ECM) and electronic counter-countermeasures (ECCM), etc., to mention but a few. Thus, the design problem of multichannel systems (multiplexing) becomes important and the techniques vary according to the application.

In the context of this thesis, the word "multiplexer" is used to mean a passive linear device that combines a number of filters representing different channels such that this device will have a single input port and a number of output ports or having a single output port and a number of input-ports depending on its use as a frequency spectrum splitter or combiner. The "diplexer" is the simplest case of the multiplexer, since it only combines two channel filters. However, if all of the channel filters of the multiplexer have bandpass characteristics, the multiplexer is referrred to as "band pass/band pass" or simply a "band pass channel multiplexer". On the other hand a multiplexer may consists of a cascade of a number of diplexers with each diplexer consisting of a low pass and a high pass channel and may be called a "low pass/high pass". However, the design problem of the multiplexer whether it is a bandpass

one or a cascade of low pass/high pass diplexers, is not an easy task as it might at first seem. This is because of the interaction effects which usually occur when a number of ordinary filters are simply connected together. Unless the filters and their interconnections are carefully designed whilst taking into account the interaction effects, the whole performance of the system will be disrupted. Several methods have been used to decouple the filters and thus reducing or avoiding their interaction by combining them with passive devices such as circulators, hybrid junctions or by using directional filters. For details of these methods one can see Chapter 16 of reference [28]. An extensive discussion of the advantages and the limitations of these methods is also presented in [29] and [30].

This chapter is devoted to presenting a new design procedure for bandpass channel multiplexers without using any extra device except the bandpass channel filters.

3.2 INTRODUCTION.

Most of the previous multiplexers design techniques have adopted an approach based upon singly terminated bandpass channcels inherently resulting in 3dB crossover points between channels (continguous) e.g. [31], [32]. Such designs exhibit good return loss over the channel bandwidths and guardbands. However dummy channels have to be included to imitate absent channels at the edges of the total multiplexer bandwidth, thus forming an addition annulling network. These redundant elements are necessary for the compensation of the channel interactions to produce a channel performance comparable to the individual channels based upon a singly terminated prototype.

In general, contiguous band multiplexers based upon the singly terminated filter design are non-optimum because they need a higher degree filter than necessary in each channel in addition to an annulling network. Furthermore, if the singly terminated designs are to be used for crossover levels in excess of 3dB, which is the case in most communication systems, the passband return loss rapidly deteriorates if a further annulling network is not used. A general design procedure was recently presented in [33] for multiplexers based upon doubly terminated channel filters where the parameters associated with the first two resonators of each individual channel filter are modified in terms of a well defined band separation factor. The process is powerful and flexible but has a number of limitations mentioned in [33] for the simple series connection of channels. For example, the channels may not be spaced too closely in frequency, the procedure will give inaccurate results when the channel return loss is greater than 20dB and the lowest and highest frequency channels suffer a severe deterioration for most specifications containing 3 or more channels.

In this chapter a new general design procedure is presented for bandpass channel prototype multiplexers having any number of Chebyshev channel filters, with arbitrary degrees, bandwidths, and interchannel spacings without the necessity of having a manifold feed. The design procedure commences from the element values of a doubly terminated low-pass prototype filter satisfying an equiripple response which is obtained from the closed form formulas given in [7], and review in Chapter 2 of this thesis and the individual channel filters can be realized in a direct coupled cavity form connected in series at a common junction. The multiplexer design procedure modifies all of the elements in each channel filter and preserves a complete match at the two point of perfect transmission closest to the bandedges of each channel filter,

whilst taking into account the frequency dependence across each channel. An optimization process has been used to modify the elements of each channel in turn and the convergence of the process is normally achieved if the insertion loss of the neighbouring channels cross over at greater than 3dB. The resulting multiplexer is canonic without an immittance compensating annulling network or a manifold feed. Finally, it is shown that this process gives very good results for a wide variety of specifications, as demonstrated by the computer analysis of several multiplexer examples.

3.3 THE DESIGN PROCEDURE.

The design procedure commenced from lumped element doubly terminated channel filters operating is isolation satisfying an equripple passband amplitude response with the maximum number of ripples. Thus, there is perfect transmission at n points $\omega = \omega_i$ $(i = 1 \rightarrow n)$, where n is the degree of transfer function.

The assumed normalized low pass prototype filter satisfies an optimum equiripple amplitude passband response I.L. sketched in Fig. 3.1 and given by the formula:

$$I.L. = 1 + \varepsilon^2 T_n^2(\omega) \qquad (3.1)$$

where

$$T_n(\omega) = \cos(n \cos^{-1} \omega)$$

and has the equivalent circuit shown in Fig. 3.2 with the explicit design formulas [7].

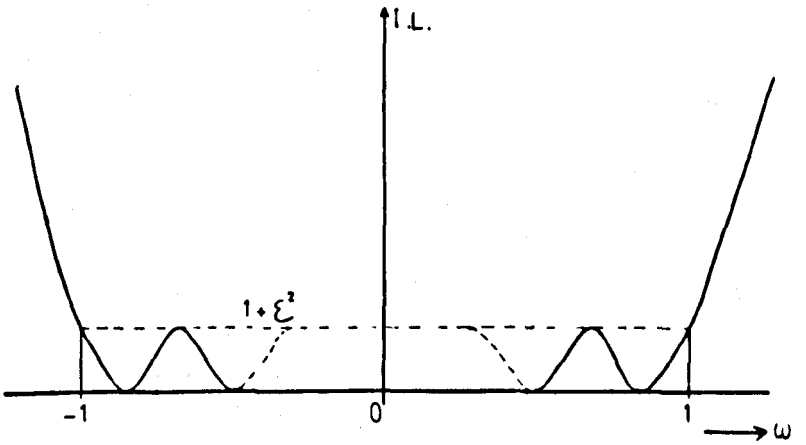

Fig. 3.1 Insertion loss response of the low pass filter

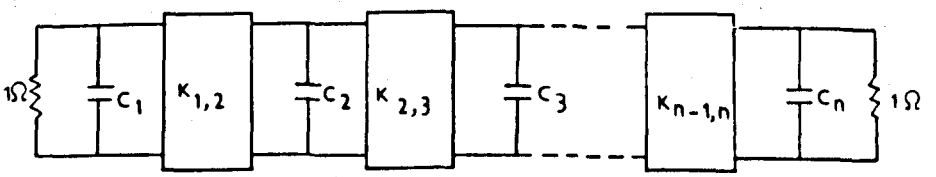

Fig. 3.2 Low pass prototype filter

$$
\left.
\begin{aligned}
C'_r &= \frac{2 \sin\left[\frac{(2r-1)\pi}{2n}\right]}{\eta} && r = 1 \to n \\
K_{r,r+1} &= \frac{\sqrt{\eta^2 + \sin^2(r\pi/n)}}{\eta} && r = 1 \to n-1 \\
\eta &= \sinh\left[\frac{1}{n}\sinh^{-1}\left(\frac{1}{\varepsilon}\right)\right]
\end{aligned}
\right\} \qquad (3.2)
$$

The band pass channels based on this lowpass can be designed as individual doubly terminated filters with the correct bandwidths and centre frequencies by applying the frequency transformation

$$\omega' \to (\omega - I_i)/\beta_i \qquad (3.3)$$

where

I_i and β_i are the ith channel centre frequency and bandwidth scaling factor respectively.

Assuming the lower and upper band edges frequencies of the individual bandpass channels ω_{1i} and ω_{2i} are known, then

$$I_i = \frac{(\omega_{1i} + \omega_{2i})}{2} \qquad (3.4)$$

The frequency transformation given in (3.3) changes all of the capacitors C'_r into capacitors C_{ir} in parallel with a frequency invariant susceptances B_{ir}, where

$$C_{ir} = \frac{C'_r}{\beta_i} \qquad (3.5)$$

$$B_{ir} = -C_{ir} I_i \qquad (3.6)$$

and preserves the equiripple amplitude response.

The design principle used here modifies all of the elements in each channel filter taking into account the frequency variation across each channel and the interaction due to other channels.

A perfect transmission is preserved with the correct overall phase shift in the auxiliary variable η at the two points of perfect transmission (F_{1i} and F_{2i}) closest to the band edges of each channel. However, when channel j (j = 1,2,3,---L) is modified the remaining channels i(i = 1,2,3,---$\neq$j, --- L) are replaced by their input impedances calculated at F_{1j} and F_{2j} and the modification process may be repeated until no more change in the element values is possible.

The two points of perfect transmission closest to the band edges of channel i, (F_{1i} and F_{2i}) can be obtained by solving the following set of linear equations formed by preserving the same argument value of $T_n(\omega)$ at the band edges and the two points of perfect transmission closest to the low pass band edges, after applying the bandpass frequency transformation given earlier in expressions (3.3). Hence,

$$\frac{I_i - \omega_{1i}}{\beta_i} = 1 \tag{3.7}$$

$$\frac{I_i - F_{1i}}{\beta_i} = \cos(\pi/2n_i) \tag{3.8}$$

$$\frac{I_i - \omega_{2i}}{\beta_i} = -1 \tag{3.9}$$

$$\frac{I_i - F_{2i}}{\beta_i} = -\cos(\pi/2n_i) \tag{3.10}$$

From equations (3.7) and (3.9)

$$\beta_i = I_i - \omega_{1i} = \omega_{2i} - I_i \tag{3.11}$$

From equation (3.8)

$$F_{1i} = I_i - \beta_i \cos(\pi/2n_i) \tag{3.12}$$

and from equation (3.10)

$$F_{2i} = I_i + \beta_i \cos(\pi/2n_i) \tag{3.13}$$

Now, if each bandpass channel i is assumed to be operating in isolation, terminated at both ends by 1 ohm resistors, then at $\omega = F_{1i}$, the transfer matrix for the entire network of channel i would be:

$$\prod_{r=1}^{n_i - 1} \frac{1}{\sqrt{n_i^2 + \sin^2(\frac{r\pi}{n_i})}} \begin{bmatrix} -\sin(\frac{r\pi}{n_i}) & jn_i \\ jn_i & -\sin(\frac{r\pi}{n_i}) \end{bmatrix} \tag{3.14}$$

Also, at $w = F_{2i}$ the transfer matrix for the entire network of channel i would be

$$\prod_{r=1}^{n_i - 1} \frac{1}{\sqrt{n_i^2 + \sin^2(\frac{r\pi}{n_i})}} \begin{bmatrix} \sin(\frac{r\pi}{n_i}) & jn_i \\ jn_i & \sin(\frac{r\pi}{n_i}) \end{bmatrix} \tag{3.15}$$

This has been shown by Rhodes [7] and represents a cascade of passive all-pass sections in the auxiliary parameter $-jn$ or jn.

The insertion loss characteristics of an L-channel multiplexer, indicating the insertion losses from the common port to the L - output ports, is shown in Fig. 3.3, where the ripple level of the channels are not necessarily identical. The L - channel, series connected multiplexer is shown in Fig. 3.4. The effect on the passband response of one channel due to the interaction of the others is to create a frequency dependent complex load at one end. Since the value of this load is different at the two critical bandedge frequencies where all-pass behaviour in the auxiliary parameter occurs, an impedance scaling within the network must occur coupled with additional phase shift. Hence, the transfer matrix for the entire network of channel i operating in a multiplexer of L-channels calculate at $\omega = F_{1i}$ from general image parameter theory for

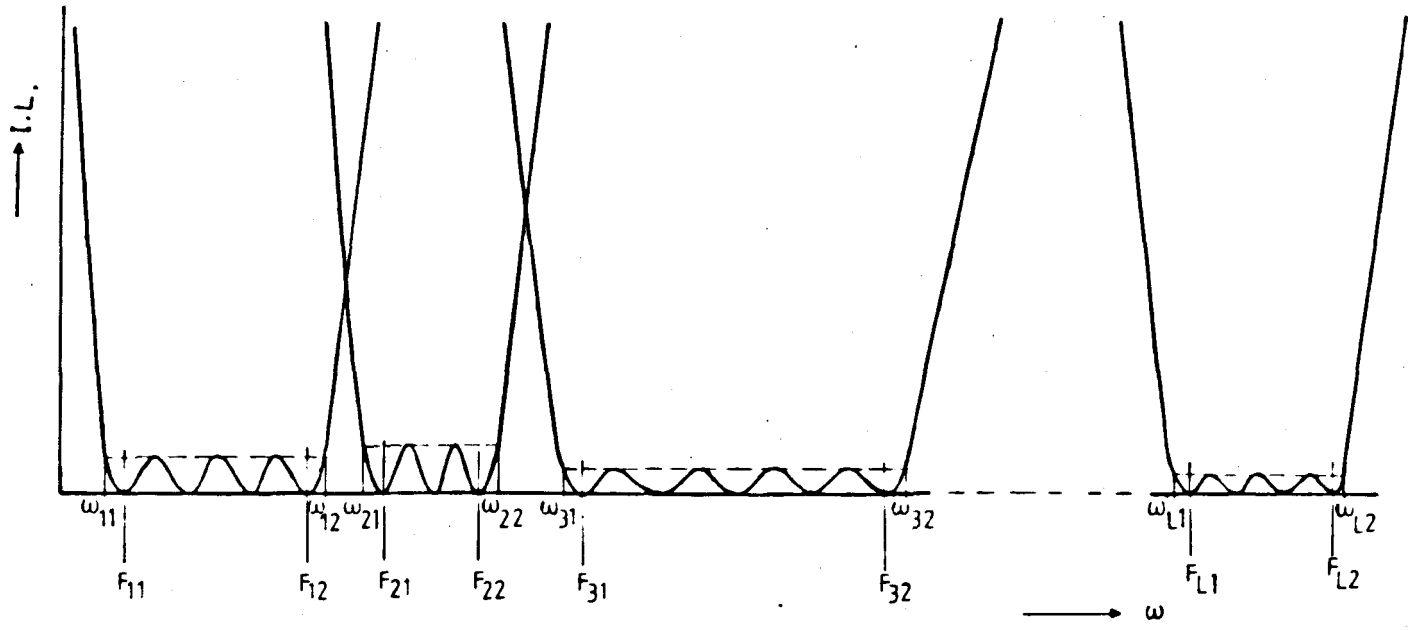

Fig. 3.3 Insertion loss of a multiplexer

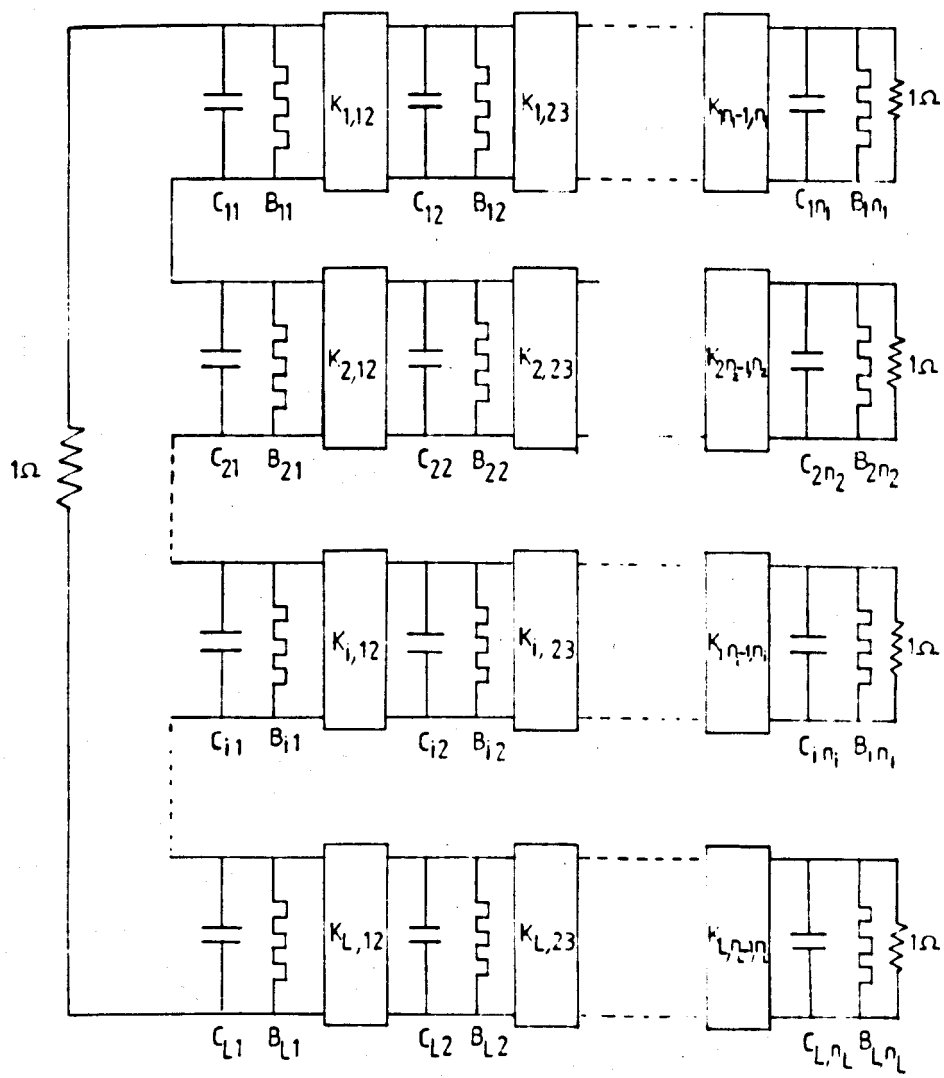

Fig. 3.4 Series connected multiplexer

matched sections is given by:

$$\prod_{r=1}^{n_i-1} \frac{1}{\sqrt{(\eta^2{}_i + S^2{}_{ir})(1+t^2{}_{i,r})}} \begin{bmatrix} \sqrt{Z_{1i,r}} & 0 \\ 0 & \frac{1}{\sqrt{Z_{1i,r}}} \end{bmatrix} \begin{bmatrix} 1 & jt_{i,r} \\ jt_{i,r} & 1 \end{bmatrix}$$

$$\begin{bmatrix} -S_{i,r} & j\eta_i \\ j\eta_i & -S_{i,r} \end{bmatrix} \begin{bmatrix} \frac{1}{\sqrt{Z_{1i,r+1}}} & 0 \\ 0 & \frac{1}{\sqrt{Z_{1i,r+1}}} \end{bmatrix} \tag{3.16}$$

or

$$\prod_{r=1}^{n_i-1} \frac{1}{\sqrt{(\eta^2{}_i+S^2{}_{i,r})(1+t^2{}_{i,r})}} \begin{bmatrix} -\sqrt{\frac{Z_{1i,r}}{Z_{1i,r+1}}}\,(S_{i,r}+\eta_i t_{i,r}) & j\sqrt{Z_{1i,r}Z_{1i,r+1}}\,(\eta_i - S_{i,r}t_{i,r}) \\ j\frac{(\eta_i - S_{i,r}t_{i,r})}{\sqrt{Z_{1i,r}Z_{1i,r+1}}} & -\sqrt{\frac{Z_{1i,r+1}}{Z_{1i,r}}}\,(S_{i,r}+\eta_i t_{i,r}) \end{bmatrix} \tag{3.17}$$

Similarly at $\omega = F_{2i}$ the transfer matrix for the entire network of channel i may be represented by

$$\prod_{r=1}^{n_i-1} \frac{1}{\sqrt{(\eta^2{}_i+S^2{}_{i,r})(1+t^2{}_{i,r})}} \begin{bmatrix} \sqrt{Z_{2i,r}} & 0 \\ 0 & \frac{1}{\sqrt{Z_{2i,r}}} \end{bmatrix} \begin{bmatrix} 1 & jt_{i.r} \\ jt_{i,r} & 1 \end{bmatrix}$$

$$\begin{bmatrix} S_{i,r} & j\eta_i \\ j\eta_i & S_{i,r} \end{bmatrix} \begin{bmatrix} \frac{1}{\sqrt{Z_{2i,r+1}}} & 0 \\ 0 & \sqrt{Z_{2i,r+1}} \end{bmatrix} \tag{3.18}$$

$$\prod_{r=1}^{n_i-1} \frac{1}{\sqrt{(\eta_i{}^2{}_i+S^2{}_{i,r})(1+t^2{}_{i,r})}} \begin{bmatrix} \sqrt{\frac{Z_{2i,r}}{Z_{2i,r+1}}}(S_{i,r}-\eta_i t_{i,r}) & j\sqrt{Z_{2i,r}Z_{2i,r+1}}\,(\eta_i+S_{i,r}t_{i,r}) \\ j\,\frac{(\eta_i+S_{i,r}t_{i,r})}{\sqrt{Z_{2i,r}Z_{2i,r+1}}} & \sqrt{\frac{Z_{2i,r+1}}{Z_{2i,r}}}\,(S_{i,r}-\eta_i t_{i,r}) \end{bmatrix} \tag{3.19}$$

where $S_{i,r} = S_{in}(r\pi/n_i)$

$t_{i,r}$ is a phase correcting factor introduced to preserve the all pass characteristic of channel i at F_{1i} and F_{2i}.

$Z_{1i,r}$ and $Z_{2i,r}$ are the image impedances of the rth section of channel i and required to be different at F_{1i} and F_{2i}.

In order to modify the element values of channel j(j=1,2,3 --- L). the remaining channels of the multiplexer $i \neq j$ may be replaced by their equivalent input impedances evaluated at $\omega = F_{1j}$ and $\omega = F_{2j}$ which are connected in series with the 1 Ohm generator load as shown in Fig. 3.5 and given by

$$R_{1t}(F_{1j}) = \sum_{i\neq j}^{L} R_{1i}(F_{1j}) \tag{3.20a}$$

$$y_{1t}(F_{1j}) = \sum_{i\neq j}^{L} X_{1i}(F_{1j}) \tag{3.20b}$$

$$R_{2t}(F_{2j}) = \sum_{i\neq j}^{L} R_{2i}(F_{2j}) \tag{3.20c}$$

and

$$X_{2t}(F_{2j}) = \sum_{i\neq j}^{L} X_{2i}(F_{2j}) \tag{3.20d}$$

where

$R_{1t}(F_{1j})$ and $R_{2t}(F_{2j})$ are the sum of the real parts of the input impedances of the individual channels evaluated at F_{ij} and F_{2j} respectively.

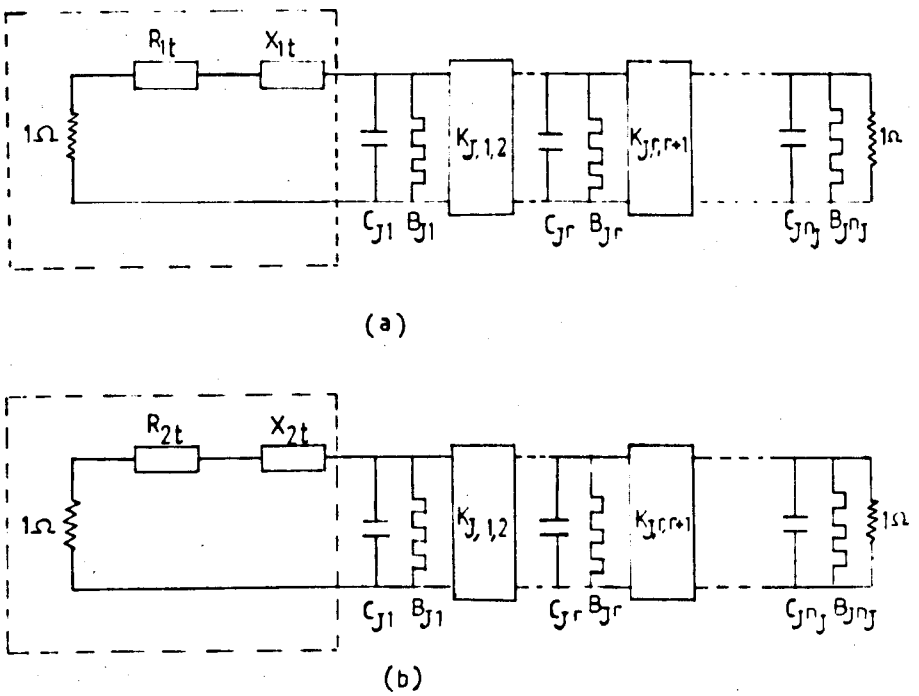

Fig.3.5 Equivalent circuit of the multiplexer (Series connected load)

(a) at $\omega = F_{1J}$

(b) at $\omega = F_{2J}$

$X_{1t}(F_{1j})$ and $X_{2t}(F_{2j})$ are the sum of the imaginary parts of the input impedances of the individual channels evaluated at F_{1j} and F_{2j} respectively.

For convenience, the load from the common junction side to channel j is replaced by its shunt equivalent circuit as shown in Fig. 3.6 where $G_{1t}(F_{1j})$ and $G_{2t}(F_{2j})$ are the real parts, $Y_{1t}(F_{1j})$ and $Y_{2t}(F_{2j})$ are the imaginary parts. Hence, they are given by

$$G_{1t}(F_{1j}) = (1 + R_{1t}(F_{1j}))/((1+R_{1t}(F_{1j}))^2 + X^2_{1t}(F_{1j})) \tag{3.21a}$$

$$Y_{1t}(F_{1j}) = - X_{1t}(F_{1j})/((1+R_{1t}(F_{1j}))^2 + X^2_{1t}(F_{1j})) \tag{3.21b}$$

$$G_{2t}(F_{2j}) = (1 + R_{2t}(F_{2j}))/((1+R_{2t}(F_{2j}))^2 + X^2_{2t}(F_{2j})) \tag{3.21c}$$

and

$$Y_{2t}(F_{2j}) = - X_{2t}(F_{2j})/((1+R_{2t}(F_{2j}))^2 + X^2_{2t}(F_{2j})) \tag{3.21d}$$

Now let i = j in matrix (3.17) whose basic section can be decomposed into a transfer matrix of a shunt resonator and an admittance inverter [34]. Hence, the overall admittance of the shunt resonator can be described by

$$C_{j,r}\{F_{1j} - I_{j,r}\} = \frac{-1}{Z_{1j,r}}\left\{\frac{(S_{j,r} + \eta_j t_{j,r})}{(\eta_j - S_{j,r} t_{j,r})} + \frac{(S_{j,r-1} + \eta_j t_{j,r-1})}{(\eta_j - S_{j,r-1} t_{j,r-1})}\right\} \tag{3.22}$$

and the characteristic admittance of the inverter is given by

$$K_{j,r,r+1} = \frac{\sqrt{(\eta^2_j + S^2_{j,r})(1 + t^2_{j,r})}}{\sqrt{Z_{ij,r} Z_{ij,r+1}}\,(\eta_j - S_{j,r} t_{j,r})} \tag{3.23}$$

Similarly from matrix (3.19)

$$C_{j,r}\{F_{2j} - I_{j,r}\} = \frac{1}{Z_{2j,r}}\left\{\frac{(S_{j,r} - \eta_j t_{j,r})}{(\eta_j + S_{j,r} t_{j,r})} + \frac{(S_{j,r-1} - \eta_j t_{j,r-1})}{(\eta_j + S_{j,r-1} t_{j,r-1})}\right\} \tag{3.24}$$

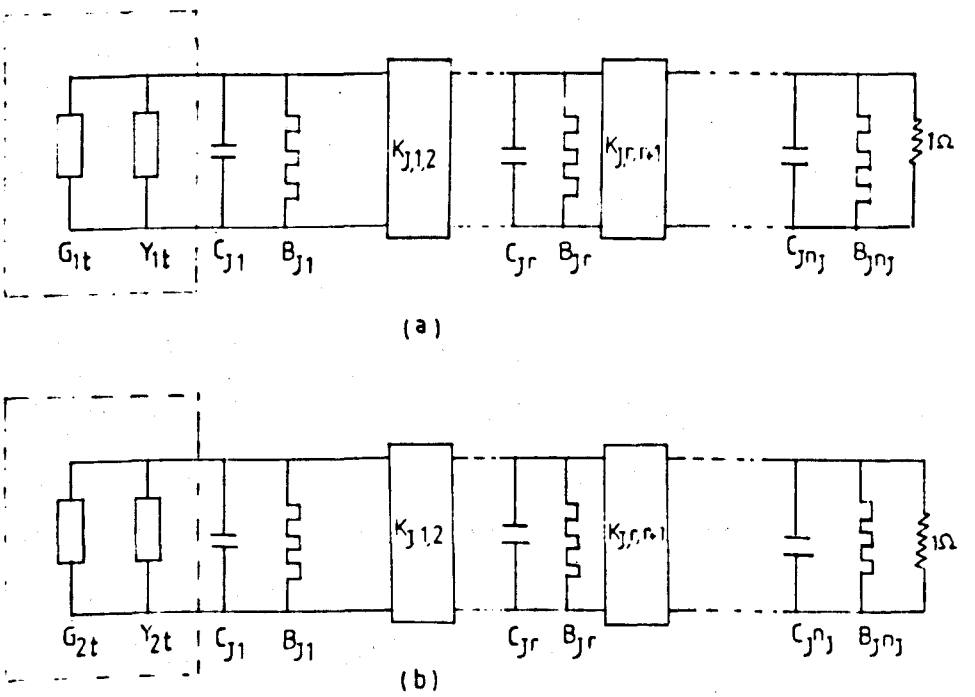

Fig.3.6 Equivalent circuit of the multiplexer
(Parallel connected load)
(a) at $\omega = F_{1j}$
(b) at $\omega = F_{2j}$

and

$$K_{j,r,r+1} = \frac{\sqrt{(\eta^2_j + S^2_{j,r})(1 + t^2_{j,r})}}{\sqrt{Z_{2j,r}Z_{2j,r+1}}(\eta_j + S_{j,r}t_{j,r})} \tag{3.25}$$

Since $K_{j,r,r+1}$ is the characteristic admittance of a frequency independent invertor, from (3.23) and (3.25) we have

$$R_{oj,r+1} = \frac{1}{R_{oj,r}} \left(\frac{\eta_j + S_{j,r}t_{j,r}}{\eta_j - S_{j,r}t_{j,r}}\right)^2 \tag{3.26}$$

where

$$R_{oj,r} = \frac{Z_{1j,r}}{Z_{2j,r}} \tag{3.27}$$

In addition it has been found, after trying different relationships, that if the individual channel network is originally symmetrical, then the required impedance variation level through it can be approximately expressed by the following expressions which give the best possible return loss over the entire passband.

$$Z_{1j,r+1} = (Z_{1j,r})^{1/4} \tag{3.28a}$$

$$Z_{2j,r+1} = (Z_{2j,r})^{1/4} \tag{3.28b}$$

and consequently

$$R_{oj,r+1} = (R_{oj,r})^{1/4} \tag{3.28c}$$

Furthermore, for the all-pass behaviour in the auxiliary parameter for each channel at its critical frequencies we must have

$$Z_{1j,1} = 1/G_{2t}\,(F_{1j})$$

and

$$Z_{2j,1} = 1/G_{2t}\,(F_{2j})$$

So, from equation (3.26) an expression for $t_{j,r}$ can be written as

$$t_{j,r} = (\eta_j / S_{j,r}) \left(\frac{\sqrt{R_{oj,r} R_{oj,r+1}} - 1}{\sqrt{R_{oj,r} R_{oj,r+1}} + 1} \right) \tag{3.29}$$

and

$$t_{j,o} = 0$$

The modified values of the elements associated with the first resonator of channel (j) can be obtained by solving the following two equation for $C_{j,1}$ and $I_{j,1}$.

$$Y_{1t} (F_{1j}) + C_{j1} \{F_{1j} - I_{j1}\} = -A_{oj,1} \tag{3.30}$$

$$Y_{2t} (F_{2j}) + C_{j1} \{F_{2j} - I_{j1}\} = B_{oj,1} \tag{3.31}$$

to give

$$C_{j,1} = \frac{Y_{1t} (F_{1j}) - Y_{2t} (F_{2j}) + A_{oj,1} + B_{oj,1}}{(F_{2j} - F_{1j})} \tag{3.32}$$

and

$$I_{j1} = F_{1j} + \{Y_{1t} (F_{1j}) + A_{o,j,1}\}/C_{j1} \tag{3.33}$$

where

$$A_{oj,1} = G_{1t} (F_{1j}) \left(\frac{S_{j,1} + \eta_j t_{j,1}}{\eta_j - S_{j,1} t_{j,1}} \right) \tag{3.34}$$

$$B_{oj,1} = G_{2t} (F_{2j}) \left(\frac{S_{j,1} - \eta_j t_{j,1}}{\eta_j + S_{j,1} t_{j,1}} \right) \tag{3.35}$$

The modified value of the remaining resonators of channel (j) can be obtained by solving equation (3.22) and (3.24) for C_{jr} and I_{jr}

$$C_{jr} = \left\{ \frac{A_{o\ j,r}}{Z_{1\ j,r}} + \frac{B_{o\ j,r}}{Z_{2\ j,r}} \right\} / \ (F_{2j} - F_{1j}) \qquad (r = 2 \rightarrow n_j) \tag{3.36}$$

$$I_{jr} = F_{1j} + \frac{A_{o\ j,r}}{Z_{1\ j,r}} C_{jr} \qquad (r = 2 \rightarrow n_j) \tag{3.37}$$

where

$$A_{o\,j,r} = \frac{S_{j,r} + \eta_j\, t_{j,r}}{\eta_j - S_{j,r}\, t_{j,r}} + \frac{S_{j,r-1} + \eta_j\, t_{j,r-1}}{\eta_j - S_{j,r}\, t_{j,r-1}} \qquad (3.38)$$

$$B_{o\,j,r} = \frac{S_{j,r} - \eta_j\, t_{j,r}}{\eta_j + S_{j,r}\, t_{j,r}} + \frac{S_{j,r-1} - \eta_j\, t_{j,r-1}}{\eta_j + S_{j,r-1}\, t_{j,r-1}} \qquad (3.39)$$

The modified characteristic impedance of the inverter $K_{j,r,r+1}$ can be obtained by using either equation (3.23) or (3.25).

A computer program has been written to perform the modification process. This process is then repeated channel by channel until all the elements values converge. No proof of convergence is offered but it has been found that if the channel cross over insertion loss levels are in excess of 3dB the process appears to converge.

3.4 PROTOTYPE EXAMPLES AND COMPUTER ANALYSIS.

i) The generality of this procedure is demonstrated here by an asymmetric 8-channel multiplexer whose individual channel filters are designed with varying number of resonators, bandwidths and interchannel separations, but are identical in their inband return loss of 20dB, (there is no restriction in this theory against designing the individual filters to have varying inband return loss as well). The design specifications are given in Table 1, and the computer analysis of the common port return loss of the resulting multiplexer is shown in Fig. 3.7. It may be seen that all of the channels have a good match even for such complicated multiplexer.

R.L.(dB)
35
30
25
20
15
10
5
0
i = 1
i = 2
0·75
1·0
1·5
2·0
2·5
3·0
R.L.(dB)
i = 4
6·0
6·5
7·0
7·5
8·0

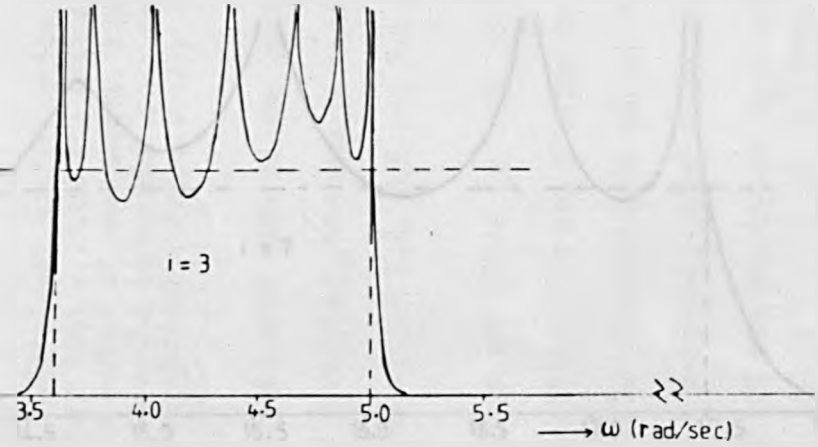
i = 3
3·5
4·0
4·5
5·0
5·5
ω (rad/sec)

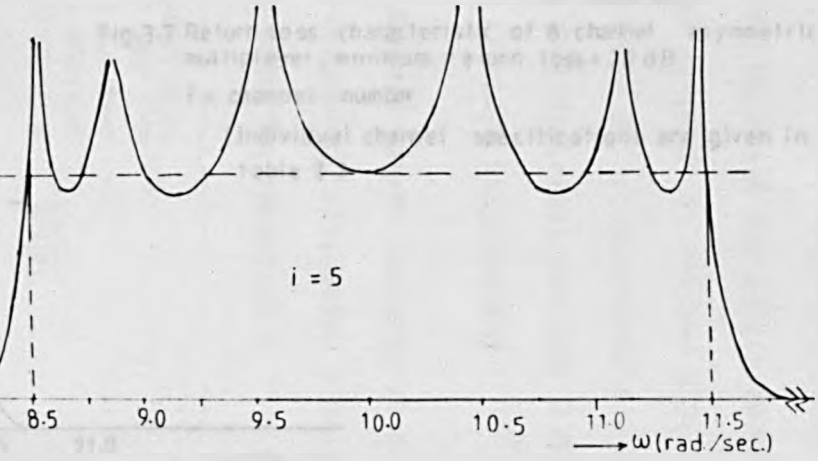
i = 5
8·5
9·0
9·5
10·0
10·5
11·0
11·5
ω (rad./sec.)

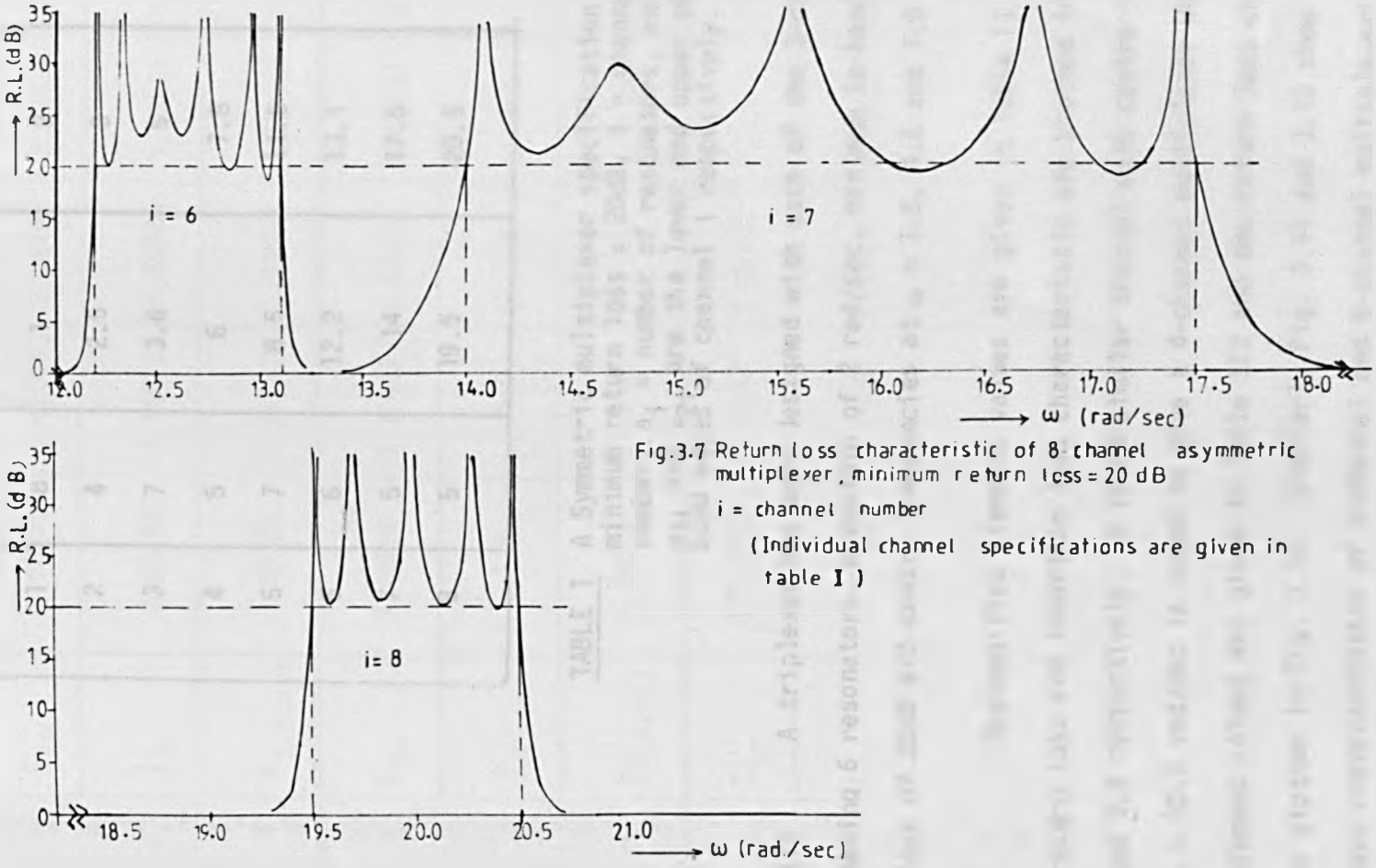

Fig.3.7 Return loss characteristic of 8 channel asymmetric multiplexer, minimum return loss = 20 dB

i = channel number

(Individual channel specifications are given in table I)

i	n_i	ω_{1i}	ω_{2i}
1	8	1	2
2	4	2.5	3
3	7	3.6	5
4	5	6	7.8
5	7	8.5	11.5
6	6	12.2	13.1
7	5	14	17.5
8	5	19.5	20.5

TABLE 1 A Symmetric multiplexer specification: minimum return loss = 20dB, i = channel number, n_i = number of resonators, and ω_{1i} and ω_{2i} are the lower and upper pass band edges of channel i respectively.

ii) A triplexer has been designed with each of the 3-channels having 6 resonators, bandwidth of 2 rad/sec, minimum in bands return loss of 26dB and centre frequencies at ω = 1.5, 4.5 and 7.5 respectively.

The modified elements values are given in Table II and the return loss and insertion loss characteristic are plotted in Fig. 3.8 and 3.9 respectively. A fourth similar channel with centre frequency at ω = 10.5 rad/sec is added to give a 4-channel multiplexer whose modified element values are given in Table III and the return loss characteristic is plotted in Fig. 3.10. Similarly Fig. 3.11 and 3.12 show the return loss characteristics of 5-channel and 6-channel multiplexers respectively. These examples demonstrate the applicability of this design procedure to a high return loss specification and show that the parameters associated with the first resonator of each individual channel suffer the larger modification while the last resonator parameters suffer the least modification.

	r	1	2	3	4	5	6
Channel 1 $n_1=6, \omega_{11}=.5, \omega_{12}=2.5$	C_{1r}	0.587586	1.97644	2.88192	2.93414	2.15776	0.790699
	I_{1r}	0.632983	1.40632	1.48548	1.49618	1.49853	1.49899
	$K_{1,r,r+1}$	1.00325	1.56137	1.79859	1.65239	1.25728	0
Channel 2 $n_2=6, \omega_{21}=3.5, \omega_{22}=5.5$	C_{2r}	1.02058	2.10667	2.9333	2.94736	2.16019	0.790922
	I_{2r}	4.5	4.5	4.5	4.5	4.5	4.5
	$K_{2,r,r+1}$	1.18079	1.63249	1.81896	1.65706	1.25817	0
Channel 3 $n_3=6, \omega_{31}=6.5, \omega_{32}=8.5$	C_{3r}	0.587586	1.97644	2.88192	2.93414	2.15776	0.790699
	I_{3r}	8.36702	7.59368	7.51452	7.50382	7.50147	7.50101
	$K_{3,r,r+1}$	1.00325	1.56137	1.79859	1.65239	1.25728	0

TABLE II Element Values of 3-channel multiplexer.
(Minimum return loss = 26dB for all channels)

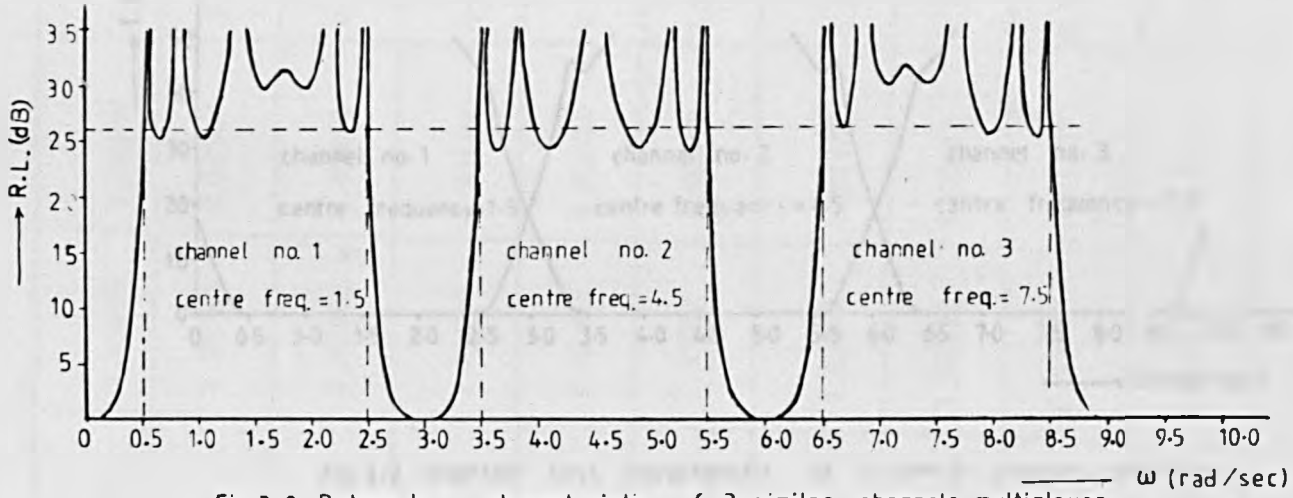

Fig. 3.8 Return loss characteristic of 3-similar channels multiplexer
n = 6 resonator, minimum return loss = 26 dB, bandwidth = 2

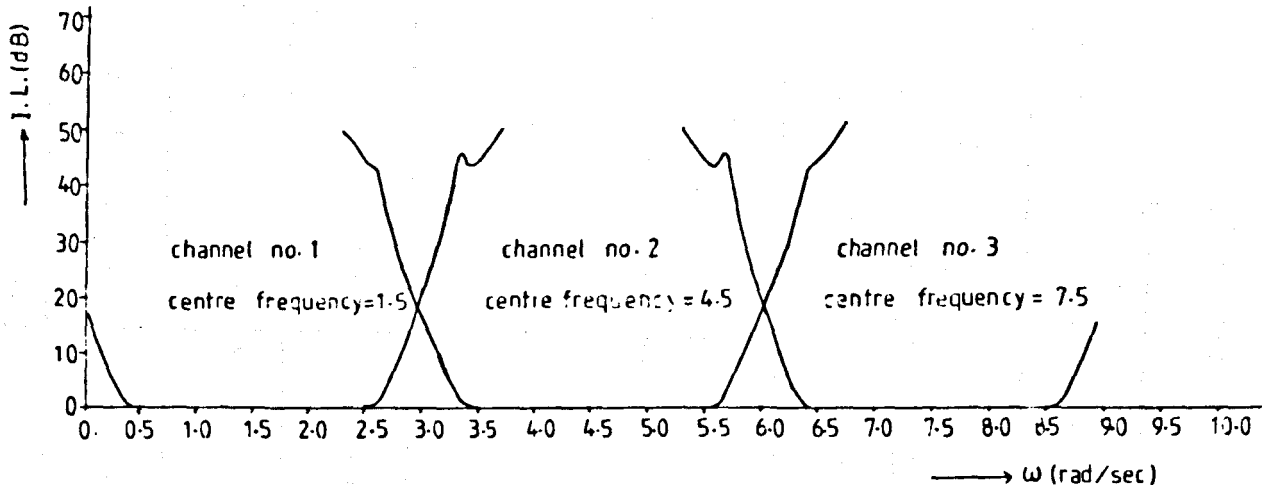

Fig.3.9 Insertion loss characteristic of 3-similar channels multiplexer
n = 6 resonator, minimum return loss = 26 dB, bandwidth = 2

	r	1	2	3	4	5	6
Channel 1 $n_1=6, \omega_{11}=.5, \omega_{12}=2.5$	C_{1r}	0.499742	1.92122	2.85953	2.92833	2.15669	0.790601
	I_{1r}	0.422453	1.38863	1.48271	1.49545	1.49825	1.4988
	$K_{1,r,r+1}$	0.933194	1.53098	1.78968	1.65033	1.25689	0
Channel 2 $n_2=6, \omega_{21}=3.5, \omega_{22}=5.5$	C_{2r}	1.01613	2.09368	2.92807	2.94601	2.15995	0.790899
	I_{2r}	4.39607	4.46498	4.49459	4.49858	4.49945	4.49962
	$K_{2,r,r+1}$	1.16215	1.62514	1.81688	1.65658	1.25808	0
Channel 3 $n_3=6, \omega_{31}=6.5, \omega_{32}=8.5$	C_{3r}	1.01613	2.09368	2.92807	2.94601	2.15995	0.790899
	I_{3r}	7.60393	7.53502	7.50541	7.50142	7.50055	7.50038
	$K_{3,r,r+1}$	1.16215	1.62514	1.81688	1.65658	1.25808	0
Channel 4 $n_4=6, \omega_{41}=9.5, \omega_{42}=11.5$	C_{4r}	0.499742	1.92122	2.85953	2.92833	2.15669	0.790601
	I_{4r}	11.5775	10.6114	10.5173	10.5045	10.5018	10.5012
	$K_{4,r,r+1}$	0.933194	1.53098	1.78968	1.65033	1.25689	0

TABLE III Element Values of 4-channel multiplexer

(Minimum return loss = 26dB for all channels)

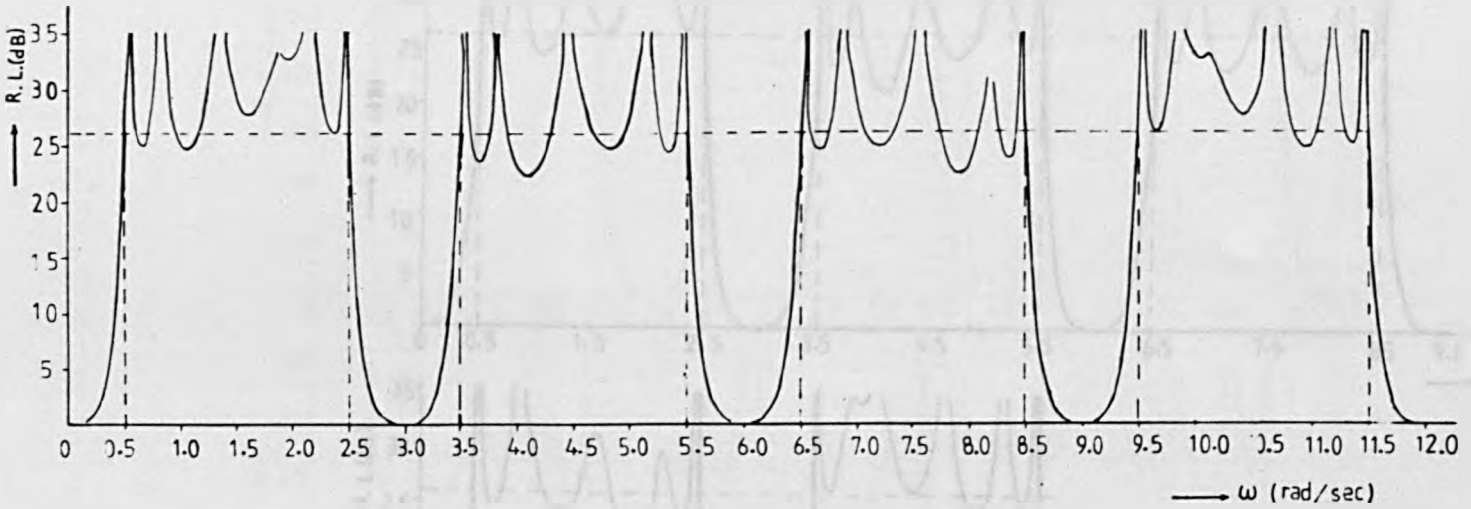

Fig. 3.10 Return loss characteristic of 4-similar channels multiplexer (minimum return loss = 26 dB)

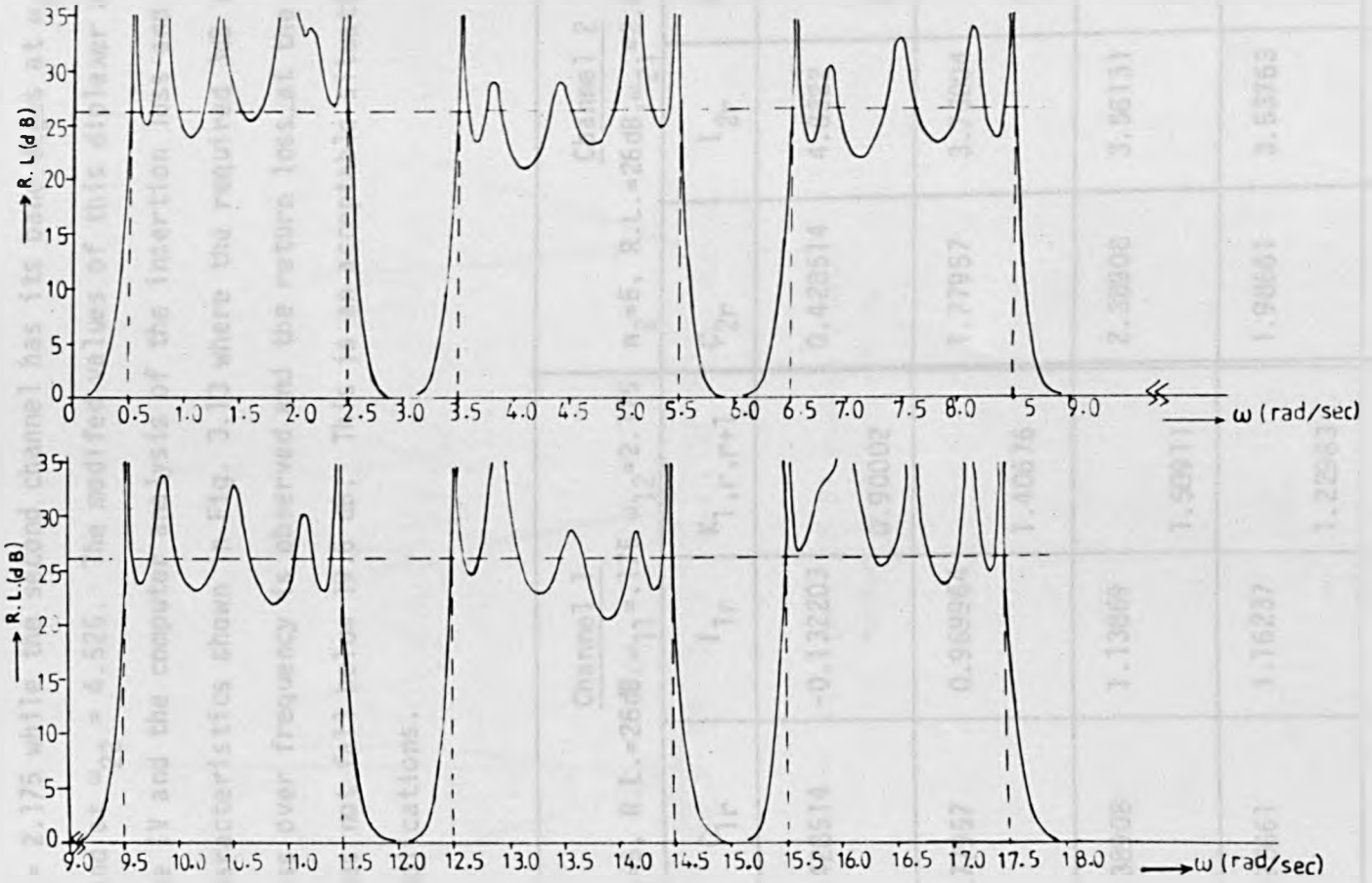

Fig. 3.12 Return loss characteristic of 6-similar channels multiplexer (minimum return loss=26dB)

iii) A contiguous Diplexer.

The validity of this design procedure has been tested for a limiting contiguous case of a diplexer of degree 5, with a return loss of 26dB for both channels, the first channel has band edges at ω_{11} = 0.175 and at ω_{12} = 2.175 while the second channel has its band edges at ω_{21} = 2.525 and at ω_{22} = 4.525. The modifed values of this diplexer are given in Table IV and the computer analysis of the insertion loss and return loss characteristics shown in Fig. 3.13 where the required 3dB loss at the cross over frequency is observed and the return loss at the common port does not fall below 19.6 dB. This is an acceptable situation for many applications.

	Channel 1 n_1=5, R.L.=26dB, ω_{11}=.175 ω_{12}=2.175			Channel 2 n_2=5, R.L.=26dB, ω_{21}=2.525, ω_{22}=4.525		
r	C_{1r}	I_{1r}	$K_{1,r,r+1}$	C_{2r}	I_{2r}	$K_{2,r,r+1}$
1	0.428514	-0.132203	0.90002	0.428514	4.8322	0.90002
2	1.77957	0.969964	1.40676	1.77957	3.73004	1.40676
3	2.38908	1.13869	1.50911	2.38908	3.56131	1.50911
4	1.98661	1.16237	1.22983	1.98661	3.53763	1.22983
5	0.764275	1.16664	0	0.764275	3.53336	0

TABLE IV. Element values of a contiguous prototype BP/BP diplexer

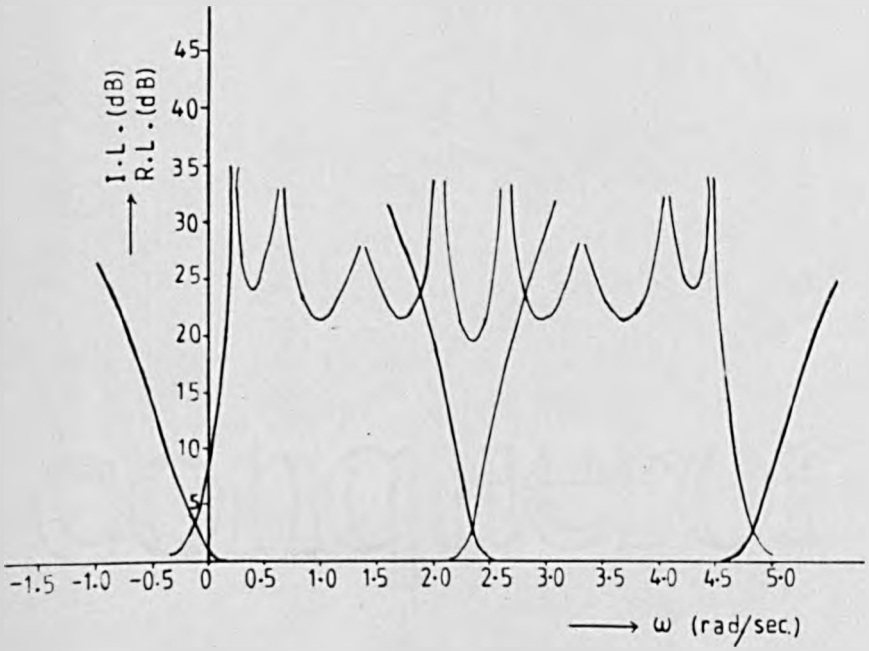

Fig.3.13 A contiguous BP/BP channels diplexer
n = 5, minimum return loss = 26 dB

From the many examples which have been designed and analysed by a computer, several points of interest arise. The design procedure is a very general one in the sense that it can handle the design of complicated asymmetric multiplexer with only a slight mismatch in some channels. The resulting multiplexers designed according to this technique are canonic (the degrees of the multiplexer is equal to the sum of the degrees of the individual channel filters), because there is no necessity for annulling immittance networks, or dummy channels to be added to the multiplexer. Furthermore this optimum doubly terminated design procedure shares the advantage of an increase of at least 6dB in the attenuation level over the pass band regions of all other channels, similar to other common junction multiplex design methods based upon doubly terminated prototype [e.g. 33].

3.5 CONCLUSIONS.

A new general design procedure has been presented for bandpass Chebysheve channel multiplexers without the addition of immittance compensation networks or dummy channels. This design procedure is also an approximate one since an exact synthesis procedure has not yet been found for this type of L-port network. It is believed that a further improvement could be made if an exact expression could be derived for the internal impedance level variation through each individual channel instead of the approximate one given in equations 3.28 a,b, and c. If a correct all pass equivalent form could be obtained at a third point of perfect transmission different from those closest to the pass-band edges of each individual channel, an improvement could be made. Attempts to obtain this solution has so far not been successful. However, this design procedure for a direct connection of all chanells at a common junction results in an excellent design without the necessity for annulling network and represents a strictly canonical solution.

CHAPTER 4

DESIGN AND PERFORMANCE OF EXPERIMENTAL MICROWAVE MULTIPLEXERS

4.1 INTRODUCTION

This chapter describes the application of the new procedure developed in the last chapter for designing microwave multiplexers using direct coupled cavity waveguide filters connected in series at a common junction by a wave-guide feed.

The design process commences with the specifications which define the number of channels, the band edges of each channel or the bandwidths and centre frequencies, the inband return loss (dB) and the rejection of each channel over the neighbouring channel passbands (dB) or the number of resonators in each channel. However, the given specifications should be related to prototype values, since the multiplexer design procedure was given in terms of such values. Finding the prototype element values of each channel in isolation, then one can proceed to obtain the modified values. Having obtained these, the direct coupled cavity waveguide realization is very simple for relatively narrow-band specifications.

This chapter presents a design process of a 4-channel multiplexer and explains the steps taken beginning with the given specifications and finishing with the physical dimensions. The computer analysis of the prototype multiplexer is plotted showing the insertion loss response of each channel and the common port return loss. The 4-channel microwave multiplexer was built in a standard rectangular waveguide WG16 (wR 90) structure, tuned and tested by using a swept-frequency reflectometer arrangement. The experimental insertion loss and return loss characteristics have been established.

4.2 DIRECT COUPLED-CAVITY WAVEGUIDE FILTERS

The design of direct-coupled-cavity band-pass filters using a rectangular waveguide realization based on a lumped low-pass prototype is now a well established technique. The oldest comprehensive method is that introduced by Cohn [35], who was the first to show the close relationship between an ideal immittance inverter and the shunt inductive coupling embedded in a negative length of waveguide. Cohn's method gives good results for bandwidth up to approximately 20 percent if, in the case of Chebyshev response, the voltage standing wave ratio (VSWR) is not too close to unity. A decade later Levy [36] presented a new theory for designing direct-coupled cavity filters in transmission line or waveguide structure and satisfying a Chebyshev response. Levy's theory based originally on a different type of prototypes but it degenerates to that by Cohn for narrow-band applications. Hence, any of these two methods can be used in designing the filter of interest, which consists of half wavelength cavities of electrical length $\theta_o = \pi$ at the design frequency which is normally chosen to be the mid-band frequency f_o, directly coupled by shunt inductive irises or posts as shown in Fig.4.2. The coupling elements (irises or posts) can be adequately described by shunt inductive susceptances of magnitude $Y_{r,r+1}$ at f_o, symmetrically embedded in a length of waveguide of electrical length $\phi_{r,r+1} = \phi_o$ at midband.

However, it is convenient to treat the frequency dependent quantities in waveguide filters whether they are lengths of line or susceptances,in terms of normalized guide wavelength i.e. $\lambda g_o/\lambda g$. Where λg is the guide wavelength and λg_o is the guide wave length at f_o. It is also simpler to operate with normalized values of susceptances by considering the characteristic impedance of the waveguide to be unity.

In order to derive the design formulas for the direct coupled cavity filter in terms of the prototype element values, the equivalent circuit for a typical section of the direct coupled cavity filter may first be established following the same procedure given in |35| and |36|.

Consider firstly a typical shunt inductive coupling element of susceptance $-jY_{r,r+1}\ \lambda g/\lambda g_o$ symmetrically located in a unit characteristic impedance piece of waveguide having an electrical length $\phi_{r,r+1}\ \lambda g_o/\lambda g$ as shown in Fig.4.3.a. The overall transfer matrix of this combination is

$$\begin{bmatrix} \cos(\phi_{r,r+1}/2) & j\sin(\phi_{r,r+1}/2) \\ j\sin(\phi_{r,r+1}/2) & \cos(\phi_{r,r+1}/2) \end{bmatrix} \begin{bmatrix} 1 & 0 \\ -jY_{r,r+1}\frac{\lambda g}{\lambda g_o} & 1 \end{bmatrix} \begin{bmatrix} \cos(\phi_{r,r+1}/2) & j\sin(\phi_{r,r+1}/2) \\ j\sin(\phi_{r,r+1}/2) & \cos(\phi_{r,r+1}/2) \end{bmatrix}$$

$$= \begin{bmatrix} \cos(\phi_{r,r+1}) + \frac{\lambda g\, Y_{r,r+1}}{2\lambda g_o}\sin(\phi_{r,r+1}) & j\{\sin(\phi_{r,r+1}) + \frac{\lambda g\, Y_{r,r+1}}{2\lambda g_o}(1-\cos(\phi_{r,r+1}))\} \\ j\{\sin(\phi_{r,r+1}) - \frac{\lambda g\, Y_{r,r+1}}{2\lambda g_o}(1+\cos(\phi_{r,r+1}))\} & \cos(\phi_{r,r+1}) + \frac{\lambda g\, Y_{r,r+1}}{2\lambda g_o}\sin(\phi_{r,r+1}) \end{bmatrix}$$

- - - -(4.1)

As shown in |36| the shunt inductive coupling element symmetrically located in a piece of waveguide is approximated by a frequency dependant immittance inverter possessing a transfer matrix

$$\begin{bmatrix} 0 & j\frac{\lambda g_o}{K'_{r,r+1}\ \lambda g} \\ jK'_{r,r+1}\frac{\lambda g}{\lambda g_o} & 0 \end{bmatrix} \quad - - - -(4.2)$$

This in turn may be splitted into three parts representing two transformers with turn ratios $\sqrt{\lambda g_o/\lambda g}$ and $\sqrt{\lambda g/\lambda g_o}$ separated by an ideal

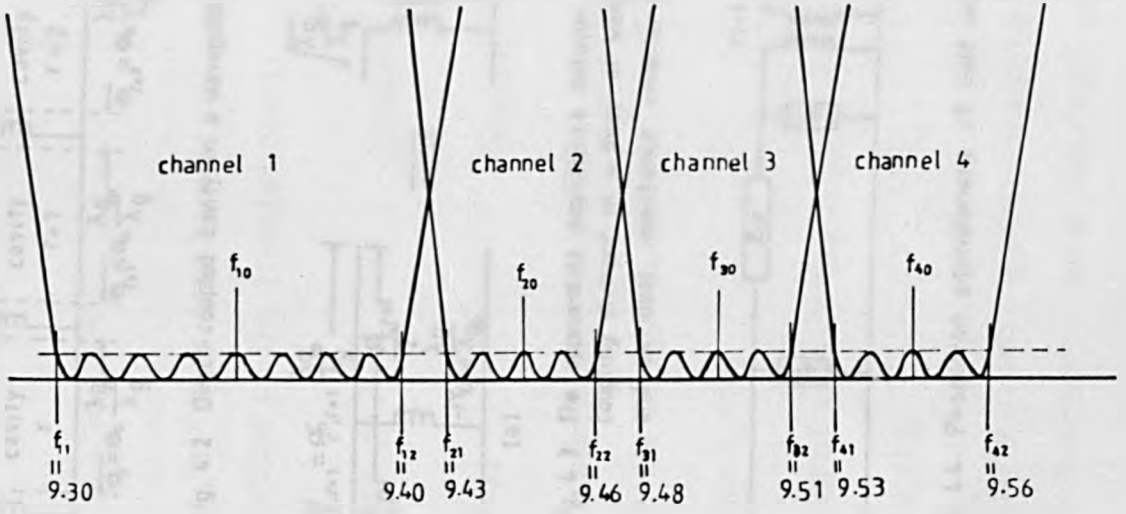

Fig. 4.1 The channels lay out

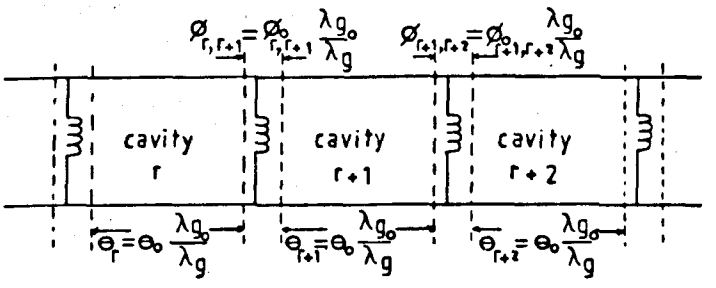

Fig. 4.2 Direct-coupled cavity in a waveguide filter

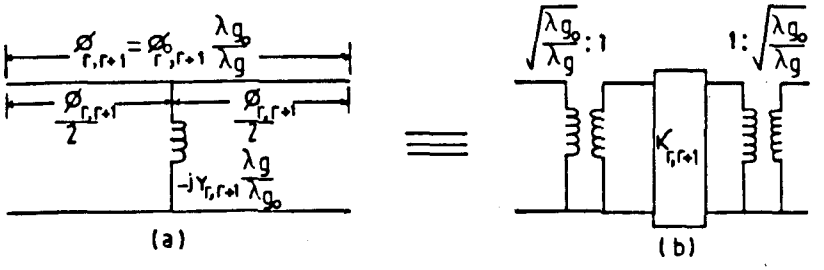

Fig. 4.3 The approximate equivalence between a shunt coupling element in a piece of waveguide (a) and an ideal immittance inverter (b)

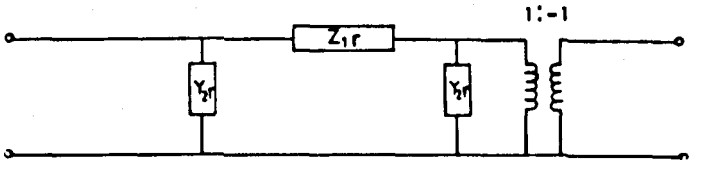

Fig. 4.4 Pi-section equivalenece of half -wave length cavity

immittance inverter of characteristic impedance $K'_{r,r+1}$ as illustrated in Fig.4.3.b.

Equating matrix (4.2) to the righthand side of (4.1) at midband i.e. $\lambda g = \lambda g_o$ yields [35]

$$\left.\begin{aligned} \phi_{or,r+1} &= -\mathrm{Cot}\left(\frac{Y_{r,r+1}}{2}\right) \\ Y_{r,r+1} &= K'_{r,r+1} - 1/K'_{r,r+1} \end{aligned}\right\} \qquad (4.3)$$

Secondly, a half wave length cavity of electrical length $\theta_o = \pi$ at λg_o characterized by the transfer matrix

$$\begin{bmatrix} \mathrm{Cos}(\pi\lambda g_o/\lambda g) & j\mathrm{Sin}(\pi\lambda g_o/\lambda g) \\ j\mathrm{Sin}(\pi\lambda g_o/\lambda g) & \mathrm{Cos}(\pi\lambda g_o/\lambda g) \end{bmatrix} \qquad (4.4)$$

has P_i-section equivalent circuit given in [35] and shown in Fig.4.4 where the impedance of the series arm is

$$Z_{1_r} = -j\ \mathrm{Sin}(\pi\lambda g_o/\lambda g) \qquad (4.5)$$

and the admittance of each of the shunt arms is

$$Y_{2_r} = -\mathrm{Cot}(\pi\lambda g_o/\lambda g) \qquad (4.6)$$

The latter is usually a small quantity compared with the large adjacent admittance of the inverter. Hence the shunt arms may be neglected. The 1:-1 transformer has only a phase correcting effect.

However, neglecting the shunt arms of the P_i-section equivalence of the cavity and scaling out the frequency dependant transformers in the equivalent circuit of the shunt coupling element across the filter, yields the approximate circuit of a typical section of a waveguide direct

coupled cavity filter shown in Fig.4.5.

The direct comparison with the lumped low-pass prototype in the dual format shown in Fig.4.6. implies the frequency transformation [36] given by

$$\omega \rightarrow \alpha \frac{\lambda g}{\lambda g_o} \mathrm{Sin}(\pi \lambda g_o / \lambda g) \qquad (4.7)$$

where ω is the lumped prototype frequency variable and α is a scaling constant. Furthermore, Levy |36| has shown that to a second degree of approximation around $\lambda g = \lambda g_o$ (justified for narrow band applications), the relationship (4.7) tends to

$$\omega \rightarrow -\alpha\pi \left(1 - \frac{\lambda g}{\lambda g_o}\right) \qquad (4.8)$$

and his method inherently leads to that used by Cohn [35].

However, the final design equations for the direct coupled cavity waveguide filter based upon the lumped low-pass prototype shown in Fig.4.6 may be given by:

$$\alpha = \frac{\omega_c}{\pi} \left(\frac{\lambda g_1 + \lambda g_2}{\lambda g_1 - \lambda g_2}\right) \qquad (4.9)$$

where

ω_c is the cut-off frequency of the lumped low-pass prototype (normally $\omega_c = 1$ rad/sec)

λg_1 and λg_2 are the guide wavelength at the lower and upper band edge frequencies.

The coupling between the rth and r + 1th cavities is given by

$$Y_{r,r+1} = \frac{\alpha \sqrt{g_r\, g_{r+1}}}{K_{r,r+1}} - \frac{K_{r,r+1}}{\alpha \sqrt{g_r\, g_{r+1}}} \qquad r = 0 \rightarrow n \qquad (4.10)$$

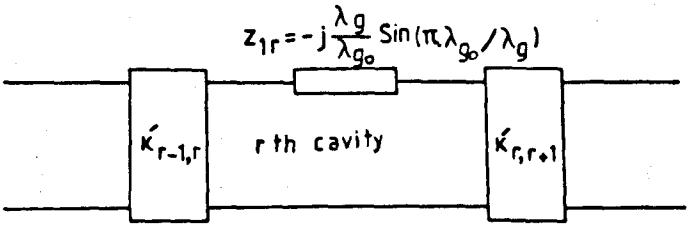

Fig. 4.5 Equivalent circuit of a typical section of a direct coupled cavity waveguide filter

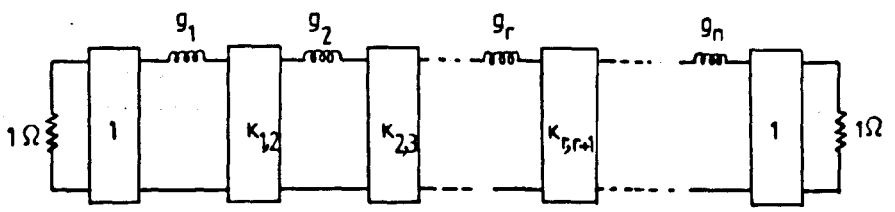

Fig. 4.6 Lumped low-pass prototype filter

where

$K_{r,r+1}$ is the characteristic impedance of the prototype inverter and the terminating loads are:

$$g_o = g_{n+1} = 1/\alpha \qquad (4.11)$$

The electrical length of the rth resonant cavity is

$$\psi_r = \theta_{or} - \frac{1}{2}\phi_{r-1,r} - \frac{1}{2}\phi_{r,r+1} \qquad r = 1 \rightarrow n \qquad (4.12)$$

where

$$\phi_{r,r+1} = \text{Cot}^{-1}\frac{Y_{r,r+1}}{2}$$

$\theta_{o_r} = \pi$ corresponds to a physical length of $\lambda g_o/2$

and

$$\lambda g_o = \frac{\lambda_{g1} + \lambda_{g2}}{2} \qquad (4.13)$$

Having reviewed the design procedure for the direct coupled cavity waveguide filter, one can now proceed with the multiplexer design example.

4.3. THE MULTIPLEXER DESIGN SPECIFICATIONS

Number of channels = 4

All channels satisfy a Chebyshev response with inband return loss = 20dB

The rest of the specification are given in the table below:

i Channel Number	n_i No. of Resonators	f_{i1}(GHZ) Lower bandedge	f_{i2}(GHZ) Upper bandedge
1	8	9.3	9.4
2	4	9.43	9.46
3	4	9.48	9.51
4	4	9.53	9.56

4.4 CALCULATION OF THE PROTOTYPE VALUES

The structure of interest here is the standard rectangular waveguide WG16 (WR90) which has the following properties [37]:

(i) The inside dimensions:

b = height (narrow dimension) = 0.4"

a = width (broad dimension) = 0.9"

the walls thickness = 0.05"

(ii) Recommended frequency range for TE10 mode from 8.20 → 12.5 GHZ

(iii) Cut off frequency f_c in MHZ = 6570.5860

(iv) Cut off wavelength λ_c is given by

$$\lambda_c = \frac{2ab}{(n^2b^2+m^2a^2)} \qquad (4.13)$$

where

n = number of half waves variation of the field in the a-direction (n = 0,1,2,3 - - -)

m = number of half waves variation of the field in the b-direction (m = 0,1,2,3 - - -)

For waveguide WG16 supporting TE10 mode

$$\lambda_c = 1.8"$$

(v) The guide wavelength λg is given by

$$\lambda g = \frac{\lambda}{(1 - (\lambda/\lambda_c)^2)^{\frac{1}{2}}} \qquad (4.14)$$

where

λ is the free space wavelength

$$\lambda = \frac{c}{f} \qquad (4.15)$$

and c is velocity of light in free space

$= 11.80315 \times 10^9$ inch/sec

However, in order to proceed in the multiplexer design process, the given frequency specification in GHZ must be related to prototype values in rad/sec. One suitable prototype may be obtained by setting f_{i2} = 9.4GHZ to correspond to unity rad/sec on the prototype frequency scale and using the transformation

$$\omega \rightarrow \beta\pi\lambda g \qquad (4.16)$$

where

ω is the prototype frequency variable rad/sec

β is a scaling constant

λg can be calculated by using equation (4.14)

For channel i = 1

The free space wavelengths at the bandedges frequencies are:

$$\lambda_{11} = \frac{11.80315 \times 10^9}{9.3 \times 10^9} = 1.269156"$$

$$\lambda_{12} = \frac{11.80315 \times 10^9}{9.4 \times 10^9} = 1.255654"$$

The corresponding guide wavelengths are

$$\lambda g_{11} = 1.789759"$$

$$\lambda g_{12} = 1.752479"$$

Now, using the relationship in (4.16) for λg_{12} corresponding to $\omega_{11} = 1$ yields

$$\beta = \frac{\omega_{11}}{\pi \lambda g_{12}} = \frac{1}{1.752479\pi} = 0.181634 \qquad (4.17)$$

Thus,

$$\omega_{12} = \beta \pi \lambda g_{11} = 1.021272 \text{ rad/sec}$$

Similarly,

For channel i = 2

$$\lambda_{21} = 1.25166" \quad , \quad \lambda_{22} = 1.24769"$$

$$\lambda g_{21} = 1.74167" \quad , \quad \lambda g_{22} = 1.731021"$$

and

$$\omega_{21} = \beta \pi \lambda g_{22} = 0.987755 \text{ rad/sec}$$

$$\omega_{22} = \beta \pi \lambda g_{21} = 0.993832 \text{ rad/sec}$$

For channel i = 3

$\lambda_{31} = 1.245058"$, $\lambda_{32} = 1.24113"$

$\lambda g_{31} = 1.724013"$, $\lambda g_{32} = 1.713629"$

and

$\omega_{31} = \beta\pi\lambda g_{32} = 0.977831$ rad/sec

$\omega_{32} = \beta\pi\lambda g_{31} = 0.983756$ rad/sec

For channel i = 4

$\lambda_{41} = 1.238526"$, $\lambda_{42} = 1.234639"$

$\lambda g_{41} = 1.706795"$, $\lambda g_{42} = 1.696665"$

and

$\omega_{41} = \beta\pi\lambda g_{42} = 0.968151$ rad/sec

$\omega_{42} = \beta\pi\lambda g_{41} = 0.973931$ rad/sec

The prototype channels layout is shown in Fig.4.7.

However, in practical design cases, the number of resonators in each channel may not be given, instead the rejection LA_i in (dB) of each channel over the adjacent ones is given. In this case the number of resonators n_i may be calculated at this stage of the design process by using the following relationship [7].

$$n_i \geq \frac{LA_i + LR_i + 6}{20 \log (\delta_i + \sqrt{\delta_i - 1})} \qquad (4.18)$$

where

LR_i is the inband return loss (dB)

$$\delta_i = \frac{A_i}{B_i}$$

A_i and B_i are as defined in Fig.4.7.

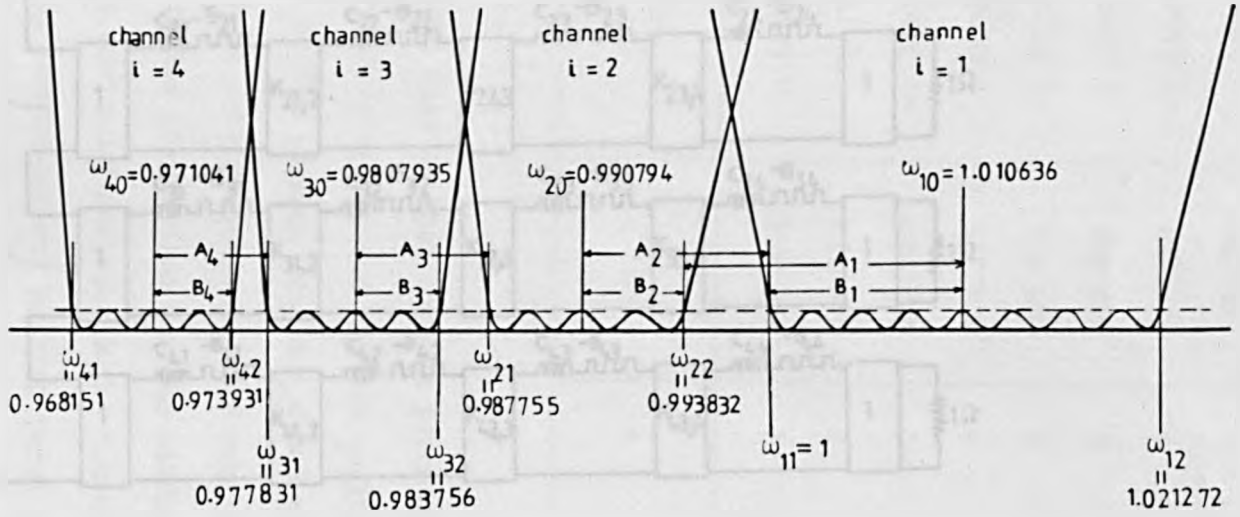

Fig. 4.7 The prototype channels layout

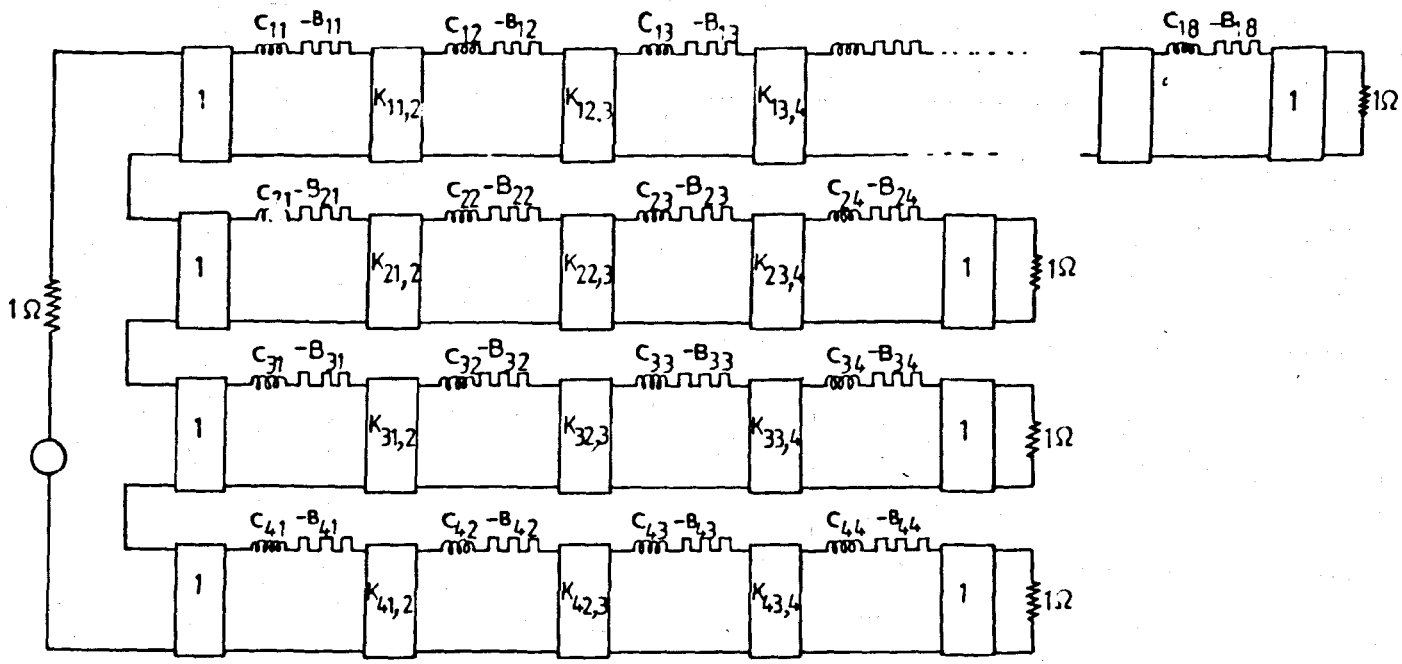

Fig. 4.8 The prototype 4-channel multiplexer

If equation (4.18) is used, one should keep in mind the advantage of multiplexer design procedures based on doubly terminated prototypes which give an improvement of more than 6(dB) in the offband insertion loss, and consequently result in saving of at least one cavity per channel.

Having calculated the required prototype design values, they can be now supplied as input data to the programmed design procedure introduced in the last chapter. The obtained prototype modified element values of the four bandpass channel multiplexer are given in Table 1.A and 1.B. For convenience, the prototype multiplexer is used in the dual form shown in Fig 4.8 where the four channel may be seen seriesly connected at a common junction and for practical reasons a normalized impedance inverter is introduced at both ends of each channel.

Channel i = 1

$n_1 = 8$, $\varepsilon = .1$, $\omega_{11} = 1$, $\omega_{12} = 1.021272$

r	C_{1r}	I_{1r}	$K_{1r,r+1}$
1	89.3355	-1.01473	1.26534
2	260.719	-1.01105	2.03759
3	402.929	-1.0107	2.58891
4	479.376	-1.01065	2.78696
5	480.416	-1.01064	2.60654
6	407.498	-1.01064	2.09683
7	272.319	-1.01064	1.41246
8	95.6289	-1.01064	0

Table 1.A Modified element values of channel i = 1 of the prototype multiplexer

	r	1	2	3	4
Channel i=2 $n_2=4$, $\epsilon_2=.1$, $\omega_{21}=.987755$ $\omega_{22}=.993832$	C_{2r}	366.867	730.754	737.69	306.288
	I_{2r}	-0.990667	-0.990766	-0.990787	-0.990789
	$K_{2r,r+1}$	1.27823	1.56264	1.31665	0
Channel i=3 $n_3=4$, $\epsilon_3=.1$, $\omega_{31}=.977831$ $\omega_{32}=.983756$	C_{3r}	357.757	740.474	753.919	313.859
	I_{3r}	-0.980155	-0.98064	-0.980755	-0.980771
	$K_{3r,r+1}$	1.23784	1.54845	1.3136	0
Channel i=3 $n_4=4$, $\epsilon_4=1$, $\omega_{41}=968151$ $\omega_{42}=.973931$	C_{4r}	207.00	693.042	754.968	319.851
	I_{4r}	-0.968558	-0.97082	-0.970985	-0.971008
	$K_{4r,r+1}$	0.983823	1.46013	1.29439	0

Table 1.B Modified element values of channel 2,3 and 4 of the prototype multiplexer

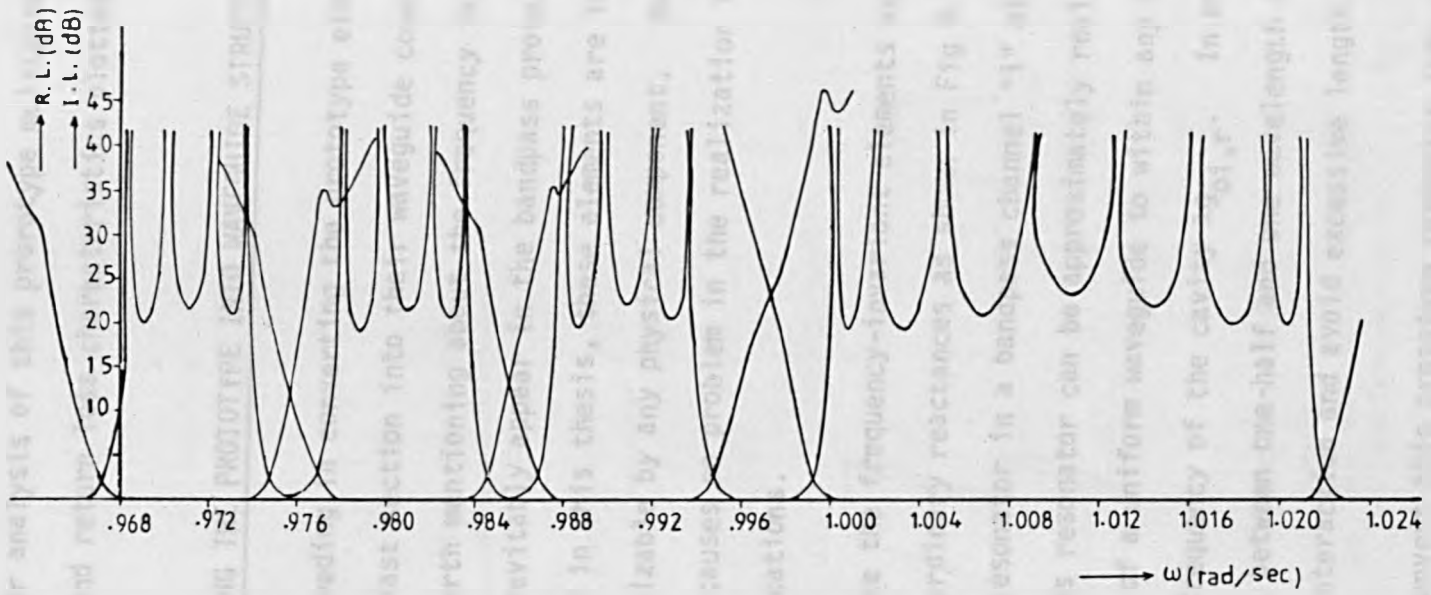

Fig. 4.9 The computer analysis of the prototype multiplexer showing the insertion loss (I.L.) and return loss (R.L.) characteristics

The computer analysis of this prorotype multiplexer yields the insertion loss and return loss characteristics plotted in Fig 4.9.

4.5 CONVERTING THE PROTOTYPE INTO WAVEGUIDE STRUCTURE

Before proceeding in converting the prototype element values obtained in the last section into their waveguide counterparts, few more words are worth mentioning about the frequency invariant reactive elements which inevitably appear in the bandpass prototype. As mentioned earlier in this thesis, these elements are imaginary. Hence they are not realizable by any physical component. But their existance in the prototype causes no problem in the realization for relatively narrow band applications.

However, since the frequency-invariant elements usually occur in conjunction with ordinary reactances as shown in Fig 4.10 which represents a typical series resonator in a bandpass channel "i" of the multiplexer in question. This resonator can be approximately realized by an equivalent length of a uniform waveguide to within any half wavelength at the resonance frequency of the cavity $\lambda g_{oi,r}$. In practice, the length of guide should be between one-half and one wavelength long to prevent evanescent modes interaction and avoid excessive length.

However, to convert this prototype resonator into a waveguide structure, the familiar reactance slope technique (see for example [35] and [28]) may be applied, such that the magnitude and the first derivative with respect to λg_r of the reactance of the prototype resonator in Fig 4.10 are respectively equated to the magnitude and the first derivative of the reactance of the waveguide resonant cavity, all evaluated at $\lambda g_{i,r} = \lambda_{goi,r}$.

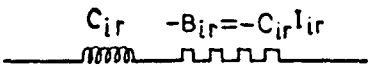

Fig. 4.10 A typical prototype series resonator

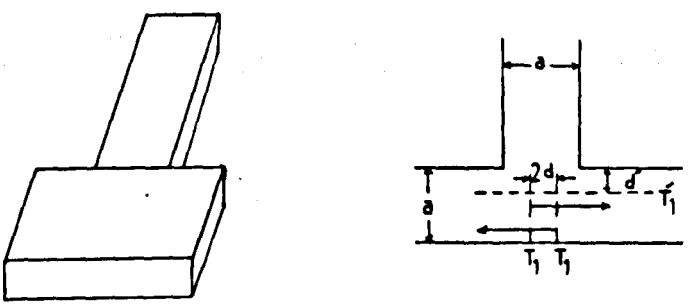

(a) (b)

Fig. 4.11 H-plane, Tee-junction

(a) General view

(b) Top view showing the position of the reference planes

Thus,

$$\nu_{i,r}\left[C_{i,r}\,\beta\,\pi\,\lambda g_{i,r} - I_{i,r}\,C_{i,r}\right] = \pi\left[\frac{\lambda g_{i,r}}{\lambda g_{oi,r}} - 1\right] \qquad (4.19)$$

where $\nu_{i,r}$ is a scaling constant still to be determined. At resonance i.e $\lambda g_{i,r} = \lambda g_{oi,r}$, this equation becomes

$$\nu_{i,r}\left[C_{i,r}\,\beta\,\pi\,\lambda g_{oi,r} - I_{i,r}\,C_{i,r}\right] = 0 \qquad (4.20)$$

Yielding,

$$\lambda g_{oi,r} = \frac{I_{i,r}}{\beta\,\pi} \qquad (4.21)$$

where β for this particular design example = 0.181634 (obtained from equation 4.17).

Now, calculating the first derivatives of both sides of equation (4.19) with respect to $\lambda g_{i,r}$ at $\lambda g_{i,r} = \lambda g_{oi,r}$ results in

$$\nu_{i,r}\,C_{i,r}\,\beta\,\pi = \frac{\pi}{\lambda g_{oi,r}} \qquad (4.22)$$

Hence,

$$\nu_{i,r} = \frac{\pi}{C_{i,r}\,I_{i,r}} \qquad (4.23)$$

On the other hand, the inductive coupling susceptance $Y_{i,r,r+1}$ between the rth and (r+1)th cavity can be determined by using an equivalent form to equation (4.10) as:

$$\left.Y_{i,r,r+1} = \frac{1}{K_{i,r}\sqrt{\nu_{i,r}\,\nu_{i,r+1}}} - K_{i,r}\sqrt{\nu_{i,r}\,\nu_{i,r-1}}\right\}_{r=1 \rightarrow n_i} \qquad (4.24a)$$

and the first and the last coupling at each channel can be obtained

respectively from

$$Y_{i,0,1} = \frac{1}{\sqrt{\nu_{i,1}}} - \sqrt{\nu_{i,1}} \qquad (4.24b)$$

$$Y_{i,n_i,n_i+1} = \frac{1}{\sqrt{\nu_{i,n_i}}} - \sqrt{\nu_{i,n_i}} \qquad (4.24c)$$

The electrical length of the rth resonant cavity is given by

$$\psi_{i,r} = \pi - \frac{1}{2}\tan^{-1}\left[\frac{2}{Y_{i,r-1,r}}\right] - \frac{1}{2}\tan^{-1}\left[\frac{2}{Y_{i,r,r+1}}\right] \quad \Big\}_{r=1 \to n_i} \qquad (4.25)$$

where π corresponds to a physical length of $\lambda g_{oi,r}/2$. Thus, the calculated waveguide element values for channels $i=1 \to 4$ are given in Tables 2.A,B,C and D respectively.

Table 2.A: The waveguide element values of channel i = 1

r	$\lambda g_{01r} = \frac{I_{1r}}{\beta\pi}$ Inch	$\nu_{1r} = \frac{\pi}{I_{1r}C_{1r}}$	ψ_{1r} (rad)	$Y_{1r,r+1}$
0				5.185528
1	1.778294	0.0034656	2.931828	38.861053
2	1.771845	0.011918	3.096348	51.165343
3	1.771231	0.007714	3.103751	54.597921
4	1.771126	0.006484	3.105236	55.380145
5	1.771126	0.00647	3.105234	54.592437
6	1.771126	0.007628	3.10372	51.088974
7	1.771126	0.011415	3.094828	36.72675
8	1.771126	0.032506	2.936014	5.366196

Table 2.B: The waveguide element values of channel i = 2

r	$\lambda g_{02r} = \frac{I_{2r}}{\beta\pi}$ Inch	$\nu_{2r} = \frac{\pi}{I_{2r}C_{2r}}$	ψ_{2r} (rad)	$Y_{2r,r+1}$
0				10.662825
1	1.736124	0.008644	3.041058	127.735666
2	1.736297	0.004339	3.127017	148.181251
3	1.73633	0.004298	3.126062	113.854663
4	1.73634	0.010352	3.031415	9.726769

Table 2.C: The waveguide element values of channel i = 3

r	$\lambda g_{03r} = \frac{I_{3r}}{\pi\beta}$ Inch	$\nu_{3r} = \frac{\pi}{I_{3r} C_{3r}}$	ψ_{3r} (rad)	$Y_{3r,r+1}$
0				10.470366
1	1.717702	0.008959	3.039516	129.758755
2	1.718552	0.004326	3.127248	150.624996
3	1.718753	0.004249	3.126304	115.593447
4	1.718781	0.010206	3.023563	8.996155

Table 2.D: The waveguide element values of channel i = 4

r	$\lambda g_{04r} = \frac{I_{4r}}{\pi\beta}$ Inch	$\nu_{4r} = \frac{\pi}{I_{4r} C_{4r}}$	ψ_{4r} (rad)	$Y_{4r,r+1}$
0				7.863582
1	1.697378	0.015669	3.00869	118.828249
2	1.701342	0.004669	3.126645	153.091799
3	1.701632	0.004286	3.126539	117.326
4	1.701672	0.010115	3.032834	9.842418

The next step in the design process is to convert the electrical values of $\psi_{i,r}$ and $Y_{i,r,r+1}$ into physical dimensions. The conversion of $\psi_{i,r}$ is a straightforward operation since the corresponding values of $\lambda g_{oi,r}$ are already known as tabulated in Tables 2.A,B,C and D. Yielding the physical length of most of $\psi_{i,r}$ to be slightly less than $\lambda g_{oi,r}/2$. However, the physical realization of $Y_{i,r,r+1}$ can be obtained by using irises or posts. Their physical dimensions can then be determined from standard experimental or theoretical data e.g. [37] and |38| among others. In this design example the structure of interest is equal diameter post in a standard rectangular waveguide WG16 (WR90). Therefore, the appropriate graphs of reference [39] have been used to determine the suitable configuration and the physical dimensions of the posts. These graphs are enclosed in the appendix of this chapter.

Each channel filter used three posts of the same dimeter (0.065") for the input and output coupling susceptances and five posts having the same diameter (0.065") for the internal couplings. Tuning screws were located at the centre of each cavity of the channel filters.

The series connection of the channels at a common junction was made with simple H-plane, Tee-junctions [38] as that shown in Fig 4.11 to waveguide WG16 main feed. The feed has a common port at one end and short circuited at the other. Standard square connecting flanges are used at each channel output port and at the common input port. The final structure of the multiplexer is sketched in Fig 4.12.

However, the dimensions "d" and 'd' associated with the reference plans T_1 and T'_1 of the H-plane, Tee-junction shown in Fig 4.11 are as indicated in [37]. They have been calculated here by using the graph

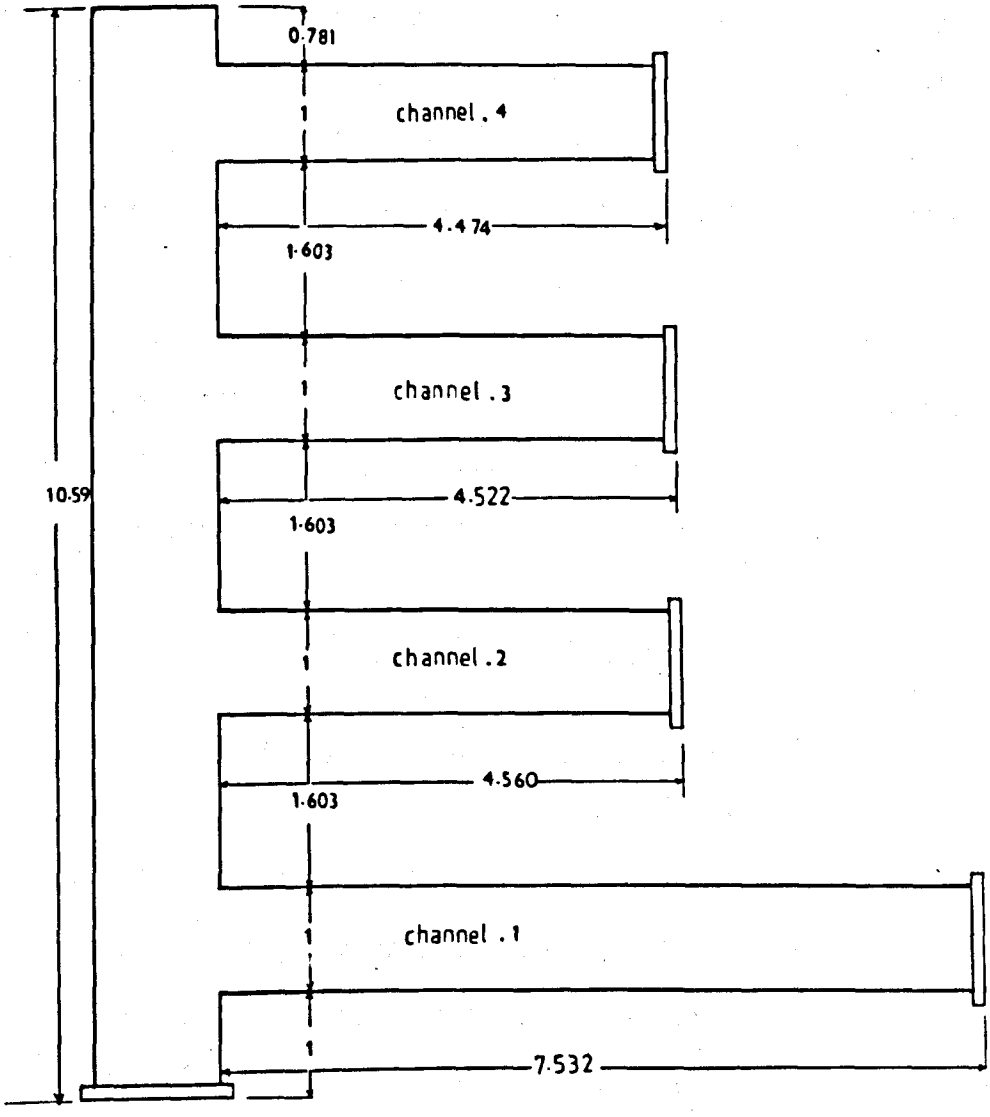

Fig. 4.12 The 4 - channel waveguide multiplexer
(all dimensions are in inches)

shown in Fig.6.5.5. of Reference [37] with the required value of λg is at the suitably chosen frequency of 9.47 GHZ, yielding d = 0.045" and d' = 0.252".

The dimensions of the channel-separating lengths and other length of the main guide feed shown in Fig 4.12 have been calculated from the fact that the distance from the short circuited end of the feed to the appropriate reference plane of the Tee-junction of channel i should be odd multiple of $\lambda g/4$. This λg can be taken as the guide wavelength at the centre frequency of the nearest channel to the closed end (channel 4 in this example). In calculating these dimensions, one should taken into account the practical considerations such as the dimensions of the connecting flanges, the engineering of the device and the feed should not be too long, otherwise it will act as a frequency dependant manifold which will disrupt the performance of the device.

4.6. THE PERFORMANCE OF THE MULTIPLEXER

The multiplexer was tuned using a swept frequency reflectometer arrangement connected to the common port whilst the other ports of the device were terminated with matched loads. However, since this multiplexer design procedure was originally based on the doubly terminated prototype filter, hence the same simple criterion for tuning such filters is used. Its based upon minimizing the reflection in the passband with the correct centre frequency and bandwidth. For example the technique introduced by Dishal [40] for tuning filters may be followed. The relatively easy tuning of the multiplexer is one more advantage of the doubly terminated design procedures over those based on the singly terminated prototypes which usually require special alignment procedures e.g. [32].

The measured insertion loss and return loss response are shown in Fig 4.13 and Fig 4.14 respectively.

4.7. CONCLUDING REMARKS

The application of the multiplexer design procedure developed in Chapter 3 has been presented by considering a 4-channel multiplexer designed and constructed in the standard rectangular waveguide WG16. The individual channels were realized in the form of direct coupled cavity filters. Hence, this chapter started with a brief review of the available design procedures for these filters and the design formulas were also given. Then the modified prototype element values of the channels were obtained starting with the given design specifications. The steps taken in the design process were fully explained. The final physical dimensions were obtained using the experimental data [39] for equal diameter posts coupling in WG16. The limitation of these data should be noticed when an equal diameter post coupling is required for bandwidths less than 30 MHZ at the band of operation.

The device was constructed as shown in Fig 4.12. It was tuned and tested using a swept frequency reflectometer arrangement. Although the tuning of multiplexers designed on the doubly terminated basis is relatively easier than those designed on singly terminated prototypes, still it is a time consuming operation because of the interaction of the channel filters. The tuning of the multiplexers becomes even harder for asymmetrical cases such as in this example. In this particular design example the modified resonance frequency of each cavity has been taken into account in calculating the length of the corresponding cavity. But the length of the waveguide at the input of each channel and the associate coupling have not been modified

in the theory and this left to tuning to take care of. This in turn make the small screws which have been added to slightly adjust the coupling between the cavities, have larger effect on the tuning than it was expected.

Finally judging from the response obtained that the practical devices can be directly produced from the theory with no or little empirical adjustment. The shape of the device shown in Fig 4.12 has no special significance and the channels can be dropped alternatively on either side of the common feed if required.

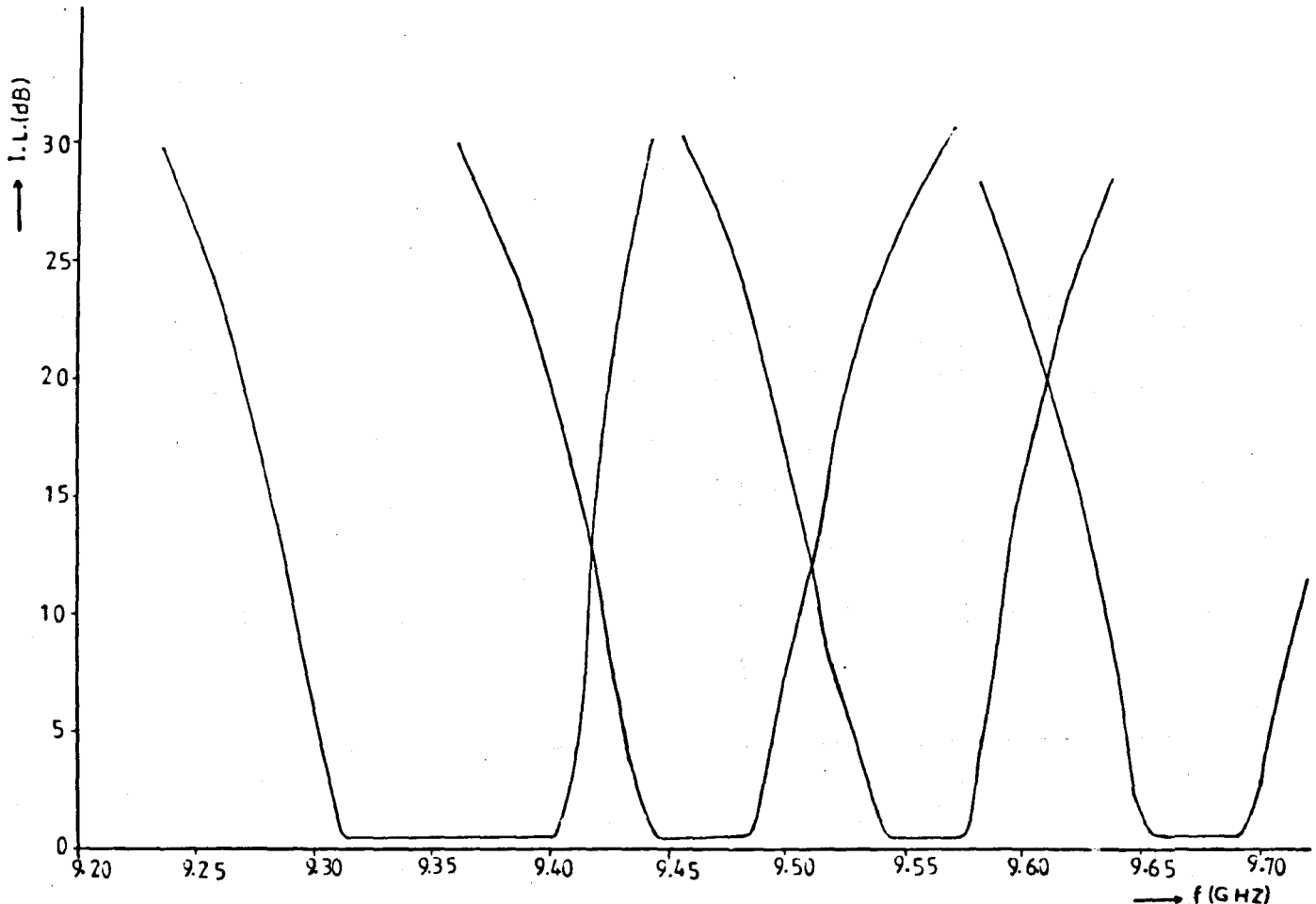

Fig. 4.13 The measured Insertion loss response of the experimental multiplexer

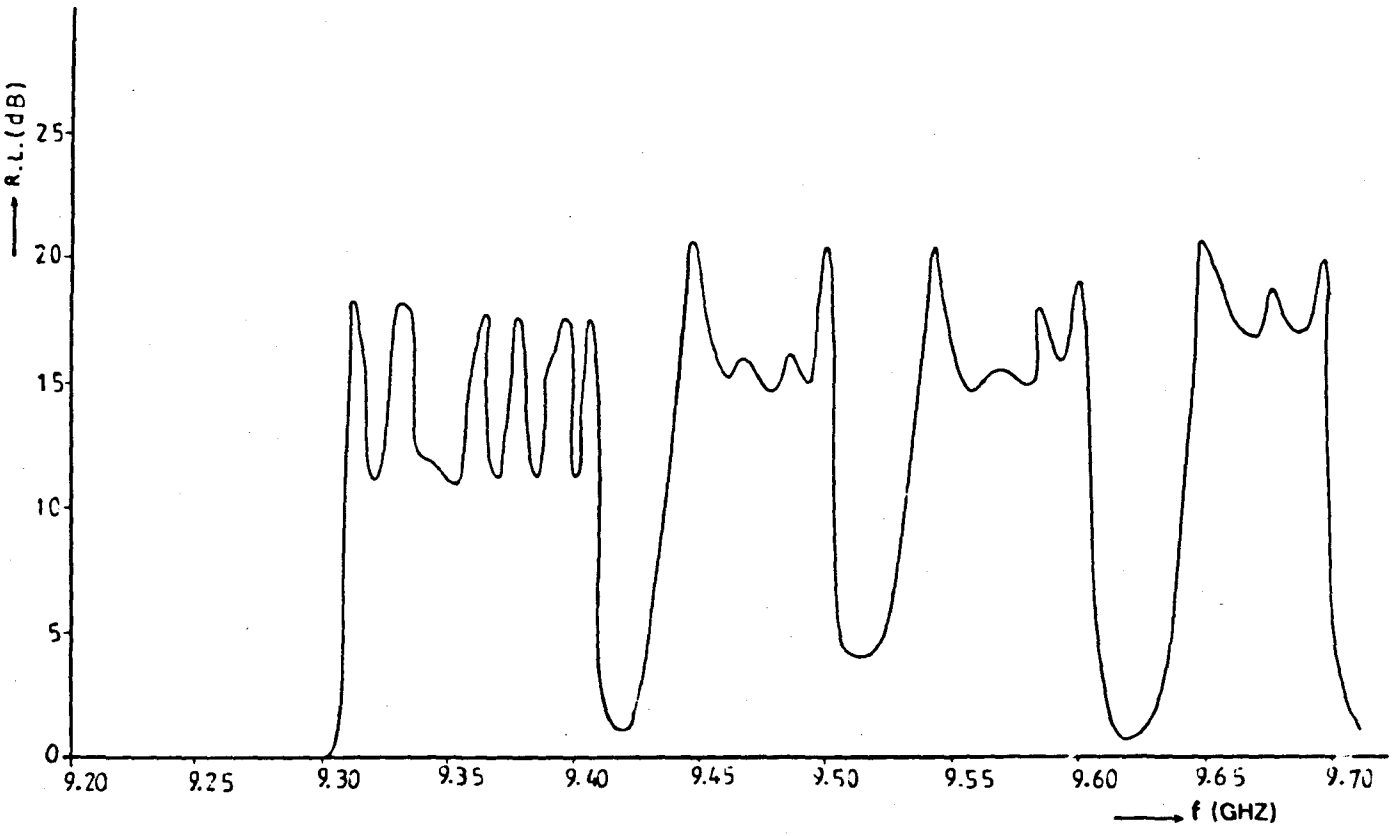

Fig. 4.14 The measured return loss response of the experimental multiplexer

4.8 APPENDIX

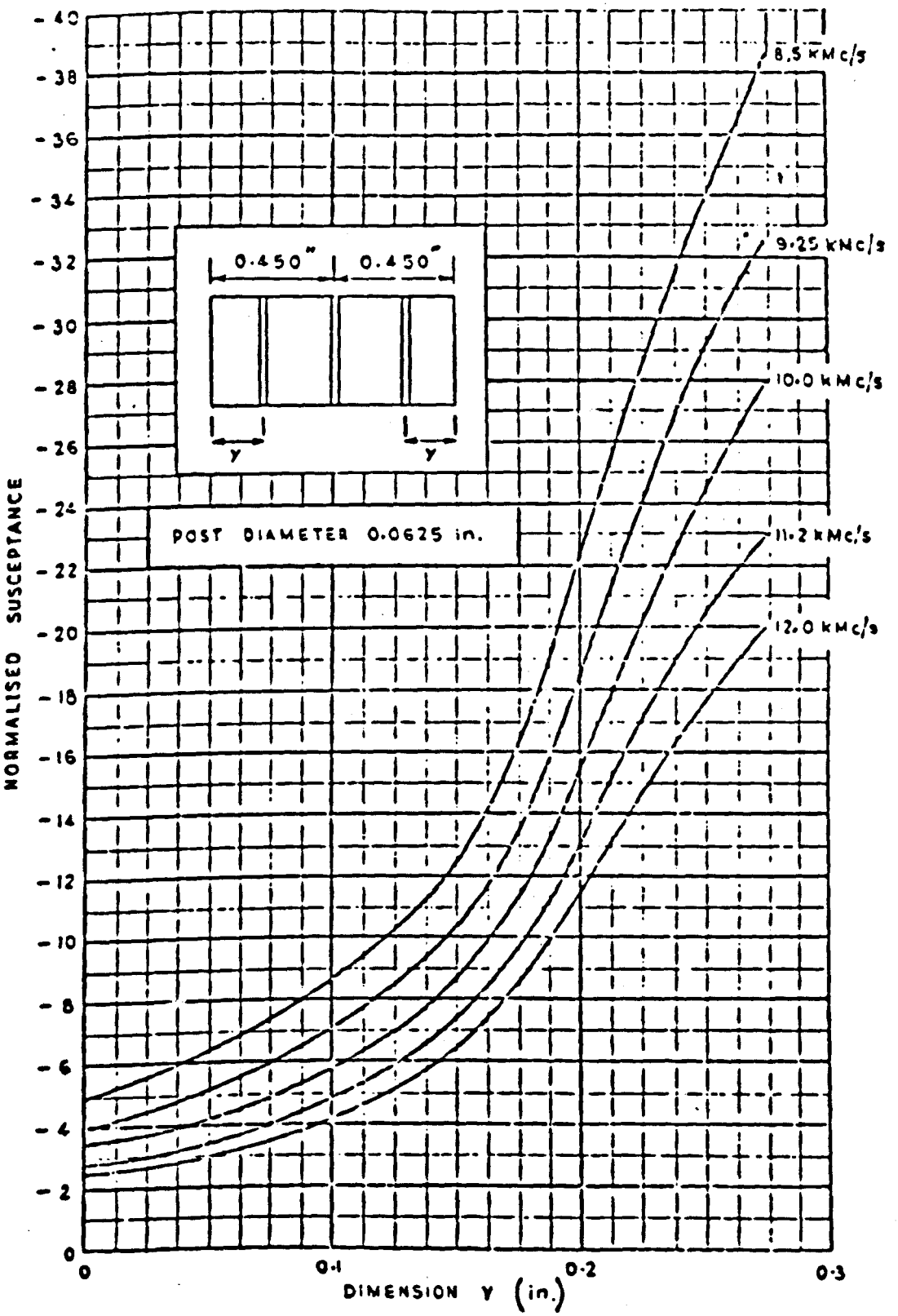

FIGURE 4.15 NORMALISED SUSCEPTANCE FOR THREE SYMMETRICAL POSTS IN WAVEGUIDE 16

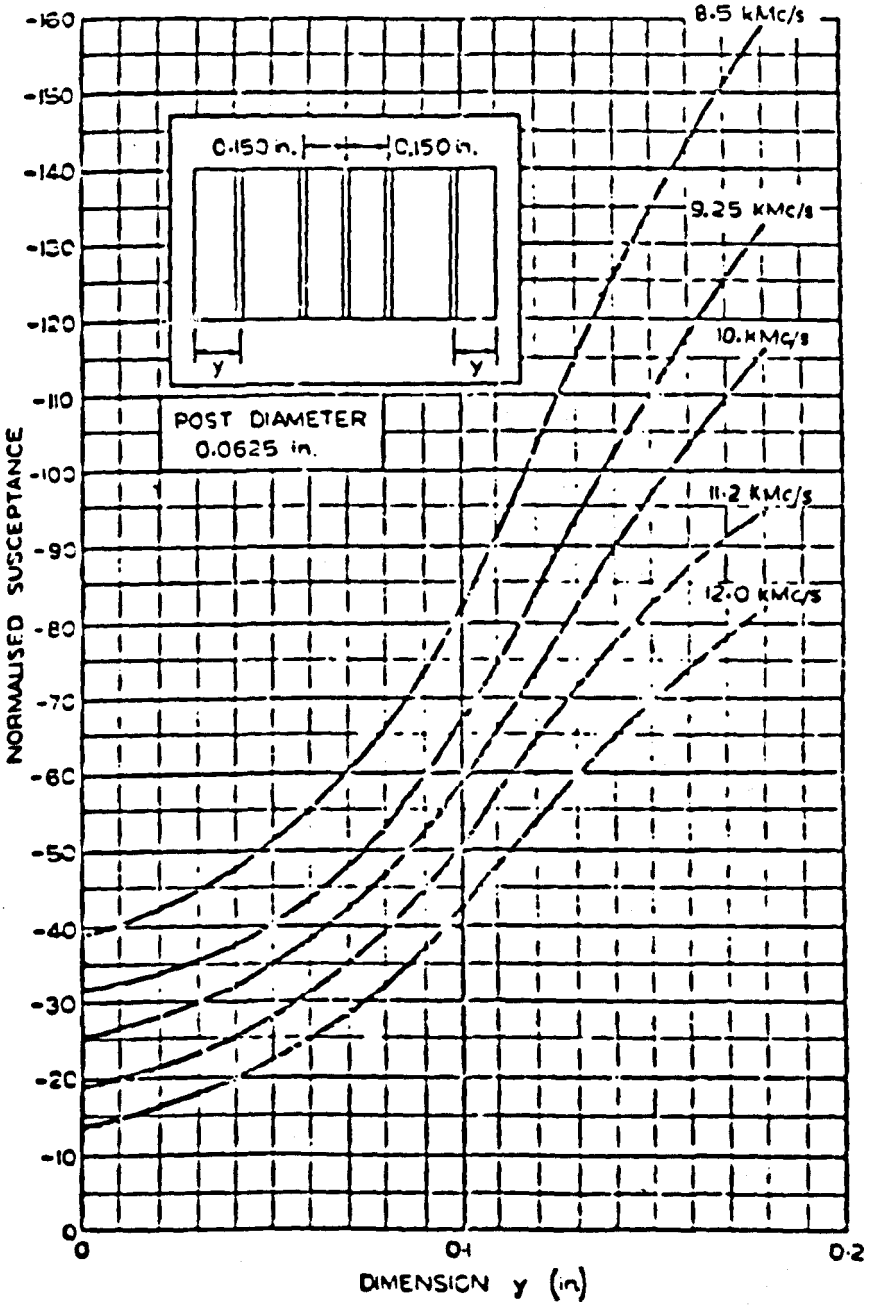

FIGURE 4.16 NORMALISED SUSCEPTANCE FOR FIVE SYMMETRICAL POSTS IN WAVEGUIDE 16

CHAPTER 5

FUNDAMENTALS OF DISTRIBUTED NETWORKS AND DESIGN OF TEM MODE MICROWAVE FILTERS

5.1 INTRODUCTION

This chapter is especially concerned with the design and realization of microwave filter structures for which the wave propagation is Transverse Electro-Magnetic (TEM), that is to say, the structures in which the electric and magnetic field components in the direction of propagation are zero. These structures are in contrast with the waveguide structures which normally operate high order modes, where some of the field components may exist in the direction of propagation.

The TEM networks generally incorporate finite lengths of transmission line in one form or another as circuit elements. Therefore they are sometimes referred to as "transmission line networks".

However, this chapter begins with a brief review of the basic concepts of the "distributed circuits" for which the TEM networks belong. These concepts are given here in a parallel manner to those of the lumped networks mentioned in Chapter 1 of this thesis. An important part of this chapter is devoted to a class of TEM networks known as "the multi-wire-line" structure. The topics presented include the description of the multi-wire-line structures, an exact synthesis procedure for the combline filter satisfying an equiripple passband response of arbitrary bandwidth, and a design example of an octave bandwidth microwave combline filter was realized and built in a coaxial form using parallel coupled rectangular bars. Its experimental performance is also given. A comparison between combline filters consisting of all distributed elements and their counterparts utilizing mixed lumped/distributed

elements is included. A new design technique for TEM networks having equal diameter coupled circular cylindrical rods between parallel ground plane is introduced.

Finally, the microwave integrated circuits (MIC_s) are briefly discussed. A design example is given based on the generalized Chebyshev low-pass prototype having three transmission zeros at infinity and the remainder at the same finite real frequency. The microwave low-pass filter was realized by utilizing a suspended substrate stripline structure. Its experimental response is established.

5.2 BASIC CONCEPTS

Electrical circuits can be conventionally divided into circuits with lumped elements (defined in Chapter 1) and circuits with distributed elements. The latter type consists of combinations of resistors, ideal transformer, and finite lengths of transmission line. These lengths of transmission line are restricted to be "commensurate" i.e. of a proportionate measure or they are multiples of a basic length of line.

The original idea of the commensurate lines as circuit elements is due to Richards [41]. He also showed that networks composed of lumped resistors, ideal transformers and commensurate lengths of transmission line behave in a manner analogous to lumped element networks under the frequency transformation

$$p \rightarrow t = \tanh(ap) \qquad (5.1)$$

where

$p = \sigma + jw$. The lumped network complex frequency variable

a is frequency scaling constant, determined by the quarter wavelength real frequency

Let,

$t = \sigma + j\omega$. The complex frequency variable of the distributed networks.

Also,

$$t = \tanh(ap) = \frac{\ell^{ap} - 1}{\ell^{ap} + 1} \tag{5.2}$$

However, the transformation given in equation (5.1) is well known as"Richard's transformation". It ensures that the driving point immittances of distributed circuits will be rational functions in ℓ^{ap} or t. Consequently if Z(t) is a finite rational driving point immittance function describing passive network, then

$$\left.\begin{aligned} &Z(t) \text{ is a positive real function} \\ \text{i.e.}\quad &\operatorname{Re} Z(t) \geq 0 \text{ for } \operatorname{Re} t \geq 0 \\ \text{and}\quad &Z(t) \text{ real for } t \text{ real} \end{aligned}\right\} \tag{5.3}$$

Furthermore, the reflection scattering coefficient in the distributed domain is a bounded real function.

$$\left.\begin{aligned} &S_{11}(t) \text{ real for } t \text{ real} \\ &|S_{11}(t)| \leq 1 \text{ for } \operatorname{Re} t \geq 0 \end{aligned}\right\} \tag{5.4}$$

and the transfer function $S_{12}(t)$ is a rational function in t and $|S_{11}(j\omega)|^2 \leq 1$

For minimum phase transfer function in the distributed domain, the relationships between the amplitude and the phase responses at real frequencies appear in the form of Wiener - Lee transform [2].

$$\begin{aligned} \alpha(\omega) &= \alpha_0 + \sum_{i=1}^{\infty} \alpha_i \operatorname{Cos}(2ia\omega) \\ -\psi(\omega) &= \sum_{i=1}^{\infty} \alpha_i \operatorname{Sin}(2ia\omega) \end{aligned} \tag{5.5}$$

However, at real lumped frequency $p = j\omega$, the Richard's transformation given in (5.1) becomes

$$t = j\tau = j \tan(a\omega) \tag{5.6}$$

Hence, the real frequency response in the lumped domain becomes periodic in the distributed domain as shown in Fig 5.1 for the ideal low-pass amplitude characteristic.

Under Richard's transformation, the capacitors in a lumped network may be replaced by open-circuited lines, and inductors may be replaced by short-circuited lines. All these lines or "stubs" are of the same electrical length and can be completely described in terms of their characteristic immittances e.g. Y_{oc} & Z_{oL}, which are proportional to the corresponding lumped element values, and the frequency variable $j \tan(a\omega)$. i.e.

$$\left.\begin{aligned} Y &= j\omega C \rightarrow j\, Y_{oc} \tan(a\omega) \\ Z &= j\omega L \rightarrow j\, Z_{oL} \tan(a\omega) \end{aligned}\right\} \tag{5.7.a}$$

where

$$\left.\begin{aligned} Y_{oc} &= \beta C \\ Z_{oL} &= \beta L \end{aligned}\right\} \tag{5.7.b}$$

One additional distributed circuit element has no direct lumped domain counterpart. It is a two port network consisting of a commensurate length of lossless transmission line. Such a line of length ℓ and characteristic impedance Z_0 shown symbolically in Fig 5.2 has the transfer matrix given by

$$\begin{bmatrix} V_1 \\ I_1 \end{bmatrix} = \begin{bmatrix} \cosh(p\ell/v) & Z_0 \mathrm{Sinh}(p\ell/v) \\ \dfrac{\mathrm{Sinh}(p\ell/v)}{Z_0} & \mathrm{Cosh}(p\ell/v) \end{bmatrix} \begin{bmatrix} V_2 \\ I_2 \end{bmatrix} \tag{5.8}$$

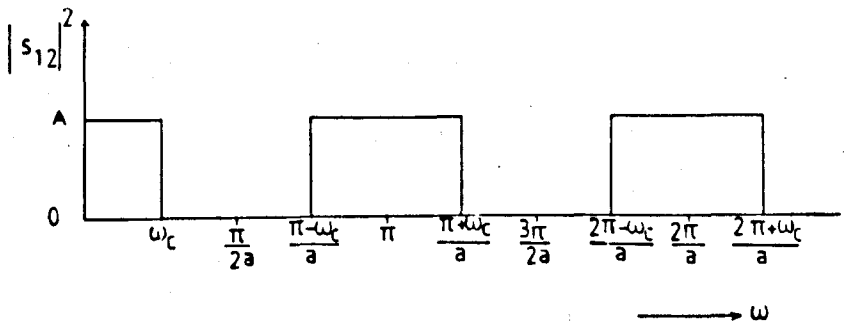

Fig. 5.1 The ideal low pass amplitude characteristic in the distributed domain

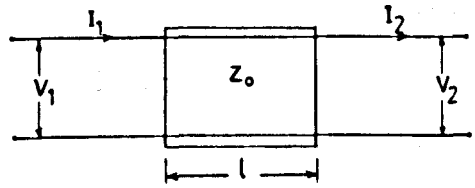

Fig. 5.2 The Unit Element

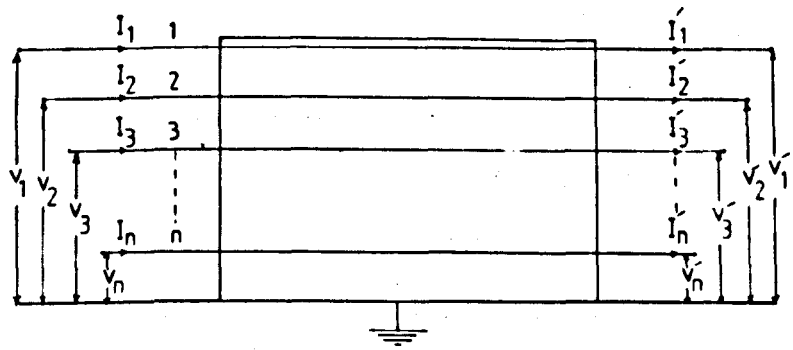

Fig. 5.3 Parallel coupled line arrays over a ground plane

where

v is the phase velocity of TEM wave propagating on the line and ℓ/v is the delay time of the wave on the line section. ℓ/v is the same or of an integer multiple relationship for the commensurate lines in the network.

Describing this matrix in terms of Richard's variable, it becomes

$$\begin{bmatrix} V_1 \\ I_1 \end{bmatrix} = \frac{1}{\sqrt{1 - t^2}} \begin{bmatrix} 1 & Z_o t \\ \frac{t}{Z_o} & 1 \end{bmatrix} \begin{bmatrix} V_2 \\ I_2 \end{bmatrix} \qquad (5.9)$$

This distributed element was originally called a "Unit Element" by Ozaki and Ishii [42] and became known by this name eversince. The Unit Element has many practical advantages in designing and constructing numerous types of microwave passive devices. For example, the Unit Elements may be introduced to be between every pair of stubs in the microwave structures based on the conventional lumped low-pass or high-pass prototypes similar to those shown in Fig 2.9. Although the introduction of the unit elements in this case is redundant in an electrical or mathematical sense (i.e. they do not contribute to the response characteristic), it is a practical necessity for realization especially when they accompanied by the application of four network identities known as "Kuroda's identities" [42] or in their general form "Kuroda-Levy's identities" [43]. For further discussion on the use of unit elements in a redudant manner one can see for example Wenzel [44] and Horton and Wenzel [45].

However, there are many types of microwave structures which could not be designed directly from a certain lumped prototype. Because they did not possess such a prototype. In these structures, the unit elements are generally non-redundant. Thus they contribute to the electrical response and transmission zeros at $t=\pm 1$ should be taken into account in the approximation of the transfer function $S_{12}(t)$. These types include configurations such as the interdigital filter whose distributed prototype consists of a mixed of stubs-unit elements, and the stepped impedance whose prototype composed only of a cascade of unit elements. Synthesis of these circuits can be achieved by using "Richard's theorem". This is an important theory in TEM network synthesis and in some types of lumped network as well. It states: If $Z_{in}(t)$ is a positive real function (p.r.f) and $Z_{in}(t)/Z_{in}(1)$ is not identically equal to t or 1/t, then

$$Z'(t) = \frac{Z_{in}(t) - t\, Z_{in}(1)}{1 - t\, Z_{in}(t)/Z_{in}(1)} \tag{5.10}$$

is p.r.f., Furthermore, if

$$Z_{in}(t) + Z_{in}(-t)\Big|_{t=1} = 0 \tag{5.11}$$

Then,

$$\text{the degree of } Z'(t) = \text{the degree of } Z_{in}(t) - 1 \tag{5.12}$$

For proof and details of this theorem, reference [46] may be consulted.

However, in some cases there is no need to recourse to this formal synthesis technique, since sets of closed form design formulas are available for different types of microwave structures e.g. the most widely used interdigital and stepped impedance filters can be simply designed by using the formulas given in [7].

No further attention will be given in this chapter for the synthesis of

these types, since the main concern of this chapter is the design and construction of classes of TEM filters for broadband applications in which unit elements are not essentially involved. They are based on exactly synthesized lumped Lc prototypes. However these microwave structures may contain a redundant unit element at either end for connection purposes. Lumped components may also be utilized in these microwave structures. The first type to be discussed here is the combline filter. It belongs to a wider class of networks known as "the multi-wire-lines" or "parallel coupled lines" which also include the interdigital filter.

5.3. MULTI-WIRE-LINE NETWORKS

A multi-wire-line structure consists of n-parallel coupled line arrays over a ground plane representing the common return for all lines, as shown symbolically in Fig 5.3. This structure supports a TEM mode and is utilized in several microwave passive devices such as filters, directional couplers and matching networks.

The multi-wire line structure is characterized by the transfer matrix [47] given by

$$\begin{bmatrix} V_1 \\ V_2 \\ \vdots \\ V_n \\ I_1 \\ I_2 \\ \vdots \\ I_n \end{bmatrix} = \frac{1}{\sqrt{1-t^2}} \begin{bmatrix} [1] & [\varepsilon]t \\ & \\ [\eta]t & [1] \end{bmatrix} \begin{bmatrix} V_1' \\ V_2' \\ \vdots \\ V_n' \\ I_1' \\ I_2' \\ \vdots \\ I_n' \end{bmatrix} \qquad (5.13)$$

where

[1] is a unitary matrix

$$[\eta] = \begin{bmatrix} \eta_{11} & -\eta_{12} & -\eta_{1n} \\ -\eta_{12} & \eta_{22} & -\eta_{2n} \\ \vdots & & \\ -\eta_{1n} & -\eta_{2n} & \eta_{nn} \end{bmatrix} \tag{5.14}$$

is the characteristic admittance matrix of the n-wire line.

And

$$[\varepsilon] = [\eta]^{-1} \tag{5.15}$$

is its characteristic impedance matrix.

The necessary and sufficient condition for physical realization of a network of this type is that [η] being symmetrical hyperdominant matrix [48] i.e. all of its diagonal terms must be non-negative or zero and the sum of all elements in every row and column must be non-negative

$$\left.\begin{aligned} \eta_{ij} = \eta_{ji} &\geq 0 \qquad && i \neq j \\ \eta_{ii} = \eta_{ie} + \sum_{j \neq i} \eta_{ij} &&& i,j = 1,2,3 \text{ --- } n \end{aligned}\right\} \tag{5.16}$$

where η_{ie} is the self-admittance of line i to ground.

The analysis of wave propagation along a multi-wire line is not simple if the wires are lossy and their geometrical arrangements are not symmetrical. But it can be simplified if either assuming there is no dissipation or the wires are symmetrically arranged. A general treatment of multi-wire networks is given [46]. Wenzel [48] gives a comprehensive description of TEM propagation on an array of parallel coupled lines in terms of the static capacitance matrix. There are many other contributions dealing with the analysis of TEM parallel coupled lines. All these methods

show that neglecting the direct coupling between non-adjacent lines simplifies the analysis and synthesis of the networks without causing any series limitation of most practical applications.

One of the most popular parallel coupled line structures is the interdigital bandpass filter. This filter was first introduced by Matthaei [49]. He also gave an approximate design method for narrowband applications. Later on an exact design theory has been developed by Wenzel [50] and commented on by Riblet [51]. On the other hand Rhodes provided a rigorous mathematical treatment [52] and the explicit design formulas for this filter [7].

The interdigital filter is constructed from the general n-wire-line when every line is alternatively short circuited to ground at one end and the other ends are either open circuited or capacitively loaded. Each line is one-quarter wave long at band centre, when their ends are open circuited. These lines (resonators) can be made shorter than one-quarter wavelength at band centre and the filter becomes more compact by capacitvely loading the open circuited ends of the resonators.

Another even more compact structure of the parallel coupled lines is the combline filter which will be discussed in some detail in the following section.

5.4 THE COMBLINE FILTER

5.4.1 Background

The combline filter occupies a distinguished place among microwave band-pass filters specially for moderate to octave bandwidth applications. The popularity of the combline compared to other filters can be attributed to the small size, broad stopband, and ease of manufacturing.

It consists of parallel coupled arrays between two paralle ground planes. All these arrays are short-circuited to ground on the same side and capacitvely loaded on the other. The capacitances are necessary to the functioning of the filter, since there is no coupling between quarterwave length digital resonators when they are all grounded on one side and open circuited on the other. The bars are typically one-eighth of a wavelength long at midband. The first spurious passband then does not occur until past the fourth harmonic frequency. This property of a broader stopband makes it attractive in designing bandpass channel multiplexers and this application will be discussed in the next chapter of this thesis.

The combline filter was first introduced and described by Matthaei [53], who gave an approximate design method based on the conventional low-pass prototype. His method is suitable for bandwidths less than 15 percent. Kurzrok [54], [55] presented a modified version of the original combline by introducing transverse decoupling posts between the adjacent resonators. This modified version is particularly useful for tunable filters, where it is desired to keep the absolute bandwidth constant as the filter is tuned. The decoupling posts are also useful to reduce the size of very narrow bandwidth filters, where the resonators might be widely separated to achieve the loose coupling necessary for such bandwidths. Another modified version of the combline filter was given by Cristal [56]. His modification based on utilizing series lumped capacitive coupling at the input and output of the filter instead of the transmission line matching section, hence a size reduction might be achieved. But this version of combline has some mechanical drawbacks due to the difficulty of realizing series capacitors.

Until the early years of this decade, no design procedure was

known for broadband combline filter when Pregla [57] has described a design procedure for this filter and other related structures consisting of coupled lines and lumped capacitances. Later on Wenzel [58] presented an exact synthesis method for combline filters and capacitvely loaded interdigital filters of arbitrary bandwidth. This section presents an exact synthesis procedure for the combline filter based on the lumped prototype used by Wenzel [58] and shown in Fig.5.4.

5.4.2 Exact Synthesis Procedure For Lumped Band-Pass Prototype

The protytype network shown in Fig.5.4 can be used in designing several band-pass microwave filters. It is adopted here for designing a microwave combline filter satisying a generalized Chebyshev response given by

$$|S_{12}(j\omega)|^2 = \frac{1}{1 + \varepsilon^2 F_N^2(\omega)} \qquad (5.17)$$

where, $F_N(\omega)$ is a generalized Chebyshev function defined by the prescribed transmission zeros and may be written as

$$F_N(\omega) = \cosh\left\{ (N-1)\cosh^{-1}\left[\frac{\omega^2 - \alpha^2}{1 - \alpha^2}\right]^{\frac{1}{2}} + \cosh^{-1}\left[\frac{1}{\omega}\left[\frac{\omega^2 - \alpha^2}{1 - \alpha^2}\right]^{\frac{1}{2}}\right]\right\} \qquad (5.18)$$

where

N is an even number equal to the total number of transmission zeros. The transmission zeros are of order (N-1) at $\omega = \infty$ and one at $\omega = 0$.

α is a bandwidth factors, its value is always less than unity when the upper bandedge frequency ω_2 is normalized to one as shown in Fig 5.5

However, this generalized Chebyshev function is derived by following a similar procedure to that given in Section 2.6 of this thesis. The major difference is the Z-transformed variable must be defined here for the

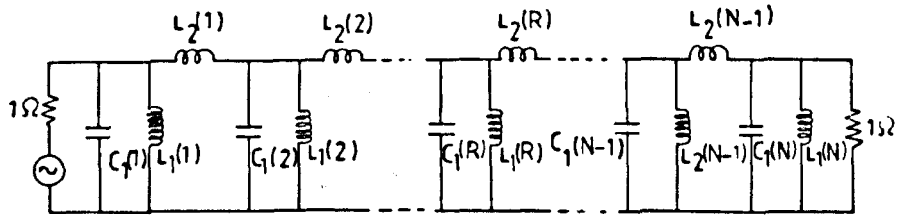

Fig. 5.4 The lumped prototype combline filter

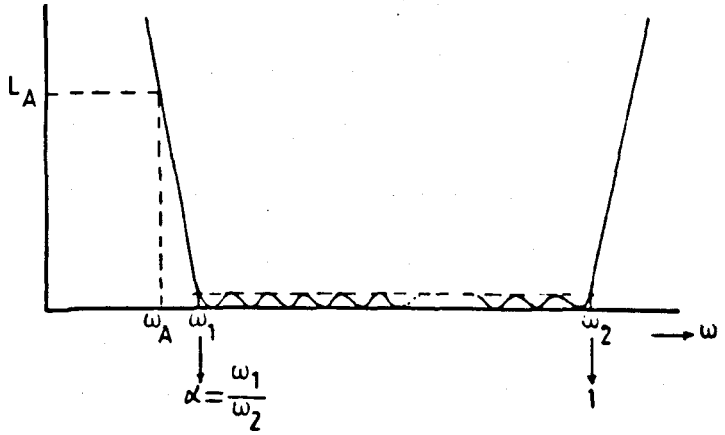

Fig. 5.5 The bandpass prototype combline filter equiripple response

bandpass case as [24], [25]

$$Z^2 = \frac{p^2 + \omega_2^2}{p^2 + \omega_1^2} \tag{5.19}$$

and after normalizing ω_2 to unity, it becomes

$$\dot{Z}^2 = \frac{p^2 + 1}{p^2 + \alpha^2} \tag{5.20}$$

From this transformation, the location of the transmission zeros at $\omega = \infty$ becomes at $Z = 1$ and that at $\omega = 0$, becomes at $Z = 1/\alpha$. Substituting for Z in equations (2.125.a and b) by the value in (5.20) and for Z_i in (2.125.b) by $1/\alpha$ results in the first and second terms of the right side of equation (5.18) respectively.

However, it has been found that it is quite possible to synthesis a network satisfying this response and of degrees up to 18 using the conventional p-plane element extraction technique and when the alternating pole synthesis technique introduced earlier in this thesis is applied, the element values of networks of degrees up to 30 can be obtained with little loss of accuracy. It was also found that synthesizing such networks using the alternating pole technique requires the construction of both Y_e and Y_c and the typical zero location of $(1 + \varepsilon P_N(p))$ for these bandpass networks is as illustrated in Fig 5.6 for N = 12.

In either case (the conventional p-plane synthesis and the alternating pole techniques) the entire synthesis process was programmed on a computer. The process commences by supplying the input data N, ε and α and ends by obtaining the element values, then establishing the theoretical insertion and return loss characteristics.

Since the application of the alternating pole synthesis technique to the band-pass networks is no different in principle from the low-pass

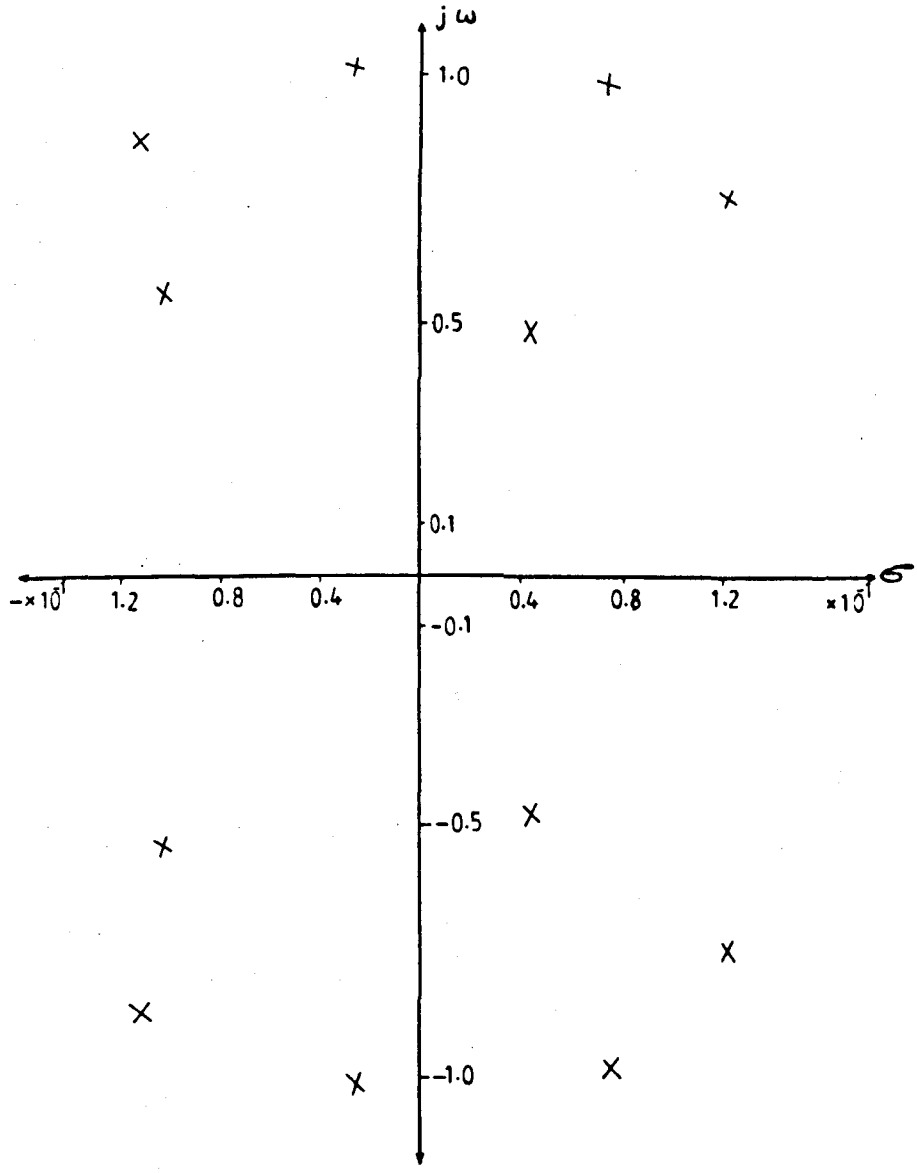

Fig. 5.6 Typical zero location of $(1+\varepsilon P_N(p))$

$N=12$, $\alpha=0.5$

case, then, there is no need to repeat it here. On the other hand the synthesis cycle of the network shown in Fig 5.4 may be explained by using the standard Darlington's procedure as follows:

By constructing

$$S_{11}(p)\, S_{11}(-p) = \frac{-\varepsilon^2 P_N(p)}{1 - \varepsilon^2 P_N{}^2(p)} \tag{5.21}$$

where

$$P_N(p) = j\, F_N(\omega)$$

and forming a Hurwitz factorization of the denominator and numerator, the reflection coefficient $S_{11}(p)$ is obtained, then the relationship

$$Y_{in}(p) = \frac{1 + S_{11}(p)}{1 - S_{11}(p)} \tag{5.22}$$

Yields the input admittance of the network. The synthesis cycle commences by total removal of the shunt capacitor $C_1(1)$ from $Y_{in}(p)$ leaving $Y_1(p)$ as

$$Y_1(p) = Y_{in}(p) - C_1(1)p \tag{5.23}$$

Then, the shunt inductor $L_1(1)$ is partially removed from $Y_1(p)$ and its numerical value can be easily obtained by applying certain conditions such as making all the shunt capacitors equal. The partial extraction of $L_1(1)$ leaves

$$Y_2(p) = Y_1(p) - {}^1/L_1(1)p \tag{5.24}$$

Holding $L_1(1)$ as unknown quantity for the times being, moving to the next step and totally remove the series inductor $L_2(1)$ from $Z_2(p) = {}^1/Y_2(p)$ leaving

$$Z_3(p) = Z_2(p) - L_2(1)p \tag{5.25}$$

Where the value of $L_2(1)$ can be expressed in terms of $L_1(1)$, yielding

$Z_3(p)$ as a second order expression in $L_1(1)$. Proceeding to the next cycle by total extraction of $C_1(2)$ from $Y_3(p) = {}^1/Z_3(p)$ and applying the condition $C_1(2) = C_1(1)$. Then $L_1(1)$ is solved for and the root which gives positive values of $L_2(1)$ is chosen. The cycle is repeated until all the element values are obtained.

The synthesis process may be illustrated further by the following simple numerical example.

Numerical Example No.5.1

Synthesize the doubly terminated network shown in Fig 5.7 of degree $N = 4$, $\varepsilon = 0.1$ and $\alpha = 0.5$.

Solution

The Hurwitz factorization of equation (5.21) gives the following poles and zeros of $S_{11}(p)$

The poles: $p_1 = -0.355345 \pm j1.17456$

$p_2 = -0.355378 \pm jo.245938$

The zeros $p'_2 = \pm jo.927768$

$p'_2 = \pm jo.57162$

Thus,

$$S_{11}(p) = \frac{1 + 4.22222p^2 + 3.55554p^4}{1 + 4.27728p + 7.81392p^2 + 5.0538p^3 + 3.55539p^4}$$

and

$$Y_{11}(p) = \frac{2 + 4.27728p + 12.0361p^2 + 5.0538p^3 + 7.11093p^4}{4.27728p + 3.5917p^2 + 5.0538p^3}$$

The first shunt capacitor is totally removed by complete pole extraction at infinity

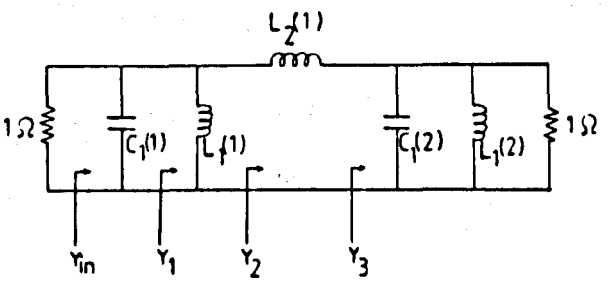

Fig. 5.7 The doubly terminated network of example 5.1

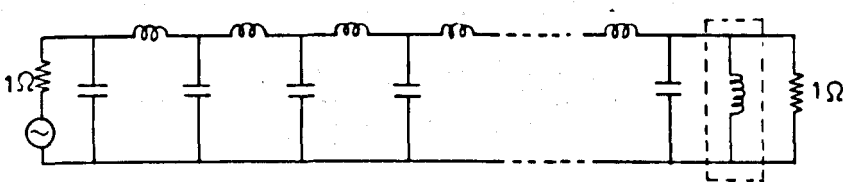

Fig. 5.8 A non redundant format of the prototype combline network

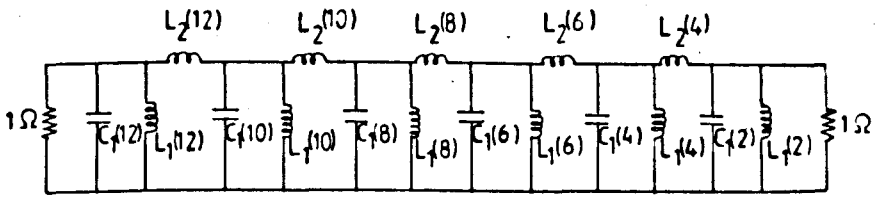

Fig. 5.9 The prototype combline network of degree 12

$$C_1(1) = Y_{in}(p)/p \Big|_{p=\infty} = \frac{7.11093}{5.0538} = 1.40705$$

$$Y_1(p) = \frac{2 + 4.27728p + 6.0178p^2}{4.27728p + 3.5917p^2 + 5.0538p^3}$$

removing the shunt inductance $L_1(1)$ partially from $Y_1(p)$ as in (5.24), yields

$$Y_2(p) = \frac{G(o) + G(1)p + G(2)p^2}{F(1)p + F(2)p^2 + F(3)p^3}$$

where

$$G(i) = x(i) - F(i+1)/L_1(1) \qquad i = 0 \rightarrow 2$$

$$x(o) = 2 \ , \ x(1) = 4.27728 \ , \ x(2) = 6.0178$$

$$F(1) = 4.27728 \ , \ F(2) = 3.5917 \ , \ F(3) = 5.0538$$

$$Z_2(p) = \frac{1}{Y_2(p)} = \frac{F(1)p + F(2)p^2 + F(3)p^3}{G(0) + G(1)p + G(2)p^2}$$

The series inductor $L_2(1)$ is totally removed by complete pole extraction at infinity,

$$L_2(1) = Z_2(p)/p \Big|_{p=\infty} = F(3)/G(2)$$

leaving $Z_3(p)$ as described in Equation (5.25). Hence

$$Z_3(p) = \frac{H(1)\,p}{G(0) + G(1)p + G(2)p^2}$$

where

$$H(1) = F(1) - L_2(1)\,G(0) = F(1) - F(3)\,G(0)/G(2)$$

$$Y_3(p) = 1/Z_3(p) = \frac{G(0) + G(1)p + G(2)p^2}{H(1)p}$$

Now, the next shunt capacitor $C_1(2)$ is totally removed

$$C_1(2) = Y_3(p)/p \Big|_{p=\infty} = G(2)/H(1)$$

Applying the condition $C_1(2) = C_1(1) = 1.40705$ and substituting for $G(2)$ and $H(1)$, results in

$$1.40705 = \frac{G(2)}{H(1)} = \frac{6.0178 - 5.0538/L_1(1)}{4.27728 - \{\dfrac{10.1076 - 21.6165/L_1(1)}{6.0178 - 5.0538/L_1(1)}\}}$$

after simplification, it becomes

$$\left[\frac{1}{L_1(1)}\right]^2 - 2.38148/L_1(1) + 0.55669 = 0 \qquad (5.26)$$

Therefore,

$$1/L_1(1) = \frac{-(-2.38148) \pm \{(-2.38148)^2 - 4 \times 0.55669\}^{\frac{1}{2}}}{2}$$

$$1/L_1(1) = \frac{2.38148 - 1.85598}{2} = 0.262747$$

or

$$1/L_1(1) = \frac{2.38148 + 1.85598}{2} = 2.11873$$

The right value of $L_1(1)$ is 1/0.262747 = 3.80589. The other root is neglected.

Substituting back in the expression for $L_2(1)$, results in

$$L_2(1) = \frac{F(3)}{G(2)} = \frac{5.0538}{6.017753 - 5.0538/3.80589} = 1.07759$$

The last shunt inductance $L_1(2)$ is totally removed as $L_1(2) = G(0)/H(1) = 3.804589$ and the load resistance

$$R_L = \frac{H(1)}{G(1)} = 1\Omega$$

However, if equation (5.26) is written in general form as

$$\left[1/L_1(R)\right]^2 + U/L_1(R) + V = 0 \qquad (5.27)$$

It has been found that the correct value of $1/L_1(R)$ is always obtained by taking the root:

$$1/L_1(R) = \frac{-U - [U^2 - 4V]^{\frac{1}{2}}}{2} \qquad (5.28)$$

because this is the only value which satisfies the fact that the values

of all the shunt capacitors $C_1(R)$ and the series inductors $L_2(R)$ should be positive.

In general, it is also possible to synthesize these prototype networks with either all of their shunt inductors or their series inductors being equal, following the same principles as in the equal shunt capacitors case. Furthermore, the prototype network which is shown in Fig 5.4 in its redundant format can be synthesize in a non-redundant equivalent format as shown in Fig 5.8, where the shunt inductor may be completely removed in one step. The network can be brought back to the redundant form, if required by scaling the inductive arrays [50].

5.5 DESIGN AND PERFORMANCE OF MICROWAVE BROADBAND COMBLINE FILTER

5.5.1 The Specifications

The microwave combline bandpass filter is to be built with all of its elements are commensurate lines (stubs) operates in 50Ω system and satisfies the following specifications:

Number of resonators = 6 i.e. N = 12

The passband limits of f_1 = 3 GHZ and f_2 = 6 GHZ

With minimum return loss = 20dB corresponding to $\varepsilon = 0.1$.

The stubs are $\lambda/4$ long at f_0 = 15 GHZ.

The value of f_0 is not so critical. It is usually taken in the middle of arbitrary chosen upper stopband.

In most practical design specifications, the number of resonators or the degree of the transfer function is not given. But it should be calculated to satisfy a given attenuation level in one or both stopbands. Wenzel [58] has given an expression of estimating the number of resonators in terms of attenuation levels at actual frequencies in both stopbands. It has been

found here that N can be easily estimated from the following expression using lumped domain frequencies.

$$N = 1 + \frac{\cosh^{-1}\left[\frac{1}{\varepsilon}\left(10^{A/10} - 1\right)^{\frac{1}{2}}\right] - \text{Sin } h^{-1}\left[\frac{1}{\omega_0}\left(\frac{\alpha^2 - \omega_A^2}{1 - \alpha^2}\right)^{\frac{1}{2}}\right]}{\text{Sin } h^{-1}\left[\frac{\alpha^2 - \omega_A^2}{1 - \alpha^2}\right]^{\frac{1}{2}}} \qquad (5.29)$$

where

$\omega_A < \alpha$ and A is the insertion loss (dB) at ω_A

5.5.2 The Prototype Element Values

The corresponding parameters to the microwave specifications are obtained by applying the Richard's transformation

$$\omega \rightarrow \beta\tan(af)$$

and equating the lumped and distributed frequency domains at the bandedges, results in the following equations

$$\alpha = \beta\tan(af_1) \qquad (5.30.a)$$

$$1 = \beta\tan(af_2) \qquad (5.30.b)$$

Since the stubs are required to be 90 electrical degree long at 15 GHZ, hence

$$af_0 = 90 \qquad (5.30.c)$$

$\therefore$ a = 90/15 = 6

From equations (5.30.b) and (5.30.a)

$\beta = 1/\tan(6x6) = 1.37638$

and

$$\alpha = \frac{\tan(af_1)}{\tan(af_2)} = \frac{\tan(6x3)}{\tan(6x6)} = 0.447214$$

Then, by supplying the input data N, ε and α to the programmed synthesis procedure, the element values of the prototype network are obtained as given in Table 5.1. This prototype network is shown in Fig 5.9 and its computer analysis showing the insertion and return loss is plotted

Table 5.1: The prototype element values of the combline filter

Section R	Shunt capacitor $C_1(R)$	Shunt inductor $L_1(R)$	Series inductor $L_2(R)$
12	1.79117	1.83351	1.61719
10	1.79117	8.18398	2.32676
8	1.79117	3.88507	2.4191
6	1.79117	3.88507	2.32676
4	1.79117	8.18398	1.61719
2	1.79117	1.83351	-

in Fig 5.10.

5.5.3 Conversion of the Lumped Element Values to Commensurate Lines

Since all the elements of the microwave combline structure of interest are required to be of the distributed type, then each capacitor in the lumped prototype must be replaced by an open-circuited (O/C) stub and each inductor must be replaced by a short circuited (S/C) stub. For convenience the normalized characteristic admittances of these stubs are calculated from the relationships

$$Y_{C_1}(R) = \beta C_1(R) \qquad (5.31.a)$$

$$Y_{L_1}(R) = 1/\beta L_1(R) \qquad (5.31.b)$$

$$Y_{L_2}(R) = 1/\beta L_2(R) \qquad (5.31.c)$$

The numerical values of these admittances are given in Table 5.2.

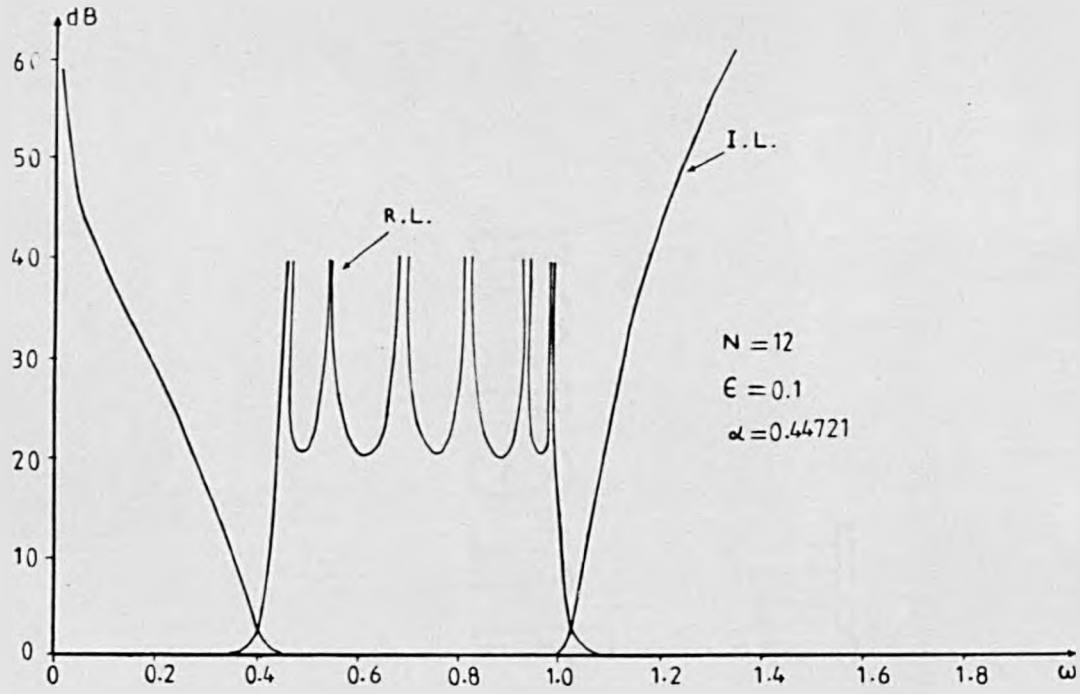

Fig. 5.10 The insertion and return loss for the combline prototype network

Table 5.2: The characteristic admittances of the O/C and S/C stubs

R	$Y_{C_1}(R)$	$Y_{L_1}(R)$	$Y_{L_2}(R)$
12	2.46533	0.396258	0.449262
10	=	0.088776	0.312255
8	=	0.187009	0.300336
6	=	0.187009	0.312255
4	=	0.088776	0.449262
2	=	0.396258	-

As previously mentioned that combline filters consist of arrays of parallel lines between two parallel ground planes. These arrays are usually fabricated either in the form of parallel bars having rectangular cross sections or in parallel cylindrical rods having circular cross sections. In either case the physical dimension of the structure are obtained from the calculated self and mutual normalized capacitances per unit length of the lines. These capacitances are related to the characteristic immittances of the lines.

Getsinger's procedure [59] is used for designing parallel coupled rectangular bars and it will be followed here in calculating the dimensions of this filter. Methods for designing structures having circular cross section rods will be discussed in the next section.

However, all of the rectangular parallel coupled bars are designed with the same t/b ratio. Where b is distance between the two ground planes

and t is the thickness of each bar as shown in Fig 5.11. Moreover, it is practically desirable to make all of the bars having similar widths as possible. In order to achieve that, the admittance matrix of the inductive arrays of the network should be scaled such that the inductance to ground at the internal nodes have the same value. The inductive arrays of the network in question is shown in Fig 5.12 and its admittance matrix is given by:

$$
\begin{array}{c}
\\ \\ n'\rightarrow \\ \\ \\ n'\rightarrow \\ \\
\end{array}
\begin{array}{c}
\begin{array}{cccccc}
 & \downarrow n' & & & \downarrow n' & \\
\end{array}\\
\begin{bmatrix}
Y_{L_1}(12)+Y_{L_2}(12) & -Y_{L_2}(12) & 0 & 0 & 0 & 0 \\
-Y_{L_1}(12) & Y_{L_1}(10)+Y_{L_2}(10)+Y_{L_2}(12) & -Y_{L_2}(10) & 0 & 0 & 0 \\
0 & -Y_{L_2}(10) & Y_{L_1}(8)+Y_{L_2}(8)+Y_{L_2}(10) & -Y_{L_2}(8) & 0 & 0 \\
0 & 0 & -Y_{L_2}(8) & Y_{L_1}(6)+Y_{L_2}(6)+Y_{L_2}(8) & -Y_{L_2}(6) & 0 \\
0 & 0 & 0 & -Y_{L_2}(6) & Y_{L_1}(4)+Y_{L_2}(4)+Y_{L_2}(6) & -Y_{L_2}(4) \\
0 & 0 & 0 & 0 & -Y_{L_2}(4) & Y_{L_1}(2)+Y_{L_2}(4)
\end{bmatrix}
\end{array}
\qquad \text{- - - - -(5.32.a)}
$$

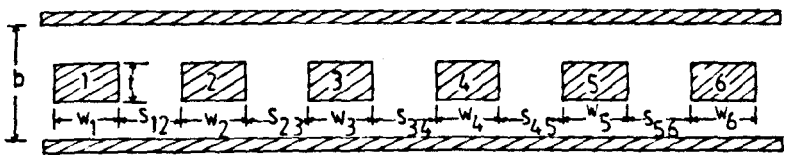

Fig. 5.11 Cross section for parallel coupled bars between two parallel ground planes

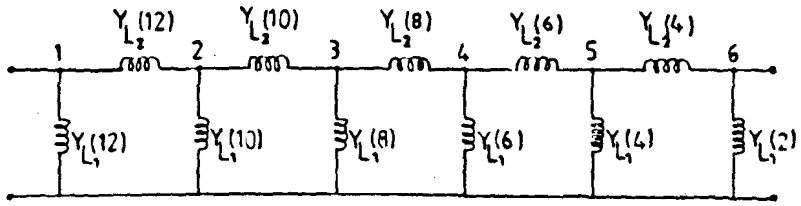

Fig. 5.12 The inductive arrays of the combline filter

It may be seen from the values of $Y_{L_1}(R)$ and $Y_{L_2}(R)$ in Table 5.2 that it is most convenient to scale rows 2 and 5 and their corresponding columns by a positive scaling factor n'. The value of n' is determined by equating the total inductance to ground at the scaled nodes to its counterpart at any other internal unscaled node, e.g. node 3. Thus

$$-Y_{L_2}(12)n' + [Y_{L_1}(10)+Y_{L_2}(10)+Y_{L_2}(12)]n'^2 - Y_{L_2}(10)n'$$

$$= - Y_{L_2}(10)n' + Y_{L_1}(8) + Y_{L_2}(8) + Y_{L_2}(10) - Y_{L_2}(8)$$

rearranging the terms gives

$$n'^2[Y_{L_1}(10)+Y_{L_2}(10)+Y_{L_2}(12)] - n'Y_{L_2}(12) - [Y_{L_2}(10)+Y_{L_1}(8)] = 0 \quad (5.32.b)$$

Substituting for the admittances and solving for n', results in:

$n' = 1.07471$

and the values of the characteristic admittances of the stubs are given in Table 5.3. Although the scaling of node 2 and 5 effects the shunt O/C stubs at these nodes, the change in their characteristic admittances was neglected in the design and it can be compensated for by tuning afterwards.

Table 5.3: The scaled values of the characteristic admittances of the stubs

R	$Y_{C_1}(R)$	$Y_{L_1}(R)$	$Y_{L_2}(R)$
12	2.46533	0.362693	0.482827
10	2.84747	0.16368	0.335584
8	2.46533	0.16368	0.300336
6	2.46533	0.16368	0.300336
4	2.84747	0.16368	0.482827
2	2.46533	0.362693	-

The O/C stubs are realized in dielectric filled coaxial form. The dielectric material is P.T.F.E. of dielectric constant $\sqrt{\varepsilon_r} = 1.45$

Since the characteristic impedance of a coaxial cable is given by

$$Z_o = \frac{60}{\sqrt{\varepsilon_r}} \ln \frac{b_1}{a_1} \qquad (5.33)$$

where b_1 is the inner diameter of the outer conductor and a_1 is the diameter of the inner conductor.

For the O/C stubs $Z_o = \frac{50}{Y_{C_1}(R)} = \frac{50}{2.46533} = 20.28123\Omega$

Then,

$$b_1/a_1 = 1.63253$$

The values of b_1 and a_1 are approximated to suit the dielectric material which is available in a cylindrical tube form. Thus a_1 = 0.04", b_1 = 0.064". The O/C stub is quarter wavelength long in the dielectric at 15 GHZ. Thus,

$$\ell_o = \lambda_d/4 = \frac{v}{4\sqrt{\epsilon_r} f_o} = \frac{11.80315 \times 10^9}{4 \times 1.45 \times 15 \times 10^9} = 0.135668"$$

On the other hand the shunt S/C stubs are quarter wavelength long in the air filled structure, hence

$$\ell_s = \lambda_o/4 = \frac{v}{4 f_o} = \frac{11.80315 \times 10^9}{4 \times 15 \times 10^9} = 0.196719"$$

Proceed in calculating the dimensions of the bars and their separating distances starting by the relationship [59]

$$(C/\epsilon) = \frac{\eta}{Z\sqrt{\epsilon_r}} \qquad (5.34)$$

which relates the characteristic impedance Z of a lossless uniform transmission line operating in TEM mode to (C/ϵ) the ratio of its static capacitance per unit length to the permittivity medium. η is the impedance of free space = 376.7 Ω and $\sqrt{\epsilon_r}$ is the relative dielectric constant of the medium in which the wave propagages. For 50 Ω terminations and air filled structure, the static capacitances of the shunt S/C stubs are given by

$$(C_i/\epsilon) = (C_R/\epsilon) = 7.534\ Y_{L_1}(R) \qquad \left.\begin{array}{l} i = 1,2 \text{ --- } 6 \\ R = 12,10\text{-- } 2 \end{array}\right\} \qquad (5.35)$$

Similarly, the static capacitances of the series S/C stubs are given by

$$(\Delta C_{i,1+1}/\epsilon) = (\Delta C_R/\epsilon) = 7.534\ Y_{L_2}(R) \qquad \left.\begin{array}{l} i = 1,2 \text{ --- } 5 \\ R = 12,10\text{-- } 4 \end{array}\right\} \qquad (5.36)$$

The calculated values of (C_i/ε) and $(\Delta C_{i,i+1}/\varepsilon)$ are given in Table 5.4.

Table 5.4: The values of the shunt static capacitances of the S/C stubs

Bar No. i	R	$C_i/\varepsilon = C_R/\varepsilon$	$\Delta C_{i,i+1}/\varepsilon = \Delta C_R/\varepsilon$
1	12	2.73253	3.63762
2	10	1.23317	2.52829
3	8	1.23317	2.26273
4	6	1.23317	2.52829
5	4	1.23317	3.63762
6	2	2.73253	-

Getsinger's charts [59] can now be used to determine the cross-sectional dimensions of the bars and spacing between them as follows: choose a suitable t/b ratio, then by using the values of $(\Delta C_{i,i+1}/b)$ and the chart in Fig.3 of Reference [59], the normalized spacing $(S_{i,i+1}/b)$ between the ith and i+1th bar is obtained. Also, the normalized fringing capacitance $(C'_{fe})_{i,i+1}/\varepsilon$ associated with the gaps $S_{i,i+1}$ are obtained. The normalized width W_i/b of the ith bar can be calculated from the relationship [53], [59]

$$(C_{p_i}/\varepsilon) = 2\,\frac{W_i/b}{1-t/b} \tag{5.37}$$

where C_{p_i} is the parallel plate capacitance between one side of the ith bar and the ground plane.

But

$$(C_{p_i}/\varepsilon) = \frac{1}{2} C_i/\varepsilon - C_{fe_{i-1,i}}/\varepsilon - C'_{fe_{i,i+1}}/\varepsilon \qquad (5.38)$$

Hence

$$W_i/b = \frac{1}{2} (1 - t/b) \left[\frac{1}{2} C_i/\varepsilon - C'_{fe_{i-1,i}}/\varepsilon - C'_{fe_{i,i+1}}/\varepsilon\right] \qquad i = 2 \rightarrow 5 \qquad (5.39)$$

The ground plane spacing b is usually selected to be in the range $\lambda_o/4 < b < \lambda_o/2$ to obtain the best possible response. The choice of b should minimize the losses in the passband and prevent the propagation of higher ordered modes.

In this example b = 0.315"

The chosen value of t/b = 0.2

The normalized dimensions obtained are given in Table 5.5.

Table 5.5: The normalized dimensions

S_{12}/b	=	S_{56}/b	= 0.08
S_{23}/b	=	S_{45}/b	= 0.14
S_{34}/b	=	0.13	
W_2/b	=	W_5/b	= 0.151
W_3/b	=	W_4/b	= 0.129

Getsinger's [59] has also indicated that if

$$W/b/(1 - t/b) > 0.35 \qquad (5.40)$$

Then, there is interaction of fringing fields from the neighbouring gaps and the decomposition of the total capacitance as given in equation

(5.38) is no longer accurate. Under these circumstances which are applicable in this example, the width of the bars W_i should be corrected by using the approximate formula

$$W_i'/b = \{ 0.07 (1 - t/b) + W_i/b \} / 1.2 \qquad (5.41)$$

resulting in the following

$$W_2'/b = W_5'/b = 0.173$$

$$W_3'/b = W_4'/b = 0.154$$

The width of the bars at the ends of the array i = 1 and 6 can be obtained by replacing the term $(C'_{fe_{i-1,i}}/\varepsilon)$ in equation (5.38) with C'_{f_o}/ε and adjusting the distance between each of them and its side wall. Take i = 1 as a typical case.

Then

$$(C_{p_1}/\varepsilon) = \frac{1}{2} C_i/\varepsilon - C'_{fe_{1,2}}/\varepsilon - C'_{fo_{1\omega}}/\varepsilon \qquad (5.42)$$

and because it is practically desirable to make these bars with similar width as the rest, one can make the following choice

$$W_1'/b = W_6'/b = W_2'/b = 0.173$$

From equation (5.37), this width corresponds to: $C_{p_1}/\varepsilon = C_{p_6}/\varepsilon = 0.433$. Then $C'_{fo_{1\omega}}/\varepsilon = C'_{fo_{6\omega}}/\varepsilon$ can be obtained from equation (5.42). This value which is equal to 0.835 is used in Fig.4 of Reference [59] to give $2S_{1\omega}/b = 2S_{6\omega}/b = 0.66$. Thus $S_{1\omega}/b = 0.33$. This value has been calculated under the assumption that the side wall are symmetrically located between the end bar and virtual similar one.

After obtaining the required dimensions, the combline filter was built. The input and output connectors were tapped directly to the end bars, since the use of transformer elements are not normally necessary for broadband structure. The filter was tuned and tested using a swept

frequency reflectometer. Its experimental insertion loss and return loss characteristics are shown in Fig 5.13.a and b respectively. These results are satisfactory within the mechanical tolerance in the construction of the device.

5.6 MIXED LUMPED/DISTRIBUTED COMBLINE FILTER

The compactness is one of the most attractive features of microwave combline structure. It can be improved even further if lumped capacitors rather than commensurate O/C stubs are used in their realization. Without going through the multivariable network synthesis details, Wenzels [58] has demonstrated that a mixed lumped/distributed combline network can be obtained from the distributed one by forcing the response of both networks to be identical at bandedge frequencies. This is achieved by forcing the admittance of each respective resonator to be identical at the bandedges.

Consider the typical distributed section and its mixed lumped/distributed equivalent counterpart shown in Fig 5.14.a. and b respectively. The admittance of the shunt distributed resonator is

$$Y_d(R) = j\,[Y_{C_1}(R)\tan(af) - Y_{L_1}(R)\cot(af)] \qquad (5.43)$$

and the admittance of the shunt resonator consists of a lumped capacitor $C_o(R)$ and a distributed shunt S/C stub of characteristic admittance $Y_{L_o}(R)$ is

$$Y_m(R) = j\,[C_o(R)\omega - Y_{L_o}(R)\cot(af)] \qquad (5.44)$$

Assuming $Y_{C_1}(R)$ and $Y_{L_1}(R)$ are known. Then the values of $C_o(R)$ and $Y_{L_o}(R)$ can be obtained by solving the following two simultaneous equations

$$Y_{C_1}(R)\tan(af_1) - Y_{L_1}(R)\cot(af_1) = C_o(R)\omega_1 - Y_{L_o}(R)\cot(af_1) \qquad (5.45.a)$$

$$Y_{C_1}(R)\tan(af_2) - Y_{L_1}(R)\cot(af_2) = C_o(R)\omega_2 - Y_{L_o}(R)\cot(af_2) \qquad (5.45.b)$$

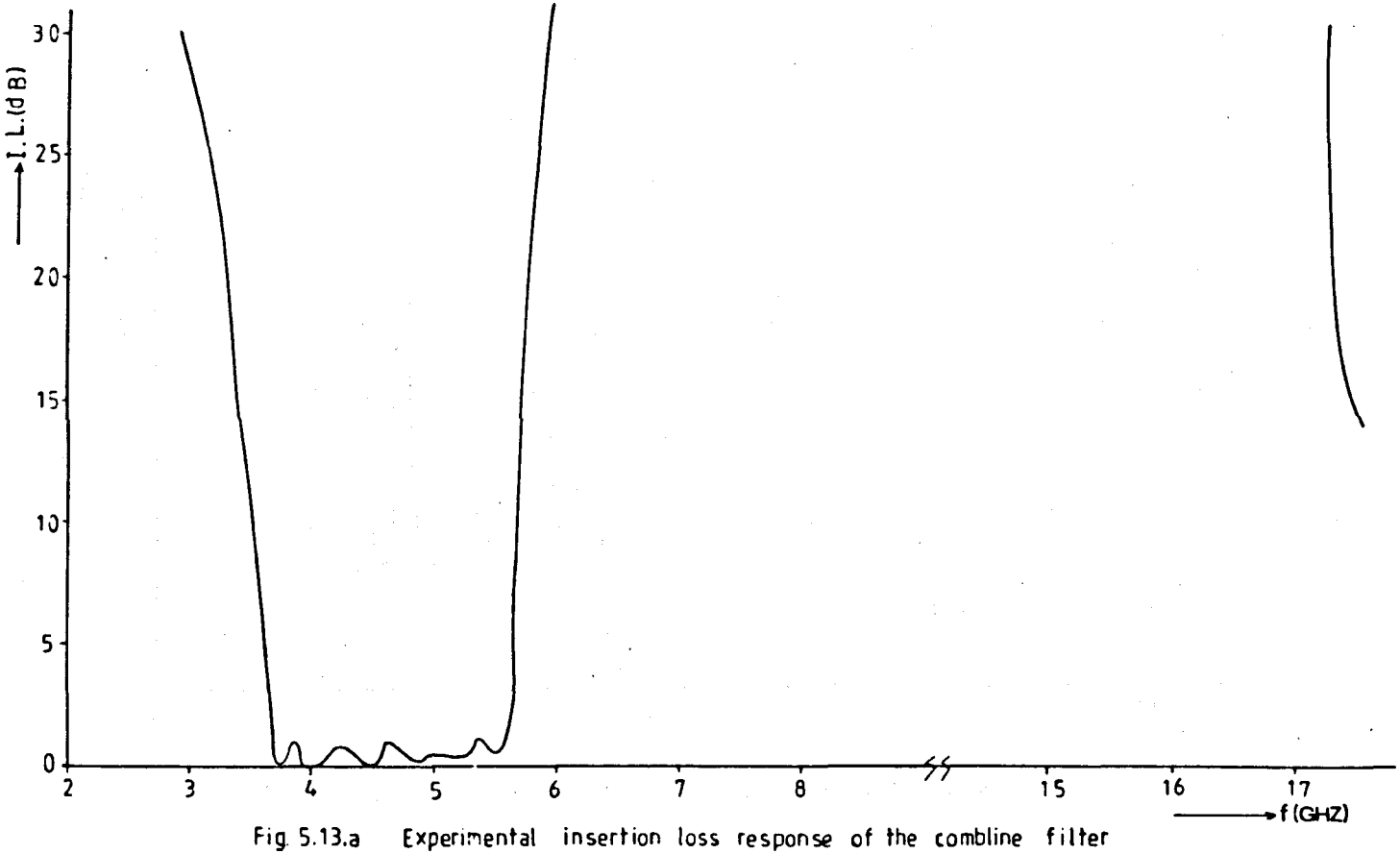

Fig. 5.13.a Experimental insertion loss response of the combline filter

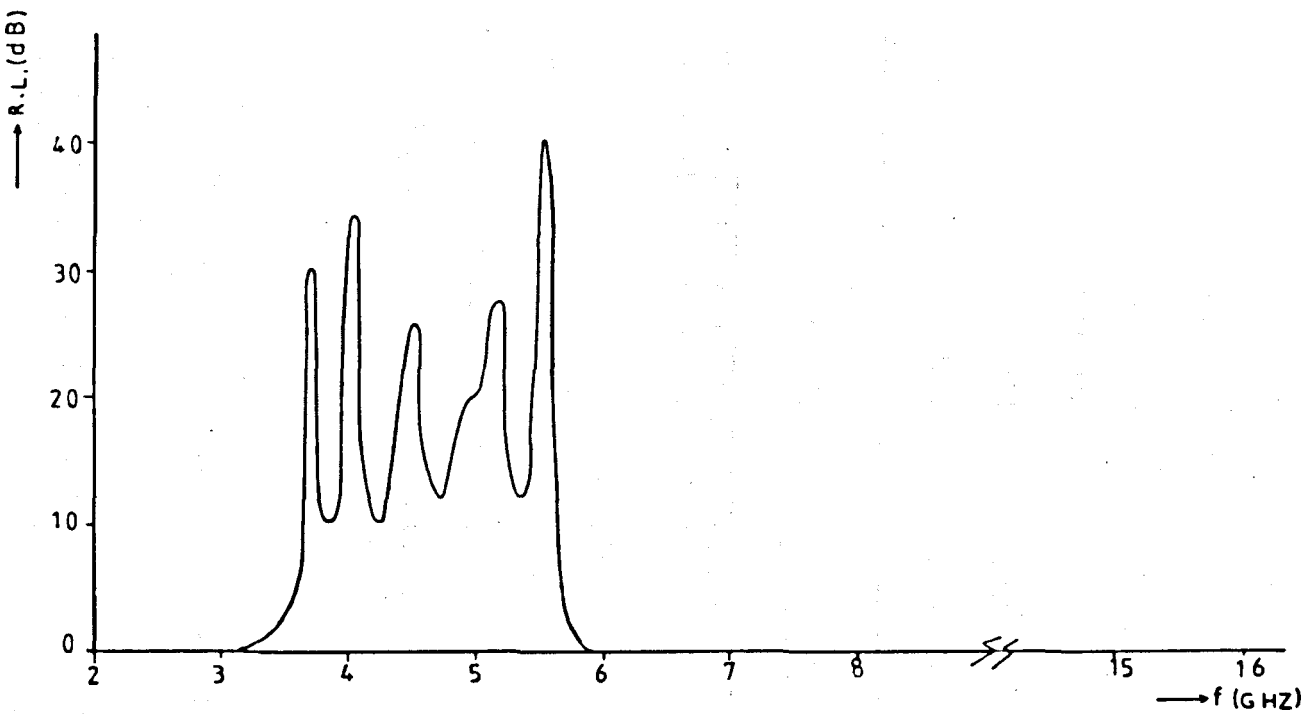

Fig. 5.13.b Experimental retune loss response of the combline filter

which gives

$$C_o(R) = Y_{C_1}(R) \left\{ \frac{\tan^2(af_1) - \tan^2(af_2)}{\omega_1 \tan(af_1) - \omega_2 \tan(af_2)} \right\} \qquad (5.46)$$

and

$$Y_{L_o}(R) = Y_{L_1}(R) + Y_{C_1}(R) \tan(af_1).\tan(af_2) \left\{ \frac{f_2 \tan(af_1) - f_1 \tan(af_2)}{f_1 \tan(af_1) - f_2 \tan(af_2)} \right\} \qquad (5.47)$$

where f_1 and f_2 are the lower and upper bandedge frequencies respectively

$$\omega_1 = 2\pi f_1 \quad \text{and} \quad \omega_2 = 2\pi f_2$$

However, this modification has been applied to the network given in the last section whose original distributed element values are given in Table 5.3. The equivalent lumped/distributed network having the element values given in table 5.6 was obtained.

Table 5.6: The element values of the Lumped/distributed network. These are equivalent to the values given in Table 5.3

R	$C_o(R) \times 10^{-9}$ Farad	$Y_{L_o}(R)$ $\mho$	$Y_{L_2}(R)$ $\mho$
12	0.307605	0.402262	0.482826
10	0.355284	0.209382	0.335584
8	0.307605	0.203249	0.300336
6	0.307605	0.203249	0.335584
4	0.355284	0.209382	0.482826
2	0.307605	0.402262	-

The computer analysis of both versions of the network is plotted in Fig 5.15. A comparison of the responses shows no change in the passband width and the return loss of the lumped/distributed version is nearly

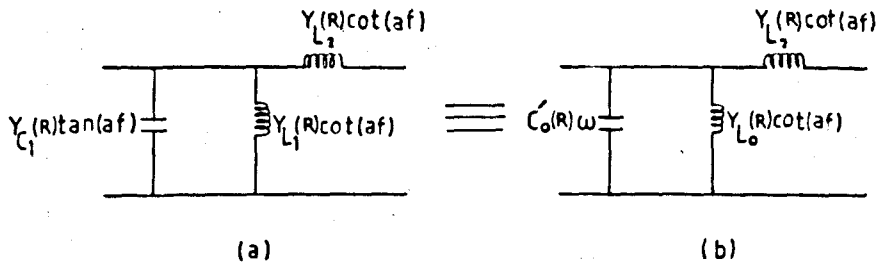

Fig. 5.14 (a) A typical distributed combline section
(b) Mixed lumped/distributed equivalent section

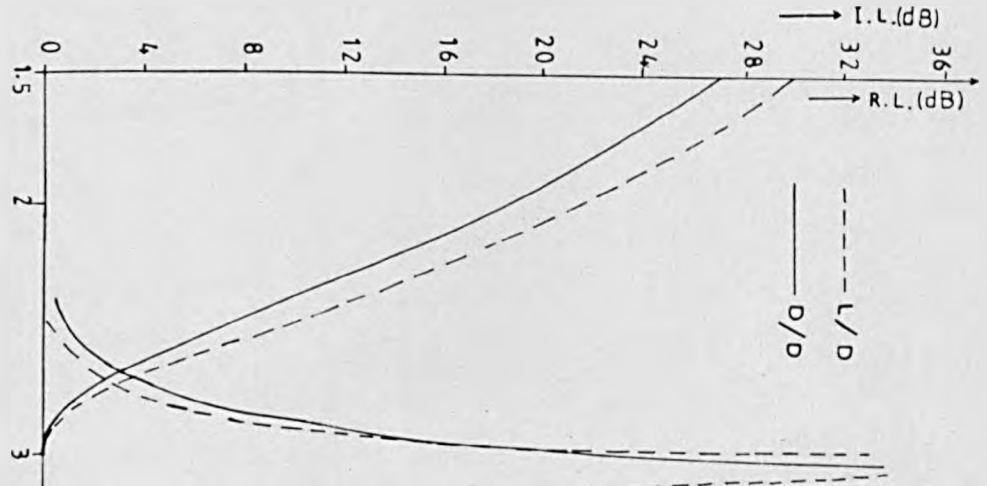
I.L.(dB)
R.L.(dB)
L/D
D/D
0
4
8
12
16
20
24
28
32
36
1.5
2
3

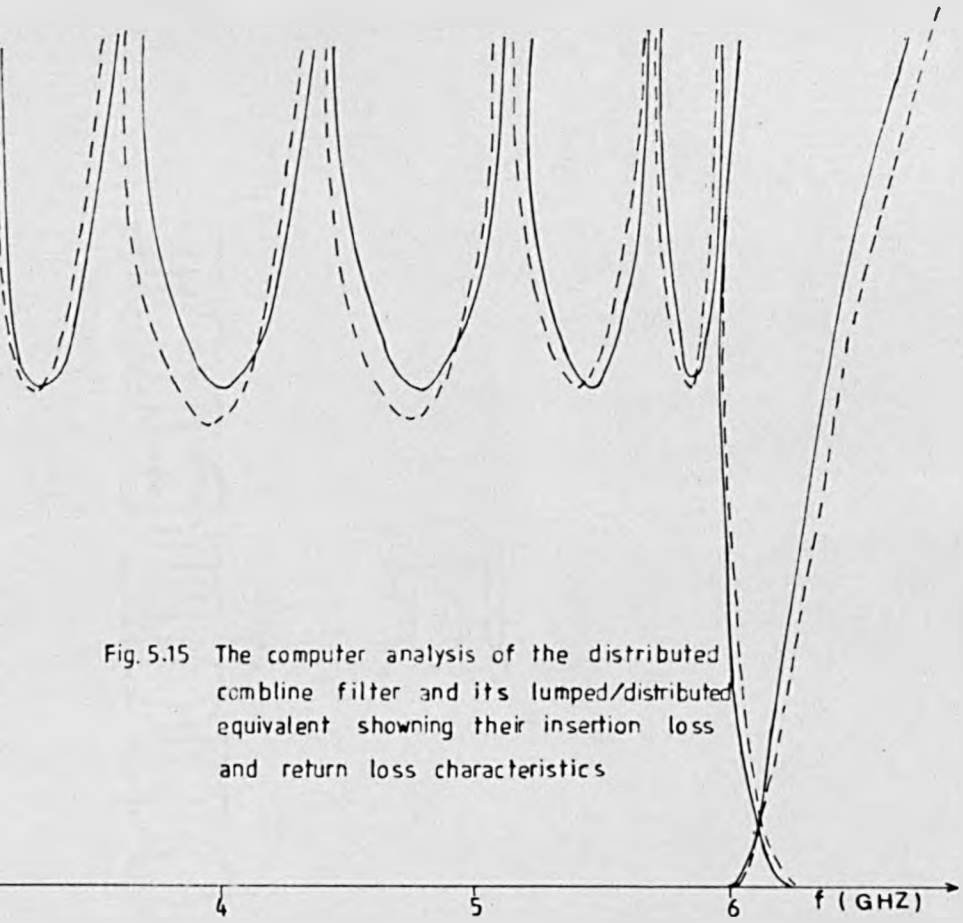

Fig. 5.15 The computer analysis of the distributed combline filter and its lumped/distributed equivalent showning their insertion loss and return loss characteristics

identical with the exact commensurate line length one. Also there is a slight change in the skirt selectivity with improvement in the low side of the lumped/distributed passband over the distributed version. The most important advantage of using lumped capacitors is the widening of the stopband by moving the second passband to higher frequencies. In this particular example, the second passband of the distributed network is moved from (24 - 27) GHZ.It was moved to higher than 32 GHZ in the lumped/distributed case and it no longer appears as perfectly shaped passband due to the destruction of the distributed domain periodicity. This advantage makes the lumped/distributed combline filter most suitable for multiplexer applications, when the broad stopband is needed to accommodate more channels.

5.7 DESIGN TECHNIQUES FOR TEM-NETWORKS HAVING COUPLED CIRCULAR CYLINDRICAL RODS

It has been pointed earlier in this chapter that parallel coupled arrays TEM networks can be realized in the coaxial structure form by using either rectangular bars or circular cylindrical rods. The physical dimensions of the TEM structure having rectangular bars are obtained by using Getsinger's procedure [59]. On the other hand, the circular cylindrical rods realization can be achieved by using Cristal charts [60]. In his work, Cristal presented an approximate design method to realize networks that require rods on non-equal diameters and spacings. The graph shown in Fig.2 of Reference [60] gives the normalized mutual capacitance (C_m/ε) against half normalized spacing $^1/2(S/b)$. In Fig.3 of Reference [62], half the normalized self capacitance $^1/2$ (C_g/ε) against $^1/2(S/b)$ is given. Both graphs are for periodic structures consist of circular cylindrical rods located between parallel ground planes. These two graphs are provided in the appendix.

This section presents a simple method based on those two graphs and the capacitance matrix to design parallel coupled transmission-line networks such as combline and interdigital filters with equal diameter rods, as shown in Fig 5.16.

5.7.1 Method [61]

As was claimed in reference [60], the use of circular cylindrical rods as resonators offers several manufacturing advantages over the rectangular bars; it is therefore, obvious that, when circular cylindrical rods of the same diameter are being used, the manufacturing process becomes much easier and the cost is reduced still further.

Consider the N-resonator prototype parallel coupled transmission-line filter shown in Fig 5.17 with a redundant normalized unit element introduced for practical reasons at each end, the admittance matrix [Y'] of which may be written as:

$$[Y']=\begin{bmatrix} 1 & -1 & 0 & 0 & 0 & - & - & 0 & 0 \\ -1 & 1+Y_1' & -K_{1,2} & 0 & 0 & - & - & - & 0 \\ 0 & -K_{1,2} & Y_2' & -K_{2,3} & 0 & - & - & - & 0 \\ 0 & 0 & -K_{2,3} & Y_3' & -K_{3,4} & - & - & - & 0 \\ 0 & 0 & 0 & -K_{3,4} & - & - & - & - & 0 \\ - & - & - & - & - & - & - & - & 0 \\ - & - & - & - & - & - & - & - & 0 \\ 0 & - & - & - & - & 0 & K_{N-1,N} & 1+Y_N' & -1 \\ 0 & 0 & - & - & - & 0 & 0 & -1 & 1 \end{bmatrix} \qquad (5.48)$$

To simply the calculations, matrix equation (5.48) may be scaled by multiplying the rows and columns by suitable constant so that all the main diagonal terms will be unity and the transformed matrix

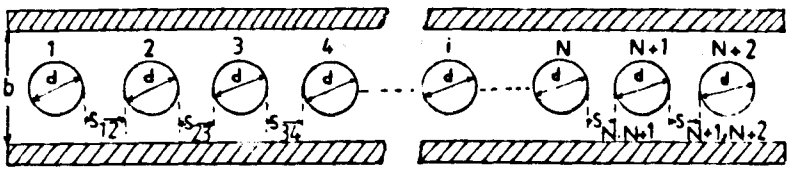

Fig. 5.16 Equal-diameter rods between two parallel planes

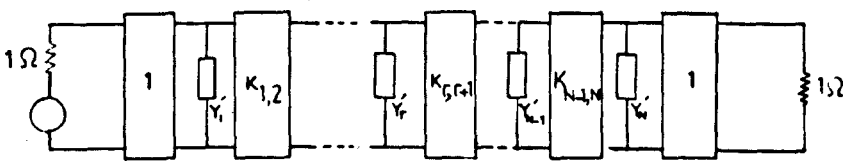

Fig. 5.17 Prototype parallel coupled lines filter with a normalised unit element at each end

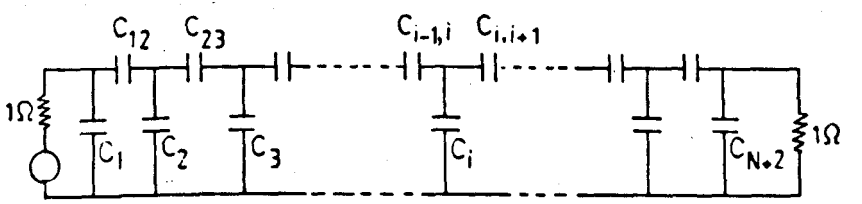

Fig. 5.18 Equivalent capacitive form of the network shown in fig. 5.14

[Y] is given by:

$$[Y] = \begin{bmatrix} 1 & -Y_{1,2} & 0 & 0 & 0 & \cdots & \cdots & \cdots & 0 \\ -Y_{2,1} & 1 & -Y_{2,3} & 0 & 0 & \cdots & \cdots & & \\ 0 & -Y_{3,2} & 1 & -Y_{3,4} & 0 & \cdots & \cdots & & 0 \\ 0 & 0 & -Y_{4,3} & 1 & & \cdots & \cdots & & 0 \\ \cdot & \cdot & & -Y_{i,i-1} & 1 & -Y_{i+1,i} & & & 0 \\ \cdot & \cdot & \cdot & \cdot & & & & & \\ \cdot & \cdot & \cdot & \cdot & & & & & \\ \cdot & \cdot & \cdot & \cdot & & & & & \\ \cdot & \cdot & \cdot & \cdot & & & & & \\ \cdot & \cdot & \cdot & \cdot & & & & 1 & -Y_{N+1,N+2} \\ 0 & 0 & \cdots & \cdots & - & & 0 & -Y_{N+2,N+1} & 1 \end{bmatrix} \quad (5.49)$$

From the [Y] matrix, the equivalent capacitance matrix may be derived using the argument described by Wenzel [48],[50]. This is given by

$$[C] = \begin{bmatrix} C_1+C_{12} & -C_{12} & 0 & 0 & \cdots & & 0 \\ -C_{21} & C_{21}+C_2+C_{23} & -C_{23} & 0 & & & \\ 0 & -C_{32} & C_{32}+C_3+C_{34} & -C_{34} & & & \\ 0 & 0 & -C_{43} & & & & \\ 0 & 0 & 0 & & & & \\ \cdot & \cdot & \cdot & & & & \\ \cdot & \cdot & \cdot & & & & 0 \\ \cdot & \cdot & \cdot & & & & -C_{N+1,N+2} \\ 0 & & 0 & 0 & & -C_{N+2,N+1} & C_{N+2}+C_{N+2,N+1} \end{bmatrix} \quad (5.50)$$

Consequently, the network in Fig 5.17 is replaced by its equivalent capactive form shown in Fig 5.18, where C_{ik} is the coupling capacitances and C_i is the self capacitances.

The necessary and sufficient condition for realization is that [C] must be a symmetrical hyperdominant matrix i.e.

(a) the diagonal terms

$$C_{i-1,i} + C_{ii} + C_{i,i+1} \geq 0 \qquad i = 2,3 \text{ ---}N-1$$

$$C_1 + C_{12} \geq 0$$

$$C_{N+2} + C_{N+1,N+2} \geq 0$$

(b) $C_{ik} = C_{ki} \quad i \neq k$

(c) $C_i \geq 0$

(d) $C_{ik} \leq 0 \quad i \neq k$

} (5.51)

The terms of matrix equation (5.50) may be obtained from matrix equation (5.49) by assuming that each conductor is coupled directly only to its nearest neighbours and using the relation given in equation (5.34). The coupling capacitances $C_{i,i+1}$ and the self capacitances C_i can be found by substituting the coupling and self admittances respectively, in equation (5.34). From matrix equation (5.49), $Y_{i,i+1}$ is the coupling characteristic admittance between conductor i and i+1, Y_i is the self characteristic admittance of conductor i and given by

$$Y_i = 1 - Y_{i-1,i} - Y_{i,i+1} \qquad i = 2 \rightarrow N+1$$

$$Y_1 = 1 - Y_{12}$$

$$Y_{N+2} = 1 - Y_{N+2,N+1}$$

} (5.52)

In most practical applications, 50 Ω terminations and air filled lines are used. Then C_i and $C_{i,i+1}$ can be found from the following relations:

$$\left.\begin{aligned}(C_{i,i+1}/\varepsilon) &= 7.534\ Y_{i,i+1}\\ (C_i/\varepsilon) &= 7.534\ Y_i\end{aligned}\right\} \qquad (5.53)$$

Having obtained all of the terms of matrix equation (5.50), one may proceed by finding the physical dimensions as follows:

(a) Choose a suitable (d/b) ratio.

(b) Determine the separation distance $\frac{1}{2}\ (S_{i-1,i}/b)$ and $\frac{1}{2}\ (S_{i,i+1}/b)$ between rod (i) $(i = 2 \rightarrow N + 1)$ and its neighbours $(i - 1)$ and $(i + 1)$ from the graph in Fig.2 of reference [60] for the given values of $C_m/\varepsilon = (C_{i,i-1}/\varepsilon)$ and $Cm/\varepsilon = (C_{i,i+1}/\varepsilon)$ respectively.

(c) Determine the total value of self capacitance $(Cg/\varepsilon = C_i'/\varepsilon)$ of rod (i) from the graph in Fig.3 of reference [60], by adding the values of the vertical coordinates of the two points on the chosen (d/b) curve whose horizontal coordinates $\frac{1}{2}\ (S_{i-1,i}/b)$ and $\frac{1}{2}\ (S_{i,i+1}/b)$ have been obtained in step (b). The value of C_i'/ε is different from that shown in matrix equation (5.50).

(d) Scale the ith row and column of matrix equation (5.50) such that its main diagonal terms will have the value of A_{ii}' where

$$A_{ii}' = (C_{i-1,i} + C_i' + C_{i,i+1})/\varepsilon \quad (i = 2 \rightarrow N+1) \qquad (5.54)$$

C_i'/ε is the self capacitance of rod (i) obtained in step (c)

And the scaling constants (n_i) are given by

$$n_i = \left[\frac{A_{ii}'}{A_{ii}}\right]^{\frac{1}{2}} \qquad (i = 2 \rightarrow N + 1) \qquad (5.55)$$

(e) Owing to the scaling process in step (d), new value of $(C_{i-1,\,i}/\varepsilon)$ and $C_{i,i+1}/\varepsilon)$ are obtained and the cycle may be repeated until the scaling constants (n_i) approach unity. And the dimensions obtained in the last scaling cycle are the required ones.

(f) The first and the last rods may be made having the same diameter as the rest by adjusting the position of the side walls of the structure as follows:

let C_o be the coupling capacitance between the first rod and its side wall

$$\therefore \quad A_{11} = (C_o + C_1 + C_{12})/\varepsilon \qquad (5.56)$$

where A_{11} is the first diagonal term of the capacitance matrix (known)

C_1 is the self capacitance of rod 1

C_{12} is the final scaled value of the coupling capacitance between rod 1 and 2 (known)

choose a reasonable separation distance between rod 1 and the wall $\frac{1}{2}$ (S_{1W}/b). From graph in Fig.2 of reference [60] find the value of $C_m/\varepsilon = C_o/\varepsilon$ and from graph Fig.3 of reference [60] find $C_g/\varepsilon = C_1/\varepsilon)$. Use the obtained values of C_o and C_1 in equation (5.56). Repeat the cycle by choosing a new value for $\frac{1}{2}$ (S_{1W}/b) until equation (5.56) is satisfied.

The method may be illustrated further by the following numerical example:

Numerical Example

A 4-resonator prototype doubly terminated by a 1 Ω resistance, shown in Fig 5.19 has been synthesised to satisfy an equiripple response in the passband between 4 GHZ and 4.5 GHZ and 20 dB minimum return loss. The resonators are quarter wavelength at 15 GHZ.

The element values are shown in Table 5.7 where $C_r' \times 10^{-9}$ are the lumped capacitors in farads, Y_r' are the characteristic admittances of the shunt short-circuited stubs in Siemens and $K_{r,r+1}'$ are the characteristic admittances of the frequency-dependant admittance inverters in Siemens.

Table 5.7: Element values of 4 resonator combline filter

r	$C_r' \times 10^{-9}$	Y_r'	$K_{r,r+1}'$
1	3.62554	7.40989	1.3188
2	8.78528	17.9608	1.57438
3	8.78528	17.9608	1.3188
4	3.62554	7.40989	

The 1 Ω unit elements at both ends of the network have been introduced for practical convenience.

The admittance matrix for the inductive array of the network may be given as:

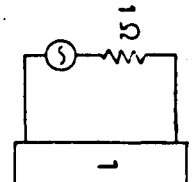
5Ω
1

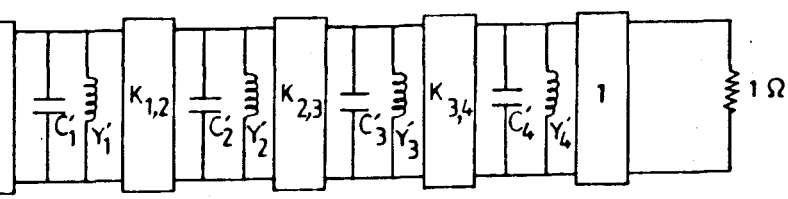

Fig. 5.19 4-resonator prototype combline filter

$$[Y'] = \begin{array}{c} \\ 1 \\ n_2 \rightarrow -1 \\ n_3 \rightarrow 0 \\ n_4 \rightarrow 0 \\ n_5 \rightarrow 0 \\ 0 \end{array} \begin{bmatrix} & n_2 \downarrow & n_3 \downarrow & n_4 \downarrow & n_5 \downarrow & \\ 1 & -1 & 0 & 0 & 0 & 0 \\ -1 & 8.40989 & -1.3188 & 0 & 0 & 0 \\ 0 & -1.3188 & 17.9608 & -1.57438 & 0 & 0 \\ 0 & 0 & -1.57438 & 17.9608 & -1.3188 & 0 \\ 0 & 0 & 0 & -1.3188 & 8.40989 & -1 \\ 0 & 0 & 0 & 0 & -1 & 0 \end{bmatrix} \qquad (5.57)$$

The scaling factors n_i are chosen such that all the diagonal terms be unity; therefore

$n_2 = 0.34483$

$n_3 = 0.235959$

and, because it is a symmetrical network,

$n_4 = n_3$

$n_5 = n_2$

after scaling we have the values shown in matrix equation (5.58):

$$[Y] = \begin{bmatrix} 1 & -0.34483 & 0 & 0 & 0 & 0 \\ -0.34483 & 1 & -0.107305 & 0 & 0 & 0 \\ 0 & -0.107305 & 1 & -0.087656 & 0 & 0 \\ 0 & 0 & -0.087656 & 1 & -0.107305 & 0 \\ 0 & 0 & 0 & -0.107305 & 1 & 0.34483 \\ 0 & 0 & 0 & 0 & -0.34483 & 1 \end{bmatrix} \qquad (5.58)$$

For 50 Ω terminations and air-filled line, the equivalent static capacitive matrix is given by

$$|C| = \begin{bmatrix} 7.534 & -2.597949 & 0 & 0 & 0 & 0 \\ -2.597949 & 7.534 & -0.808436 & 0 & 0 & 0 \\ 0 & -0.808436 & 7.534 & -0.6604 & 0 & 0 \\ 0 & 0 & -0.6604 & 7.534 & -0.808436 & 0 \\ 0 & 0 & 0 & -0.808436 & 7.534 & -2.597949 \\ 0 & 0 & 0 & 0 & -2.597949 & 7.534 \end{bmatrix} \quad (5.59)$$

with $d/b = 0.4$.

By using the elements of matrix equation (5.59) and the graphs in Reference [60] proceed in finding the dimensions.

(i) Rod 2:

(a) From the graph in Fig.2 of Reference [60]: use $C_{21}/\varepsilon = 2.597949$, intersect $(d/b) = 0.4$, find $\frac{1}{2}(C_{21}/b) = 0.06$

(b) Repeat for $(C_{23}/\varepsilon) = 0.808436 = \frac{1}{2}(S_{23}/b) = 0.193$

(c) From the graph in Fig.3 of Reference [60], use $\frac{1}{2}(S_{21}/b) = 0.06$, intersect $(d/b) = 0.4$ find $x(C_g/\varepsilon) = 1.55$

(d) Repeat for $\frac{1}{2}(S_{23}/b) = 0.193 \rightarrow (1 - x)(C_g/\varepsilon) = 2.1$

$C_2'/\varepsilon = x(C_g/\varepsilon) + (1 - x)(C_g/\varepsilon)$

$C_2'/\varepsilon = 1.55 + 2.1 = 3.65$

(ii) Rod 3:

(a) From the graph in Fig.2 of Reference [60]: use $(C_{34}/\varepsilon) = 0.6604$, intersect $(d/b) = 0.4 \rightarrow \frac{1}{2}(S_{34}/b) = 0.225$

(b) Since $(C_{32}/\varepsilon) = (C_{23}/\varepsilon) \rightarrow \frac{1}{2}(S_{32}/b) = \frac{1}{2}(S_{23}/b) = 0.193$

(c) From the graph in Fig.3 of Reference [60], use $\frac{1}{2}(S_{34}/b) = 0.225$, intersect $(d/b) = 0.4 \rightarrow X(C_g/\varepsilon) = 2.2$

Then, the capacitance matrix equation (5.59) can be transformed to that shown in matrix equation (5.60) by multiplying the ith row and column by the corresponding scaling constant n_i'

$$[C'] = \begin{bmatrix} 7.534 & -2.514253 & 0 & 0 & 0 & 0 \\ -2.514253 & 7.056385 & -0.684629 & 0 & 0 & 0 \\ 0 & -0.684629 & 5.768836 & -0.505673 & 0 & 0 \\ 0 & 0 & -0.505673 & 5.768836 & -0.684629 & 0 \\ 0 & 0 & 0 & -0.684629 & 7.056385 & -2.514253 \\ 0 & 0 & 0 & 0 & -2.514253 & 7.534 \end{bmatrix} \quad (5.60)$$

The cycle may be repeated by using the elements in matrix equation (5.60) Consequently, results in the scaling constants n_i'' at values

$$n_2'' = n_5'' = 0.990924$$

$$n_3'' = n_4'' = 0.988797$$

Similarly, by using n_i'', matrix equation (5.60) can be transformed to the matrix given in matrix equation (5.61)

$$|''C| = \begin{bmatrix} 7.534 & -2.491434 & 0 & 0 & 0 & 0 \\ -2.491434 & 6.928882 & -0.670815 & 0 & 0 & 0 \\ 0 & -0.670815 & 5.640302 & -0.494406 & 0 & 0 \\ 0 & 0 & -0.494406 & 5.640302 & -0.670815 & 0 \\ 0 & 0 & 0 & -0.670815 & 6.928882 & -2.491434 \\ 0 & 0 & 0 & 0 & -2.491434 & 7.534 \end{bmatrix} \quad (5.61)$$

(d) For $\frac{1}{2}(S_{32}/b) = 0.193 \rightarrow (1 - X)(C_g/\varepsilon) = 2.1$

$C_3'/\varepsilon = x(C_g/\varepsilon)+(1-x)(Cg/\varepsilon)$ therefore $(C_3'/\varepsilon) = 2.2 + 2.1 = 4.3$

(iii) Since the network is symmetrical, rod 4 has the same self capacitance as rod 3, and rod 5 has that of rod 2; therefore

$(C_4'/\varepsilon) = 4.3$

$(C_5'/\varepsilon) = 3.65$

The scaling operation may be performed and the scaling constants n_i' can be obtained as follows:,

(a) The scaling constant n_2':

$$A_{22}' = (C_{21} + C_2' + C_{23})/\varepsilon$$

$$A_{22}' = 2.597949 + 3.65 + 0.808436 = 7.056385$$

therefore

$$n_2' = \left[\frac{7.056385}{7.534}\right]^{\frac{1}{2}} = 0.967784$$

$$n_5' = n_2' = 0.967784$$

(b) The scaling constant n_3':

$$A_{33}' = (C_{32} + C_3' + C_{34})/\varepsilon$$

$$A_{33}' = 0.808436 + 4.3 + 0.6604 = 5.768836$$

therefore

$$n_3' = \left[\frac{5.768836}{7.534}\right]^{\frac{1}{2}} = 0.875047$$

$$n_4' = n_3' = 0.875047$$

However, repeating the cycle by using the elements in matrix equation (5.61) results in the dimensions shown in Table 5.8 and the new set of scaling factors n_i''' are

$$n_2''' = n_s''' = 0.999882$$

$$n_3''' = n_4''' = 1.00132$$

which clearly shows that $n_i''' \simeq 1$; i.e. matrix equation (5.61) is unique for the dimension shown in Table 5.8 and for d/b = 0.4.

The first rod and the last one may be made with the same diameter as the rest by adjusting the position of the side walls of the structure as follows: Use equation (5.56)

$$A_{11} = C_o + C_1 + C_{12}''$$

where

$$A_{11} = 7.534$$

$$C_{12}'' = 2.491434$$

(a) choose $\frac{1}{2}(S_{1w}/b) = 0.1$

From graph in Fig.2 of Reference [60], $C_m/\varepsilon = C_o/\varepsilon = 1.7$

From graph in Fig.3 of Reference [60], $\frac{1}{2}(C_g/\varepsilon) = \frac{1}{2}(C_1/\varepsilon) = 1.75$?

$C_1/\varepsilon = 3.50$

$A_{11} = 1.7 + 3.5 + 2.491434 = 7.691434$

$7.534 \stackrel{?}{=} 7.691434$

(b) choose a new value of $\frac{1}{2}(S_{1w}/b) = 0.11$

From Fig.2 of Reference [60], $C_m/\varepsilon = C_o/\varepsilon = 1.55$

From Fig.3 of Reference [60], $\frac{1}{2}(C_g/\varepsilon) = \frac{1}{2}(C_1/\varepsilon) = 1.78$?

$C_1/\varepsilon = 3.65$

$A_{11} = 1.55 + 3.65 + 2.491434 = 7.601434$

(c) choose another value of $\frac{1}{2}(S_{1\omega}/b) = 0.115$

From Fig.2 of Reference [60], $C_m/\varepsilon = C_o/\varepsilon = 1.48$

From Fig.3 of Reference [60], $\frac{1}{2}(C_g/\varepsilon) = \frac{1}{2}(C_1/\varepsilon) = 1.8 \rightarrow$

$C_1/\varepsilon = 3.6$

$A_{11} = 1.48 + 3.6 + 2.491434 = 7.571434$

so it can be claimed that the distance $\frac{1}{2}(S_{1\omega}/b) = 0.115$ is the right choice for $d/b = 0.4$

$S_{1\omega}/b = 0.23$

Table 5.8: Dimensions

S_{21}/b	= S_{56}/b	=	0.126
S_{32}/b	= S_{45}/b	=	0.44
S_{34}/b		=	0.53

5.8 MICROWAVE INTEGRATED CIRCUITS (MIC_s)

In certain airborne receivers, satellite systems and many others, size and weight are very important factors in the design process. The necessity and the greater demands in these applications for mass production with lower cost have pushed the trend towards smaller components and consequently led to the development of microwave integrated circuits.

The MIC_s technology is nowadays quite mature and keeps in pace with the continuous increase in the complexity and sophistication in almost every aspect of microwave devices, components, sub-systems and systems.

In passive circuits, the microstrip transmission line and the suspended substrate transmission line (strip line) are the most popular forms of

circuit for MIC_s. The microstrip shown in Fig 5.20 consists of a strip conductor separated from the ground plane by a dielectric layer. All associated circuit parameters are defined in the plane of the strip conductor. The characteristic impedance and length of lines determine the circuit properties. The propagating field lines between the strip conductor and the ground plane are distributed between the air and the dielectric substrate with the major part is contained in the latter. Hence the propagating mode along the strip is not purely TEM but a quasi TEM or even more complicated than that when the structure shown in Fig 5.20 is sealed in a closed container. A detailed and comprehensive treatment for the analysis of microstrip transmission line was given by Mitra and Itoh in [62]. However, the microstrip structure has attracted much attention in recent years and its characteristics and behaviour are still under further investigation and study in different circumstances for different applications.

On the other hand the suspended substrate strip transmission line or as simply known the strip line shown in Fig 5.21 consists of a strip conductor on the face of a dielectric substrate and the substrate is then suspended in a metal enclosure. The major part of propagating field in this structure is in the airspace between the dielectric substrate and the ground. The circuit characteristics are determined by the substrate thickness, dielectric constant, ground plane spacing and width of the strip conductor. The strip line was introduced thirty years ago and was going under intensive study in the early fiftees of this century. Therefore it may be considered as the first generation of MIC_s where the microstrip may represent the second generation. Although the strip line was known for so long, its use in microwave design did not become very popular until quite recently when new

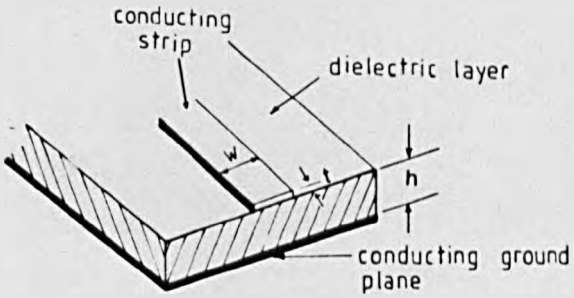

Fig. 5.20 Microstrip transmission line

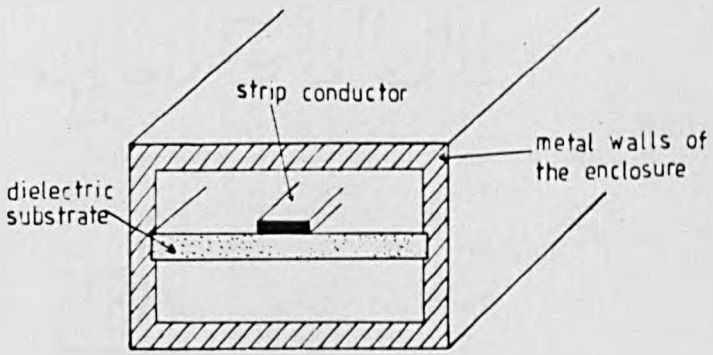

Fig. 5.21 Suspended-substrate strip line

low loss dielectric and substrate materials became available and paved the road towards the development of the different versions of MIC_s. A considerable amount of experimental and theoretical data on the MIC_s can be found in [63] and [64].

5.8.1 The MIC_s Filters

Filters are no exception from the continuous demands for smaller components and cheaper manufacturing cost either as individual components or part of MIC packages performing many functions. In the past some types of microwave filters have been built in one form of MIC_s or another. They were limited to relatively wide band applications where the selectivity is not severe. Most recently two important contributions have been reported [65], [66]. In both of these papers, the microstrip structure has been discarded because microstrip filters suffer from limitations on stopband loss due to quasi surface modes, higher in-band dissipation loss and limited range of impedance achieved which limits filter realizations, performance and design flexibility. In contrast the suspended substrate stripline (SSS) has been found to be the most suitable structure. This structure is capable of achieving very good electrical performance, temperature stability and fine tuning is possible with screws in the main enclosure.

The SSS structure has been used in Reference [65] to construct stepped impedance low-pass and broadband interdigital filters exhibiting Butterworth and conventional Chebyshev responses. In Reference [66] this form of realization was used for constructing broadband filters based on the generalized Chebyshev low-pass prototype introduced in Chapter 2 of this thesis which exhibits a single transmission zero at infinity with the

remainder at the same finite point $\omega = \pm \omega_0$.

This section presents a microwave low-pass filter design example based on the highly selective prototype introduced earlier in this thesis (Chapter 2, section 2.7.2). The design and construction technique is similar to that used in [66].

5.8.2 Design and Construction of SSS Microwave Lowpass Filter

The low-pass prototype filter satisying a generalized Chebyshev response with three transmission zeros at infinity and multiple order transmission zeros at the same finite frequency $\omega = \pm \omega_0$ has been introduced in Chapter 2. This filter has a selectivity close to the optimum elliptic function prototype but much easier to realize physically, since the variation in the impedance level is less than 2:1 comparing with about 10:1 in the elliptic function.

The microwave low-pass filter design example given here is based on the generalized Chebyshev low-pass prototype of degree N = 11 shown in Fig 5.22 and is required to satisfy the following specifications:

cut-off frequency f_b = 4 GHZ

minimum stopband insertion loss = 40 dB

and minimum passband return loss = 26 dB.

The lumped prototype element values $C_1(R)$, $L_0(R)$, $L_2(R)$ and $C_2(R)$ of this network are taken from Table 13 in Chapter 2 of this thesis. The corresponding value of ω_0 = 1.1158 is taken from Table No.16 in the same chapter.

To transform to the distributed domain, Richard's transformation

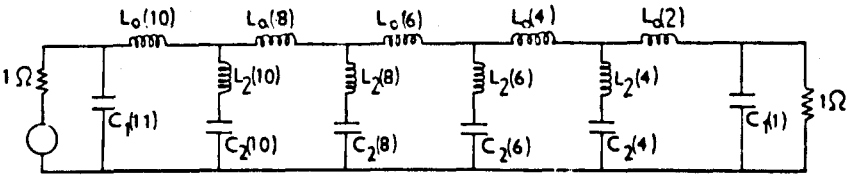

Fig. 5.22 The generalized low pass prototype of degree 11

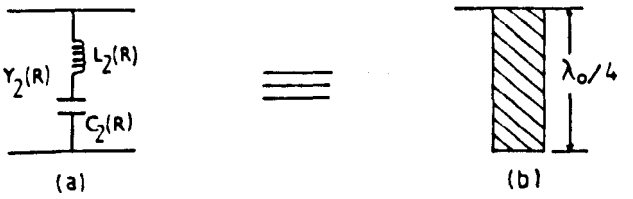

Fig. 5.23 (a) Lumped shunt resonant section
(b) Shunt o/c resonator stub

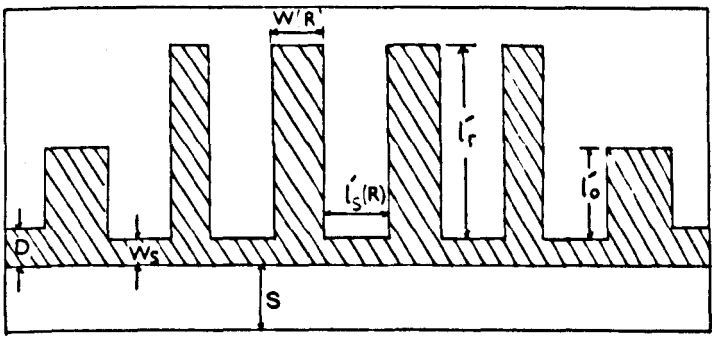

Fig. 5.24 The printed circuit board for degree 11 low-pass filter

should be applied

$$p \rightarrow \beta t = \beta \tanh(ap)$$

where the constants a and β are chosen such that the shunt resonant branch may be realized directly by uniform admittance shunt O/C stubs. Each stub is one quarter of a wavelength long at the finite transmission zero f_o.

Consider a typical lumped shunt resonant branch and its proposed microwave printed circuit realization of a uniform admittance O/C stub shown in Fig 5.23.a and b respectively. Its admittance may be written as

$$Y_2(R) = \frac{C_2(R)p}{1 + p^2/\omega_o^2} \tag{5.62}$$

where $\omega_o^2 = 1/L_2(R).C_2(R)$.

After applying Richard's transformation, it becomes

$$Y_2(R) = \frac{C_2(R)\ \beta t}{1 + \beta^2 t^2/\omega_o^2} \tag{5.63}$$

If $\beta = \omega_o$ (5.64)

Then

$$Y_2(R) = \frac{\beta\ C_2(R)\ t}{1 + t^2} \tag{5.65}$$

$$\therefore\ Y_2(R) = \tfrac{1}{2}\beta\ C_2(R)\ \tanh(2ap) \tag{5.66}$$

which clearly shows that the shunt resonant branch is realizable by a uniform admittance shunt O/C stub of characteristic admittance:

$$Y_{02}(R) = \beta\ C_2(R)/2 \tag{5.67}$$

The constant a can be obtained from the Richard's transformation at

the bandedge.

$$\omega_b = \beta \tan(af_b)$$

$$\therefore a = \frac{1}{f_b} \tan^{-1}(1/\beta) \tag{5.68}$$

from equation (5.64), $\beta = 1.1158$, and $f_b = 4$ GHZ (given). Then

$$a = 10.466817 \tag{5.69}$$

Since the O/C resonant stub should be $\lambda_o/4$ long at f_o then, from equation (5.66)

$$2af_o = 90^o \quad \Rightarrow \quad f_o = 4.2993 \text{ GHZ}$$

The length of the resonator is

$$\ell_r = \lambda_o/4 = \frac{v}{4 f_o} = 0.68634'' \tag{5.70}$$

However, as a direct result of Richard's transformation, the two shunt capacitors $C_1(11)$ and $C_1(1)$ of the lumped prototype network contributing for two out of the three transmission zero at infinity are realized by shunt O/C stubs of characteristic admittance

$$Y_{01}(11) = Y_{01}(1) = \beta C_1(11) = \beta C_1(1) \tag{5.71}$$

and they can be made a quarter wavelength long at $2f_o$. Hence, the length of the O/C stub:

$$\ell_o = \lambda_o/8 = 0.34317'' \tag{5.72}$$

The characteristic admittances of the shunt O/C resonator stubs $Y_{02}(R)$ and those of the shunt O/C stubs $Y_{01}(R)$ are calculated from equation (5.67) and (5.71) respectively and given in Table 5.9.

Table 5.9: The normalized characteristic admittances of the shunt O/C stubs of the low-pass filter

$Y_{01}(11) = Y_{01}(1) = 0.944685$
$Y_{02}(10) = Y_{02}(4) = 0.658812$
$Y_{02}(8) = Y_{02}(6) = 0.934409$

it remains to realize the series elements $L_o(R)$. These elements are responsible for the third transmission zero at infinity. Due to Richard's transformation, these elements correspond to short-circuited stubs that produce an infinite impedance when a quarter of a wavelength long at $2f_o$. At this frequency the two shunt O/C stubs are also a quarter of a wavelength long each producing an infinite admittance while the shunt O/C resonator stubs are one half of a wavelength long and hence do not contribute to the response of the filter.

Since a direct realization of a series S/C in printed circuit form is difficult, therefore an alternative approximate realization is given in [66] and adopted here. It utilizes a length of short transmission line to provide a series inductive effect on the printed circuit. This approximation is justified by holding a stopband upto about an octave above the cut-off frequency and this is suitable for several applications.

Let the length of short transmission lines which realize the series lumped inductances $L_o(R)$ in microwave frequency equal $\ell_s(R) < \lambda_o/8$ and have effective inductances $L_o'(R)$. To calculate these values, one may start by equating the impedances of length of short transmission lines to the required impedance at the cut-off frequency f_b. Thus

$$j\omega_b L_o'(R) = j R_o Z(R) \tan(af_b) \tag{5.73}$$

where $Z(R) = \beta L_o(R)$

R_o = the actual load resistance. In this example

$$R_o = 50\ \Omega$$

$\omega_b = 2\pi f_b$

$$\therefore\ L_o'(R) = \frac{R_o Z(R)}{\omega_b} \tan(af_b)$$

But $\tan(af_b) = 1/\beta$

Hence

$$L_o'(R) = \frac{R_o L_o(R)}{\omega_b} \tag{5.74}$$

which of course can be obtained directly by simple impedance and frequency scaling.

However, the lumped inductance of a short length of line $\ell_s(R)$ can be approximately given by [28].

$$L_o'(R) = \frac{Z_o \ell_s(R)}{v} \tag{5.75}$$

where v is the velocity of wave propagation

Z_o is the characteristic impedance of the line.

Then, from equation (5.74) and (5.75)

$$\ell_s(R) = \frac{L_o(R)\, v}{Z_o'} \tag{5.76}$$

where $Z_o' = Z_o/R_o$ is the normalized characteristic impedance.

Since these series inductances are also acting as connecting lines to the shunt O/C stubs, therefore the determination of Z_o' is governed by

the requirement of producing a smooth transition across the device and from the input and output coaxial connectors to the printed circuit board.

With the final configuration of the printed circuit structure shown in Fig 5.24 in mind, one may proceed in calculating $\ell_s'(R)$. In this design a ½ oz., 0.005" thick glass reinforced teflon known commercially by (RT/duriod) has been used due to its high level of tolerance on dielectric constant and the thickness of copper and dielectric. The circuit elements appear on one side of the substrate. The board is placed in the middle of a metal box of ground plane spacing b, suitably chosen to prevent the propagation of the higher order modes. In this design b = 0.07" which also ensures that b is much greater than the dielectric thickness. Within this choice the conductors are practically in air hence the variation of the overall dielectric constant with temperature will be very close to that of air ε_o and has little effect on the response. The thickness of all conductors is t = 0.00085". The width of the series conductors is chosen to be W_s = 0.025".

The characteristic impedance of the piece of centre conductor of the terminal connectors symmetrically located inside the metal box is given by [64].

$$Z_o = \frac{138}{\sqrt{\varepsilon_r}} \log \frac{4}{\pi} \frac{b}{D} \qquad (5.77)$$

For 50 Ω termination and air filled structure the diameter of the centre conductor D = 0.036". The distance from the series connecting lines to the nearest side wall S = 0.03".

Having established these values, the characteristic impedance Z_o' can be calculated, commencing by calculating the fringing capacitances using Getsinger's charts [59]. Consider the cross section of a typical short series connecting line inside the box shown in Fig 5.25.a with the associated capacitances. With $t/_b = 0.012$ and $2S/_b = 0.857$, Getsinger's charts gives: $C_f'/\varepsilon_o = 0.46$, $C_f'/\varepsilon_o = 0.51$

Since $C_p/\varepsilon_o = 2W_s/(b-t) = 0.714$

Then, the total static capacitance per unit length of the line is given by

$$C_{\ell_s}/\varepsilon_o = 2\,(C_f'/\varepsilon_o + C_{f_o}'/\varepsilon_o + C_p/\varepsilon_o) = 3.368$$

Then, applying equation (5.34)

$$Z_o' = 7.534/(C_{\ell_s}/\varepsilon_o) = 2.236\ \Omega$$

Now, the length of the short series transmission line can be calculated from equation (5.76) and their values are given in Table 5.10.

Table 5.10: The length of the series connected transmission lines

$\ell_s(10) = \ell_s(2) = 0.169"$
$\ell_s(8) = \ell_s(4) = 0.158"$
$\ell_s(6) = 0.162"$

To complete the design, the widths of the shunt O/C stubs should be found. Consider the cross section for a typical stub with the associated capacitances shown in Fig 5.25.b. Each of these stubs can be treated as being in isolation between two parallel ground planes. This is because the coupling between the parallel stubs is negligible for high $\ell_s(R)/b$ ratio

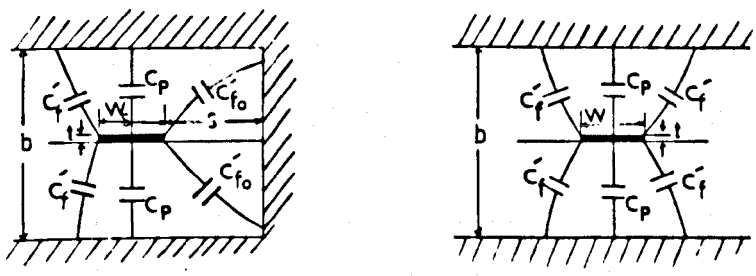

Fig. 5.25 (a) Cross-section for a typical short transmission line representing series lumped inductance showing the associated capacitances

(b) Cross-section for a typical shunt o/c stub showing the associated capacitances

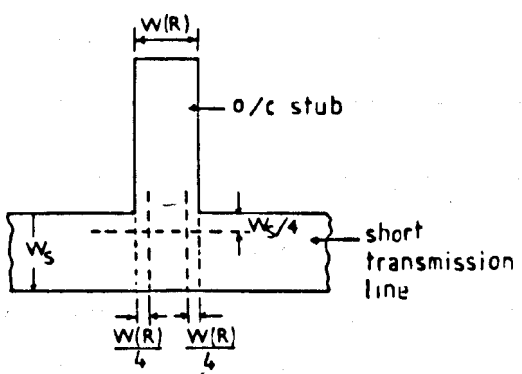

Fig 5.26 The reference planes of the T-junction

as may be clearly seen from Getsinger's charts and the coupling between the ends of the stubs and the nearest sidewall can be neglected by adjusting the distances to these walls. Hence, the total static capacitance per unit length of each shunt O/C stub is

$$C_t(R)/\varepsilon_o = 2\, C_p(R)/\varepsilon_o + 4\, C_f'/\varepsilon_o \qquad (5.78)$$

and since

$$C_t(R)/\varepsilon_o = 7.534\, Y_{02}(R) \qquad R = 10,8,6,4$$

$$C_t(R)/\varepsilon_o = 7.534\, Y_{01}(R) \qquad R = 11 \text{ and } 1$$

which can be obtained by substituting the values of $Y_{02}(R)$ and $Y_{01}(R)$ given in Table 5.9. Then $C_p(R)/\varepsilon_o$ are calculated from equation (5.78) and the widths of the stubs W(R) are followed as given in Table 5.11.

Table 5.11: The width of the O/C stubs

W(10)	= W(4)	=	0.053997"
W(8)	= W(6)	=	0.089892"
W(11)	= W(1)	=	0.09123"

However, the length dimensions obtained so far are not final. Since the shunt O/C stubs and the series short lines are connected at a Tee-junction, their lengths should be modified taking into account the junction effect. Thus, the actual lengths $\ell_s'(R)$, ℓ_r' shown in Fig 5.23 are calculated as follows:

$$\ell_r' = \ell_r - W_s/4 = 0.68"$$

$$\ell_o' = \ell_o - W_s/4 = 0.337"$$

$$\ell_s'(R) = \ell_s(R) - \frac{W(R+1)}{4} - W(R)/4 \qquad R = 10,8,6,4,2$$

35
30
25
20
15
10
5
0
I.L.(dB)
R.L.(dB)
R.L.
0
1
2
3

Fig. 5. 27 The experimental insertion loss and return loss characterstic of the low-pass printed circuit microwave filter

Thus,

$$\ell_s'(10) = \ell_s'(2) = 0.133"$$

$$\ell_s'(8) = \ell_s'(4) = 0.123"$$

$$\ell_s'(6) = 0.118"$$

These set of values are obtained under the assumption that the original values were measured from the corresponding reference planes of a simple stripline Tee-junction as given in Reference [28] and illustrated in Fig 5.26.

Having completed the design, the low-pass microwave filter has been constructed and tested using a swept frequency reflectometer arrangement. Its experimental insertion loss and return loss characteristics are obtained as shown in Fig 5.27.

5.9 CONCLUDING REMARKS

The main concern of this chapter is developing design procedures and construction of classes of TEM mode filters for broadband applications.

The chapter began by a brief introduction on the basic concepts of the distributed circuits. The analogy between these circuits and their lumped counterparts was explained by considering the well known Richard's transformation. The concept of the Unit Element was also discussed and its utilization in TEM networks either in a redundant or non-redundant form was mentioned.

After that introduction, the parallel coupled lines class of TEM-network was discussed. Within this context an exact synthesis procedure for prototype broadband combline filter was given and a new design

method to realize TEM-network in coaxial form having equal-diameter coupled circular cylindrical rods was presented.

The exact synthesis procedure was developed for arbitrary bandwidth combline filter based on a doubly terminated LC bandpass prototype satisying a generalized Chebyshev characteristic having equiripple passband response with single transmission zero at the origin and an odd multiple at infinity. The synthesis procedure was programmed on a computer and when the alternating pole synthesis technique was used, networks of up to degree 30 can be easily synthesized and their element values are obtained with little loss of accuracy. On the other hand, it has been found that networks of degree less than 18 can be synthesized using the conventional p-plane element extraction technique. However, the computer program gives the lumped prototype element values, converts them into distributed stubs or into mixed lumped capacitors and short circuited stub if required and provides the frequency analysis of the circuit.

An octave bandwidth microwave combline filter was designed using distributed stubs and constructed in coaxial form with the parallel coupled bars having rectangular cross sections. The experimental results are given in Fig 5.13. They show a shrink in the passband. Instead of (3 → 6) GHZ as expected, the measured one is approximately from (3.7 → 5.6) GHZ. This is because for such design specifications, the bars are tightly coupled and the correct width of the bars can not be calculated easily due to the interaction of the fringing capacitances. The use of the approximate formula given in equation (5.41) has not helped much in obtaining the correct value of the widths, since the resulting values still do not satisfy equation (5.40) for the chosen t/b ratio. Furthermore, Wenzel [58] has shown that the return loss and the upper

bandedge of these networks response are extremely sensitive to the value of coupling admittances $Y_2(R)$ which affect the gap between the bars. So unless a strict mechanical tolerance is considered during the construction, the return loss and the upper bandedge are altered considerably. However, the experimental results obtained here are considered satisfactory within the mechanical tolerance used. The response might be improved if a smaller t/b ratio had been chosen.

This chapter has also presented a new design method to realize TEM-networks such as combline and interdigital filters in coaxial form having equal-diameter coupled cylindrical rods. This method based on the graphs in Fig.2 and 3 of Reference [60] and the capacitance matrix. It is approximate in the sense that each conductor is coupled only to its nearest neighbours and its accuracy is governed by the accuracy of the mentioned graphs which is within the accuracy of the manufacturing process. The method permits the handling of data for filters synthesized to satisfy narrow and moderate bandwidth specifications. It should also be suitable for designing broadband filters, but because a high capacitance C_m/ε results in some broadband cases (octave bandwidth), the limitation of Fig.2 of Reference [60] should be noticed. In general the method is simple and converges very quickly. It has been found that the method usually needs no more than three cycle to converge, regardless of the number of resonators.

The last part of the chapter is concerned with the MIC_s form of realizing TEM-networks. The concepts of microstrip and stripline were given and the suitability of the latter to filter design in printed circuit form was discussed. Then a design procedure was presented for a low-pass broadband microwave filter. This filter based on the very selective prototype of degree 11 satisfying a generalized Chebyshev response with 3

transmission zeros at infinity and the remainder at a finite point on the imaginary axis. The microwave structure was constructed in suspended substrate stripline and the resonators were realized by uniform admittance O/C stubs. The selectivity of this type of filters are close to that of elliptic function, but much easier to realize considering the impedance level variation of less than 2:1 compared with about 10:1 in the elliptic function and the uniform admittance O/C stubs realization which is not possible in the elliptic function. Furthermore the experimental results shown in Fig 5.25 shows that an octave stopband can be easily achieved. This advantage make this filter even more admirable for diplexer and multiplexer applications than that used in Reference [66].

In this particular example the experimental results shows a slight reduction in the cut-off frequency due to neglecting of the effect of fringing capacitances between the resonators and the nearest side wall. However this can be easily adjusted either tuning screws or by pushing the side walls a little further away from the printed circuit board.

5.10 APPENDIX

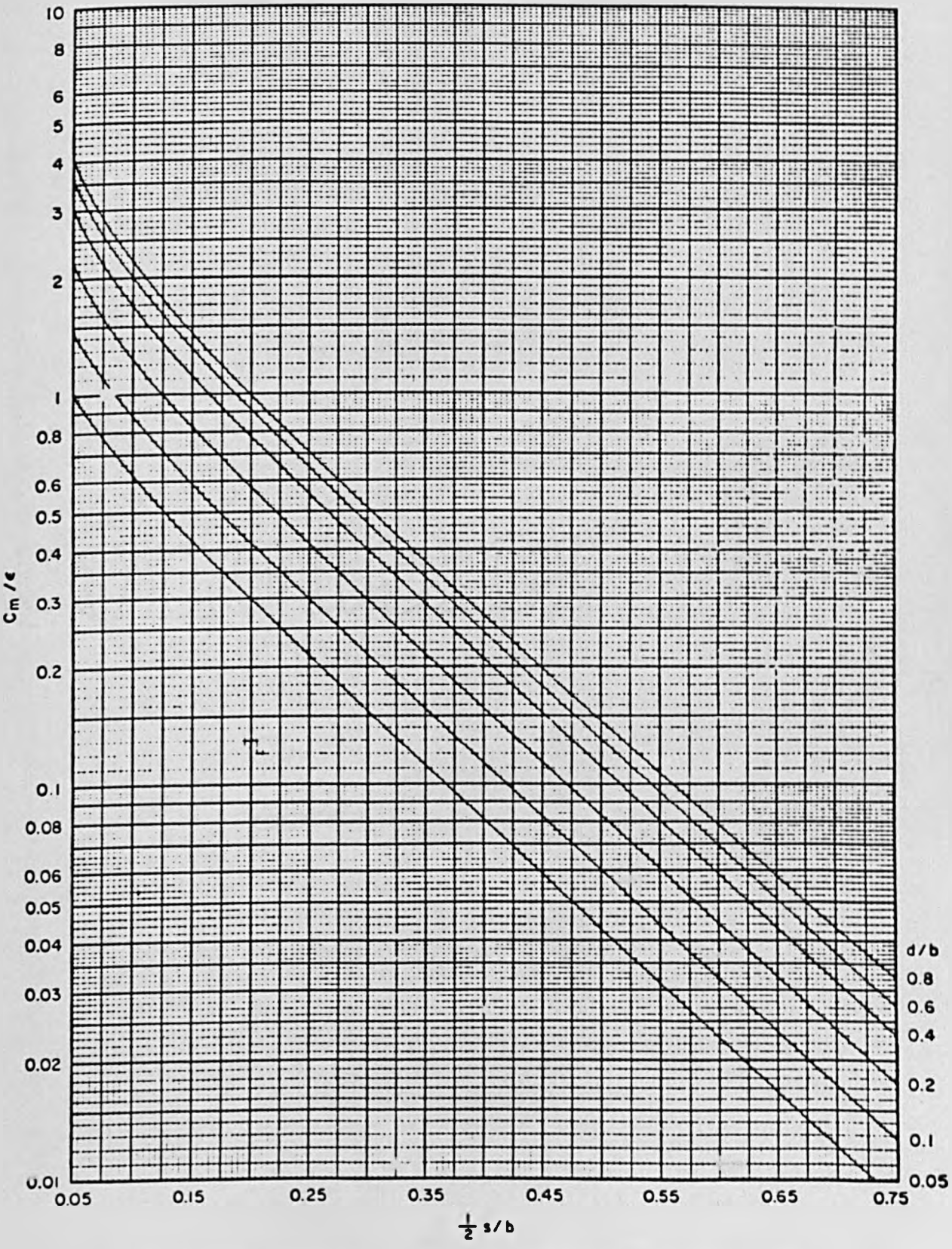

Fig. 2—Graph of C_m/ϵ (normalized mutual capacitance) vs $\frac{1}{2}(s/b)$ (normalized half spacing).

(Reference [60])

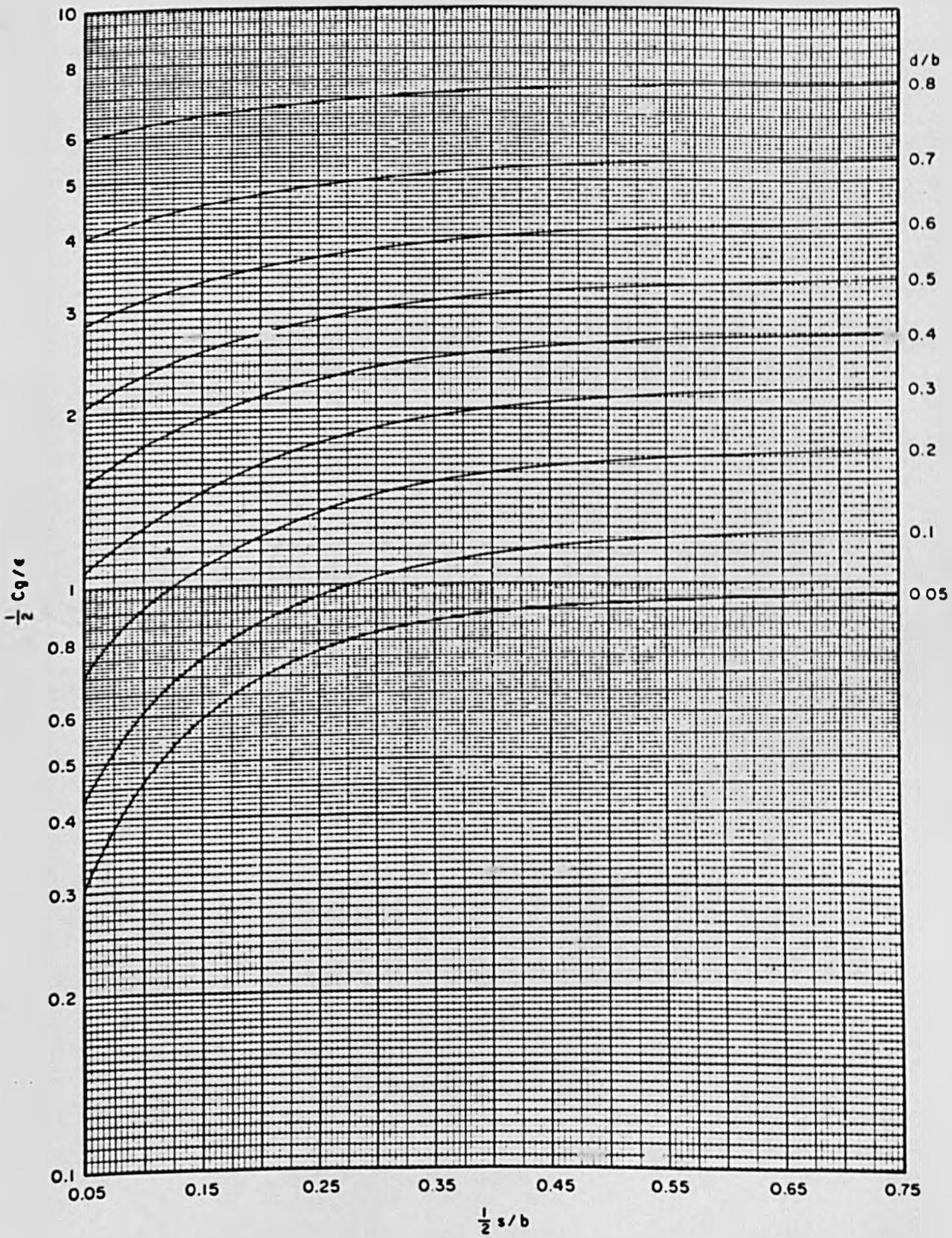

Fig. 3—Graph of $(\frac{1}{2})C_g/\epsilon$ (normalized half self capacitance) vs $(\frac{1}{2})s/b$ (normalized half spacing).

(Reference [60])

CHAPTER 6

DESIGN PROCEDURE FOR MULTI-OCTAVE COMBLINE-FILTER MULTIPLEXERS

6.1 INTRODUCTION.

Broadband multiplexers, often spanning several octaves, are most frequently used in electronic warfare applications. They allow several signals to share a common broadband device usually an antenna. Most of the multiplexers developed during the late sixties and early seventies used high-pass/low-pass or band-pass/band-stop diplexer configuration in cascade. Elliptic prototypes were used to obtain sharp cut-offs and maintain certain rejection level over very broadband e.g. [67]. These devices have the disadvantage of being both difficult and expensive to design. In addition, the number of filters used for a given number of channels is high e.g. at least five filters for a triplexer. The main reason that the cascade of diplexers approach has been used is because, during those years, it has seemed too difficult to cover a multi-octave band with a common junction bandpass multiplexer. Meanwhile, the broadband combine filter has been undergoing continual improvement. It can nowadays be constructed in straightforward manner from the theoretical prototype with bandwidths approaching 100%, stopband performance can exceed several times the upper passband edge with no spurious response. The insertion loss and the VSWR in the passband can be kept quite low even for a relatively high number of resonators filter. Therefore the attention in recent years has focussed on using combline bandpass filters to achieve smaller size, lower cost bandpass common junction multiplexers.

A design method for combline-filter multiplexers was presented more than a decade ago by Matthaei and Cristal [68]. Their design equations are based upon narrow-band approximations and the filters should be either

singly-terminated or foreshortened doubly terminated. The junction design consists of high impedance lines connected between the junction and the input resonators of the separated channel filters. However, the method was limited to a total frequency range of the order of one octave due to the narrow band approximation used in the design of individual channels. More recently LaTourrette [69], [70] and [71] presented several attempts to design a multi-octave combline filter-multiplexers. His main concern was focussed on obtaining a minimum susceptance band-pass channel filter by adding extra circuits to the original non-minimum susceptance singly terminated combline structure in order to achieve parallel connected common junction multiplexer. Although these attempts have resulted in particularly successful devices. Still their design processes are lacking in generality and in most cases the additional circuits make the manufacturing and the adjusting of these devices much more expensive and difficult to achieve.

This chapter presents a new general design procedure for multi-octave combline-filter multiplexers having any number of Chebyshev channel filters, with arbitrary number of resonators, bandwidth and interchannel spacings. This procedure may be considered as a modified version of that introduced in chapter 3 of this thesis. It commences from the element values of a doubly terminated bandpass prototype combline filter satisfying an equiripple response which is obtained from a recently introduced design equations [34]. These individual channel filters are connected at a common junction. The multiplexer design procedure modifies the elements in the nearest half to the common junction of each channel filter and as in a similar manner to that given in chapter 3, it preserves a complete match at the two points of perfect transmission closest to the passband-edges of each channel filter. However, this design procedure follows

almost the same steps in chapter 3 and has all the advantages pointed there.

The chapter begins by reviewing the combline filter design equations introduced recently by Rhodes [34]. Although these equations are approximate they have been adopted here because of their compactness and when used in a computerized multiplexer design method - as it is the case here - they are certainly required less computer time compared with the exact design method for combline filter introduced in chapter 5. Then the multi-octave multiplexer design procedure is presented. The computer analysis of several multiplexers are shown. Finally, a design example of a combline filter diplexer constructed in a coaxial form of realization is given and its experimental insertion loss and return loss characteristics are established.

6.2 DESIGN FORMULAS FOR BROADBAND COMBLINE FILTER.

The multi-octave combline-filter multiplexer design procedure commences from lumped/distributed element doubly terminated combline channel filters operating is isolation satisfying an equiripple passband amplitude response shown in Fig. 6.1 and given by [34].

$$I.L. = 10 \text{ Log } (1+\varepsilon^2 F_n^2(\omega)) \tag{6.1}$$

where

$$F_n(\omega)=\cos\left[n\cos^{-1}\left\{\frac{\omega_1\tan(a\omega_1)+\omega_2\tan(a\omega_2)-2\omega\tan(a\omega)}{\omega_2\tan(a\omega_2)-\omega_1\tan(a\omega_1)}\right\}\right.$$
$$\left.+\cos^{-1}\left\{\frac{\tan(a\omega_1)\tan(a\omega_2)(\omega_2-\omega_1)+(\tan(a\omega_2)-\tan(a\omega_1))\omega\tan(a\omega)}{\tan(a\omega).(\omega_2\tan(a\omega_2)-\omega_1\tan(a\omega_1))}\right\}\right] \tag{6.2}$$

ω_1 and ω_2 are the lower and upper bandedge frequencies

n is the number of resonators in the network shown in Fig. 6.2

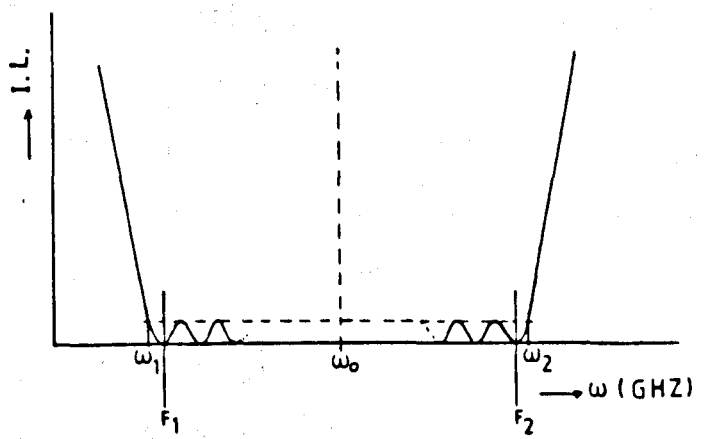

Fig. 6.1 Insertion loss response of a combline filter

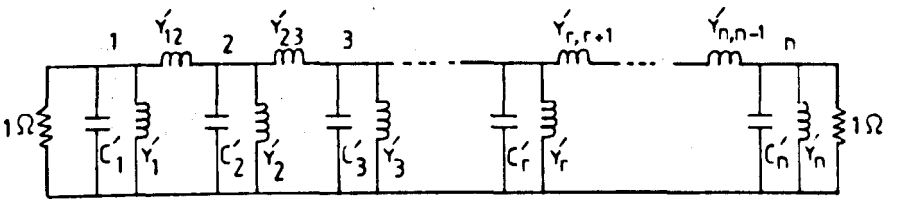

Fig. 6.2 Equivalent network of doubly terminated combline filter

whose lumped counterpart has (2n-1) transmission zeros at infinity and single transmission zero at the origin.

However, by extracting a negative shunt short circuited stub of characteristic admittance $(-Y'_{r,r+1})$ from every resonator in the network, an equivalent format consisting of resonators separated by frequency dependent admittance inverter with characteristic admittance $Y'_{r,r+1}\cot(a\omega)$ is obtained. Scaling all admittances by $\cot(a\omega)/\cot(a\omega_o)$, (where ω_o is the passband centre frequency) results in the network shown in Fig. 6.3 where the rth shunt resonator possesses an admittance:

$$B_r=j(C_r\omega\tan(a\omega)-Y_r) \tag{6.3}$$

and the resonators are separated by ideal admittance inverters of characteristic admittance $Y_{r,r+1}$, but the terminating resistances become frequency dependents i.e.

$$R_g=R_\ell = \cot(a\omega)/\cot(a\omega_o) \tag{6.4}$$

However, it has been shown by Rhodes [34], that the design formulas for this prototype network can be obtained easily with very good approximation to satisfy upto an octave bandwidth specifications using only the dominant term in $F_n(\omega)$ given in equation (6.2) such that

$$F_n(\omega) \simeq \cos\left[n\cos^{-1}\left\{\frac{\omega_1\tan(a\omega_1)+\omega_2\tan(a\omega_2)-2\omega\tan(a\omega)}{\omega_2\tan(a\omega_2)-\omega_1\tan(a\omega_1)}\right\}\right] \tag{6.5}$$

By comparing this prototype combline filter which satisfies the equiripple response in the variable $\omega\tan(a\omega)$ given in (6.5) with the low-pass prototype satisfies a conventional Chebyshev response in the variable ω, having a passband $\omega=\pm1$ and centre frequency at $\omega=0$, the approximate centre frequency ω_o of the combline is obtained when the argument of $F_n(\omega)$ is zero. Hence

$$2\omega_o\tan(a\omega_o) = \omega_1\tan(a\omega_1)+\omega_2\tan(a\omega_2) \tag{6.6}$$

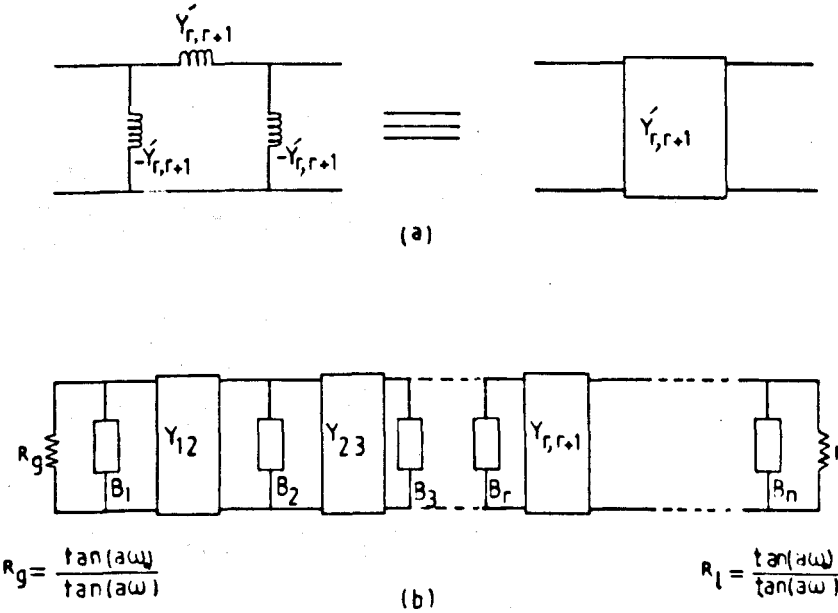

Fig. 6.3 (a) Equivalent network of an inverter of characteristic admittance $Y'_{r,r+1}$

(b) Scaled equivalent format of combline network

and the frequencies F_1 qnd F_2 where the perfect transmission occurs closest to the bandedges, can be obtained when the argument is $\pm \cos(\pi/2n)$ respectively i.e.

$$\left.\frac{\omega_1\tan(a\omega_1)+\omega_2\tan(a\omega_2)-2\omega\tan(a\omega)}{\omega_2\tan(a\omega_2)-\omega_1\tan(a\omega_1)}\right|_{\omega=F_1} = \cos(\pi/2n) \qquad (6.7)$$

and

$$\left.\frac{\omega_1\tan(a\omega)+\omega_2\tan(a\omega_2)-2\omega\tan(a\omega)}{\omega_2\tan(a\omega_2)-\omega_1\tan(a\omega_1)}\right|_{\omega=F_2} = -\cos(\pi/2n) \qquad (6.8)$$

Hence, from equation (6.7)

$$F_1\tan(aF_1) = \omega_1\tan(a\omega_1)\cos^2(\pi/4n)+\omega_2\tan(a\omega_2)\sin^2(\pi/4n) \qquad (6.9)$$

and from equation (6.8)

$$F_2\tan(aF_2) = \omega_1\tan(a\omega_1)\sin^2(\pi/4n)+\omega_2\tan(a\omega_2)\cos^2(\pi/4n) \qquad (6.10)$$

However, the values of ω_o, F_1 and F_2 can be obtained by using one of the standard numerical techniques (e.g. Newton-Raphson) in solving equations (6.6), (6.9) and (6.10) for given values of n, ω_1 and ω_2.

The derivation of the design formulas for the combline based on preserving unity transmission with the correct overall phase shift in the auxiliary parameter $-j\eta$ or $j\eta$ at the frequencies F_1 and F_2, where η is as defined in equation (3.2). For broadband applications the $\cot(a\omega)/\cot(a\omega_o)$ frequency dependence of the terminating resistances R_ℓ and R_g must be taken into account. Furthermore, the internal impedance level is allowed to vary and the sections of the network in question is only required to be image matched. Thus the overall transfer matrix of the network at F_1 is given by:

$$\prod_{r=1}^{n-1} \frac{1}{\sqrt{(n^2+S_r^2)(1+t_r^2)}} \begin{bmatrix} \sqrt{\frac{Z_{1r}}{Z_{1r+1}}}\,(S_r+nt_r) & j\sqrt{Z_{1r}Z_{1r+1}}\,(n-S_rt_r) \\ j\frac{(n-S_rt_r)}{\sqrt{Z_{1r}Z_{1r+1}}} & -\sqrt{\frac{Z_{1r+1}}{Z_{1r}}}\,(S_r+nt_1) \end{bmatrix} \tag{6.11}$$

and the overall transfer matrix of the network at F_2 is given by

$$\prod_{r=1}^{n-1} \frac{1}{\sqrt{(n^2+S_r^2)(1+t_r^2)}} \begin{bmatrix} \sqrt{\frac{Z_{2r}}{Z_{2r+1}}}\,(S_r-nt_r) & j\sqrt{Z_{2r}Z_{2r+1}}\,(n+S_rt_r) \\ j\frac{(n+S_rt_r)}{\sqrt{Z_{2r}Z_{2r+1}}} & \sqrt{\frac{Z_{2r+1}}{Z_{2r}}}\,(S_r-nt_r) \end{bmatrix} \tag{6.12}$$

Where the quantities in these two equations have similar definitions as those in chapter 3.

Implying the same argument presented in chapter 3, matrix equation (6.11) yields the characteristic admittance of the inventer.

$$Y_{r,r+1} = \frac{\sqrt{(n^2+S_r)(1+t_r^2)}}{\sqrt{Z_{1r}Z_{1r+1}}(n-S_rt_r)} \qquad r=1\rightarrow\frac{n}{2} \tag{6.13}$$

and the admittance of the rth shunt resonator between the inventers $Y_{r-1,r}$ and $Y_{r,r+1}$ is

$$C_rF_1\tan(aF_1) - Y_r = \frac{-1}{Z_{1r}}\left\{\frac{(S_r+nt_r)}{(n-S_rt_r)} + \frac{(S_{r-1}+nt_{r-1})}{(n-S_{r-1}t_{r-1})}\right\} \qquad r=1\rightarrow\frac{n}{2} \tag{6.14}$$

Similarly, from matrix equation (6.12)

$$Y_{r,r+1} = \frac{\sqrt{(n^2+S_r)(1+t_r^2)}}{\sqrt{Z_{2r}Z_{2r+1}}(n+S_r t_r)} \qquad r=1\rightarrow\frac{n}{2} \tag{6.15}$$

and

$$C_r F_2 \tan(aF_2) - Y_r = \frac{1}{Z_{2r}} \left\{ \frac{(S_r - nt_r)}{(n+S_r t_r)} + \frac{(S_{r-1} - nt_{r-1})}{(n+S_{r-1} t_{r-1})} \right\} \qquad r=1\rightarrow\frac{n}{2} \tag{6.16}$$

To match into the terminating resistances at F_1 and F_2, the internal image impedance of section r=1 must be respectively

$$Z_{11} = \frac{\tan(a\omega_o)}{\tan(aF_1)} \tag{6.17a}$$

and

$$Z_{21} = \frac{\tan(a\omega_o)}{\tan(aF_1)}$$

Since the network is symmetrical, then

$$Z_{1n} = Z_{11} \tag{6.18a}$$

$$Z_{2n} = Z_{21} \tag{6.18b}$$

and the impedance variation level can be approximately expressed by

$$Z_{1\ r+1} = (Z_{1r})^{\frac{1}{4}} \qquad r=1\rightarrow\frac{n}{2} \tag{6.19a}$$

$$Z_{2\ r+1} = (Z_{2r})^{\frac{1}{4}} \qquad r=1\rightarrow\frac{n}{2} \tag{6.19b}$$

On the other hand, since $Y_{r,r+1}$ is the characteristic admittance of a frequency independent inverter, then from equations (6.13) and (6.15), it results in

$$R_{o\ r+1} = \frac{1}{R_{or}} \left\{ \frac{n+S_r t_r}{n-S_r t_r} \right\}^2 \tag{6.20}$$

where

$$R_{or} = \frac{Z_{1r}}{Z_{2r}} = \frac{\tan(aF_2)}{\tan(aF_1)} \tag{6.21}$$

and consequently

$$R_{or+1} = (R_{or})^{\frac{1}{2}} \qquad r=1\rightarrow\frac{n}{2} \tag{6.22}$$

Rearranging equation (6.20), t_r can be expressed by

$$t_r = \frac{n}{S_r}\left\{\frac{\sqrt{R_{or}R_{or+1}}-1}{\sqrt{R_{or}R_{or+1}}+1}\right\} \qquad r=1\rightarrow\frac{n}{2} \tag{6.23}$$

Having obtained all of the values in the right hand side of equations (6.14) and (6.16), then they can be solved to gives the values of C_r and Y_r as

$$C_r = \frac{A_{or}/Z_{1r} + B_{or}/Z_{2r}}{F_2\tan(a\,F_2)-F_1\tan(a\,F_1)} \qquad r=1\rightarrow\frac{n}{2} \tag{6.24}$$

and

$$Y_r = C_rF_1\tan(aF_1) + A_{or}/Z_{1r} \qquad r=1\rightarrow\frac{n}{2} \tag{6.25}$$

where

$$A_{or} = \left\{\frac{S_r+nt_r}{n-S_rt_r} + \frac{S_{r-1}+nt_{r-1}}{n-S_{r-1}t_{r-1}}\right\} \tag{6.26}$$

and

$$B_{or} = \left\{\frac{S_r-nt_r}{n+S_rt_r} + \frac{S_{r-1}-nt_{r-1}}{n+S_{r-1}t_{r-1}}\right\} \tag{6.27}$$

6.3 THE MULTIPLEXER DESIGN PROCEDURE.

As mentioned earlier, this design procedure is for multi-octave combline filter multiplexers having any number (L) of Chebyshev channel filters, with arbitrary number of resonators, bandwidths and interchannel spacings. The design procedure is developed for bandpass combline filters connected in series at a common junction. It commences from the lumped/distributed element values of a doubly terminated prototype. These element values are obtained from the formulas given in the last section for the given values of: number of resonators $n_i (i=1\rightarrow L)$, passband edges frequencies ω_{1i} and ω_{2i}, passband minimum return loss, and the quarter wavelength frequency f_o.

The design principles used here are similar to those used in chapter 3. But only the elements in the nearest half to the common junction at each channel filter are modified here, taking into account the frequency variation across each channel and the interaction due to other channels.

A perfect transmission is preserved with the correct overall phase in the auxiliary variable η at the two points of perfect transmission (F_{1i} and F_{2i}) closest to the passband edges of each channel. However, when channel j (j=1,2,3....L) is modified the remaining channels i (i=1,2,3,... $\neq$j,...L) are replaced by their input impednaces calculated at F_{1j} and F_{2j} to create frequency dependent complex loads at one end which are connected in series with the generator resistance having values of

$$Z_{3j} = \tan(a\omega_{oj})/\tan(aF_{1j}) \tag{6.28a}$$

and

$$Z_{4j} = \tan(a\omega_{oj})/\tan(aF_{2j}) \tag{6.28b}$$

at F_{1j} and F_{2j} respectively. The equivalent circuit of the multiplexer is shown in Fig. 6.4, where

$$R_{1t}(F_{1j}) = \sum_{i\neq j}^{L} R_{1i}(F_{1j}) \tan(a\omega_{oi})/\tan(a\omega_{oj}) \tag{6.29a}$$

$$X_{1t}(F_{1j}) = \sum_{i\neq j}^{L} X_{1i}(F_{1j}) \tan(a\omega_{oi})/\tan(a\omega_{oj}) \tag{6.29b}$$

$$R_{2t}(F_{2j}) = \sum_{i\neq j}^{L} R_{2i}(F_{2j}) \tan(a\omega_{oi})/\tan(a\omega_{oj}) \tag{6.29c}$$

and

$$X_{2t}(F_{2j}) = \sum_{i\neq j}^{L} X_{2i}(F_{2j}) \tan(a\omega_{oi})/\tan(a\omega_{oj}) \tag{6.29d}$$

$R_{1t}(F_{1j})$ and $R_{2t}(F_{2j})$ are the sum of the real parts of the input impedances of the individual channels evaluated at F_{1j} and F_{2j} respectively.

$X_{1t}(F_{1j})$ and $X_{2t}(F_{2j})$ are the sum of the imaginary parts of the input impedances of the individual channels evaluated at F_{1j} and F_{2j}

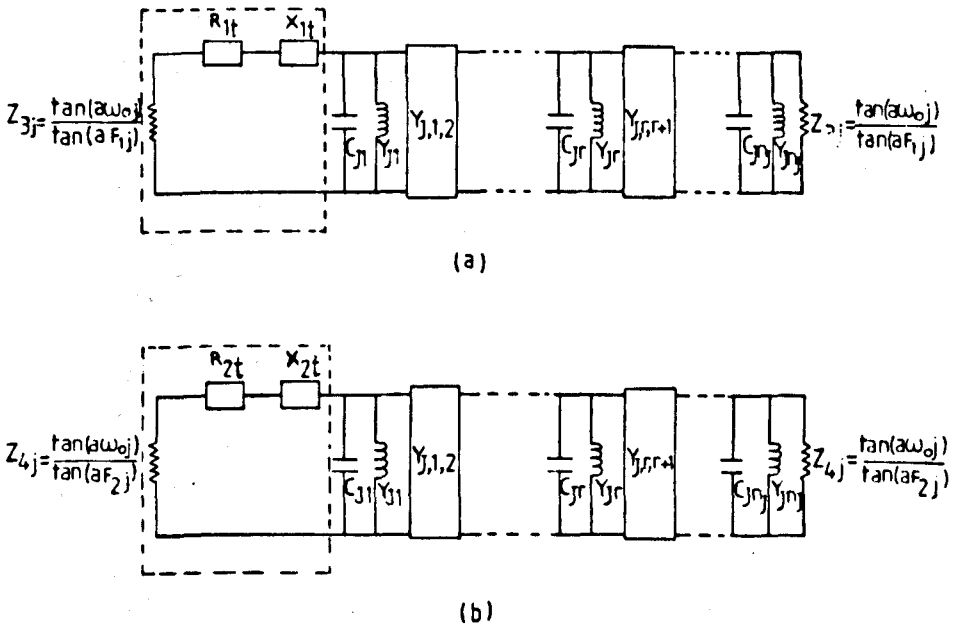

Fig.6.4 Equivalent circuit of the combline channel filter multiplexer (series connected load)

(a) at $\omega = F_{1j}$

(b) at $\omega = F_{2j}$

respectively. The real and imaginary parts of the input impedance of each individual channel may be given by:

$$R_{1i}(F_{1j}) = Z_{5i}(A_{1i}D_{1i}+B_{1i}C_{1i})/(D_{1i}^2+(Z_{5i}C_{1i})^2) \quad (6.30a)$$

$$X_{1i}(F_{ij}) = (B_{1i}D_{1i}-Z_{5i}^2A_{1i}C_{1i})/(D_{1i}^2+(Z_{5i}C_{1i})^2) \quad (6.30b)$$

$$R_{2i}(F_{2j}) = Z_{6i}(A_{2i}D_{2i}+B_{2i}C_{2i})/(D_{2i}^2+(Z_{6i}C_{2i})^2) \quad (6.30c)$$

and

$$X_{2i}(F_{2j}) = (B_{2i}D_{2i}-Z_{6i}^2A_{2i}C_{2i})/(D_{2i}^2+(Z_{6i}C_{2i})^2) \quad (6.30d)$$

where

$$Z_{5i} = \tan(a\omega_{oi})/\tan(a F_{1j}) \quad (6.31a)$$

$$Z_{6i} = \tan(a\omega_{oi})/\tan(a F_{2j}) \quad (6.31b)$$

ω_{oi} is the passband centre frequency of channel i

A_{1i}, B_{1i}, C_{1i} and D_{1i} are the entries of the overall transfer matrix of channel i calculate at F_{1j}.

A_{2i}, B_{2i}, C_{2i} and D_{2i} are the same entries calculated at F_{2j}.

For convenience, the series connected load from the common junction side to channel j is replaced by its shunt equivalent circuit as shown in Fig. 6.5 where $G_{1t}(F_{1j})$ and $G_{2t}(F_{2j})$ are the real parts, $B_{1t}(F_{1j})$ and $B_{2t}(F_{2j})$ are the imaginary parts. Hence, they are given by:

$$G_{1t}(F_{1j})=(Z_{3j}+R_{1t}(F_{1j}))/((Z_{3j}+R_{1t}(F_{1j}))^2+X_{1t}^2(F_{1j})) \quad (6.32a)$$

$$B_{1t}(F_{1j})=-X_{1t}(F_{1j})/((Z_{3j}+R_{1t}(F_{ij}))^2+X_{1t}^2(F_{ij})) \quad (6.32b)$$

and

$$G_{2t}(F_{2j})=(Z_{4j}+R_{2t}(F_{2j}))/((Z_{4j}+R_{2t}(F_{2j}))^2+X_{2t}^2(F_{2j})) \quad (6.32c)$$

$$B_{2t}(F_{2j}) = -X_{2t}(F_{2j})/((Z_{4j}+R_{2t}(F_{2j}))^2+X_{2t}^2(F_{2j})) \quad (6.32d)$$

Now consider the overall transfer matrices given in equations (6.11) and (6.12) respresenting channel j with all the remaining channels $i \neq j$ are replaced by the shunt connected load. Since the basic section of

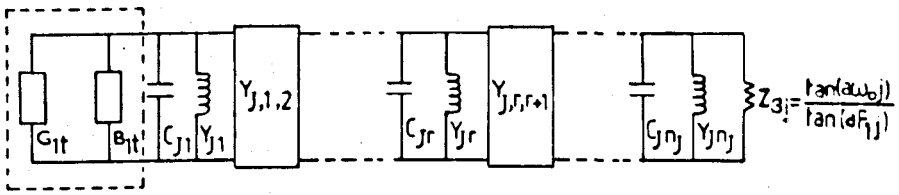

(a)

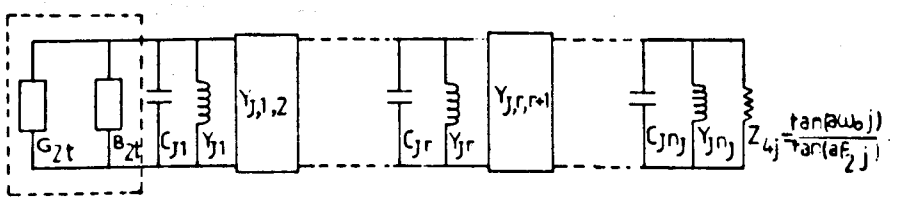

(b)

Fig. 6.5 Equivalent circuit of the combline channel filter multiplexer (parallel connected load)

(a) at $\omega = F_{1J}$

(b) at $\omega = F_{2J}$

these matrices can be decomposed into a transfer matrix of a shunt resonator and an admittance inverter, hence the overall admittance of the rth shunt resonator obtained from matrix equation (6.11) can be described by

$$C_{j,r}\,F_{ij}\tan(aF_{ij})-Y_{j,r}=\frac{-1}{Z_{1j,r}}\left\{\frac{(S_{j,r}+\eta_j\,t_{j,r})}{\eta_j-S_{j,r}t_{j,r}}+\frac{(S_{j,r-1}+\eta_j t_{j,r-1})}{\eta_j-S_{j,r-1}t_{j,r-1}}\right\} \tag{6.33}$$

and the characteristic admittance of the inverter is given by

$$Y_{j,r,r+1}=\frac{\sqrt{(\eta_j^2+S_{j,r})(1+t_{j,r}^2)}}{\sqrt{Z_{1j,r}Z_{1j,r+1}}(\eta_j-S_{j,r}\,t_{j,r})}\quad (r=1\,\frac{n_j}{2}) \tag{6.34}$$

Similarly from matrix equation (6.12)

$$C_{j,r}F_{2j}\tan(aF_{2j})-Y_{j,r}=\frac{1}{Z_{2j,r}}\left\{\frac{(S_{j,r}-\eta_j t_{j,r})}{(\eta_j+S_{j,r}t_{j,r})}+\frac{(S_{j,r-1}-\eta_j t_{j,r-1})}{(\eta_j+S_{j,r-1}t_{j,r-1})}\right\} \tag{6.35}$$

and

$$Y_{j,r,r+1}=\frac{\sqrt{(\eta_j^2+S_{j,r}^2)(1+t_{j,r}^2)}}{\sqrt{Z_{2j,r}Z_{2j,r+1}}(\eta_j+S_{j,r}t_{j,r})}\qquad r=1\rightarrow\frac{n_j}{2} \tag{6.36}$$

Once again, since $Y_{j,r,r+1}$ is frequency independent then from equations (6.34) and (6.36) the expression for $t_{j,r}$ can be written as

$$t_{j,r}=(\eta_j/S_{j,r})\left\{\frac{\sqrt{R_{oj}R_{oj,r+1}}-1}{\sqrt{R_{oj}R_{oj,r+1}}+1}\right\}\qquad r=1\rightarrow\frac{n_j}{2} \tag{6.37}$$

where $t_{j,o}=0$

$$R_{oj,r}=\frac{Z_{1j,r}}{Z_{2j,r}} \tag{6.38}$$

it has been found that the impedance level variation still follows the expression given in (6.19a and b). Furthermore, for all-pass behaviour in the auxiliary parameter for each channels at its critical frequencies F_{ij} and F_{2j}, the following relationships must be applied

$$Z_{1j,1}=1/G_{lt}(F_{1j}) \tag{6.39a}$$

$$Z_{2j,1} = 1/G_{2t}(G_{2j}) \tag{6.39b}$$

and

$$R_{oj,1} = G_{2t}(F_{2j})/G_{1t}(F_{1j}) \tag{6.39c}$$

However, the modified values of the elements associated with the first resonator of channel j can be obtained by solving the following two equations for $C_{j,1}$ and $Y_{j,1}$

$$B_{1t}(F_{1j}) + C_{j,1}F_{1j}\tan(a\ F_{1j}) - Y_{j,1} = -A_{oj,1} \tag{6.40}$$

$$B_{2t}(F_{2j}) + C_{j,1}F_{2j}\tan(a\ F_{2j}) - Y_{j,1} = B_{oj,1} \tag{6.41}$$

resulting in

$$C_{j,1} = \{A_{oj,1}+B_{oj,1}+B_{1t}(F_{ij})-B_{2t}(F_{2j})\}/(F_{2j}\tan(a\ F_{2j})-F_{1j}\tan(aF_{1j})) \tag{6.42}$$

and

$$Y_{j,1} = C_{j,1}F_{1j}\tan(a\ F_{1j})+A_{oj,1}+B_{1t}(F_{1j}) \tag{6.43}$$

where

$$A_{oj,1} = G_{1t}(F_{1j})(S_{j,1}+\eta_j\ t_{j,1})/(\eta_j-S_{j,1}\ t_{j,1}) \tag{6.44}$$

and

$$B_{oj,1} = G_{2t}(F_{2j})(S_{j,1}-\eta_j t_{j,1})/(\eta_j+S_{j,1}t_{j,1}) \tag{6.45}$$

The modified values of the elements associated with the remaining resonators in the nearest half to the common junction of channel j can be obtained by solving equations (6.33) and (6.35) for $C_{j,r}$ and $Y_{j,r}$ $(r=1\rightarrow n_j/2)$ to give

$$C_{j,r} = \left\{ \frac{A_{oj,r}}{Z_{1j,r}} + \frac{B_{oj,r}}{Z_{2j,r}} \right\} /(F_{2j}\tan(a\ F_{2j}) - F_{1j}\tan(a\ F_{1j})) \tag{6.46}$$

and

$$Y_{j,r} = C_{j,r}\ F_{2j}\tan\ (a\ F_{2j}) - B_{oj,r}/Z_{2j,r} \tag{6.47}$$

where

$$A_{oj,r} = \frac{S_{j,r}+n_j t_{j,r}}{n_j-S_{j,r}t_{j,r}} + \frac{S_{j,r-1}+n_j t_{j,r-1}}{n_j - S_{j,r}t_{j,r-1}} \tag{6.48}$$

and

$$B_{oj,r} = \frac{S_{j,r}-n_j t_{j,r}}{n_j + S_{j,r} t_{j,r}} + \frac{S_{j,r-1}-n_j t_{j,r-1}}{n_j + S_{j,r-1} t_{j,r-1}} \qquad (6.49)$$

The modified characteristic admittance $Y_{j,r,r+1}$ of the inverter can be obtained by using either equation (6.34) or (6.36).

The values of the elements associated with the other half of each channel are remained without change as in isolation.

A computer program has been written to perform the modification process. This process is then repeated channel by channel until all the element values converge, to certain values and no further change is possible.

6.4 PROTOTYPE EXAMPLES AND COMPUTER ANALYSIS.

The validity of this design procedure for multi-octave combline filter multiplexers is demonstrated by the computer analysis of several design examples for a wide variety of specifications samples of those example are given here.

i) a 5-channel multiplexer has been designed with each of its channels having 8 resonators, bandwidth of 1 GHZ, minimum return loss of 20dB. The combline channel filters are consisting of lumped capacitors and short circuited stubs. Each of these stubs is a quarter wavelength long at 15GHZ. The individual channel specifications and the modifed element values are given in table 6.1. The return loss and insertion loss characteristics are plotted in Fig. 6.6 and 6.7 respectively.

ii) A triplexer has been designed with each of the 3-channels, having 6 resonators, bandwith of 2GHZ, minimum inband return loss of 26dB. The short circuited stubs are quarter wavelength long at f_0 = 20 GHZ. The individual channel specifications and the modified element values are

	r	1	2	3	4	5	6	7	8
channel 1 $n_1=8, \omega_{11}=1, \omega_{12}=2$	C_{1r}	6.15292	16.9766	26.6197	31.8151	31.9064	26.9409	18.0062	5.72712
	Y_{1r}	1.32438	4.67732	7.10123	8.44703	8.4796	7.21645	5.08485	1.59616
	$Y_{1,r,r+1}$	1.19927	2.00606	2.57862	2.78418	2.59703	2.06586	1.38083	0
channel 2 $n_2=8, \omega_{21}=2.5, \omega_{22}=3.5$	C_{2r}	3.53269	8.38213	12.7745	15.1522	15.1747	12.8509	8.58717	2.9376
	Y_{2r}	3.53633	8.58893	12.8967	15.264	15.2871	12.9752	8.80508	3.0048
	$Y_{2,r,r+1}$	1.32225	2.05792	2.59524	2.78866	2.60489	2.08877	1.40436	0
channel 3 $n_3=8, \omega_{31}=4, \omega_{32}=5$	C_{3r}	2.11281	5.10663	7.77753	9.22878	9.24611	7.8345	5.23597	1.81499
	Y_{3r}	5.0425	12.1066	18.1972	21.5514	21.5867	18.3121	12.336	4.26759
	$Y_{3,r,r+1}$	1.32091	2.05472	2.5941	2.78834	2.60634	2.09304	1.40914	0
channel 4 $n_4=8, \omega_{41}=5.5, \omega_{42}=6.5$	C_{4r}	1.28897	3.3158	5.06887	6.02742	6.04392	5.12214	3.42365	1.1919
	Y_{4r}	5.91935	14.8966	22.4531	26.6443	26.7067	22.6514	15.2233	5.2925
	$Y_{4,r,r+1}$	1.2957	2.03933	2.58896	2.78695	2.60682	2.09447	1.41092	0
channel 5 $n_4=8, \omega_{51}=7, \omega_{52}=8$	C_{5r}	0.400102	1.9617	3.23439	3.92308	3.96027	3.35653	2.24382	0.782341
	Y_{5r}	3.56139	15.1568	24.6297	29.811	30.0801	25.5114	17.1332	5.96677
	$Y_{5,r,r+1}$	1.00144	1.90812	2.54606	2.77532	2.607	2.09502	1.41188	0

TABLE 6.1: Element Values of 5-channel combline filter multiplexer. ω_{i1} and ω_{i2} are in GHZ, $\frac{C_{ir}}{2\pi} \times 10^{-9}$ Farads Y_{ir} and $Y_{i,r,r+1}$ are in seimens·minimum return loss = 20dB for all channels.

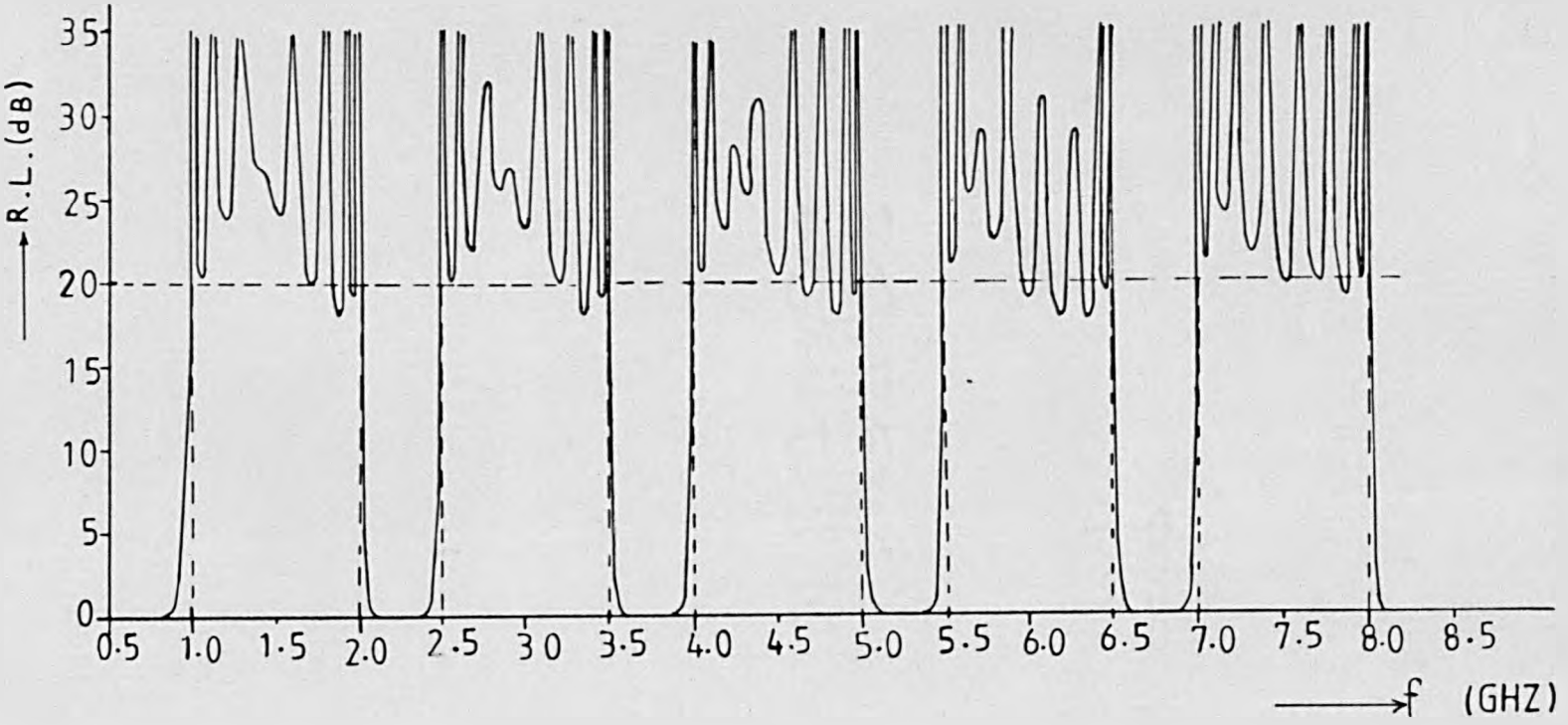

Fig. 6.6 Return loss response of 5_channel combline filter multiplexer

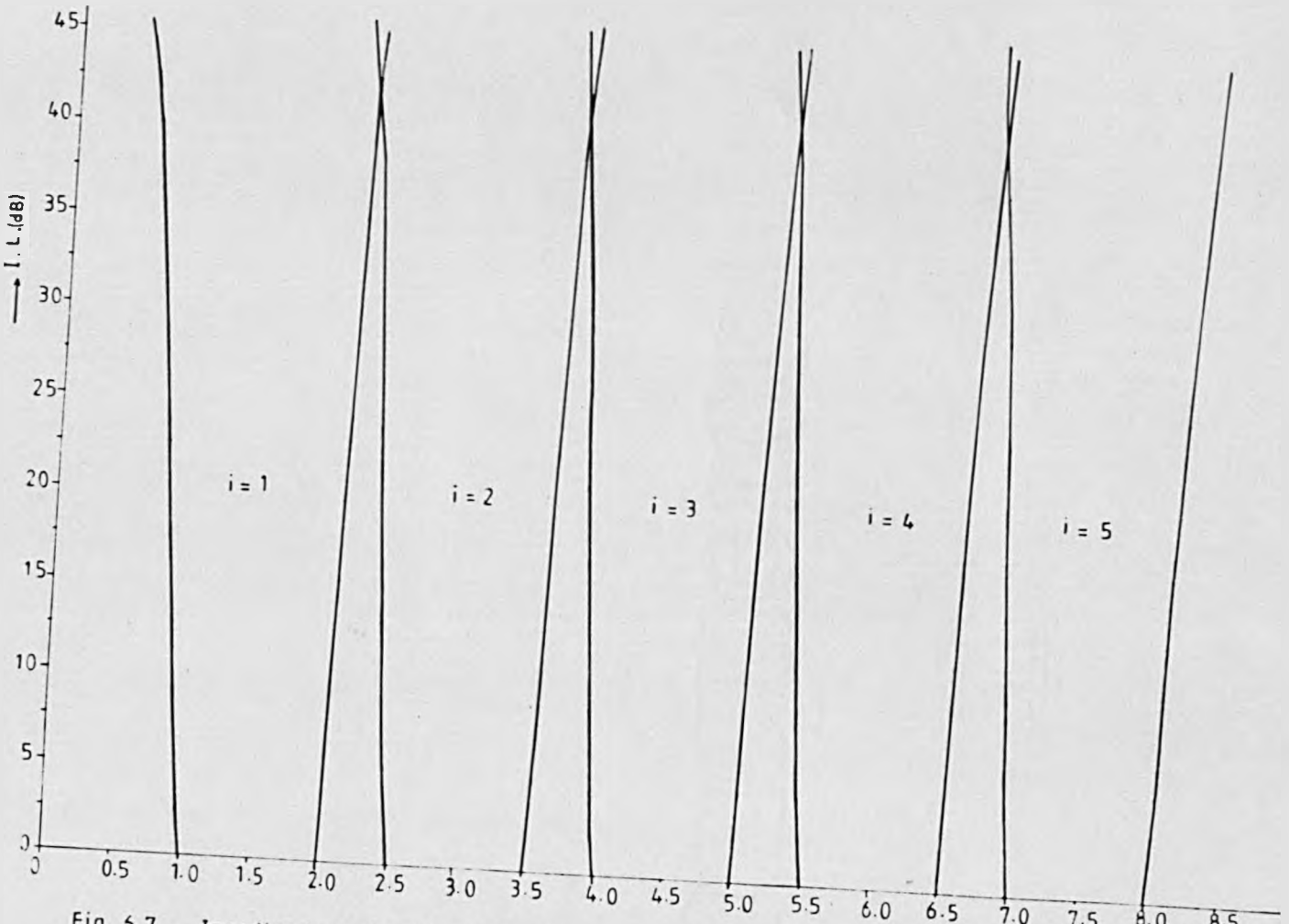

Fig. 6.7 Insertion loss characteristic of 5-channel combline filter multiplexer

given in Table 6.2. The return loss and the insertion loss characteristics are plotted in Fig. 6.8 and 6.9 respectively.

	r	1	2	3	4	5	6
Channel 1 $n_1=6$, $\omega_{11}=2$ $\omega_{12}=4$	C_{1r}	1.638657	4.09635	5.89134	5.97556	4.40932	1.4245
	Y_{1r}	1.03293	3.49723	4.80309	4.90869	3.93744	1.31704
	$Y_{1r,r+1}$	1.0506	1.57961	1.80382	1.63519	1.25028	0
Channel 2 $n_2=6$, $\omega_{21}=5$ $\omega_{22}=7$	C_{2r}	0.886556	1.89948	2.63698	2.65737	1.95072	0.688487
	Y_{2r}	2.92143	6.29414	8.44107	8.49499	6.41074	2.2872
	$Y_{2r,r+1}$	1.17441	1.62015	1.81514	1.65202	1.25809	0
Channel 3 $n_3=6$, $\omega_{31}=8$ $\omega_{32}=10$	C_{3r}	0.197274	0.934837	1.36585	1.40874	1.03374	0.370092
	Y_{3r}	2.13856	7.75791	10.8825	11.1736	8.34211	3.00667
	$Y_{3r,r+1}$	0.966651	1.52993	1.78877	1.65498	1.26054	0

TABLE 6.2 Element Values of the Combline Filter Triplexer ω_{i1} and ω_{i2} are in GHZ, $\frac{C_{ir}}{2\pi} \times 10^{-9}$ in Farads, Y_{ir} and $Y_{ir,r+1}$ in seimens. Minimum return loss = 26dB.

6.5 DESIGN AND PERFORMANCE OF COMBLINE FILTER-DIPLEXER

The combline filter diplexer has been designed with each channel haing 6-resonators, bandwidth of 0.5 GHZ, in band minimum return loss equal 20dB and the short circuited stubs are quarter wavelength long at 18 GHZ. The diplexer operates in 50Ω system. The bandedges frequencies and the element values are given in table 6.3. The computer analysis of this diplexer showing the insertion loss and the return loss characteristics is plotted in Fig. 6.10.

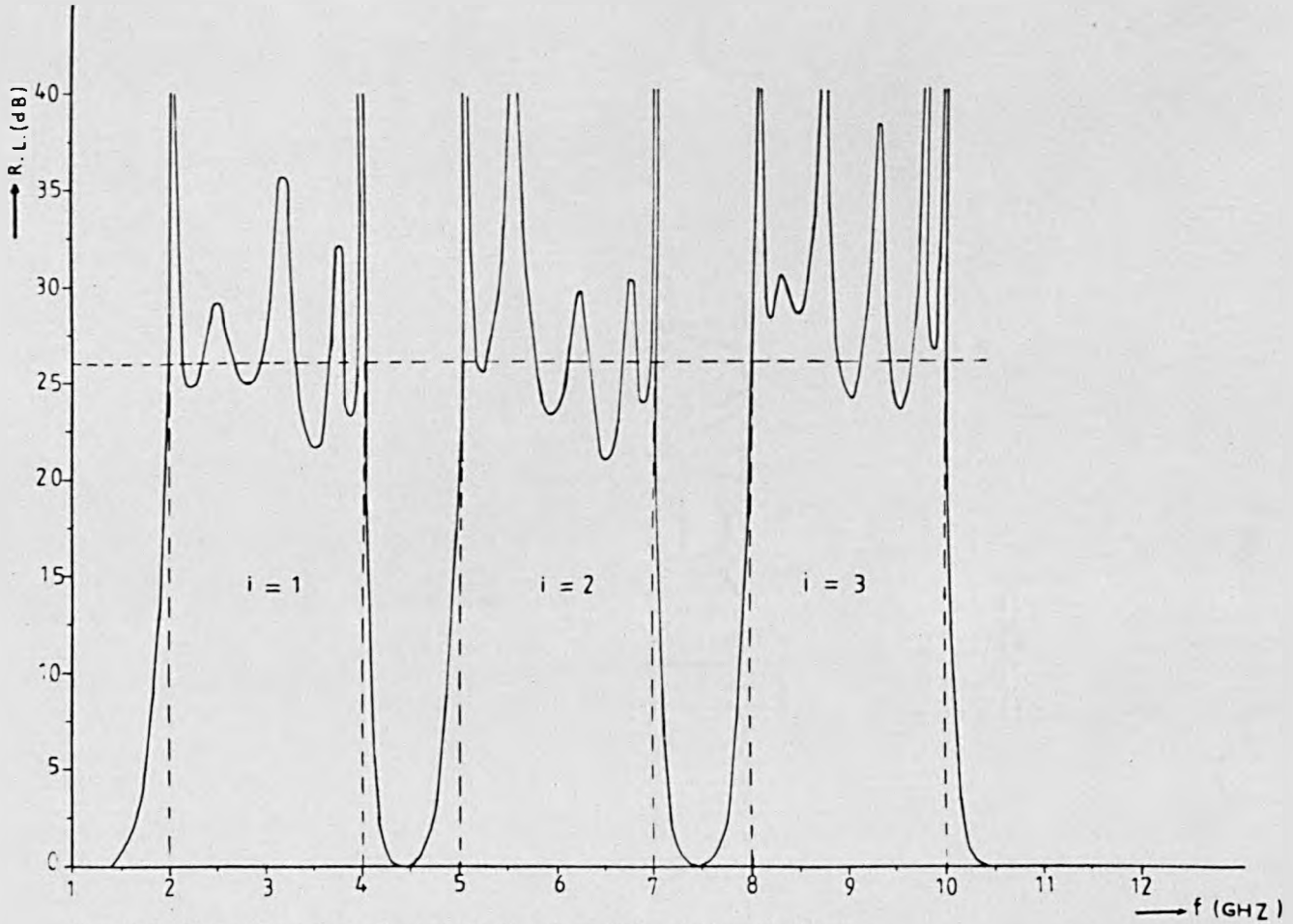

Fig. 6.8 The return loss characteristic of combline filter triplexer

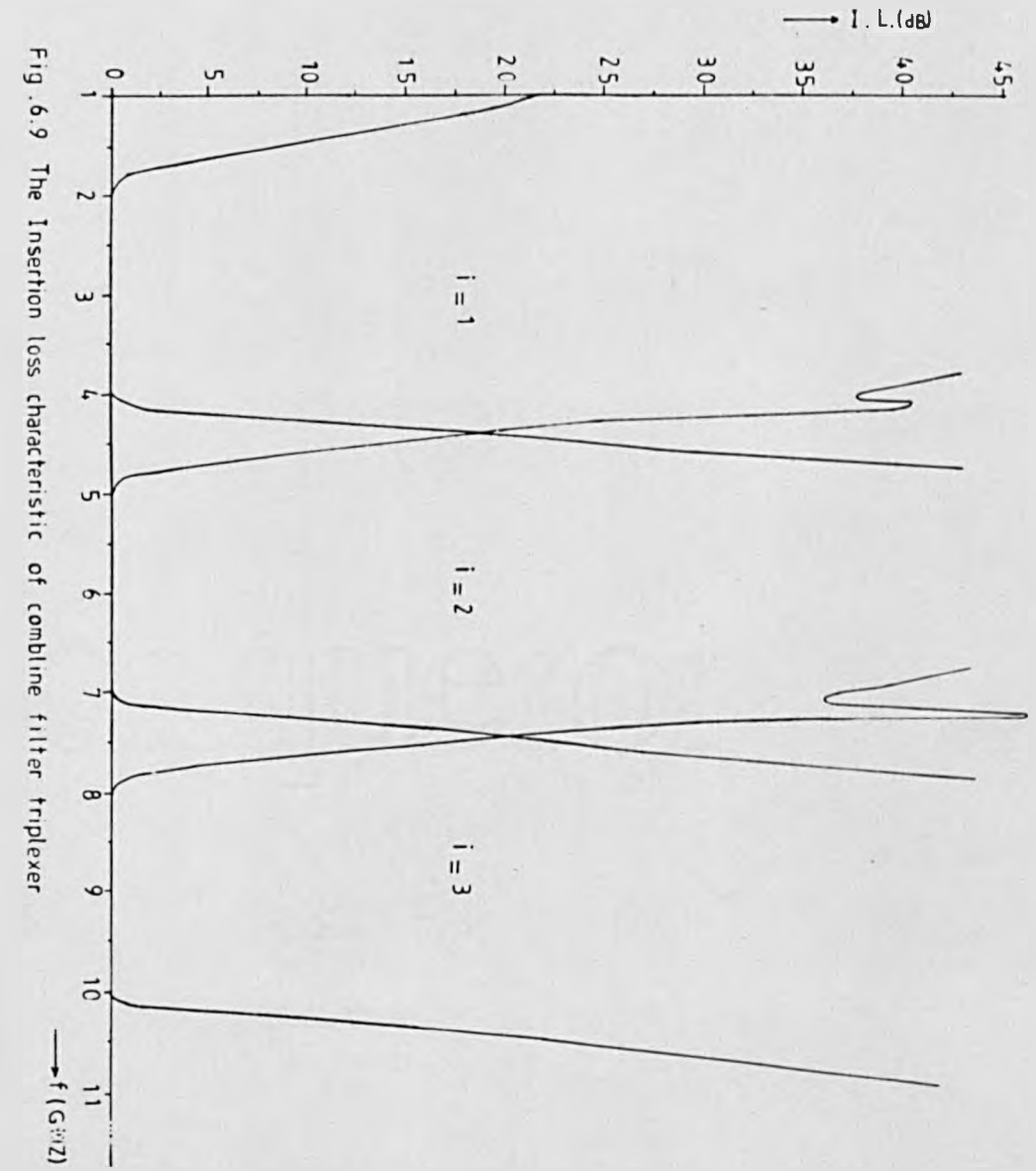

Fig .6.9 The Insertion loss characteristic of combline filter triplexer

	r	1	2	3	4	5	6
channel 1 $\eta_1=6$, $\omega_{11}=5$, $\omega_{12}=5.5$	C_{1r}	3.58442	9.78544	13.8054	13.9554	10.2167	3.73072
	Y_{1r}	8.95655	25.3634	35.8444	36.2587	26.5866	9.70533
	$Y_{1r,r+1}$	1.24406	1.88815	2.15027	1.93985	1.38577	0
channel 2 $\eta_2=6$, $\omega_{21}=5.7$, $\omega_{22}=6.2$	C_{2r}	2.82269	8.24469	11.6271	11.7664	8.61422	3.14686
	Y_{2r}	10.0143	28.2639	39.686	40.1356	29.4217	10.7453
	$Y_{2r,r+1}$	1.23932	1.88261	2.14853	1.93997	1.38592	0

TABLE 6.3. Element Values of Combline Filter Diplexer Minimum Return Loss = 20 dB in both channels. These Element Values are for 1Ω terminating loads. $\frac{C_{ir}}{2\pi} \times 10^{-9}$ Farads Y_{ir} and $Y_{ir,r+1}$ are in seimens.

This diplexer was constructed in coaxial form of realization with all of the resonators in both channels having equal diameter circular cylindrical rods. The design technique presented in section 5.7 has been used in obtaining the physical dimensions of the diplexer structure shown schematically in Fig. 6.11 its dimensions are obtained for the suitably chosen d/b = 0.4 and b = 0.3" and given in Table 6.4 when each rod has a diameter d = 0.12" and since the length ℓr should be λ/4 at 18 GHZ, thus ℓr = 0.146".

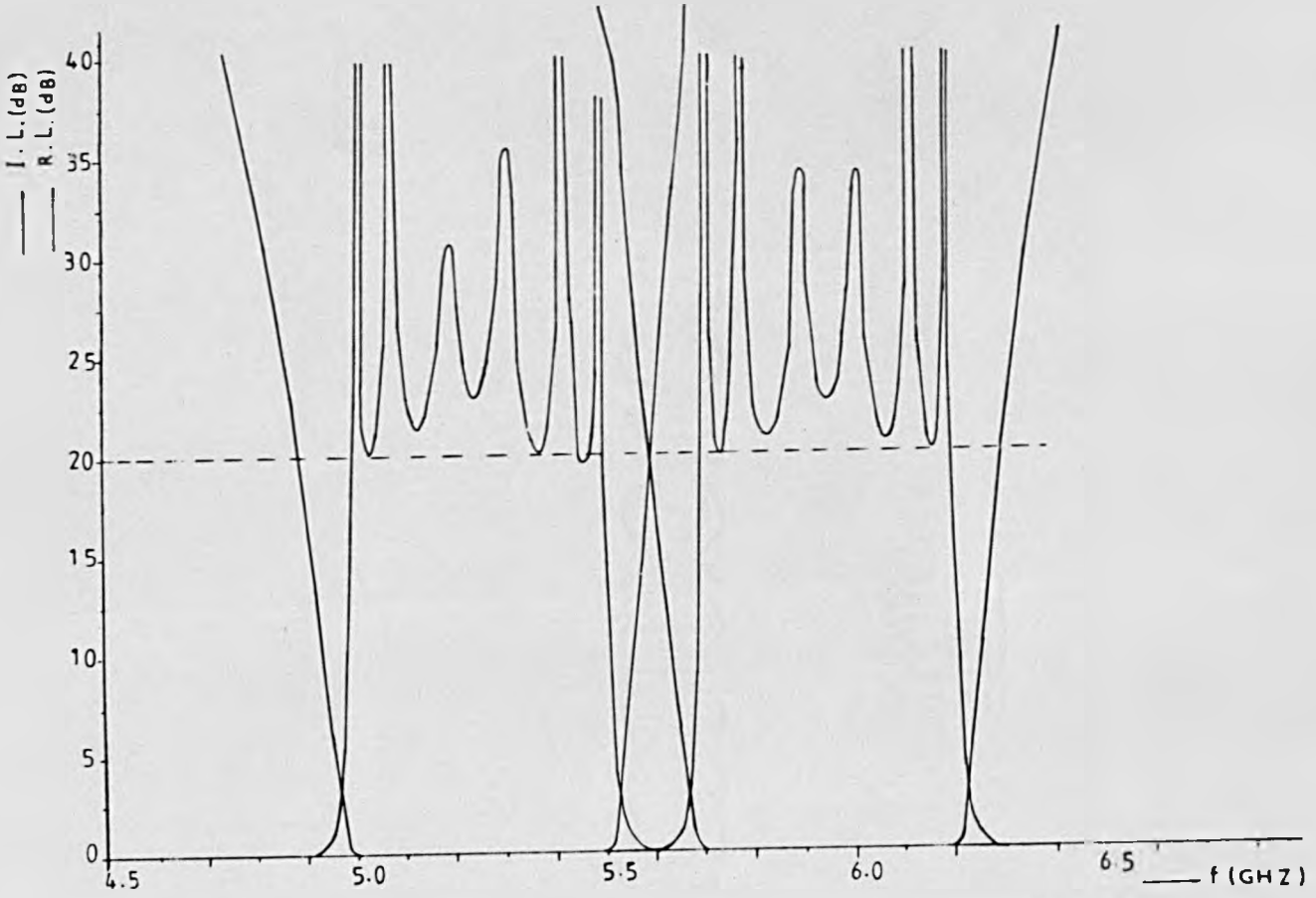

Fig. 6.10 Insertion loss and return loss characteristics of the combline filter diplexer

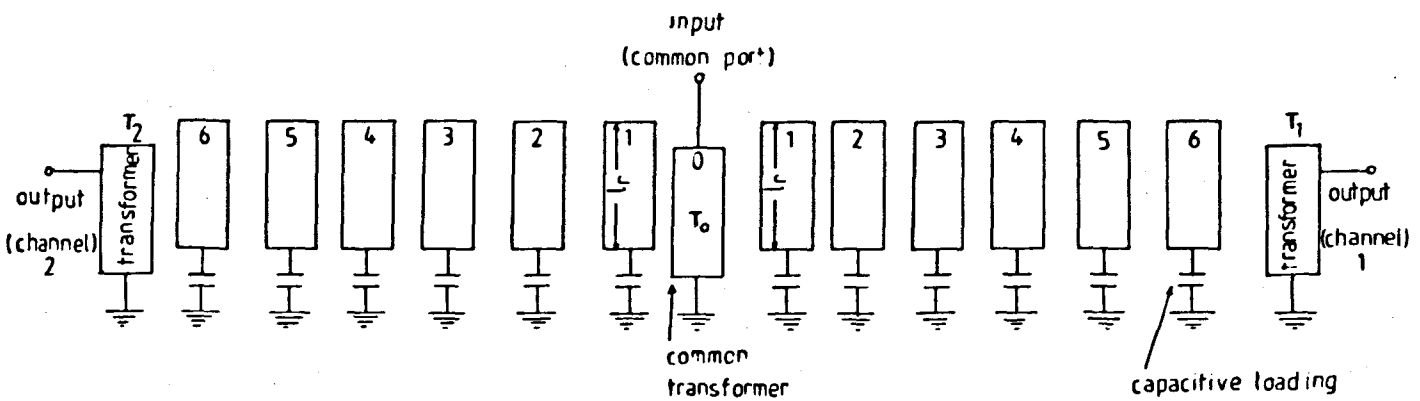

Fig. 6.11 Symbollic representation of the combline filter diplexer

channel 1	channel 2
S_{01} = 0.044"	S_{01} = 0.046"
S_{12} = 0.165"	S_{12} = 0.174"
S_{23} = 0.194"	S_{23} = 0.204"
S_{34} = 0.2"	S_{34} = 0.207"
S_{45} = 0.194"	S_{45} = 0.204"
S_{56} = 0.159"	S_{56} = 0.171"
S_{6T_1} = 0.047"	S_{6T_2} = 0.048"
S_{T_1W} = 0.045"	S_{T_2W} = 0.042"

TABLE 6.4 Distances between the rods.

The lumped capacitors have been realized by using screws. These screws form parallel plates capacitances with the end of the rods. However the distance D between the open end of the rods and the side wall of the metallic box is determined by

$$D = \frac{\varepsilon_0 A}{C} \tag{6.50}$$

where ε_0 is the free space permitivity = 8.842×10^{-2} Farad/meter

A is the cross sectional area of the rod = $\pi d^2/4$

C is the smallest value of the capacitances given in table 6.3 scales to 50Ω termination and modified according to the successive scaling operation of the admittances to obtain equal diameter rods structure. In this design example, the smallest value of C in table 6.3 is $C_{21}=2.82269 \times 10^{-9}/2\pi$ which finally became equal to 2.695×10^{-13} Farad. Thus D = 0.009".

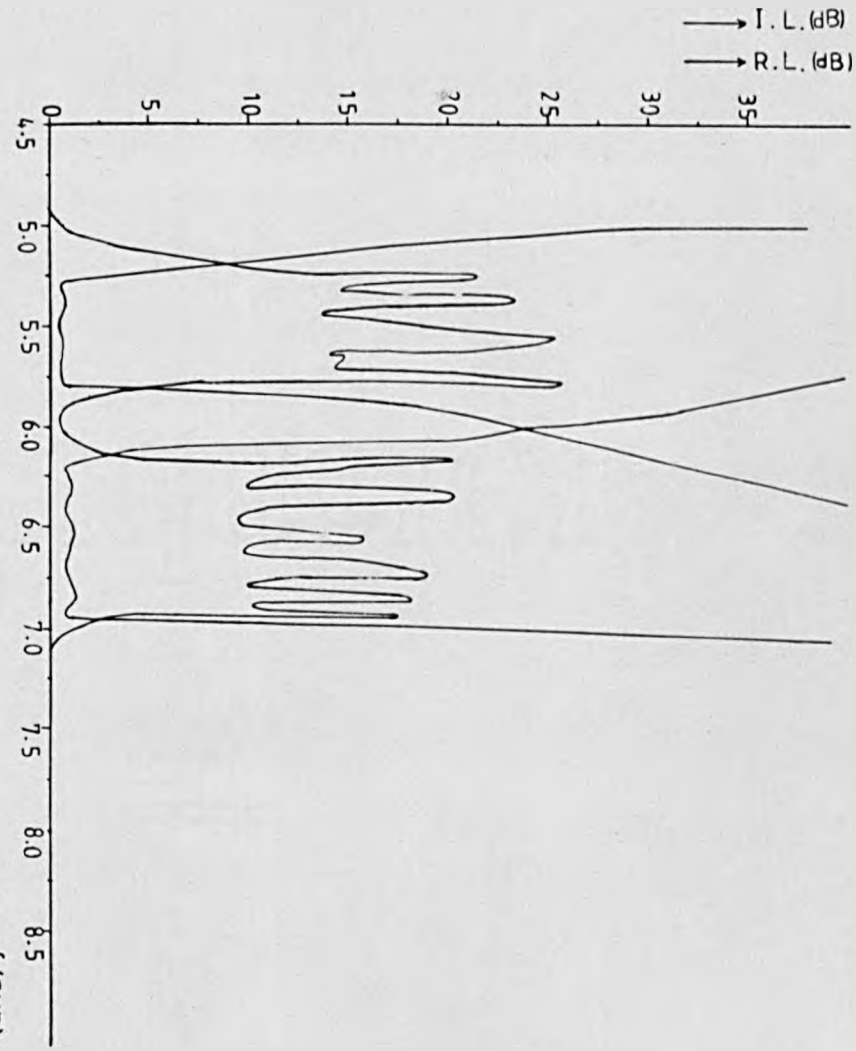

Fig. 6.12 Experimental insertion loss and return loss characteristic of the combline filter diplexer

The diplexer has been built and then tuned using a swept-frequency reflectometer arrangement connected to the common port. The other ports were terminated with 50Ω loads. The experimental insertion loss and common port return loss characteristics have been established and shown in Fig. 6.12.

6.6 CONCLUSIONS

A new general design procedure has been presented for multi-octave combline filter multiplexers. This procedure is based on the same principles of that introduced in chapter 3 and has all the merits, advantages and the approximations pointed there. In fact this procedure may be considered as an extension of the procedure introduced in chapter 3 to broadband applications. The individual combline channel filters are designed on the doubly terminated bases using the recently introduced formulas [34]. Although these formulas are approximate, they nevertheless give excellent results upto an octave bandwidth. Furthermore, they are quite compact and can easily be programmed on a computer.

The individual channels are connected in series at a common junction without the addition of immittance compensation networks or dummy channels. However, the channels may be coupled by means of a common transformer. Common transformer diplexers have been used in practice for some time, but the theory behind the use of common transformer coupling and the extension to multi-channels has not been verified until recently when Rhodes and Levy devoted a full section in [33] to the discussion of this topic.

The multiplexer design procedure presented in this chapter has been programmed on a computer. An optimization process has been used to modify the elements of each channel in turn and it has been found that the

process normally converges if the insertion loss of the neighbouring channels cross over at greater than 3dB. The very good results of this theory are demonstrated and confirmed by both the computer analysis of several multiplexers and by a practical diplexer.

CHAPTER 7

GENERAL CONCLUSIONS

The main object of this chapter is to present a brief review of the original material in this thesis and to outline the possible extension and further related work which may be carried out in future.

Considering first the material presented in Chapter 1, the fundamental principles, properties and realizability conditions of lumped passive linear networks have been briefly discussed. Special attention was given to the lossless two port networks. Further details were avoided since the main reason behind including that chapter was to serve as an introduction to the rest of the thesis and to establish the general picture and terminology used afterwards.

In Chapter 2, the approximation problem satisfying the amplitude constraints has been discussed. The three most popular rational function approximation schemes (the maximally flat, Chebyshev and elliptic function responses) have been presented. Special attention was given to the Chebyshev response in its conventional and generalized forms. This is mainly because the maximally flat and the elliptic function characteristics were not used in this thesis. The concepts of doubly terminated and singly terminated prototype ladder structures have been discussed and several low-pass prototype networks were considered. Explicit design formulas were given for the element values of prototype low-pass filters consisting of series inductors and shunt capacitors and for the modified versions consisting of either series inductors separated by impedance inverters or shunt capacitors separated by admittance inverters. These modified versions are particularly suitable for designing microwave band-pass filters e.g. direct coupled cavity waveguide filters. The prototypes considered were of a class often called "all-pole"

which have all their transmission zeros at infinity.

The most important part of Chapter 2 may have been devoted for new classes of very selective low-pass prototypes satisfying a generalized Chebyshev response with some of their transmission zeros at infinity and the remainder at the same finite point on the imaginary axis. A new computerized procedure was presented. A relatively new solution to the synthesis accuracy problem has been adopted and termed "the alternating pole synthesis technique". The superiority of this technique over the z-transformed variable technique was discussed. Special properties and practical advantages of these prototypes were also discussed. Tables of element values for typical requirements were provided. These filters are very selective classes of prototype netowrks having important applications in the design of TEM mode microwave broadband filters, diplexers and multiplexers particularly for printed circuit forms of realization.

A design example of a microwave broadband lowpass filter based on one of these prototypes having 3 transmission zeros at infinity and the remainder at a finite point on the imaginary axis was given in chapter 5. This microwave filter has been realized and constructed in a novel suspended substrate stripline form. The primary experimental results show a very good response especially in the stopband where an octave stopband can be easily achieved. This property as well as the better selectively make this prototype an equally attractive if not better than that having a single transmission zero at infinity and the remainder at a finite point on the imaginary axis, which has been extensively used in the design of microwave broadband diplexers and multiplexers e.g. [66].

However the synthesis procedures and the results given in chapter 2 for the generalized Chebyshev filters were for odd degree networks having an odd number of transmission zeros at infinity and the remainder at a finite point on the imaginary axis. Since two classes of these prototype filters having either a single transmission zero or three transmission zeros at infinity have been presented, it may seem obvious that if a third class having five transmission zeros at infinity and the remainder at a finite point on the imaginary axis is investigated and synthesized in a suitable format as an extension to the work given in chapter 2. In addition, similar prototype networks of even degrees and having an even number of transmission zeros at infinity may be synthesized using the z-transformed variable technique at least for degree 6, 8 and 10 since it is not possible to synthesize networks of higher degrees using this technique and because the alternating pole synthesis technique can not be applied to non-symmetrical even degree networks.

Chapter 3 presented a new general design procedure for multiplexers having any number of Chebyshev channel filters, with arbitrary degrees, bandwidths and inter-channel spacing. The design procedure was developed for bandpass channel filters connected in series at a common junction for narrowband applications.

Commencing with the closed form expression for element values in Chebyshev filters, the multiplexers design process modifies all of the elements in each channel filter and preserves a match at the two points of perfect transmission closest to the band edges of each channel filter, while taking into account the frequency dependence across each channel. This design procedure for a direct connection of all channels of a common junction results in an excellent design without the

necessity for any immittance compensation networks or dummy channels and represents a strictly canonical solution. It has been shown that this procedure gives very good results for a wide variety of specifications and it is valid for most combinations of contiguous and non-contiguous channels as demonstrated by the computer analysis of several multiplexer examples. It is believed that a further improvement could be made if an exact expression could be derived for the internal impedance level variation through each individual channel instead of the approximate one given in equations 3.28 a,b and c. If a correct all-pass equivalent form could be obtained at a third point of perfect transmission different from those closest to the passband edges of each individual channel, an improvement could be made.

Chapter 4 showed the application of the multiplexer design procedure developed in Chapter 3 by considering a 4-channel multiplexer designed and constructed in the standard rectangular waveguide WG16. The individual channels were realized in the form of direct coupled cavity filters. The design procedures for these filters have been reviewed and their design formulas were developed. Then the multiplexer design process has been explained in details starting from the given specification and finishing with the final physical dimensions. The most recent, equal diameter post-coupled cavity structure was used in constructing the channels. This type of coupling has many practical advantages compared with the iris-coupled cavity such as elimination of the solder fillets and waveguide cuts and to provide simpler structure with a reduced manufacturing cost. The experimental characteristics of this multiplexer was also given in Chapter 4.

Chapter 5 has been devoted for the design of TEM mode networks. The fundamental principles of the distributed circuits have been briefly discussed first. Then an exact synthesis procedure was presented for

broadband prototype combline filters and it has been pointed out that networks of degrees as high as 30 can be easily synthesized with little loss of accuracy if the alternating pole synthesis technique is used. A comparison was given between microwave combline filter realization using all distributed elements and its lumped distributed counterpart. This comparison was based upon the computer analysis of an octave bandwidth microwave combline filter. A design example was given for an octave bandwidth microwave combline filter. This filter has been realized and built in coaxial form using parallel coupled lines having rectangular cross sections. The design process has been explained in some details and the experimental return loss and insertion loss characteristics have been established. Other methods of coaxial form of realization have been discussed including a new design method for realizing TEM network using parallel coupled circular cylindrical rods having the same diameter. Its practical advantages have been indicated. The method has been explained and illustrated by a numerical example.

The microwave integrated circuit form of TEM mode networks realization has been discussed from filter design point of view and a design example was given for a broadband microwave lowpass filter, realized and constructed using a suspended substrate stripline structure. As it was mentioned earlier this microwave filter is based on the generalized Chebyshev low-pass prototype introduced in chapter 2 and having 3-transmission zero at infinity. A novel structure has been used in the realization where each shunt resonator in the prototype has been realized by a uniform admittance shunt open circuit stub. This has an important practical advantage in simplifying the design and making it even more compact and easier to manufacture than other types of selective filters e.g. elliptic function where the uniform admittance shunt O/C stubs realization is not possible.

However, certain forms of physical realization have been utilized in constructing certain TEM-mode microwave filters in Chapter 5. This should not lead to the conclusion that other forms of physical realization are not possible for the same filter as long as they still support TEM mode. For example, the combline filter which has been realized in coaxial form with parallel coupled lines having rectangular cross-sections, can also be realized if required in one suitable form of stripline structure or another. One suitable form may have been worth attempting is similar to that used in Reference [65] in designing interdigital filters. Similar argument can be applied to the generalized Chebyshev prototype which can also be realized in coaxial form as well as the printed circuit one presented in Chapter 5. However, the designer may make his own judgement on which form of realization he needs to choose according to the application and the environmental conditions under which the system will operate.

In Chapter 6 a new general design procedure has been presented for multi-octave combline filter multiplexers having any number of bandpass Chebyshev combline fhannel filters, with arbitrary number of resonators, bandwidths, and interchannel spacings. This procedure is for doubly terminated channel filters connected in series at a common junction. It results in an excellent design without the necessity for any compensating annulling network or dummy channels and represents a strictly cannonical solution. Examples of several multiplexers were given indicating that the design procedure is valid for different combinations of channels and gives very good results for a wide variety of specifications.

However, due to the similarities between the principles of this design procedure and that introduced in Chapter 3, further improvement in the response of the multi-octave combline filter-multiplexer design

procedure could also be made if an exact expression for the internal impedance level variation and a correct all pass equivalent form at a third point of perfect transmission could be obtained for each individual channel.

Although there is no limitation in this theory on the overall multiplexer bandwidth, the multiple passbands or the spurious responses of the microwave combline channel filters tend to limit the overall bandwidth of the multiplexer and this should be taken into account in practical designs.

A design example of a combline filter diplexer has been given in Chapter 6. This diplexer was realized and built in coaxial form with channels having equal diameter circular cylindrical parallel rods. The physical dimensions of this diplexer have been obtained using the new method introduced in Chapter 5. Its experimental insertion and return loss characteristics have been established.

Finally, hoping the design methods presented in this thesis have contributed something to the state-of-the-art in microwave filters and multiplexers which was described by Professor Rhodes's words [72]. "The state-of-the-art in microwave filters has changed relatively slowly compared to other areas of microwave engineering. One of the main difficulties has been design rather than technology".

REFERENCES

[1] Carlin and Giordano, "Network Theory", Prentice-Hall EE series, New Jersey, 1964.

[2] A. PaPoulis, "Fourier integral and its applications", McGraw Hill Book Company, 1962.

[3] G.I. Atabekov, "Linear network theory", Pergamon Press.

[4] E.A. Guilleman, "Synthesis of passive networks", J. Wiley & Sons, 1957.

[5] J.O. Scanlan and R. Levy, "Circuit theory Vol. 2", Oliver and Boyd, Edinburgh.

[6] S. Darlington, "Synthesis of reactance-4-Pole which produce prescribed insertion loss characteristics", J. Math. Phys., Vol. 30, pp 257-353, Sept. 1939.

[7] J.D. Rhodes, "Theory of electrical filters", J. Wiley & Sons, 1976.

[8] E. Christian and E. Eisenmann, "Filter design tables and graphs", Wiley, New York, 1966.

[9] A.I. Zverev, "Handbook of filter synthesis", J. Wiley, New York, 1967.

[10] R. Saal, "Der Entwurf Vonfiltern mit milfe des Kataloges Normurter Tiefpasse, Telefunken, G.M.B.H., Backray/Wurtemburg, W. Germany, 1964.

[11] T. Fujisawa, "Realizability theorem for mid series mid shunt low-pass ladder networks without induction", IRE Trans. on Circuit theory, CT-2, 320-325, December 1955.

[12] J. Meinguet and V. Belevitch, "On the realizability of Ladder filters", IRE Trans. on Circuit Theory Vol. CT-5, pp 253-255, (December 1958).

[13] J.D. Rhodes, "Explicit formulas for element values in elliptic function prototype network", IEEE Trans. on Circuit Theory, CT-18, pp 264-276,(March 1971).

[14] R.E. Baum, "A modification of Brune's method for narrow-band filters", IRE Trans. on Circuit Theory, Vol. CT-5,(December 1958), pp 264-267.

[15] E.L. Norton, "Constant resistance networks with applications to filter groups", Bell systems Tech. J., 16, pp 178-193, (April 1937).

[16] W.R. Bennet "Advanced problems No. 3880, 3881", Amer. Math. monthly, 45, 389-390. (June-July, 1938).

[17] V. Belevitch, "Tchebyshev filters and amplifier networks", Wireless Engineer, 29, pp 106-110 (April 1952).

[18] H. Takahasi, "On the ladder type filter network with Tchebyshev response", J. Ins. Elec. Commun. Engr. Japan, 34, pp 65-74 (February 1951).

[19] L. Weinberg and P. Slepian, "Takahasi results on Tchebyshev and Butterworth Ladder networks", IRE Trans. on Circuit Theory, CT-7, pp. 88-101, (June 1960).

[20] H.J. Orchard, "Formulae for Ladder Filters", Wireless Engr. 30, pp 3-5 (January 1953).

[21] C.B. Sharpe "A generalized rational function", Proc. IRE, pp 454-457, (February 1954).

[22] R. Levy, "Generalized rational function approximation in finite intervals using Zolotarev functions", IEEE Trans. Microwave theory Tech. (1970 Symp. Issue) Vol. MTT-18, pp 1052-1064, (December 1970).

[23] J.D. Rhodes and S.A. Alseyab, "The generalized low-pass prototype filter", The International Journal of Circuit Theory and Applications (in press).

[24] J.A.C. Bingham, "A new method of solving the accuracy problem in filter synthesis", IEEE Trans. Circuit Theory, Vol. CT-11, pp 327-341, (September 1964).

[25] H.J. Orchard and G.C. Temes, "Filter design using transformed variable, "IEEE Trans. circuit theory, Vol. CT-15, pp 385-408, (December 1965).

[26] L. Weinberg, "Network analysis and synthesis", McGraw Hill Book Company, 1962.

[27] J.K. Skwirzynski, "Design theory and data for electrical filters", D. Von Nostrand Company Ltd., 1965.

[28] G.L. Mattaei, L. Young and E.M.T. Jones "Microwave Filters, Impedance Matching Networks and Coupling Structures", McGraw-Hill, New York, 1964.

[29] J.L. Haine, "Direct design methods for electrical filters and diplexers", Ph.D. thesis, The University of Leeds, England, 1977.

[30] C.B. Barham, "Review of design and performance of microwave multiplexers", The Marconi Review, Vo. XXXV, No. 184, First Quarter 1972, pp 1-23.

[31] R.J. Webzel and W.G. Erlinger, "Narrow band contiguous multiplexing filters with arbitrary amplitude and delay response. 1976, PG-MTT Symposium Digest, pp.116-118.

[32] M.H. Chen, F. Assal and C. Mahle, "A contiguous band multiplexer", Comsat technical review, Vol. 6, No. 2, pp 285-305, Fall, 1976.

[33] J.D. Rhodes and R. Levy, "A generalized multiplexer theory", IEEE Trans. on Microwave Theory and Techniques, Vol. MTT-27, No. 2, (February, 1979).

[34] R.K. Brayton, L.O. Chua, J.D. Rhodes and R. Spence, "Modern Network Theory - An Introduction", Georgi Publishing Company, Switzerland, 1978.

[35] S.B. Cohn, "Direct-coupled-resonator filters", Proceedings of IRE, Vol. 45, pp 187-196, (February 1957).

[36] R. Levy, "Theory of Direct-Coupled-Cavity Filters", IEEE Transaction on Microwave Theory and Techniques, Vol. MTT-15, No. 6, pp 340-348, (June 1967).

[37] Microwave Engineer's Handbook, Vol. 1, edited by T.S. Saad, et al, Artech House, Inc., Dedham, Massachusetts, 1971.

[38] N. Marcuvitz, "Waveguide Handbook", MIT Radiation Lab. Series, Vol. 10, McGraw-Hill Book Company Inc., New York, 1951.

[39] Australian Ministry of Defence, Technical note EID 55.

[40] M. Dishal, "Alignment and Adjustment of Synchronously tuned multiple resonators circuit filters", Proc. IRE Vol. 39, No. 11, pp 1448-1455. 1951.

[41] P.I. Richards, "Resistor-transmission line-circuits", Proc. IRE, Vol. 36, pp 217-220, (Feb. 1948).

[42] H. Ozaki and J. Ishii, "Synthesis of class of strip-line filters", IRE Trans. on Circuit Theory, CT-5, pp 104-109, (June 1958).

[43] R. Levy, "A general equivalent circuit transformation for distributed networks", IEEE Trans. on Circuit Theory, Vol. CT-12, No. 3, pp. 457-458, (September 1965).

[44] R.J. Wenzel, "Exact design of TEM microwave network using quater-wave length lines", IEEE Trans. on Microwave Theory and Techniques, Vol. MTT-12, No. 1, pp 94-111, (January 1964).

[45] M.C. Horton and R.J. Wenzel, "General theory and design of optimum quarter-wave TEM filters", IEEE Trans. on Microwave Theory and Techniques, Vol. MTT-13, No. 3, pp 316-327, (May1965).

[46] A. Matsumoto, Editor, "Microwave Filters and Circuits", Supplement 1, Advances in Microwaves, Academic Press New York, 1970.

[47] H. Uchidea, "Fundamentals of Coupled Lines and multiwire Antennas", Sasaki Sendai, Japan, 1967.

[48] R.J. Wenzel, "Theoretical and Practical Applications of Capacitance matrix transformation to TEM network design", IEEE Trans. on Microwave Theory and Techniques, Vol. MTT-14, No. 12, pp 635-647, (December 1966).

[49] G.L. Matthaei, "Interdigital bandpass filters", IEEE Trans. on Microwave Theory and Techniques, Vol. MTT-10, No. 6, pp 479-491, (November 1962).

[50] R.J. Wenzel, "Exact theory of interdigital band-pass filters and related coupled structures", IEEE Trans. on Microwave Theory, and Techniques, Vol. MTT-13, No. 5, pp 559-575, (September 1965).

[51] H.J. Riblet, "An explicit derivation of the relationships between the parameters of an interdigital structure and the equivalent transmission line cascade", IEEE Trans. on Microwave Theory and Techniques, Vol. MTT-15, No. 3, pp 161-166, (March 1967).

[52] J.D. Rhodes, "The theory of generalized interdigital networks", IEEE Trans. on Circuit Theory, Vol. CT-16 No. 3, pp 280-288, (August 1969).

[53] G.L. Matthaei, "Combline band-pass filters of narrow or moderate bandwidth", Microwave journal, Vol. 6, pp 82-91, (August 1963).

[54] R.M. Kurzork, "Design of combline bandpass filters", IEEE Trans. on Microwave Theory and Techniques, Vol. MTT-14, No. 7, pp 351-353, (July 1966).

[55] R.M. Kurzork, "Frequency behaviour of Post Coupled TEM Combline resonators", IEEE Trans. on Microwave Theory and Techniques, Vol. MTT-16, No. 10, pp 888-889, (October 1968).

[56] E.G. Cristal, "Capacity coupling shortens combline filters", Microwaves, pp 44-50, (December 1967).

[57] R. Pregla, "Microwave filters of coupled lines and lumped capacitances", IEEE Trans. on Microwave Theory and Techniques, Vol. MTT-18, pp 278-280, (May 1970).

[58] R.J. Wenzel, "Synthesis of combline and capacitively loaded interdigital band-pass filters of arbitrary bandwidth", IEEE Trans. on Microwave Theory and Techniques, Vol. MTT-19, No. 8, pp. 678-686, (August 1971).

[59] W.J. Getsinger, "Coupled rectangular bars between parallel plates", IRE Trans. on Microwave Theory and Techniques, Vol. MTT-10, No. 1, pp 65-72, (January 1962).

[60] E.G. Cristal, "Coupled Circular Cylindrical rods between parallel ground planes", IEEE Trans. on Microwave Theory and Techniques, Vol. MTT-12, No. 4, pp 428-439, (July 1964).

[61] J.D. Rhodes and S.A. Alseyab, "Simple design technique for TEM-networks having equal-diameter coupled circular cylindrical rods between parallel ground planes", IEE Journal on Microwave, Optics, and Acoustics, Vol. 3, No. 4, pp 142-146, (July 1979).

[62] R. Mitra and T. Itoh, "Analysis of microstrip transmission lines", Advanced in Microwave, Vol. 8, Academic Press, New Yorks, 1974.

[63] L. Young, Editor, "Advanced in microwave", Vol. 8, Academic Press, New York, 1974.

[64] H. Howe Jr., "Stripline Circuit design", Artech House Inc., Massachusetts, 1974.

[65] J.P. Rooney and L.M. Underkofler, "Printed circuit integration of MW filter", Microwave Journal, Vol. 21, No. 9, pp 68-73, (September 1978).

[66] J.D. Rhodes and J.E. Dean, "MIC broadband filters and contiguous Multiplexers", proceeding of the 9th European Microwave Conference September 1979.

[67] R.J. Wenzel, "Wideband high-selectivity diplexers utilizing digital elliptic filters", IEEE Trans. on Microwave Theory and Techniques, Vol. MTT-15, No. 5, pp 669-680, (December 1967).

[68] G.L. Matthaei and E.G. Cristal, "Theory and Design of diplexers and multiplexers", Advances in Microwaves, Vol. 2, Academic Press, pp 237-326, New York, 1967.

[69] P.M. LaTourrette, "Multi-octave combline filter multiplexers", 1977 IEEE-MTT-S International Symposium Digest, pp 298-301.

[70] P.M. LaTourrette, "Combline filter multiplexers", Microwave journal, Vol. 20, No. 8, pp 55-59, August 1977.

[71] P.M. LaTourette and J.L. Roberds, "Extended junction combline multiplexers", 1978 IEEE-MTT-S International Symposium Digest, pp 214-216.

[72] J.D. Rhodes, "Technology Forecast - Filters: for printed circuit multiplexers", Microwave Systems News, Vol. 8, No. 4, April 1978.

PUBLISHED PAPERS.

1) "Simple design technique for TEM-networks having equal-diameter coupled circular cylindrical rods between parallel ground planes", IEE Journal on Microwaves, Optics and Accoustics, July, 1979, Vol. 3, No. 4.

2) "The Generalized Chebyshev Low-Pass Prototype Filter", Accepted for publication as a paper in the International Journal of Circuit Theory and Applications".

3) "A design procedure for bandpass channel multiplexers connected at a common junction", Accepted for publication as a paper in the IEEE Trans. on Microwave Theory and Techniques.

4) "A design procedure for broadband combline filter multiplexers", to be published.